4-2016

Effect of bioenergy crops and fast growing trees on hydrology and water quality in the Little Vermilion River Watershed

Tian Guo
Purdue University

Graduate School Form
30 Updated 12/26/2015

PURDUE UNIVERSITY
GRADUATE SCHOOL
Thesis/Dissertation Acceptance

This is to certify that the thesis/dissertation prepared

By Tian Guo

Entitled

Effect of Bioenergy Crops and Fast Growing Trees on Hydrology and Water Quality in the Little Vermilion River Watershed

For the degree of Doctor of Philosophy

Is approved by the final examining committee:

Bernard Engel Chair	James Kiniry
Venkatesh Merwade	
Margaret Gitau	
Indrajeet Chaubey	

To the best of my knowledge and as understood by the student in the Thesis/Dissertation Agreement, Publication Delay, and Certification Disclaimer (Graduate School Form 32), this thesis/dissertation adheres to the provisions of Purdue University's "Policy of Integrity in Research" and the use of copyright material.

Approved by Major Professor(s): Bernard Engel

Approved by: Bernard Engel 4/21/2016

Head of the Departmental Graduate Program Date

EFFECT OF BIOENERGY CROPS AND FAST GROWING TREES ON HYDROLOGY AND WATER QUALITY IN THE LITTLE VERMILION RIVER WATERSHED

A Dissertation

Submitted to the Faculty

of

Purdue University

by

Tian Guo

In Partial Fulfillment of the

Requirements for the Degree

of

Doctor of Philosophy

May 2016

Purdue University

West Lafayette, Indiana

To my family and great mentors

ACKNOWLEDGEMENTS

I want to express my gratitude for so many who invested time and effort into helping me complete this work.

The data used in this publication from the Little Vermilion River Watershed were a contribution of the Illinois Agricultural Experiment Station, University of Illinois at Urbana-Champaign as a part of Projects 10-309 and 10-301 and Southern Regional Research Project S-1004 (formerly S-249 and S-273). Supported in part with funds from USDA-CSREES under special projects 91-EHUA-1-0040 and 95-EHUA-1-0123, NRI project 9501781, and Special Project 95-34214-2266 (Purdue sub-contract 590-1145-2417-01). In addition, this work was supported with funds from the Illinois Council on Food and Agricultural Research and with the assistance of the Champaign County Soil and Water Conservation District which sponsored the installation of the County Line gaging station. Faculty from the Department of Agricultural Engineering supervising the collection and reduction of these data were: J. K. Mitchell, M. C. Hirschi, P. Kalita, and R. A.C. Cooke.

To my advisor, Dr. Bernard Engel, I thank you for your encouragement, wisdom, and support in helping me conduct independent research and complete my studies. For your frequent meeting with me and hours of work spent mentoring me, thank you. And thank you to my committee members, Dr. Indrajeet Chaubey Dr. Venkatesh Merwade, Dr. James Kiniry and Dr. Margaret Gitau, for your thoughtful guidance. I could never have completed tree growth modification in SWAT work without Dr. Kiniry's support! For all my ABE friends, thank you for providing a friendly and enriching environment and making my life much easier.

To my dear husband, Gang, thank you for being my partner in all things. Thank you for your selfless sacrifice. To my lovely baby, Decker, thank you for being such a healthy and happy baby. Your smiles always make my rough days much better. My parents and in-laws, thank you for your love and support.

TABLE OF CONTENTS

Page

Page

Page

Page

LIST OF TABLES

Table Page

Table Page

Appendix Table

LIST OF FIGURES

Figure Page

Figure Page

Figure Page

Appendix Figure

ABSTRACT

Guo, Tian. Ph.D., Purdue University, May 2016. Effect of Bioenergy Crops and Fast Growing Trees on Hydrology and Water Quality in the Little Vermilion River Watershed. Major Professor: Bernard Engel.

Energy security and sustainability require a suite of biomass crops, including woody species. Short rotation woody crops (SRWCs) such as *Populus* have great potential as biofuel feedstocks. Quantifying biomass yields of bioenergy crop and hydrologic and water quality responses to growth is important should it be widely planted in the Midwestern U.S. Subsurface tile drainage systems enable the Midwest area to become highly productive agricultural lands, but also create environmental problems like nitrate-N contamination of the water it drains. The Soil and Water Assessment Tool (SWAT) has been used to model watersheds with tile drainage, but the new tile drainage routine in SWAT2012 has not been fully tested.

The objectives of this study were to develop algorithms and growth parameters of *Populus* in Agricultural Land Management Alternative with Numerical Assessment Criteria (ALMANAC) and SWAT models, compare performance of tile drainage routines in SWAT2009 and SWAT2012 in simulating tile drainage, and simulate biomass yields of bioenergy crops and the impacts of their impacts on water quantity and quality for a typical tile-drained watershed in the Midwest USA.

The functional components and parameters of hybrid poplar Tristis #1 (*Populus balsamifera* L. × *P.tristis* Fisch) and eastern cottonwood (*Populus deltoides* Bartr.) were determined, and related algorithms improved in ALMANAC and SWAT based on improved simulation of leaf area, plant biomass and biomass partitioning. Long-term (1991-2003) field site and river station data from the Little Vermilion River (LVR)

watershed in Illinois were used to evaluate performance of tile drainage routines in SWAT2009 revision 528 (the old routine) and SWAT2012 revision 615 and 645 (the new routine). Calibrated monthly tile flow, surface flow, nitrate in tile and surface flow, sediment and annual corn and soybean yield results at field sites, and flow, sediment load and nitrate load at the river station for the old and new tile drainage routines were compared with observed values. Crop residue from corn stover, perennial grasses, switchgrass and *Miscanthus*, and hybrid poplar trees were considered as potential bioenergy crops for the LVR watershed. SWAT2012 (Revision 615) with the new tile drainage routine (DRAINMOD routine) and improved perennial grass and tree growth simulation was used to model long-term annual biomass yields, flow, tile flow, sediment load, total nitrogen, nitrate load in flow, nitrate in tile flow, soluble nitrogen, organic nitrogen, total phosphorus, mineral phosphorus and organic phosphorus under various bioenergy scenarios in the LVR watershed. Simulated results from different bioenergy crop scenarios were compared with those from the baseline.

Tree growth calibration and validation results showed that improved algorithms of leaf area index (LAI) and biomass simulation and suggested values and potential parameter range for hybrid poplar Tristis #1 and Eastern cottonwood (*Populus deltoides* Bartr.) were reasonable, and performance of the modified ALMANAC in simulating LAI, aboveground biomass and root biomass of *Populus* was good. Performance of the modified SWAT simulated hybrid poplar LAI and aboveground woody biomass (P_{BIAS}: -57 ~ 7%, NSE: 0.94 ~ 0.99, and R^2: 0.74 ~ 0.99), and cottonwood aboveground biomass, seasonal mean runoff, mean sediment, mean nitrate-N and total nitrate-N were satisfactory (P_{BIAS}: -39 ~ 11%, NSE: 0.86 ~ 0.99, and R^2: 0.93 ~ 0.99). Additionally, tile drainage calibration and validation results indicated that the new routine provides acceptable simulated tile flow (NSE = 0.50 ~ 0.68), and nitrate in tile flow (NSE = 0.50 ~ 0.77) for field sites, while the old routine simulated tile flow (NSE = -0.77~ -0.20) and nitrate in tile flow (NSE = -0.99 ~ 0.21) for the field site with constant tile spacing were unacceptable. The new modified curve number calculation method in revision 645 (NSE = 0.56 ~ 0.82) better simulated surface runoff than revision 615 (NSE = -5.95 ~ 0.5). Bioenergy crop simulation results showed that 38% corn stover removal (66,439 Mg/yr) with combination of *Miscanthus*

both on highly erodible areas and marginal land (19,039 Mg/yr) provided the highest biofeedstock production. Flow, tile flow, erosion and nutrient losses were slightly reduced under bioenergy crop scenarios of *Miscanthus*, switchgrass, and hybrid poplar on highly erodible areas, marginal land and marginal land with forest. The increase in sediment load and nutrient losses resulting from corn stover removal could be offset under scenarios with various combinations of bioenergy crops. Corn stover removal with bioenergy crops both on highly erodible areas and marginal land could provide more biofuel production relative to the baseline, and was beneficial to hydrology and water quality at the watershed scale.

The modified ALMANAC and SWAT can be used for biofeedstock production modeling for *Populus*. The modified SWAT model can be used for *Populus* biofeedstock production modeling and hydrologic and water quality response to its growth. The improved algorithms of LAI and biomass simulation for tree growth should also be useful for other process based models, such as SWAT, EPIC and APEX. Tile drainage calibration and validation results provided reasonable parameter sets for the old and new tile drainage routines to accurately simulate hydrologic processes in mildly-sloped watersheds. Bioenergy crop simulation results provided guidance for further research on evaluation of bioenergy crop scenarios in a typical extensively tile-drained watershed in the Midwestern US.

CHAPTER 1. INTRODUCTION

1.1 Problem Statement

1.1.1 Biofuel Production and Bioenergy Crops

World energy consumption is projected to grow by 56 percent between 2010 and 2040, and fossil fuels will supply about 80 percent of world energy use through 2040 (U.S. Energy Information Administration, 2013). Increasing energy demand has encouraged the use of alternative forms of energy. According to the Energy Independence and Security Act (EISA) of 2007, 36 billion gallons of renewable biofuels are expected to be produced by 2022 in USA. The majority of biofuel production in the USA comes from soybean oil and sugar-rich corn. However, some studies have shown that with the combination of a global increasing demand of renewable energy and food, the problems of food-fuel competition of land, higher food prices (Johansson and Azar, 2007), and lower food production (Wolf *et al*., 2003) will be created. Thus, EISA has proposed 15 billion gallons of renewable biofuels could come from conventional biofuel resources such as corn and soybean by 2022. The beneficial biofuels should provide sustainable biofeedstocks that neither compete with food crops nor cause land-clearing. Non-food bioenergy crops—crop residues (e.g. corn stover, rice straw) (Thomas, 2011a, 2014a), cellulosic perennial crops (e.g. miscanthus, switchgrass, mixed grasses) (Thomas, 2011b, 2014b), and woody biomass crops (e.g. hybrid poplar, willow) offer great potential (Tilman *et al*., 2009). Crop residue removal can provide biomass feedstock in the short term, and cellulosic perennial crops (e.g. miscanthus, switchgrass, and mixed grasses) and woody biomass crops (e.g. *populous*) are expected to provide the remaining 21 billion gallons of biofuels.

1.1.2 Environmental Impacts of Bioenergy Crops

To meet the US biofuel goal, bioenergy crops should provide environmental sustainable and economic biofuel production. Many researchers have suggested that bioenergy crops can improve soil structure and fertility of degraded lands but may cause reductions in water availability and deteriorating water scarcity. Other issues like land use change (e.g. biodiversity losses), reduced sediment load in reservoirs, rivers and irrigation channels, greenhouse gas emissions and forest conversion and cropland expansion also receive much attention (Bauen *et al.*, 2009). For instance, planting fast growing poplar trees has been shown to reduce total nitrogen and phosphorus loading to meet the requirement of the Total Maximum Daily Loads in the Millsboro Pond Watershed (Aditya and William, 2010). Additionally, Thomas (2009) qualified the water quality impacts of land management changes related to increasing demands for corn as a biofuel feedstock in US and demonstrated that agricultural management decisions would have great impacts on nutrient, runoff, erosion, and pesticide losses from agricultural fields and further research was needed to fully understand the water impacts of land management decisions related to corn grain for biofuel production. Moreover, Parajuli and Duffy (2013) studied the impacts of bioenergy crops on hydrology and water quality in Town Creek Watershed (TCW) in Mississippi and concluded that different bioenergy crops have different environmental benefits. Growing miscanthus can attain the highest feedstock yield in TCW, and switchgrass and miscanthus had lower sediment yield than corn and soybeans. Thus, it is necessary and important to investigate the environmental impacts of bioenergy crops on water quantity and quality.

1.1.3 Bioenergy Crops Growth Simulation Using Computation Modeling Tools

On the basis of soil characteristics, land cover, elevation, management practices and climate data, the influence of bioenergy crop production scenarios on hydrologic processes and water quality can be simulated by computational modeling tools, such as Groundwater Loading Effects of Agricultural Management System and National Agricultural Pesticide Risk Analysis (GLEAMS-NAPRA), Environmental Policy Integrated Climate (EPIC), Agricultural Policy/Environmental Extender (APEX), Soil and Water Assessment Tool

(SWAT), Revised Universal Soil Loss Equation Version 2 (RUSLE2) and Wind Erosion Prediction System (WEPS) (Engel *et al*., 2010; Muth *et al*., 2013). Some researchers investigated impacts of biofeedstock production on water quantity and quality using Soil and Water Assessment Tool (SWAT), and demonstrated that the SWAT model can simulate bioenergy crop growth and impacts of bioenergy crops on hydrologic phenomenon and nutrient loadings at watershed scales (Parajuli *et al*., 2008; Love and Nejadhashemi, 2011; Nair *et al.,* 2011; Powers *et al.,* 2011; Wu *et al*., 2012 a, b, c; Parajuli and Duffy, 2013). Moreover, production impacts of perennial biofuel feedstocks, such as switchgrass and miscanthus and woody biofuel crops like hybrid poplar, may not be easily represented in SWAT (Engel *et al*, 2010), since the plant dataset in the model does not include scientific and detailed information to represent these second generation biofuel crops. To obtain a better representation of perennial bioenergy crop growth in the SWAT model, the parameters in the plant dataset should be developed and improved, and then impacts of biofuel crops production on hydrologic processes and water quality can be simulated appropriately.

1.1.4 Environmental Impacts of Bioenergy Crops Simulation in Watersheds with SWAT

Some researchers have debated about impacts of land use changes on hydrological schemes for years (Stednick, 1996; Finch, 1998; Roberts, 2000). The SWAT model has shown the ability to simulate bioenergy crop growth and hydrologic and water quality responses to their growth. For the study of evaluating the influence of bioenergy crops on water quantity and quality, sediments and nutrient losses, the watershed is an appropriate carrier incorporating bioenergy crops, soil and water-related mediums — river, stream, channel and reach. Parajuli and Duffy (2013) studied hydrologic and water quality responses to corn, soybean, switchgrass and *miscanthus* in Town Creek Watershed (TCW) in Mississippi, USA and found that producing a perennial grass in the TCW can provide the largest biomass feedstock source with the least environmental impact. Raj (2013) developed 13 bioenergy scenarios in Wildcat Creek watershed and simulated the impacts on streamflow, sediments and nutrients and compared by an improved SWAT model and

found that simulated streamflow, sediment erosion and nutrient loading at the watershed outlet with bioenergy scenarios, compared with watershed with baseline scenario (corn and soybean).

1.1.5 Tile Drainage and Impacts on Hydrology and Nutrient Loads

Drainage expanded to a broad scale when Europeans settled the Midwestern U.S., during which large proportions of the Midwest were swampland unsuited to normal cultivation (NRCS/ARS/University of Illinois, 2014). Poorly draining soils can prevent timely fieldwork and cause stress on growing plants (Wright and Sands, 2001). Thus, artificial drainage has been used to increase crop yields in agricultural lands. Subsurface drainage can make excess water leave the field through a network of drain tiles installed below the soil surface. The percentage of cropland tiled in Illinois, Indiana, Ohio and Iowa is 35%, 50%, 25% and 25%, respectively (Kalita *et al.*, 2007).

The North Central Region of the U.S is the major source of nutrient loading to Mississippi River (Alexander *et al.*, 2008). Moreover, Illinois has been estimated to provide 15% of Mississippi River N loading and 10% of P loading (Kalita *et al.*, 2007). Models that link Mississippi River discharge with Gulf of Mexico hypoxia showed that increasing water discharge and nitrogen within the discharge would cause worse hypoxia; on the other hand, reducing nitrogen load to surface waters would reduce oxygen demand (Rabalais *et al.*, 1999). Thus, reducing nutrient loading from tile-drained watersheds in the Midwest area is necessary and urgent.

1.1.6 Tile Drainage Routine Development in the SWAT

Because of the old tile drainage routines incorporated in SWAT2002, modeled subsurface flow and stream discharge results by SWAT2002 were not always satisfactory (Arnold *et al.*, 1999; Du *et al.*, 2005). The simulation of water table dynamics was improved in SWAT2005, and monthly flow and subsurface tile drainage simulated by the modified SWAT has been improved as compared to SWAT2000 (Du *et al.*, 2005). Koch *et al.* (2013) demonstrated that the tile drainage routine in SWAT2005 could simulate the impact of subsurface drainage on hydrology at watershed scales satisfactorily. Additionally, the

drawdown time parameter (TDRAIN) and the drain tile lag time (GDRAIN) were added in the new tile drainage routine in SWAT. With the new tile drainage routine in SWAT2012, peak drain flow is controlled by the drainage coefficient (DRAIN_CO). However, research on testing new drainage routines in SWAT2012 and application of realistic parameters is rare. Boles (2013) parameterized the new tile drainage simulation method and compared simulated tile flow, stream flow, and nitrogen and phosphorus results with data from reviewed literature and found that the new drain flow routine in SWAT2012 could simulate tile flow and nitrate transported by tiles realistically. However, it is important to implement the new drainage routines in tile-drained watersheds to figure out how to select realistic parameters and simulate the influence of tile drainage on water balance well.

1.1.7 The Impacts of Bioenergy Crop Growth on Tile Drain Flow and Nutrient Loss

Tile flow hydrology and nutrient transport were studied at the Water Quality Field Station in West Lafayette, IN including conventional bioenergy crops, and results showed that switchgrass could decrease nitrate concentrations and loadings in tile lines and miscanthus could decrease tile flow volume; while, two of the four switchgrass plots decreased tile flow, the other two switchgrass plots increased tile flow as compared to control tiles (Trybula, 2012). Modeling studies about the influence of bioenergy crops on tile flow and water quality in tile flow are rare. Boles (2013) simulated effects of switchgrass growth on tile drained lands in the Matson Ditch watershed in Indiana and found that scenario converting all corn, soybean, wheat, hay and alfalfa lands was the most effective at reducing sediment and nutrient losses; filter strip application to corn, soybean and wheat lands was found to decrease total N and P while increasing mineral P and nitrate. Since hydrologic and water quality responses to bioenergy crop growth are unique in tile-drained areas, it is important to include tiles as a consideration to understand the environmental impacts of bioenergy crops.

Generally, tree growth simulation in the SWAT model has not been fully developed and modeling studies including bioenergy crop and fast growing tree growth and hydrologic and water quality impacts at the watershed scale or tile drains modeling based on the new tile drain routine in the SWAT are few. Given that the necessity to understand and quantify

bioenergy crop growth and hydrologic and water quality impacts of tile-drained watersheds by SWAT, the research goals and objectives were determined and shown below (1.2).

1.2 Overall Goal of the Study

The overall goal of this study is to understand and quantify watershed-scale environmental sustainability assessment of biofuel crop (corn, corn stover, switchgrass and *Miscanthus*) and fast growing tree (*Populus* 'Tristis #1' (*Populus balsamifera* L. × *P.tristis* Fisch)) production. The research will estimate the influence of bioenergy crops including fast growing trees on hydrologic processes and water quality on a watershed scale and provide guidance for the selection, placement and management of energy crops. The Soil and Water Assessment Tool (SWAT) was chosen to simulate hydrologic and water quality impacts of energy crops. The research will establish growth parameters of hybrid poplar in the SWAT2012 plant dataset based on poplar and hybrid poplar growth and nutrient loading data in research sites in Wisconsin and Mississippi. The impacts of hybrid poplar, switchgrass, miscanthus, corn, corn stover and soybeans under various land cover and management scenarios will be simulated in a typical Midwestern US tile-drained watershed, the Little Vermilion River watershed (LVRW) located in east-central Illinois. Generally, the study is to solve the issues:

(1) Establishment of *Populus* parameters in the plant dataset in SWAT and improvement and modification of *Populus* growth simulation in SWAT;

(2) Simulation of *Populus* growth and its influence on water quantity and quality;

(3) Comparison of model results (streamflow, tile drain flow and nutrient losses in tile drain) simulated by new tile drainage routines in SWAT2012 with results modeled by old tile drainage routines in SWAT2009 in a tile-drained watershed;

(4) Evaluation of biomass yields of bioenergy crops (corn, corn stover, switchgrass, *Miscanthus*, hybrid poplar) in a tile-drained watershed under different bioenergy crop scenarios;

(5) Evaluation of the impact of bioenergy crop growth on water balance and nutrient loadings including tiles as a consideration under different bioenergy crop scenarios;

(6) Determination of bioenergy crop scenarios with the highest biomass yields and the least hydrologic and water quality impacts, water quality improvement in typical tile-drained watersheds in the Midwestern US.

1.3 Objectives of the Study

To reach the goals mentioned above, three objectives were established for this study as below:

Objective 1: Development and improvement of the simulation of woody bioenergy crops (*Populus* 'Tristis #1' (*Populus balsamifera* L. × *P.tristis* Fisch) and Eastern cottonwood (*Populus deltoides* Bartr.)) in the Soil and Water Assessment Tool (SWAT) model.

Objective 2: Comparison of the performance of tile drainage routines in the SWAT2009 and SWAT2012 at the Little Vermilion River (LVR) Watershed.

Objective 3: Quantification of bioenergy crop growth and the impacts of bioenergy crops on water quantity and quality in LVR watershed using SWAT.

1.4 Thesis Organization

This thesis is composed of six chapters. The first chapter, the introduction, reviews needs of bioenergy crops, environmental impacts of bioenergy crops, modeling tools (including SWAT) used for bioenergy crops growth and hydrologic and water quality impacts, tile drainage routines in the SWAT, and impacts of bioenergy crops and tile drainage on hydrology and nutrient loads.

Objective 1 "Development and improvement of the simulation of woody bioenergy crops—hybrid poplar in the Soil and Water Assessment Tool (SWAT) model" is covered in chapter two and three. Chapter two, "Functional Approach to Simulating Short Rotation Woody Crops in Process Based Models", describes adding new algorithms and parameter for *Populus* 'Tristis #1' *(Populus balsamifera L.* × *P.tristis* Fisch*)* in ALMANAC,

calibration and validation of modified ALMANAC model based on comparison between modeled and measure values of annual LAI and biomass yield of hybrid poplar trees with various spacing. This chapter also includes preliminary results covering improved algorithms and parameters for LAI and dropping leaves weight estimation, estimation of *Populus 'Tristis #1'* growth parameters, and model simulation and validation for hybrid poplar growth.

Chapter three "Development and Improvement of the Simulation of Woody Bioenergy Crops (*Populus* 'Tristis #1' (*Populus balsamifera* L. × *P.tristis* Fisch) and Eastern Cottonwood (*Populus deltoides* Bartr.)) in the Soil and Water Assessment Tool (SWAT) Model" demonstrates adding new algorithms and parameters for *Populus* 'Tristis #1' (*Populus* balsamifera L. × P.tristis Fisch) and Eastern Cottonwood (*Populus* deltoides Bartr. in the SWAT model, calibration and validation of modified SWAT model based on comparison between modeled and measured values of LAI, biomass yield, runoff, sediment and nitrate-N in runoff. This chapter also includes preliminary results covering improved algorithms and parameters for LAI and dropping leaves weight estimation, sensitivity analysis and estimation of *Populus* growth parameters, and model simulation and validation for hybrid poplar and cottonwood growth.

The fourth chapter (Objective 2) " Comparison of the performance of tile drainage routines in the SWAT2009 and SWAT2012 at the Little Vermilion River (LVR) Watershed" describes tile drainage routine development in the SWAT, tile drainage impacts on hydrology and water quality in Midwestern US, and comparison of tile flow, surface flow, sediment, and nitrate in tile flow and surface flow at field sites, and flow, sediment load and nitrate load at river station simulated by the new and old tile drainage routines in SWAT in the LVR watershed.

The fifth chapter (Objective 3) "Predictions of bioenergy crop growth and the impacts of bioenergy crops on streamflow, tile drain flow and nutrient loss in the LVRW using SWAT" demonstrates various biofuel crop scenarios designed in the LVRW, bioenergy crop representations in the SWAT, uncertainty analysis of selected parameters in SWAT

and prediction of biomass yields of bioenergy crop and the impacts on streamflow, tile drain flow and nutrient loss under different bioenergy crop scenarios in the LVRW.

Chapter six provides an overview of major research findings of this study and recommendations for further research. Appendices A and B are supplementary information for Chapters two and three, respectively.

1.5 References

Aditya, S., & William F, R. (2010). Evaluation of Best Management Practices in Millsboro Pond Watershed Using Soil and Water Assessment Tool (SWAT) Model. Journal of Water Resource and Protection, 2010.

Alexander, R. B., Smith, R. A., Schwarz, G. E., Boyer, E. W., Nolan, J. V., & Brakebill, J. W. (2007). Differences in phosphorus and nitrogen delivery to the Gulf of Mexico from the Mississippi River Basin. *Environmental Science & Technology*, *42*(3), 822-830.

Arnold, J. G., P. W. Gassman, K. W. King, A. Saleh, & U. Sunday.(1999). Validation of the subsurface tile flow component in the SWAT model. Presented at the ASAE/CSAE-SCGR Annual International Meeting. ASAE Paper No. 992138. St. Joseph, Mich.: ASAE.

Bauen, A., Berndes, G., Junginger, M., Londo, M., Vuille, F., Ball, R., & Mozaffarian, H. (2009). Bioenergy: a sustainable and reliable energy source. A review of status and prospects.

Boles, C. M. (2013). *SWAT model simulation of bioenergy crop impacts in a tile-drained watershed* (Mater thesis), Purdue University.

Briefing, U. S. (2013). International Energy Outlook 2013.

Du, B., Arnold, J. G., Saleh, A., & Jaynes, D. B. (2005). Development and application of SWAT to landscapes with tiles and potholes. *Trans. ASAE*, *48*(3), 1121-1133.

Engel, B., Chaubey, I., Thomas, M., Saraswat, D., Murphy, P., & Bhaduri, B. (2010). Biofuels and water quality: challenges and opportunities for simulation modeling. *Biofuels*, *1*(3), 463-477.

Finch, J. W. (1998). Estimating direct groundwater recharge using a simple water balance model–sensitivity to land surface parameters. *Journal of Hydrology*, *211*(1), 112-125.

Johansson, D. J., & Azar, C. (2007). A scenario based analysis of land competition between food and bioenergy production in the US. *Climatic Change*, *82*(3-4), 267-291.

Kalita, P. K., Cooke, R. A. C., Anderson, S. M., Hirschi, M. C., & Mitchell, J. K. (2007). Subsurface drainage and water quality: The Illinois experience. *Trans. ASABE*, *50*(5), 1651-1656.

Koch, S., Bauwe, A., & Lennartz, B. (2013). Application of the SWAT model for a tile-drained lowland catchment in North-Eastern Germany on subbasin scale. *Water resources management*, *27*(3), 791-805.

Muth Jr, D. J., & Bryden, K. M. (2013). An integrated model for assessment of sustainable agricultural residue removal limits for bioenergy systems. *Environmental Modelling & Software*, *39*, 50-69.

Nair, S. S. , King, D. W. , Witter, J. D. , Sohngen, B. L. & Fausey, N. R. (2011). Importance of Crop Yield in Calibrating Watershed Water Quality Simulation Tools. *Journal of the American Water Resources Association*, 47(6), 1285-1297.

NRCS/ARS/University of Illinois. University of Illinois Extension: Bioreactor, Water Table Management, and Water Quality.(2014).Retrieved from website: http://web.extension.illinois.edu/bioreactors/history.cfm.

Parajuli, P. B., Mankin, K. R., & Barnes, P. L. (2008). Applicability of targeting vegetative filter strips to abate fecal bacteria and sediment yield using SWAT. *Agricultural water management*, *95*(10), 1189-1200.

Parajuli, P. B., & Duffy, S. E. (2013). Quantifying Hydrologic and Water Quality Responses to Bioenergy Crops in Town Creek Watershed in Mississippi. *Journal of Sustainable Bioenergy Systems*, *3*, 202.

Powers, S. E., Ascough II, J. C., Nelson, R. G., & Larocque, G. R. (2011). Modeling water and soil quality environmental impacts associated with bioenergy crop production and biomass removal in the Midwest USA. *Ecological Modelling*, *222*(14), 2430-2447.

Rabalais, N. N., Turner, R. E., Justic, D., Dortch, Q., & Wiseman Jr, W. J. (1999). *Characterization of hypoxia: Topic 1 Report for the Integrated Assessment of Hypoxia in the Gulf of Mexico*. NOAA Coastal Ocean Program, 46-47.

Raj, C. (2013). *Optimal land use planning on selection and placement of energy crops for sustainable biofuel production*. (Doctoral dissertation), Purdue University.

Roberts, J. (2000). The influence of physical and physiological characteristics of vegetation on their hydrological response. *Hydrological Processes*, *14*(16-17), 2885-2901.

Schilling, K. E., Jha, M. K., Zhang, Y. K., Gassman, P. W., & Wolter, C. F. (2008). Impact of land use and land cover change on the water balance of a large agricultural watershed: Historical effects and future directions. *Water Resources Research*, *44*(7), 1-12. DOI:10.1029/2007WR006644.

Stednick, J. D. (1996). Monitoring the effects of timber harvest on annual water yield. *Journal of Hydrology*, *176*(1), 79-95.

Thomas, M. A., Ahiablame, L. M., Engel, B. A., Chaubey, I., & Mosier, N. (2014a). Modeling Water Quality Impacts of Cellulosic Biofuel Production from Corn Silage. *BioEnergy Research*, *7*(2), 636-653.

Thomas, M.A., L. M. Ahiablame, B.A. Engel, I. Chaubey. (2014b). Modeling Water Quality Impacts of Growing Corn, Switchgrass, and *Miscanthus* on Marginal Soils. *Journal of Water Resource and Protection*, 6, 1352-1368.

Thomas, M. A., Engel, B. A., & Chaubey, I. (2011a). Multiple corn stover removal rates for cellulosic biofuels and long-term water quality impacts. *Journal of Soil and Water Conservation*, *66*(6), 431-444.

Thomas, M. A. (2011b). *Environmental implications of feedstock production practices for bioenergy* (Doctoral dissertation), Purdue University.

Thomas, M. A., Engel, B. A., & Chaubey, I. (2009). Water quality impacts of corn production to meet biofuel demands. *Journal of Environmental Engineering*, *135*(11), 1123-1135.

Tilman, D., Socolow, R., Foley, J. A., Hill, J., Larson, E., Lynd, L., & Williams, R. (2009). Beneficial biofuels—the food, energy, and environment trilemma. *Science*, *325*(5938), 270.

Trybula, E. (2012). *Quantifying ecohydrologic impacts of perennial rhizomatous grasses on tile discharge: A plot level comparison of continuous corn, upland switchgrass, mixed prairie, and Miscanthus x giganteus* (Master thesis), Purdue University.

U.S. Environmental Protection Agency, National Agriculture Compliance Assistance Center. (2014). Drainage. Retrieved from website: http://www.epa.gov/oecaagct/ag101/cropdrainage.html.

Wolf, J., Bindraban, P. S., Luijten, J. C., & Vleeshouwers, L. M. (2003). Exploratory study on the land area required for global food supply and the potential global production of bioenergy. *Agricultural systems*, *76*(3), 841-861.

Wright, J., & Sands, G. (2001). Planning an agricultural subsurface drainage system. *College of Agricultural, Food and Environmental Sciences, University of Minnesota. BU-07685*, 1-10. Retrieved from website:http://www.extension.umn.edu/agriculture/water/planning-a-subsurface-drainage-system/.

Wu, M., Demissie , Y., & Yan, E. (2012a). Simulated impact of future biofuel production on water quality and water cycle dynamics in the Upper Mississippi river basin. *Biomass and Bioenergy*, *41*, 44-56.

Wu, Y., Liu, S., & Li, Z. (2012b). Identifying potential areas for biofuel production and evaluating the environmental effects: a case study of the James River Basin in the Midwestern United States. *GCB Bioenergy*, *4*(6), 875-888.

Wu, Y., & Liu, S. (2012c). Impacts of biofuels production alternatives on water quantity and quality in the Iowa River Basin. *Biomass and Bioenergy*, *36*, 182-191.

CHAPTER 2. FUNCTIONAL APPROACH TO SIMULATING SHORT ROTATION WOODY CROPS IN PROCESS BASED MODELS

2.1 Abstract

Short rotation woody crops (SRWCs) such as *Populus* have great potential as biofuel feedstocks. Biomass yields and yield stability at potential sites are important considerations when SRWCs are widely planted. The process-based, daily time-step simulation model Agricultural Land Management Alternative with Numerical Assessment Criteria (ALMANAC) offers promise as a useful tool to evaluate tree growth over large ranges of conditions. The objective of this study was to develop algorithms and growth parameters of hybrid poplar 'Tristis #1' (*Populus balsamifera* L. × *P.tristis* Fisch) and eastern cottonwood (*Populus deltoides* Bartr.) in ALMANAC, and to improve simulation of leaf area index (LAI) and plant biomass as well as biomass partitioning. ALMANAC with the improved algorithms for LAI and weight of falling leaves was applied to hybrid poplar plots in Wisconsin and cottonwood plots in Mississippi, and the modeled biomass yield, and LAI were compared with measured data to modify and evaluate the location specific ALMANAC models. Improved algorithms for LAI and biomass simulation and suggested values and potential parameter ranges for hybrid poplar and cottonwood were reasonable (NSE: 0.81 ~ 0.99, and R^2: 0.76 ~ 0.99). ALMANAC with modified algorithms and parameters for *Populus* growth realistically simulated LAI, aboveground woody biomass and root biomass of *Populus*. Thus, this model can be used for biofeedstock production modeling for *Populus*. The improved algorithms of LAI and biomass simulation for tree growth should also be useful for other process based models, such as SWAT, EPIC and APEX.

2.2 Introduction

Increasing energy demand and high sustained oil prices have encouraged the use of alternative forms of energy. The majority of biofuel production in the USA comes from sugar-rich maize (*Zea mays* L.) and soybean (*Glycine max* (L.) Merr) oil. However, with the combination of a global increasing demand for renewable energy and food, the problems of food-fuel competition for land, higher food prices (Johansson & Azar, 2007), and lower food production (Wolf *et al*., 2003) will be created. Thus, beneficial biofuels should provide sustainable biofeedstocks that neither compete with food crops nor cause clearing of native forests. Non-food bioenergy crops—crop residues (Thomas *et al*., 2009, 2011; Cibin *et al*., 2012; Raj, 2013; Thomas *et al*., 2014b), cellulosic perennial crops (e.g. miscanthus (*Miscanthus* ×*giganteus*), switchgrass (*Panicum virgatum* L.), mixed grasses) (Casler, 2010; Cortese *et al*., 2010; Schmer *et al*., 2010; Thomas, 2011; Boles, 2013; Kiniry *et al*., 2013; Behrman *et al*., 2014; Thomas *et al*., 2014a; Trybula *et al*., 2014), and woody biomass crops (e.g. *Populus*), offer great potential (Tilman *et al*., 2009).

Short-rotation intensive culture of trees is considered a promising way to increase wood biomass productivity (U. S. Department of Agriculture, 1980). Dry matter production of wood plus bark in short rotation hardwood plantations are up to 20,000 kg/ha/yr, 3 to 5 times more than that for some natural stands (Hansen & Baker, 1979). Interest has increased in growing short rotation plantations for energy production, since the oil embargo in 1973 (Hansen, 1991). The *Populus* genus is highly productive under short rotation intensive culture system and is a good raw material for reconstituted forest products, due to its genetic diversity, rapid growth, vegetative propagation ease, and coppice regeneration (Hansen, 1983).

Biomass productivity may increase with narrower tree spacing under short rotation intensive culture system. Strong and Hansen (1993) concluded that biomass differences related to spacing were minor in hybrid poplar plantations with 18 clone/spacing combinations for up to 16 year growth periods in northern Wisconsin. Productivity of hybrid poplar was mainly influenced by clone, irrigation and disease. Similarly, Cannell and Smith (Cannell & Smith, 1980) showed that close spacing was not essential for high

biomass yield of hybrid poplar. However, tree spacing can affect time to canopy closure and the time needed to achieve maximum mean annual biomass increment (MABI). Hybrid poplar trees with wide tree spacing have longer rotations, and more flexible harvest scheduling as well as lower costs (Cannell & Smith, 1980; Strong & Hansen, 1993).

Prediction of *Populus* growth is critical for managers and policy makers to establish and manage short rotation woody crops (SRWCs) and to obtain high yields. Some researchers studied simulation of hybrid poplar growth using tree growth models. For instance, Ek (1979) used a model for regression estimation of branch weights of *Populus* which was found to be more precise than the models based on branch diameter. An individual-tree-based stand simulation model, FOREST, was used to simulate the periodic growth of hybrid poplar and showed that plot design, establishment techniques, cultural and environmental factors, measurement procedures and model limitation can explain differences between the projected and observed harvest (Isebrands *et al*., 1982). Meldahl (Meldahl, 1979) modified the FOREST model to simulate biomass yields of hybrid poplar and reduce the differences between projected and observed values. Moreover, Landsberg and Wright (Landsberg & Wright, 1989) simulated annual biomass production of two hybrid *Populus* clones in two locations using an energy conversion which assumes that plant biomass is proportional to the radiant energy absorbed by the canopy. Use of a radiant energy equation, also used in the ALMANAC models as described below, resulted in better simulation performance of *Populus* biomass yields than other simulations based on tree branch weight or stand (Landsberg & Wright, 1989).

The ALMANAC model (Kiniry *et al*., 2008) is a process-based, daily time step simulation model that has been parameterized and validated for a wide range of crop (corn and soybean), grass (switchgrass, miscanthus) and northern tree species (MacDonald *et al*., 2008) (lodgepole pine (*Pinus contorta* Douglas ex Loudon), white spruce (*Picea glauca* var. *glauca*), black spruce (*Picea mariana*), and trembling aspen (*Populus tremuloides* Michx.)). The model uses readily available USDA-NRCS soils data and readily available daily temperature, and rainfall data. ALMANAC plant growth simulation processes include light interception, dry matter production and biomass partitioned into plants

(Kiniry *et al*., 2008; Kiniry *et al*., 2012). Biomass is calculated based on light interception and species-specific radiant use efficiency (RUE), which is the amount of dry biomass produced per unit of intercepted light (Kiniry *et al*., 1999; Kiniry *et al*., 2007). Three attributes useful for quantifying potential plant growth are: RUE, LAI, and the light extinction coefficient (k) used to calculate the fraction of light intercepted by leaves (Kiniry, 1998).

Generally, RUE values for woody species are between 1.3 and 1.9 g/MJ intercepted photosynthetically active radiation (PAR), and for crops are between 2.2 and 3.5 g/MJ intercepted PAR (Kiniry *et al*., 1989). Kiniry measured RUE values for eastern red cedar (*Juniperus virginiana*) (1.6 g/MJ intercepted PAR) and honey mesquite (*Prosopis glandulosa*) (1.61 g/MJ intercepted PAR) to allow better prediction of their growth in ALMANAC (Kiniry, 1998). Mean RUE values were 1.5 for poplar in Wisconsin and Pennsylvania, USA (Landsberg & Wright, 1989) and RUE values were between 2.4 and 3.4 for intensively cultured poplar in Scotland (Cannell *et al*., 1988). The standard RUE values (g/MJ) should be multiplied by 10, to obtain the values (kg/ha)/(MJ/m2) used in the ALMANAC and Soil and Water Assessment Tool (SWAT) (Arnold *et al*., 2011).

Nineteen parameters for annual and long-term forest growth were incorporated and modified in the model to simulate successional forest regrowth after disturbance of forest ecosystems. Ranges of parameters were derived from scientific literature or yields tables. The range of RUE and k values for mixed forest used in ALMANAC were determined as 15-20 and 0.5-0.55, respectively (MacDonald *et al*., 2008; Johnson *et al*., 2009). However, research on biomass yields of trees simulated by ALMANAC is limited, since parameters and equations modified in the model are for mixed forest stands consisting of various woody species rather than a specific woody species (MacDonald *et al*., 2008).

Moreover, accurate LAI, biomass yield and biomass partitioning simulation for *Populus* in ALMANAC has not been adequately developed, and it is important to quantify fast growing tree growth accurately. In ALMANAC and SWAT, leaf area development, a sigmoid curve, is a function of the growing season for mature plants, during which mature plants can reach maximum LAI with the increase of heat units (Arnold *et al*., 2011). As

LAI for juvenile trees cannot increase to maximum LAI, the leaf area algorithm used in the model was not suitable for juvenile tree growth simulation. Thus, ALMANAC can only simulate plant growth after plants reach maturity (Arnold *et al.*, 2011). However, SRWCs were usually harvested once they reach maturity or even before maturity and short-rotation Populus trees usually reach maturity at the 5th or 6th year since planting (Hansen, 1983). Thus, it is also important to improve the model to reasonably simulate tree growth from tree planting to maturity.

This work is a first effort to improve *Populus* growth algorithms and parameters in ALMANAC with published region-specific *Populus* growth data. The objectives of this study were to: (1) develop algorithms and growth parameters of hybrid poplar 'Tristis #1' (*Populus balsamifera* L. × P.*tristis* Fisch) and eastern cottonwood (*Populus deltoides* Bartr.) in ALMANAC, and to improve simulation of leaf area and plant biomass as well as biomass partitioning; (2) use the modified model to simulate LAI and aboveground woody biomass of hybrid poplar in Wisconsin and aboveground woody biomass and root biomass of cottonwood in Mississippi; and (3) compare simulated LAI and biomass results from the modified model with observed values for verification of improved algorithms and growth parameters of *Populus*.

2.3 Materials and Methods

2.3.1 Hybrid Poplar Site in Northern Wisconsin and Cottonwood Site in Western Mississippi

This study was conducted using data in the literature from two study sites (Figure 2.1). The Poplar Site was a short rotation intensive culture plantation at the USDA Forest Service Harshaw Experimental Farm near Rhinelander, Wisconsin, US (45.6° N, 89.5° W) (Hansen *et al.*; Nelson & Michael, 1982) (Data A.1). Hybrid poplar cuttings were planted in early June, 1970, on a prepared site (Ek & Dawson, 1976a). The site was sowed to rye, plowed, and rototilled before planting (Strong & Hansen, 1993). The soil of the plantation is the Padus series, a silt loam, overlaying sand and gravel at depths of 30 to 60 cm with slope

reaching at most 1%. The pH is from 6.7 to 7.0 (Ek & Dawson, 1976a). The average growing season of hybrid poplar in this region is 120 days.

The Cottonwood Site was at the Delta Research and Extension Center at Stoneville, Mississippi in the Tennessee Valley region (Joslin & Schoenholtz, 1997), which was on agricultural land with a Bostket silt loam soil, a fine loamy, mixed, thermic Mollic Hapludalfs. The slope gradient is 0.2% (Data A.2). Soil quality changes were determined based on soil physical characteristics measured at the site in 1995 (prior to tree establishment) and in 1997 (at the end of growing season) (Tolbert *et al.*, 1998). Cottonwood cuttings 20-30 cm long were planted with spacing of 1.2 × 3.6 m (population: 23 trees/ 100 m^2) on 3 February, 1995 (Thornton *et al.*, 1998) and harvested during 1-20 November, 1997 (Pettry *et al.* 1997, unpublished annual progress report).

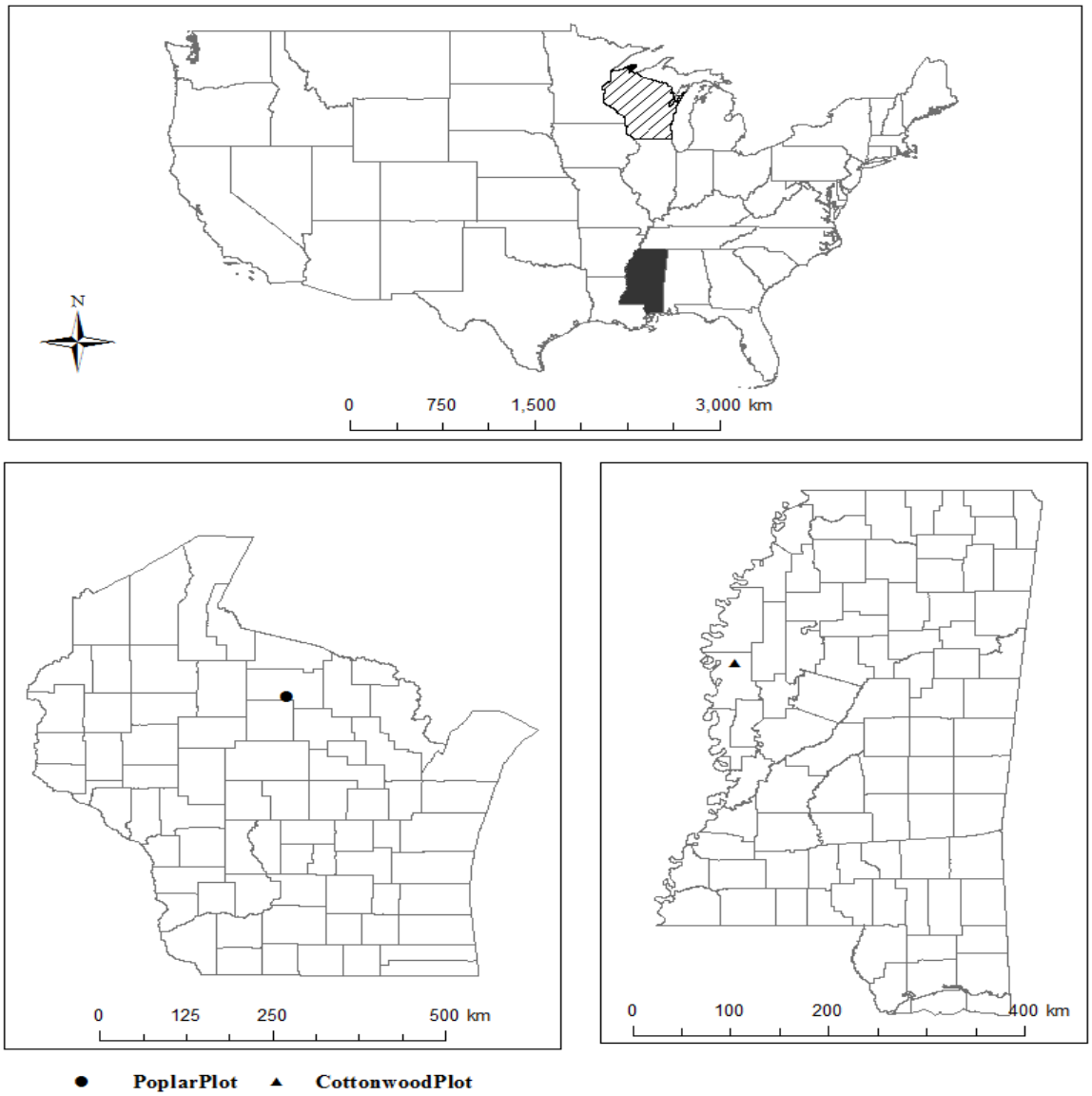

Figure 2.1 Location of hybrid poplar site at the USDA Forest Service Harshaw Experimental Farm near Rhinelander, Wisconsin and cottonwood site at the Delta Research and Extension Center at Stoneville, Mississippi

2.3.2 ALMANAC Model Setup and Management Schedules

ALMANAC 2011 (Version 1.0.3 Beta 2) with Interface (Version 1.0.3) was used in this project. A new crop named "Poplar Tian Low" and "Cottonwood" were added to represent hybrid polar and cottonwood, respectively. Lat 45.6°, Long 89.5° and Lat 33.34°, Long 90.85° were used for the Hybrid Poplar and Cottonwood Sites, respectively. The fraction of total tree biomass partitioned to roots was assumed to be 0.5 for hybrid poplar (Hansen, 1983) and 0.2 for cottonwood (Pettry *et al.* 1997, unpublished annual progress report). Table 2.1 describes the primary data required for ALMANAC model setup (Data A.3).

Table 2.1 Data for hybrid poplar and cottonwood growth simulation by ALMANAC

Plant	Data type	Source	Format	Date
Hybrid poplar	SSURGO[a]	USDA[b] Web Soil Survey	Polygon Shapefile	
	Precipitation and temperature	NCDC[c]		1970 - 1980
	Annual aboveground woody biomass yield (metric ton (mt)/ha)	Scientific literature[c]		1970 - 1980
	Annual LAI	Scientific literature[d]		1970 - 1980
Cottonwood	SSURGO[a]	USDA[b] Web Soil Survey	Polygon Shapefile	
	Precipitation and temperature	NCDC[c]		1995-1997
	Annual aboveground biomass yield (mt/ha)	Unpublished report[e]		1995-1997
	Annual root biomass (mt/ha)	Unpublished report[e]		1995-1997

[a] SSURGO: Soil Survey Geographic Database
[b] USDA: U.S. Department of Agriculture
[c] NCDC: National Climate Data Center
[d] Hansen, 1983
[e] Pettry *et al.* 1997, unpublished annual progress report

ALMANAC management includes planting and end of schedule dates, yearly tillage, pesticide and nutrient application rates. Tables 2.2 and 2.3 represented management operations for hybrid poplar growth in 1970, and cottonwood growth in 1995. Fertilizer and auto irrigation were also added to these two location-specific models to ensure *Populus* growth was not under water stress or nutrient stress. Nutrient application dates and rates for hybrid poplar growth from years 1971 to 1980, and cottonwood growth during years

1996 and 1997 were the same as nitrogen and phosphorus application in Tables 2.2 and 2.3, respectively. Hybrid poplar planting was on 22 May, 1970, and harvest was on 1 May, 1980. Cottonwood planting was on 3 February, 1995, and harvest was on 30 Nov, 1997.

Table 2.2 Management operations for hybrid poplar site at the USDA Forest Service Harshaw Experimental Farm near Rhinelander, Wisconsin

Plant	Date	Management Operation	Rate
Hybrid poplar	30-May	Tillage, Roto-Tiller (mixing depth: 5 mm, mixing efficiency: 0.80)	
	1-June	Planting	
	1-June	Pesticide Application (as Linuron)	2.2 kg/ha[a,b]
	1-June	Nitrogen Application (as Anhydrous Ammonia)	200 kg/ha[a,b]
	1-June	Phosphorus Application (as Elemental Phosphorus)	50 kg/ ha[a,b]
	31-Dec	The end of the operation scheduling for a year	

[a] Ek and Dawson, 1976a
[b] Srinivasan and Cibin 2014, personal communication

Table 2.3 Management operations for cottonwood site at the Delta Research and Extension Center at Stoneville, Mississippi

Plant	Date	Management Operation	Rate
Cottonwood	3-Feb	Tillage, Roto-Tiller (mixing depth: 5 mm, mixing efficiency: 0.80)	
	3-Feb	Planting	
	3-Feb	Pesticide Application (as Linuron)	2.2 kg/ha[a,b]
	1-June	Nitrogen Application (as Anhydrous Ammonia)	200 kg/ha[a,b]
	1-June	Phosphorus Application (as Elemental Phosphorus)	30 kg/ha[a,b]
	31-Dec	The end of the operation scheduling for a year	

[a] Thornton *et al.* 1998; Joslin and Schoenholtz, 1997
[b] Srinivasan and Cibin 2014, personal communication

2.3.3 Algorithm and Parameter Changes in the Model

Deciduous tree LAI increases both within each growing season prior to late season senescence and among years as the maximum seasonal LAI increases. The seasonal leaf area development curve in the model can be used in years prior to maturity year after adjusting each year's potential LAI. Published yearly LAI and aboveground biomass values for *Populus* trees with various planting densities ranged from 8 to 1111 trees/100 m^2 (Tables A.1 and A.2). The increase in maximum seasonal LAI across years for *Populus* with various densities was similar to the equation of loss of leaf late in the season (Kiniry

et al., 1992). This served as the starting point to derive a new leaf development algorithm to simulate maximum seasonal LAI each year with various densities.

$$y_{yr} = y_{yr-1} * 10^{log10^{\left(\frac{yr}{x_1}\right)} * x_2} \quad (2.1)$$

where yr is current growth year, y_{yr} is LAI value for current year, y_{yr-1} is LAI value for previous year, x_1 is number of years until maximum LAI is attained (CLAIYR), and x_2 is a new tree leaf factor (TreeD) in the LAI algorithm, representing how LAI increases to the maximum potential LAI (DMLA) with varying densities.

CLAIYR values for *Populus* trees with various densities were obtained from a previous study (Hansen, 1983). A specific density of *Populus* trees has an associated TreeD value representing its LAI development. Based on published LAI values for different years and CLAIYR values, TreeD in Equation (2.1) was calibrated manually for various populations to match observed values.

The management parameter "POPULATION" is the number of trees per 100 m^2. Previously, ALMANAC did not include a specific parameter for population effects on maximum seasonal LAI over years. In this new version, TreeD values in the crop database is used for different populations for *Populus* trees to calculate these seasonal maximums.

Total tree biomass consists of root biomass, senescent dropped leaf weight, and aboveground biomass (leaves, stems and branches). To accurately simulate *Populus* tree biomass partitioning, the algorithm used for dropping leaves was improved (Data A.4).

2.3.4 Values and Ranges of Parameters Determined before Model Calibration

Two-week moving average daily temperatures at the USDA Forest Service Harshaw Experimental Farm in Wisconsin and the Stoneville site in Mississippi were obtained using Matlab2013 based on NOAA daily temperature data to determine base temperature (TG). The period of emergence was assumed from 1 to 20 April for hybrid poplar and 20 March to 10 April for cottonwood (Isebrands & Nelson, 1983; Michael *et al.*, 1988; Michael *et al.*, 1990), which were Day of Year 90 to 110 and 78 to 98, respectively.

Values of PHU for hybrid poplar growth in Wisconsin and cottonwood growth in Mississippi were calculated based on accumulation of heat units during the growing season (Neitsch *et al*., 2011). The growing season of hybrid poplar on the Harshaw experiment farm and cottonwood at the Stoneville site was assumed from 1 April to 11 October and from 20 March to 31 October, respectively (Isebrands & Nelson, 1983; Michael *et al*., 1988; Michael *et al*., 1990) (Data A.5).

Values of hybrid poplar and cottonwood growth parameters maximum rooting depth (RDMX), rate of decline in RUE per unit increase in vapor pressure deficit (WAVP), plant nitrogen (N) at emergence (BN_1), 50% maturity (BN_2), and maturity (BN_3), phosphorus fraction at emergence (BP_1), 50% maturity (BP_2) and maturity (BP_3) (Kiniry, 1998; MacDonald *et al*., 2008), and harvest index (HI) for optimal growing conditions (Michael *et al*., 1990; Arnold *et al*., 2011) were derived from previous studies (Data A.5).

Values of plant maximum stomatal conductance (GSI) and maximum canopy height (HMX) for *Populus* growth simulation in the model were assumed before model calibration based on personal communication (Kiniry 2014) (Data A.5).

2.3.5 ALMANAC Model Calibration and Parameterization

Previous hybrid poplar growth studies at the USDA Forest Service Harshaw Experimental Farm in Wisconsin (Zavitkovski, 1981; Hansen, 1983; McLaughlin *et al*., 1987; Landsberg & Wright, 1989; Black *et al*., 2002)suggested values for RUE (called WA in the model), k (called EXTINC in the model), DMLA, two points on optimal leaf development curve parameters (DLAP1 and DLAP2), fraction of growing season when leaf area starts declining (DLAI), plant N fraction in harvested biomass (CNY) and plant P fraction in harvested biomass (CNP) (see details in appendix), providing reasonable ranges of these tree growth parameters for model calibration. Ranges of PHU values were calculated before model calibration. The model was calibrated by changing these *Populus* growth parameters manually to obtain a good fit with published hybrid poplar LAI and aboveground biomass values. Values of WA, EXTINC, DMLA, DLAP1 and DLAP2, DLAI, CNY and PHU were determined after model calibration (Data A.6).

The LAI and aboveground woody biomass data of hybrid poplar with various spacings and aboveground biomass and root biomass of cottonwood with medium density used for model calibration and validation were summarized in Table 2.4.

Table 2.4 Hybrid poplar and cottonwood growth data for model calibration and validation

Populus	population (trees/100 $m^{2)}$	Density level	Outputs (Annual aboveground woody biomass (AAWB), LAI, annual aboveground biomass (AAB) and root biomass (RB))	Data usage
Hybrid poplar	278	high	LAI	model calibration
	278	high	AAWB (mt/ha)	
	69	medium	AAWB (mt/ha)	
	17	low	LAI	
	17	low	AAWB (mt/ha)	
	1111	high	AAWB (mt/ha)	model validation
	83	high	LAI	
	83	high	AAWB (mt/ha)	
	25	medium	LAI	
	25	medium	AAWB (mt/ha)	
	8	low	AAWB (mt/ha)	
Cottonwood	23	medium	AAB (mt/ha)	
	23	medium	RB (mt/ha)	

2.3.6 Validation of the Modified ALMANAC Model

The methods used for verifying the model performance (Kumar & Merwade, 2009) include percent bias/ percent error (P_{BIAS} [%]), Nash-Sutcliffe model efficiency coefficient (NSE), and coefficient of determination (R^2). Value of P_{BIAS} (Gupta *et al.*, 1999) is a measure of the average tendency of the simulated data to be larger or smaller than the measured data. The value of 0.0 is the optimal value of P_{BIAS}. Negative values represent overestimation bias, and positive values represent underestimation bias. The NSE (Nash & Sutcliffe, 1970) describes how well measured versus simulated data plot match the 1:1 line. The NSE value ranges from $-\infty$ to 1, and the optimal value is 1. We assumed a NSE value of greater than 0.5 meant model performance is satisfactory (Moriasi *et al.*, 2007). Values of $0.36 \leq NSE \leq 0.72$ and $NSE \geq 0.75$ also have been considered satisfactory and good simulated results, respectively (Van Liew *et al.*, 2003; Larose *et al.*, 2007). The R^2 value indicates the strength

of the linear relationship between the measured and simulated data. We assumed an R^2 value of greater than 0.5 indicated reasonable model performance (Moriasi *et al*., 2007).

2.4 Results and Discussion

2.4.1 Algorithm and Parameter Changes in the Model

Leaf area cover, as defined by leaf area index (LAI), is a driving variable determining amount of light intercepted and thus biomass via the RUE approach. Simulated LAI also drives potential transpiration, an important component of the total evapotranspiration of the system. Deciduous tree LAI increases both within each growing season prior to late season senescence and among years. Values for LAI also vary with planting density of trees. Within each growing season, LAI decreases late in the season with leaf senescence. Tree spacing was converted to population (Table 2.5). TreeD, CLAIYR, observed DMLA and DMLA for various spacings used in LAI simulation in the modified ALMANAC are shown in Table 2.5. For high density (population of 1111, 278 or 83 trees/100 m^2) and medium density (population of 69 or 25 trees/100 m^2) hybrid poplar trees, a shorter time (6 years) is needed to attain DMLA. For low density (population of 17 or 8 trees/100 m^2) hybrid poplar trees, a longer time (7 years or 9 years) is needed to attain DMLA.

Table 2.5 Hybrid poplar tree growth parameters for various spacing for used in LAI simulation in the modified ALMANAC

Population (trees/100 m^2)	Spacing (m×m)	DMLA (maximum LAI) in ALMANAC)	Observed DMLA	TreeD (LAI factor)	CLAIYR (year to attain maximum LAI)
1111	0.3×0.3	9.5	8.6	0.5	6
278	0.6×0.6	9.5	8.6	0.75	6
83	1.1×1.1	9.5	8.6	1.5	6
69	1.2×1.2	9.5	8.6	2.5	6
25	2×2	9.5	8.6	3	6
17	2.4×2.4	9.5	8.6	2	7
8	3.6×3.6	9.5	8.6	4.5	9

Based on TreeD and tree spacing values (Table 2.5) for high and medium density hybrid poplar trees (Figure 2.2), TreeD is linearly related to tree spacing (Equation (2.2)). Equation (2.2) was assumed suitable for short rotation *Populus* trees which can attain

DMLA in 6 years. For *Populus* trees attaining DMLA in 6 years, the higher tree spacing (smaller tree population) is associated with higher TreeD values. For *Populus* trees which attain DMLA in 7 to 9 years, the TreeD values can be found in Table 2.5.

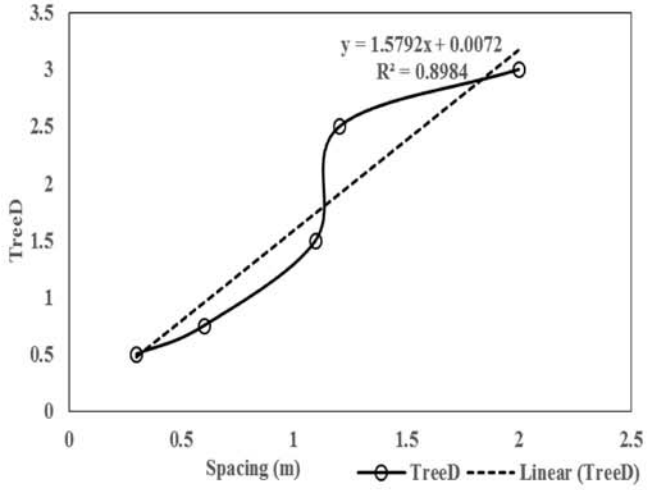

Figure 2.2 ALMANAC TreeD parameters for hybrid poplar trees with various spacings

$$y = 1.579 * x + 0.007, R^2 = 0.898 \quad (2.2)$$

Where y is TreeD parameter, x is tree planting spacing (m).

Maximum seasonal LAI values of hybrid poplar with different populations calculated by Equation (2.1) are shown in Figure 2.3. For high density hybrid poplar trees, LAI can increase significantly at the beginning (years 1 to 3) and attain maximum LAI in a shorter time (6 years). For low density hybrid poplar trees, LAI increases slowly at the beginning (years 1 to 3) and attains maximum LAI at a later time (7 or 9 years). Thus, tree spacing can affect time to canopy closure, and wide tree spacing allows longer rotations of hybrid poplar if canopy closure by harvest year is desirable. This is consistent with results of Strong and Hansen (1993)'s research.

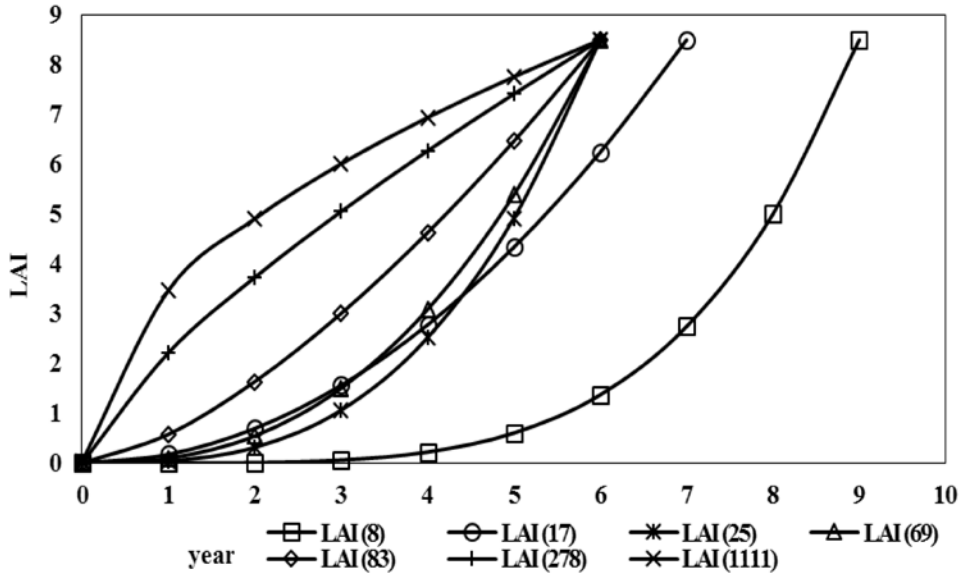

Figure 2.3 Simulated LAI curve for hybrid poplar trees with various populations (number in parentheses is population (trees/100 m^2) of hybrid poplar trees)

The algorithm used for dropping leaves was improved to more accurately simulate weight of dropping leaves.

$$y = F_{BIO\_LEAF} * x \quad (2.3)$$

y is weight of dropping leaves, x is annual accumulated tree biomass, F_{BIO_LEAF} is a user defined fraction in plant dataset.

2.4.2 Values and Ranges of Parameters Determined before Model Calibration

Two-week moving average daily temperature plots of hybrid poplar and cottonwood growth were shown in Figure 2.4. The grey bands were the period of emergence for hybrid poplar (Figure 2.4(a)) and cottonwood (Figure 2.4(b)) growth, respectively. Temperatures in the grey bands were the ranges of TG for *Populus* growth. TG was chosen as 4℃ for hybrid poplar (within the expected range 0-6 ℃ (Srinivasan R 2014, personal communication)) and 8 ℃ for cottonwood. The generic optimal temperature for warm season plants, 25 ℃, was chosen for optimal temperature (TB) of hybrid poplar and cottonwood growth in this study (Arnold *et al*., 2011).

(a) Hybrid Poplar Site in Wisconsin (b) Cottonwood Site in Mississippi

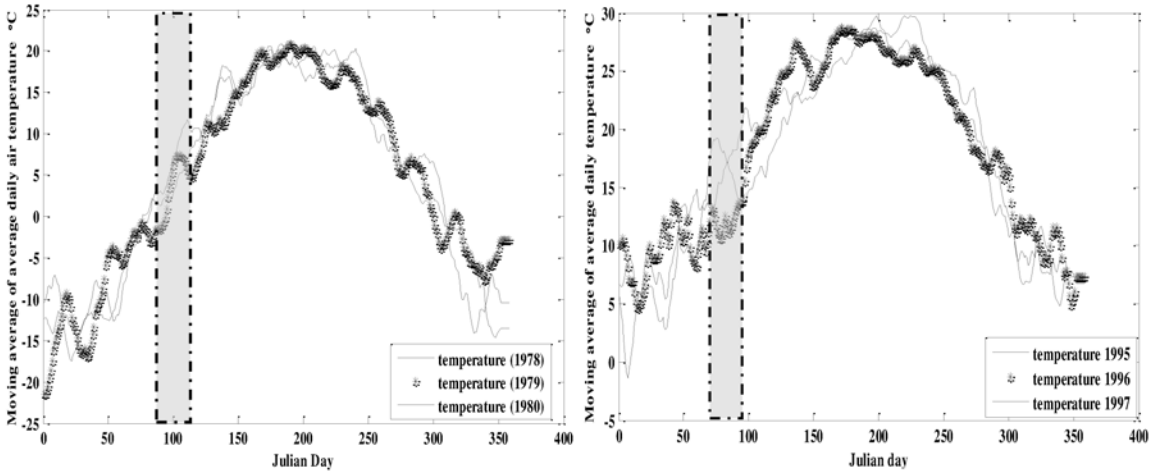

Figure 2.4 Two-week moving average daily temperatures at Harshaw Experiment Farm in Wisconsin and at Stoneville Site in Mississippi (grey bands are periods of emergence)

The PHU values were calculated during each growing season from 1974 to 1980 for hybrid poplar and from 1995 to 1997 for cottonwood (Table 2.6).The range of possible values for PHU is 1670-2150 for hybrid poplar in Wisconsin and 2421-2899 for cottonwood in Mississippi.

Table 2.6 Potential heat units for *Populus* during each growing season of different years

Plant	Year	PHU
Hybrid poplar	1974	1670
	1975	1999
	1976	2047
	1977	2149
	1978	1956
	1979	1893
	1980	1986
Cottonwood	1995	2899
	1996	2818
	1997	2421

Assumed values and ranges of RDMX, WAVP, BN_1, BN_2, BN_3, BP_1, BP_2, BP_3, HI, GSI and HMX for hybrid poplar and cottonwood growth are summarized in Table 2.7.

2.4.3 ALMANAC Model Calibration for Hybrid Poplar Growth in Wisconsin

Calibrated annual LAI values by ALMANAC were compared with published values for hybrid poplar with populations of 278 (high density) and 17 (low density) trees/100 m^2 (Figure 2.5). Calibrated annual aboveground woody biomass values were compared with published values for hybrid poplar with populations of 278, 69 (medium density) and 17 trees/100 m^2 (Figure 2.6).

Simulated annual LAI of hybrid poplar with populations of 278 and 17 trees/100 m^2 had a reasonable good match with observed values, except that the simulated LAI value at year 9 (population of 17 trees/100 m^2) was slightly higher than the observed value (Figure 2.5).

Projected annual aboveground woody biomass of hybrid poplar with populations of 278, 69 and 17 trees/100 m^2 fit the observed values reasonably well, except that simulated annual aboveground woody biomass values at years 2 and 3 (population of 278 trees/100 m^2) were higher than the observed values (Figure 2.6). Simulated annual aboveground woody biomass values at years 2, 3 and 4 (population of 17 trees/100 m^2) were higher than the observed values.

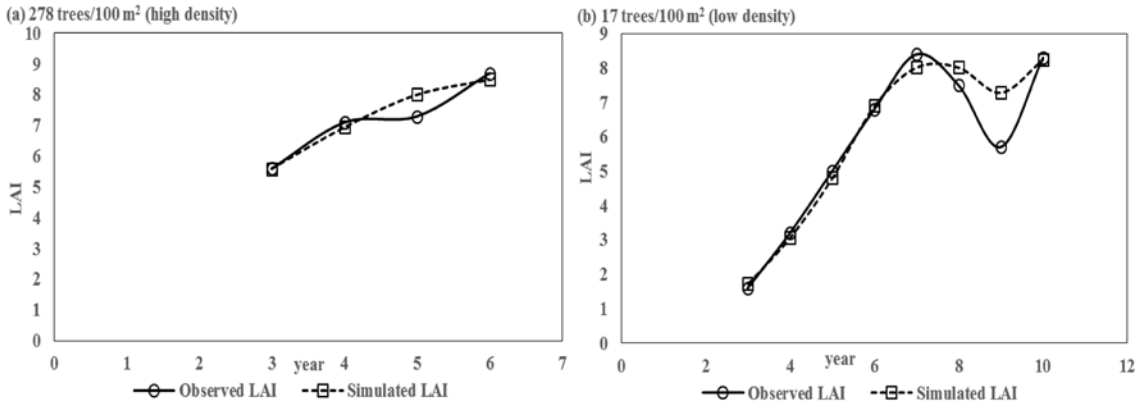

Figure 2.5 Yearly observed and calibrated ALMANAC (modified) simulated LAI during calibration of hybrid poplar with populations of 278 (a) and 17 (b) trees/100 m^2

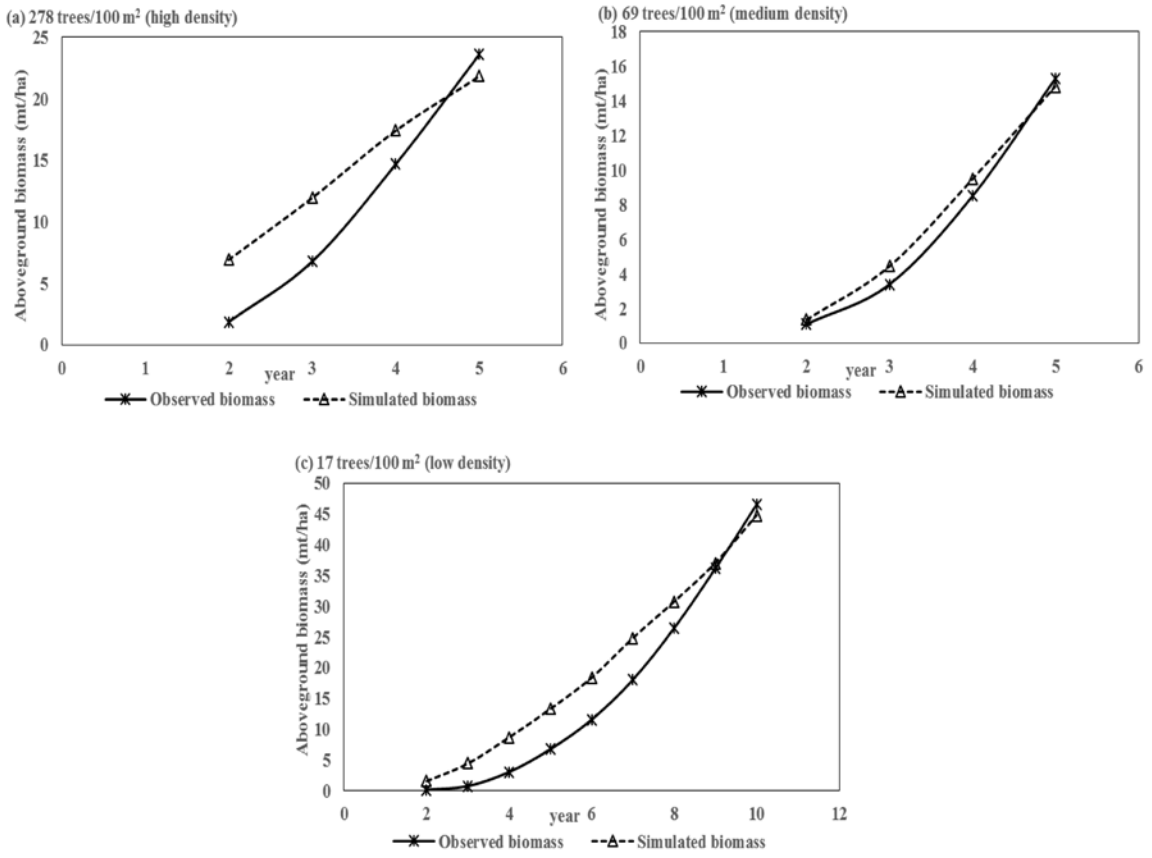

Figure 2.6 Yearly observed and calibrated ALMANAC (modified) simulated aboveground woody biomass during calibration of hybrid poplar with populations of 278 (a), 69 (b), and 17 (c) trees/100 m^2

2.4.4 Suggested Values and Potential Parameter Range for Hybrid Poplar and Cottonwood in ALMANAC Model

ALMANAC realistically simulated annual LAI and aboveground woody biomass yield of hybrid poplar with various spacings. Suggested values and potential parameter ranges for hybrid poplar and cottonwood were determined (Table 2.7). Existing values or ranges of growth parameters used in ALMANAC are globally approximated, since it is time consuming and difficult to obtain growth data in detail for each species. The existing values or ranges can be adjusted in specific regions before used for plant growth simulation.

Table 2.7 Suggested values and potential parameter ranges for hybrid poplar and cottonwood compared to current parameters for *Populus* in ALMANAC crop database

Parameter Acronym in ALMANAC	Parameter definition	Hybrid poplar 'Tristis #1' *Populus balsamifera* L. × *P.tristis* Fisch (HYPO)		Eastern cottonwood *Populus deltoides* Bartr. (HYPO)		*Populus* (POPL)
		Suggested value	Range	*Suggested value*	Range	Database value
TG[a]	Base Temperature (°C)		0-6		7-15	
[PHU][a,c]	Heat Units to Maturity	4 [1750]	[2150-1500]	8 [2818]	[2900-2200]	10 -
TB[b]	Optimal Temperature (°C)	25	25-30	25	25-30	30
WA[c,d]	Radiation Use Efficiency in ambient CO_2 (kg/ha)/(MJ/m^2)	20	20-35	41	30-58	30
EXTINC[c,d]	Light Extinction Coefficient	0.30	0.20-0.60	0.60	0.20-0.60	0.45
DMLA[c,e,f]	Maximum LAI	9.50	5.00-9.50	9.50	5.00-9.50	5.00
DLAI[c,e,f]	Point in growing season when LAI declines	0.99	0.99	0.99	0.99	0.99
TREED[c,e]	Tree leaf area decline factor	0.500-4.500	0.500-4.500	0.500-4.500	0.500-4.500	
BP_1[g,h]	Plant P fraction at emergence (whole plant)	Existing value	Existing value	Existing value	Existing value	0.0007
GSI[b]	Maximum stomatal conductance	0.0070	0.0040-0.0070	0.0070	0.0040-0.0070	0.0040
HMX[b]	Maximum canopy height	Existing value	7.00-15.00	10.00	10.00-15.00	7.50
BN_1[g,h]	Plant N fraction at emergence (whole plant)	Existing value	Existing value	Existing value	Existing value	0.0060
BN_3[g,h]	Plant N fraction at maturity (whole plant)	Existing value	Existing value	Existing value	Existing value	0.0015
BN_2[g,h]	Plant N fraction at 50% maturity (whole plant)	Existing value	Existing value	Existing value	Existing value	0.0020
RDMX[g,h]	Maximum rooting depth	Existing value	Existing value	Existing value	Existing value	3.50
CNY[c,i,j]	Plant N fraction in harvested biomass	0.0005	0.0005-0.0015	0.0005	0.0005-0.0015	0.0015
CPY[c,k]	Plant P fraction in harvested biomass	0.0002	0.0002-0.0003	0.0002	0.0002-0.0003	0.0003

Table 2.7 Continued.

BP_2[g,h]	Plant P fraction at 50% maturity (whole plant)	Existing value	Existing value	Existing value	Existing value	0.0004
BP_3[g,h]	Plant P fraction at maturity (whole plant)	Existing value	Existing value	Existing value	Existing value	0.0003
WAVP[g,h]	Rate of decline in RUE per unit increase in vapor pressure deficit	Existing value	Existing value	Existing value	Existing value	8.00
CHTYR[e,f]	Number of years required for tree species to reach full development (years)	6-9	6-9	6-9	6-9	10
HI[l,m]	Harvest index for optimal growing conditions	0.65	0.45-0.70	0.60	0.40-0.65	0.76
Optimal Leaf Development Curve Parameters						
	Fraction of growing season coinciding with 1st point	0.05	0.05-0.07	0.05	0.05-0.07	0.05
DLAP1 [c,e,f]	Fraction of DMLA corresponding to 1st point	0.05	0.05-0.30	0.05	0.05-0.30	0.05
	Fraction of growing season coinciding with 2nd point	0.40	0.40-0.45	0.40	0.40-0.45	0.40
DLAP2 [c,e,f]	Fraction of DMLA corresponding to 2nd point	0.95	0.95-0.98	0.95	0.95-0.98	0.95

[a] Maximum and minimum daily temperature from NOAA
[b] Assumed
[c] Modified parameter from hybrid poplar growth simulation
[d] Landsberg and Wright, 1989
[e] Hansen, 1983
[f] Zavitkovski, 1981
[g] Kiniry *et al.*, 1999
[h] MacDonald *et al.*, 2008
[i] Black *et al.*, 2002
[j] McLaughlin *et al.*, 1987
[k] Kiniry 2014, personal communication
[l] Michael *et al.*, 1988
[m] Arnold *et al.*, 2011

2.4.5 Modified ALMANAC Model Validation for Hybrid Poplar and Cottonwood Growth

Comparison of annual LAI values modeled by the modified ALMANAC with published values for hybrid poplar with populations of 83 (high density) and 25 (medium density) trees/100 m^2 are shown in Figure 2.7. Comparison of annual aboveground woody biomass modeled values with published values for hybrid poplar with populations of 1111 (high density), 83, 25 and 8 (low density) trees/100 m^2 are shown in Figure 2.8. Comparison of modeled annual aboveground biomass and root biomass with published values for cottonwood with a population of 23 trees/100 m^2 (medium density) are shown in Figure 2.9. The modified model was validated based on the percent bias (P_{BIAS}, %), Nash-Sutcliff (NSE), and coefficient of determination (R^2) methods. Evaluation results of modeled outputs were shown in Table 2.8. Projected MABI values by the modified ALMANAC were compared with measured yields and projected values from the original ALMANAC and FOREST and modified FOREST models for hybrid poplar growth in Rhinelander, Wisconsin (Table 2.9).

Projected annual LAI of hybrid poplar with populations of 83 and 25 trees/100 m^2 had a good match with observed values (Figure 2.7). Moreover, NSE (R^2) values for modeled LAI of hybrid poplar with populations of 83 and 25 trees/100 m^2 were 0.96 (0.76) and 0.98 (0.98), respectively (Table 2.8). Overall performance of the modeled LAI of hybrid poplar (83 and 25 trees/100 m^2) was satisfactory (since NSE $\geq$ 0.75 and $R^2 \geq$ 0.5). 0 is the optimal value of P_{BIAS}, and 4% (83 trees/100 m^2) was close to 0, which also represented accurate model simulation. However, P_{BIAS}= -11% (25 trees/100 m^2) meant that simulated annual LAI results were slightly overestimated, which also could be found from Figure 2.7 (b). Simulated annual LAI values for years 3 and 4 were higher than observed values.

Overall performance of the modeled aboveground woody biomass yields of hybrid poplar (1111, 83, 25 and 8 trees/100 m^2) was satisfactory (since NSE $\geq$ 0.75 and $R^2 \geq$ 0.5). Projected annual aboveground woody biomass of hybrid poplar with populations of 1111, 83, 25 and 8 trees/100 m^2 fit observed values well (Figure 2.8). Moreover, NSE (R^2) values

for simulated aboveground woody biomass of hybrid poplar with populations of 1111, 83, 25 and 8 trees/100 m^2 were 0.81 (0.98), 0.95 (0.79), 0.96 (0.96) and 0.99 (0.99), respectively (Table 2.8). P_{BIAS} values of aboveground woody biomass of hybrid poplar with populations of 1111 and 8 trees/100 m^2 were 2% and 1%, which also represented accurate model simulation. However, P_{BIAS} values of hybrid poplar with populations of 83 and 25 trees/100 m^2 were -9% and -22% respectively, indicating that modeled annual aboveground woody biomass results were slightly overestimated, which also could be found from Figure 2.8 (b) (83 trees/100 m^2) and Figure 2.8 (c) (25 trees/100 m^2). Modeled annual aboveground woody biomass for years 2 and 3 were higher than observed values.

Projected annual aboveground biomass and root biomass of cottonwood with a population of 23 trees/100 m^2 fit the observed values well (Figure 2.9). Moreover, NSE (R^2) values for modeled aboveground biomass and root biomass of cottonwood were 0.99 (0.99) and 0.99 (0.99), respectively (Table 2.8). Overall performance of the modeled aboveground and root biomass yields of cottonwood was satisfactory (since NSE $\geq$ 0.75 and $R^2 \geq 0.5$). P_{BIAS} values of modeled aboveground and root biomass were -0.3% and 2%, respectively, which also represented accurate model simulation.

Performance of MABI simulation by the modified ALMANAC was superior to the original ALMANAC and FOREST and the modified FOREST models. Measured MABI of the 5-year old hybrid poplar planting with a population of 69 trees/100 m^2 was 7.6 mt/ha/year (Table 2.9). The modified ALMANAC, original ALMANAC and FOREST (Ek & Dawson, 1976a, 1976b) projections were 8% (7.0 mt/ha/year) lower, 32% (10.0 mt/ha/year) higher, and 42% (10.8 mt/ha/year) higher than the measured value, respectively.

Additionally, measured MABI of the 10-year old hybrid poplar planting with a population of 17 trees/100 m^2 was 10.4 mt/ha/year (Table 2.9). The modified ALMANAC, original ALMANAC and FOREST (Ek & Dawson, 1976a, 1976b) and the modified FOREST (Meldahl, 1979) projections were 12% (9.2 mt/ha/year) lower, 82% (1.9 mt/ha/year) lower, 96% (20.4 mt/ha/year) higher, and 81% (18.8 mt/ha/year) higher than the measured value, respectively.

Measured MABI of the 9-year old hybrid poplar planting with a population of 8 trees/100 m^2 was 6.2 mt/ha/year (Table 2.9). The modified ALMANAC, original ALMANAC and FOREST (Ek & Dawson, 1976a, 1976b) projections were 18% (7.3 mt/ha/year) higher, 65% (2.2 mt/ha/year) lower, and 182% (17.5 mt/ha/year) higher than the measured value, respectively.

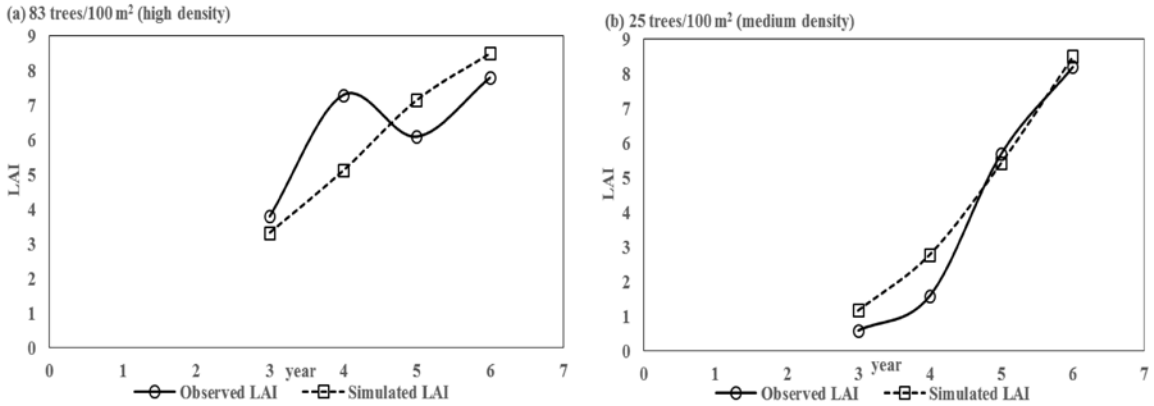

Figure 2.7 Yearly observed and calibrated ALMANAC (modified) simulated LAI during validation of hybrid poplar with populations of 83 (a) and 25 (b) trees/100 m^2

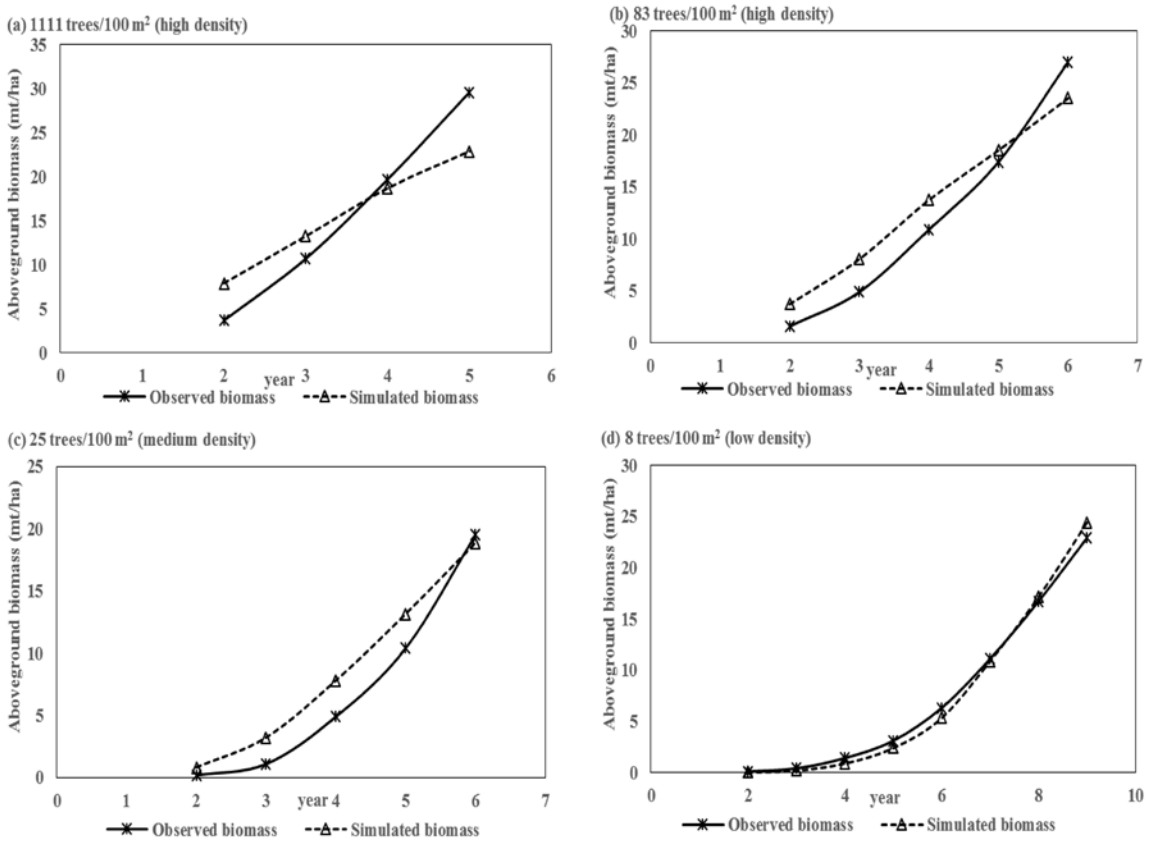

Figure 2.8 Yearly observed and calibrated ALMANAC (modified) simulated aboveground woody biomass during validation of hybrid poplar with populations of 1111 (a), 83 (b), 25 (c) and 8 (d) trees/100 m^2

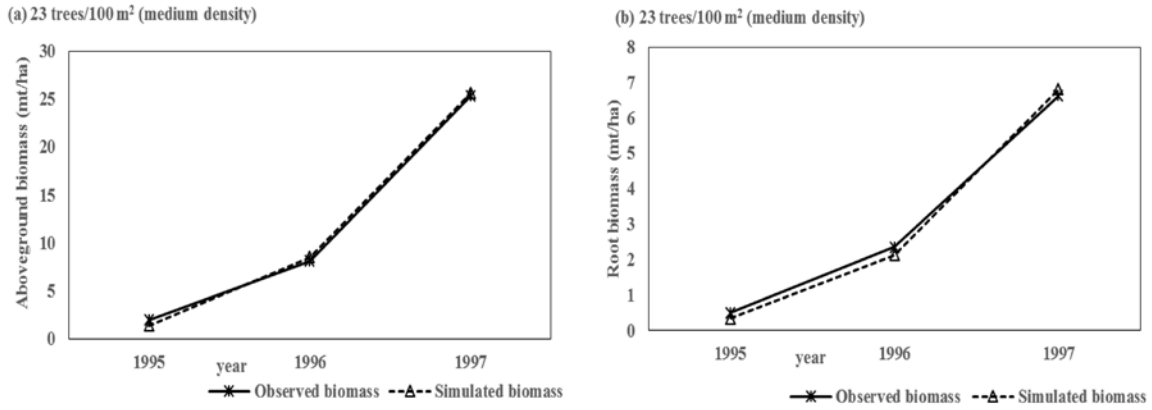

Figure 2.9 Yearly observed and calibrated ALMANAC (modified) simulated aboveground biomass (a) and root biomass (b) during validation of cottonwood with a population of 23 trees/100 m^2

Table 2.8 Evaluation of model outputs with various populations for the modified ALMANAC

Plant	Population (trees/100 $m^{2)}$	Density level	Outputs Aboveground Woody Biomass (AWB), LAI, Aboveground Biomass (AB), Root Biomass (RB)	P_{BIAS} (%)	NSE	R^2
Hybrid poplar	1111	high	AWB (mt/ha)	2	0.81	0.98
	83	high	LAI	4	0.96	0.76
			AWB (mt/ha)	-9	0.95	0.79
	25	medium	LAI	-11	0.98	0.98
			AWB (mt/ha)	-22	0.96	0.96
	8	low	AWB (mt/ha)	1	0.99	0.99
Cottonwood			AB (mt/ha)	-0.3	0.99	0.99
	23	medium	RB (mt/ha)	2	0.99	0.99

Table 2.9 Comparison of projected and measured MABI of 5-, 9- and 10-year-old short rotation intensively cultured hybrid poplar grown with various spacing in Wisconsin (number in parentheses represents rate of increase/decrease of simulated results to related measured results)

Variables	Age (year(yr))	Spacing (m×m)	Population (trees/100 m^2)	Measured harvest	Modeled yields (mt/ha/yr)			
					Modified ALMANAC	ALMANAC	FOREST	Modified FOREST
MABI mt/ha/yr	5	1.2×1.2	69	7.6[a]	7.0[b] (-8%)	10.0[b] (32%)	10.8[c,d] (42%)	-
MABI mt/ha/yr	10	2.4×2.4	17	10.4[e]	9.2[b] (-12%)	1.9[b] (-82%)	20.4[c,d] (96%)	18.8[f] (81%)
MABI mt/ha/yr	9	3.6 ×3.6	8	6.2[e]	7.3[b] (18%)	2.2[b] (-65%)	17.5[c,d] (182%)	-

[a] Isebrands *et al.*, 1979
[b] Present study
[c] Ek and Dawson, 1976a
[d] Ek and Dawson, 1976b
[e] Hansen, 1983
[f] Meldahl, 1979

2.5 Conclusions

SRWCs such as hybrid poplar and cottonwood are important biofuel feedstocks. To simulate biomass yields of hybrid poplar and cottonwood appropriately, the functional components and parameters of hybrid poplar and cottonwood were determined, and related algorithms improved in ALMANAC for leaf area, plant biomass, and biomass partitioning. The improved tree growth simulation in ALMANAC was applied to hybrid poplar plots in Wisconsin and cottonwood plots in Mississippi. The simulated LAI, total biomass, and

biomass partitioning between above-ground and roots were compared with published data to modify and evaluate the location specific ALMANAC model parameters.

Simulated aboveground woody biomass and LAI results from the modified ALMANAC for the Hybrid Poplar Site with various spacings in Wisconsin were satisfactory (P_{BIAS}: -22 ~ 4, NSE: 0.81 ~ 0.99, and R^2: 0.76 ~ 0.99). Additionally, modeled aboveground biomass and root biomass for the Cottonwood Site in Mississippi were good (P_{BIAS}: -0.3 ~ 2, NSE: 0.99 ~ 0.99, and R^2: 0.99 ~ 0.99). Generally, simulations by the modified ALMANAC model of LAI and biomass yield of *Populus* were good (P_{BIAS}: -22 ~ 4, NSE: 0.81 ~ 0.99, and R^2: 0.76 ~ 0.99), and improved relative to simulations by the original ALMANAC, FOREST, and modified FOREST models. Thus, the new algorithm for estimating LAI development for *Populus* (Equation (2.1)), the new equation for calculating falling leaves weight (Equation (2.3)), and suggested values of newly added parameter tree leaf factor (Table 2.5 and Equation (2.2)) for various populations (high, medium and low density) were reasonable. The suggested values and potential parameter range for hybrid poplar and cottonwood (Table 2.7) were reasonable, which provide guidance for simulation of poplar growth in the midwestern U.S. and cottonwood growth in the southern U.S. The modified ALMANAC model is able to simulate biofeedstock production of juvenile and mature *Populus* trees with various populations. The improved algorithms of LAI and biomass simulation for tree growth could also be used in other process based models, such as Soil and Water Assessment Tool (SWAT), Environmental Policy Integrated Climate (EPIC) and Agricultural Policy/Environmental eXtender (APEX).

The LAI and biomass yields data of *Populus* trees used in this work were from previous studies during 1970-1980 or 1995-1997. The data were limited (for some tree populations, only four years data were observed). Moreover, tree planting techniques and applied pesticide were different from those in recent hybrid poplar trials. Short rotation woody crop growth models and parameters could potentially be improved using additional *Populus* tree growth data. Moreover, suggested ranges and values for *Populus* growth parameters could be adjusted in specific regions before used for tree growth simulation.

2.6 References

Arnold, J., Kiniry, J., Srinivasan, R., Williams, J., Haney, E., & Neitsch, S. (2011). Soil and water assessment tool input/output file documentation version 2009. Texas Water Resources Institute Technical Report. (365).

Behrman, K. D., Keitt, T. H., & Kiniry, J. R. (2014). Modeling Differential Growth in Switchgrass Cultivars Across the Central and Southern Great Plains. *BioEnergy Research*. doi: 10.1007/s12155-014-9450-8

Black, B. L., Fuchigami, L. H., & Coleman, G. D. (2002). Partitioning of nitrate assimilation among leaves, stems and roots of poplar. *Tree Physiology, 22*(10), 717-724.

Boles, C. M. (2013). *SWAT model simulation of bioenergy crop impacts in a tile-drained watershed* (Mater thesis), Purdue University.

Cannell, M., Sheppard, L., & Milne, R. (1988). Light use efficiency and woody biomass production of poplar and willow. *Forestry, 61*(2), 125-136.

Cannell, M., & Smith, R. (1980). Yields of minirotation closely spaced hardwoods in temperate regions: review and appraisal. *Forest Science, 26*(3), 415-428.

Behrman, K. D., Keitt, T. H., & Kiniry, J. R. (2014). Modeling Differential Growth in Switchgrass Cultivars Across the Central and Southern Great Plains. *BioEnergy Research*. doi: 10.1007/s12155-014-9450-8

Black, B. L., Fuchigami, L. H., & Coleman, G. D. (2002). Partitioning of nitrate assimilation among leaves, stems and roots of poplar. *Tree Physiology, 22*(10), 717-724.

Cannell, M., Sheppard, L., & Milne, R. (1988). Light use efficiency and woody biomass production of poplar and willow. *Forestry, 61*(2), 125-136.

Cannell, M., & Smith, R. (1980). Yields of minirotation closely spaced hardwoods in temperate regions: review and appraisal. *Forest Science, 26*(3), 415-428.

Casler, M. D. (2010). Changes in mean and genetic variance during two cycles of within-family selection in switchgrass. *BioEnergy Research, 3*(1), 47-54.

Cibin, R., Chaubey, I., & Engel, B. (2012). Simulated watershed scale impacts of corn stover removal for biofuel on hydrology and water quality. *Hydrological Processes, 26*(11), 1629-1641.

Cortese, L. M., Honig, J., Miller, C., & Bonos, S. A. (2010). Genetic diversity of twelve switchgrass populations using molecular and morphological markers. *BioEnergy Research, 3*(3), 262-271.

Ek, A. R. (1979). Notes: A model for estimating branch weight and branch leaf weight in biomass studies. *Forest Science, 25*(2), 303-306.

Ek, A. R., & Dawson, D. H. (1976a). Actual and projected growth and yields of *Populus*' Tristis# 1'under intensive culture. *Canadian Journal of Forest Research, 6*(2), 132-144.

Ek, A. R., & Dawson, D. H. (1976b). Yields of intensively grown *Populus*: actual and projected. USDA Forest Service General Technical Report NC, 21: 5-9.

Gupta, H. V., Sorooshian, S., & Yapo, P. O. (1999). Status of automatic calibration for hydrologic models: Comparison with multilevel expert calibration. *Journal of Hydrologic Engineering, 4*(2), 135-143.

Hansen, E., & Baker, J. (1979). *Biomass and nutrient removal in short rotation intensively cultured plantations.* Paper presented at the Impact of intensive harvesting on forest nutrient cycling, State University of New York, College of Environmental Science and Forestry.

Hansen, E. A. (1983). Intensive plantation culture: 12 years research. General Technical Report, North Central Forest Experiment Station, USDA Forest Service (NC-91).

Hansen, E. A. (1991). Poplar woody biomass yields: a look to the future. *Biomass and Bioenergy, 1*(1), 1-7.

Hansen, E. A., McNeel, H., Netzer, D. A., Phipps, H. M., Roberts, P. S., Strong, T. F., Tolsted, D., & Zavitkovski, J. *Short-rotation intensive culture practices for northern Wisconsin.* Paper presented at the Proceedings, 16th Annual Meeting, North American Poplar Council, Joint Meeting of the United States and the Canadian Chapters.

Isebrands, J., Ek, A., & Meldahl, R. (1982). Comparison of growth model and harvest yields of short rotation intensively cultured *Populus*: a case study. *Canadian Journal of Forest Research, 12*(1), 58-63.

Isebrands, J., & Nelson, N. (1983). Distribution of [14C]-labeled photosynthates within intensively cultured *Populus* clones during the establishment year. *Physiologia Plantarum, 59*(1), 9-18.

Isebrands, J., Sturos, J., & Crist, J. (1979). Integrated utilization of biomass: A case study of short-rotation intensively cultured *Populus* raw material. Technical Association of the Pulp and Paper Industry (USA).

Johansson, D. J. A., & Azar, C. (2007). A scenario based analysis of land competition between food and bioenergy production in the US. *Climatic Change, 82*(3-4), 267-291. doi: 10.1007/s10584-006-9208-1

Johnson, M.-V. V., MacDonald, J. D., Kiniry, J. R., Arnold, J., & Gassman, P. (2009). ALMANAC: A potential tool for simulating agroforestry yields and improving SWAT simulations of agroforestry watersheds. *International Agricultural Engineering Journal, 18*(1-2), 51-58.

Joslin, J., & Schoenholtz, S. (1997). Measuring the environmental effects of converting cropland to short-rotation woody crops: A research approach. *Biomass and Bioenergy, 13*(4), 301-311.

Kiniry, J. (1998). Biomass accumulation and radiation use efficiency of honey mesquite and eastern red cedar. *Biomass and Bioenergy, 15*(6), 467-473.

Kiniry, J., Burson, B., Evers, G., Williams, J., Sanchez, H., Wade, C., Featherston, J., & Greenwade, J. (2007). Coastal bermudagrass, bahiagrass, and native range simulation at diverse sites in Texas. *Agronomy Journal, 99*(2), 450-461.

Kiniry, J., Jones, C., O'Toole, J., Blanchet, R., Cabelguenne, M., & Spanel, D. (1989). Radiation-use efficiency in biomass accumulation prior to grain-filling for five grain-crop species. *Field Crops Research, 20*(1), 51-64.

Kiniry, J., MacDonald, J., Kemanian, A. R., Watson, B., Putz, G., & Prepas, E. E. (2008). Plant growth simulation for landscape-scale hydrological modelling. *Hydrological Sciences Journal, 53*(5), 1030-1042.

Kiniry, J., Tischler, C., & Van Esbroeck, G. (1999). Radiation use efficiency and leaf CO_2 exchange for diverse C_4 grasses. *Biomass and Bioenergy, 17*(2), 95-112.

Kiniry, J. R., Anderson, L., Johnson, M.-V., Behrman, K., Brakie, M., Burner, D., Cordsiemon, R., Fay, P., Fritschi, F., & Houx III, J. (2013). Perennial Biomass Grasses and the Mason–Dixon Line: Comparative Productivity across Latitudes in the Southern Great Plains. *BioEnergy Research, 6*(1), 276-291.

Kiniry, J. R., Johnson, M.-V. V., Bruckerhoff, S. B., Kaiser, J. U., Cordsiemon, R., & Harmel, R. D. (2012). Clash of the titans: comparing productivity via radiation use efficiency for two grass giants of the biofuel field. *BioEnergy Research, 5*(1), 41-48.

Kiniry, J. R., Williams, J. R., Gassman, P. W., & Debaeke, P. (1992). A general, process-oriented model for two competing plant species. *Trans. ASAE*, *35*(3), 801-810.

Kumar, S., & Merwade, V. (2009). Impact of watershed subdivision and soil data resolution on SWAT model calibration and parameter uncertainty1. *Journal of the American Water Resources Association, 45*(5), 1179-1196.

Landsberg, J., & Wright, L. (1989). Comparisons among *Populus* clones and intensive culture conditions, using an energy-conservation model. *Forest Ecology and Management, 27*(2), 129-147.

Larose, M., Heathman, G., Norton, L., & Engel, B. (2007). Hydrologic and atrazine simulation of the Cedar Creek watershed using the SWAT model. *Journal of Environmental Quality, 36*(2), 521-531.

MacDonald, J. D., Kiniry, J., Putz, G., & Prepas, E. (2008). A multi-species, process based vegetation simulation module to simulate successional forest regrowth after forest disturbance in daily time step hydrological transport models *Journal of Environmental Engineering and Science, 7*(S1), 127-143.

McLaughlin, R. A., Hansen, E. A., & Pope, P. E. (1987). Biomass and nitrogen dynamics in an irrigated hybrid poplar plantation. *Forest Ecology and Management, 18*(3), 169-188.

Meldahl, R. S. (1979). *Yield projection methodology and analysis of hybrid poplars based on multispacial plots.* (PhD Thesis), University of Wisconsin, Madison. ((University Microfilm No 80-0506))

Michael, D., Dickmann, D., Isebrands, J., & Nelson, N. (1990). Photosynthesis patterns during the establishment year within two *Populus* clones with contrasting morphology and phenology. *Tree Physiology, 6*(1), 11-27.

Michael, D., Isebrands, J., Dickmann, D., & Nelson, N. (1988). Growth and development during the establishment year of two *Populus* clones with contrasting morphology and phenology. *Tree Physiology, 4*(2), 139-152.

Moriasi, D. N., Arnold, J. G., Van Liew, M. W., Bingner, R. L., Harmel, R. D., & Veith, T. L. (2007). Model evaluation guidelines for systematic quantification of accuracy in watershed simulations. *Trans. ASABE*, *50*(3), 885-900.

Nash, J., & Sutcliffe, J. (1970). River flow forecasting through conceptual models part I—A discussion of principles. *Journal of hydrology, 10*(3), 282-290.

Neitsch, S., Arnold, J., Kiniry, J., & Williams, J. (2011). Soil and water assessment tool theoretical documentation version 2009. Texas Water Resources Institute Technical Report.

Nelson, N. D., & Michael, D. (1982). Photosynthesis, leaf conductance, and specific leaf weight in long and short shoots of *Populus* 'Tristis# 1' grown under intensive culture. *Forest Science, 28*(4), 737-744.

Raj, C. (2013). *Optimal land use planning on selection and placement of energy crops for sustainable biofuel production.* (Doctoral dissertation), Purdue University.

Schmer, M. R., Mitchell, R., Vogel, K., Schacht, W., & Marx, D. B. (2010). Spatial and temporal effects on switchgrass stands and yield in the Great Plains. *BioEnergy Research, 3*(2), 159-171.

Strong, T., & Hansen, E. (1993). Hybrid poplar spacing/productivity relations in short rotation intensive culture plantations. *Biomass and Bioenergy, 4*(4), 255-261.

Thomas, M., Engel, B., & Chaubey, I. (2009). Water quality impacts of corn production to meet biofuel demands. *Journal of Environmental Engineering, 135*(11), 1123-1135.

Thomas, M., Engel, B., & Chaubey, I. (2011). Multiple corn stover removal rates for cellulosic biofuels and long-term water quality impacts. *Journal of Soil and Water Conservation, 66*(6), 431-444.

Thomas, M. A. (2011). *Environmental implications of feedstock production practices for bioenergy.* (Doctoral dissertation), Purdue University.

Thomas, M. A., Ahiablame, L. M., Engel, B. A., & Chaubey, I. (2014a). Modeling Water Quality Impacts of Growing Corn, Switchgrass, and *Miscanthus* on Marginal Soils. *Journal of Water Resource and Protection, 06*(14), 1352-1368. doi: 10.4236/jwarp.2014.614125

Thomas, M. A., Ahiablame, L. M., Engel, B. A., Chaubey, I., & Mosier, N. (2014b). Modeling Water Quality Impacts of Cellulosic Biofuel Production from Corn Silage. *BioEnergy Research, 7*(2), 636-653.

Thornton, F. C., Dev Joslin, J., Bock, B. R., Houston, A., Green, T., Schoenholtz, S., Pettry, D., & Tyler, D. D. (1998). Environmental effects of growing woody crops on agricultural land: first year effects on erosion, and water quality. *Biomass and Bioenergy, 15*(1), 57-69.

Tilman, D., Socolow, R., Foley, J. A., Hill, J., Larson, E., Lynd, L., Pacala, S., Reilly, J., Searchinger, T., & Somerville, C. (2009). Beneficial biofuels—the food, energy, and environment trilemma. *Science, 325*(5938), 270.

Tolbert, V. R., Thornton, F. C., Joslin, J. D., Bock, B. R., Bandaranayake, W. E., Tyler, D. D., Pettry, D., Green, T. H., Makik, R., & Houston, A. E. (1996). *Soil and water quality aspects of herbaceous and woody energy crop production: lessons from research-scale comparisons with agricultural crops*. BioEnergy, OCT 9.

Trybula, E. M., Cibin, R., Burks, J. L., Chaubey, I., Brouder, S. M., & Volenec, J. J. (2014). Perennial rhizomatous grasses as bioenergy feedstock in SWAT: parameter development and model improvement. *Global Change Biology Bioenergy*. doi: 10.1111/gcbb.12210

U. S. Department of Agriculture, F. S. (1980). Energy & wood from intensively cultured plantations: research and development program. Gen. Tech. Rep. St. Paul, MN. North Central Forest Experiment Station, (NC-58), 28. http://www.nrs.fs.fed.us/pubs/gtr/gtr_nc058.pdf. Accessed 1 July 2014.

Van Liew, M., Arnold, J., & Garbrecht, J. (2003). Hydrologic simulation on agricultural watersheds: Choosing between two models. *Trans. ASAE, 46*(6), 1539-1551.

Wolf, J., Bindraban, P., Luijten, J., & Vleeshouwers, L. (2003). Exploratory study on the land area required for global food supply and the potential global production of bioenergy. *Agricultural Systems, 76*(3), 841-861.

Zavitkovski, J. (1981). Characterization of light climate under canopies of intensively-cultured hybrid poplar plantations. *Agricultural Meteorology, 25*, 245-255.

CHAPTER 3. IMPROVEMENT OF THE SIMULATION OF WOODY BIOENERGY CROPS (*POPULUS* 'TRISTIS #1' (*POPULUS BALSAMIFERA* L. × *P.TRISTIS* FISCH) AND EASTERN COTTONWOOD (*POPULUS DELTOIDES* BARTR.)) IN THE SOIL AND WATER ASSESSMENT TOOL (SWAT)

3.1 Abstract

Energy security and sustainability require a suite of biomass crops, including woody species. *Populus* has the potential to produce significant quantities of biofuel. Quantifying hydrologic and water quality responses to *Populus* growth is important should it be widely planted. *Populus* growth and its impacts on runoff, sediment and nitrate-N losses were simulated by the Soil and Water Assessment Tool (SWAT). SWAT tree growth algorithms and parameters for hybrid poplar (*Populus balsamifera* L. × *P.tristis* Fisch) in Midwestern US and cottonwood (*Populus deltoides* Bartr.) in Southern US were improved based on hybrid poplar and cottonwood site data. Tree growth representation led to SWAT2012 code changes including a new leaf area parameter (TREED), new leaf area index algorithm, and leaf biomass algorithm, while fraction of tree biomass accumulated each year converted to residue during dormancy (BIO_LEAF) was removed. The modified SWAT simulated LAI, biomass yield, runoff, sediment and nitrate-N losses of *Populus* growth were compared with observed values. Performance of the modified SWAT simulated hybrid poplar LAI and aboveground woody biomass (P_{BIAS}: -57 ~ 7%, NSE: 0.94 ~ 0.99, and R^2: 0.74 ~ 0.99), and cottonwood aboveground biomass, seasonal mean runoff, mean sediment, mean nitrate-N and total nitrate-N were satisfactory (P_{BIAS}: -39 ~ 11%, NSE: 0.86 ~ 0.99, and R^2: 0.93 ~ 0.99). Improved algorithms and associate parameters, and values and potential parameter ranges for *Populus* were reasonable. Thus, the modified SWAT model can be used for *Populus* biofeedstock production modeling and hydrologic and water quality response to its growth.

3.2 Introduction

Sustainability, energy independence and security, and other social and environmental concerns have prompted an increasing interest in bioenergy as renewable energy sources. In particular, cellulosic perennial crops and short rotation woody crops are potential sources of biofeedstock for bioenergy production. Short-rotation intensive culture (SRIC) of trees is considered a promising way to increase wood biomass productivity (U. S. Department of Agriculture, 1980; Guo *et al*., 2015). The purpose of tree SRIC system establishment is to maximize biomass yield of trees per unit area, to meet high economical wood fiber demand and create revenue on marginal sites (Zavitkovski, 1978; Fege *et al*., 1979; Hansen & Baker, 1979; Anderson *et al*., 1983). Dry woody biomass production in hardwood plantations under SRIC is up to 20,000 kg ha^{-1} yr^{-1}, three to five times more than that of some natural stands (Hansen & Baker, 1979). Since global increasing demand for food and renewable energy will face challenges, such as higher food prices (Johansson & Azar, 2007; Manning *et al*., 2014), lower food production (Wolf *et al*., 2003) and land competition between fuel and food, biofuels should require biofeedstocks that neither compete with food crops nor cause natural forest decline (Guest *et al*., 2013; Guo *et al*., 2015). As a potential non-food bioenergy crop, *Populus* is highly productive under SRIC, because of its rapid growth, genetic diversity, and coppice regeneration (Hansen, 1983). *Populus* could serve as a predominant temperate zone crop with the worldwide improvement of woody biomass/fuel crop species (Haissig *et al*., 1987).

Biomass production often increases with decrease of tree spacing in SRIC plantations. Hansen and Baker (1979) found that tree spacing could influence the time needed to reach the maximum mean annual biomass increase, and forest management practices were more flexible in wide tree spacing in scheduling thinning and harvesting with fewer operational damages (Cannell & Smith, 1980; Strong & Hansen, 1993). However, Strong and Hansen (1993) demonstrated that the relationship between biomass productivity and spacing was minor when they studied the relationship between tree spacing and biomass yields for hybrid poplar plantations with 18 clone/spacing combinations for 16 years duration in

northern Wisconsin. In that study, productivity of hybrid poplar was mainly influenced by clone, irrigation and disease.

Short rotation woody crops have environmental impacts (Sixto *et al*., 2014), including changes in nutrient cycle, site quality, and water movement. Poplars can uptake and degrade the chlorinated solvent Trichloroethylene in aquifers to aerobic degradation products (Strand *et al*., 1995). Additionally, sediment loss from a cottonwood site (2.3 Mg ha^{-1}) was lower than that from a conventional tilled cotton site (16.2 Mg ha^{-1}) over 14 months in Mississippi (Thornton *et al*., 1998). Nutrient movement from woody crops was less than agricultural crops in the years after the establishment year (Tolbert *et al*., 1997; Thornton *et al*., 1998). Aditya and William (2010) demonstrated that planting fast growing poplar trees could decrease total nitrogen (N) and phosphorus (P) loading in Millsboro Pond Watershed.

Populus growth prediction is essential for managers and policy makers to establish and manage *Populus* under SRIC plantations (Guo *et al*., 2015). Numerous tree growth models have been used for *Populus* growth simulation to assist with establishment and management of *Populus* under SRIC systems. For example, a regression model was used for estimation of branch weights of *Populus*, which was more accurate than models based on branch diameter (Ek, 1979). Isebrands *et al*. (1982) used FOREST, an individual-tree-based stand simulation model, to simulate hybrid poplar growth. The FOREST model was modified to simulate hybrid poplar biomass yields and the differences between measured and simulated values were reduced (Meldahl, 1979). There is a long history of bottom-up modeling for poplar (*Populus*) based on tree inventory and field data (Hansen, 1983; Ceulemans, 1990; Stettler & Bradshaw, 1994; Liski *et al*., 2014). Host *et al*. (1990) linked an ecophysiologic growth process model (ECOPHYS) (Rauscher *et al*., 1990) with the Environmental Policy Integrated Model (EPIC) (Williams *et al*., 1989) to estimate poplar growth and management impacts on site productivity and erosion. A harmonized equation was used for predicting hybrid poplar woody biomass in the Pacific Northwest (Clendenen, 1996). Stand to EcosystemCaRbon and EvapoTranspiration Simulator (SECRETS) (Deckmyn *et al*., 2004) and Physiological Principles to Predict Growth (3PG) (Amichev *et*

al., 2010; Amichev *et al*., 2011) were used for simulating field-scale effects of soil, irrigation, N fertilization and rotation cycle on biomass yields for poplar and aspen (Nair *et al*., 2011). Wang *et al*. (2013) predicted yield potential of poplar plantations using the Ecosystem Demography 2 (ED2) model and demonstrated that simulated poplar yield matched observed data well.

Biomass is assumed proportional to the radiant energy absorbed by the plant canopy in an energy conversion model, which has been used for simulation of biomass yields of *Populus* (Landsberg & Wright, 1989). The energy conversion equation (Landsberg & Wright, 1989) was also used in Soil and Water Assessment Tool (SWAT), Agricultural Land Management Alternative with Numerical Assessment Criteria (ALMANAC), EPIC and Agricultural Policy/Environmental eXtender (APEX) models (Guo *et al*., 2015).

Simulation models have been enhanced and updated in various ways in recent years. For example, the EPIC (Williams *et al*., 1984; Williams *et al*., 1989) crop growth model was added in SWAT to account for growth annual variation, auto-fertilization and auto-irrigation as management options (Neitsch *et al*., 2011). SWAT has been used for simulating impacts of bioenergy crops on hydrology and water quality at a wide range of scales around the world (Love & Nejadhashemi, 2011; Nair *et al*., 2011; Powers *et al*., 2011; Boles, 2013; Parajuli & Duffy, 2013; Raj, 2013).

The fundamental concepts of plant algorithms used in SWAT (Arnold *et al*., 2012) are identical to those used in the ALMANAC model (Kiniry *et al*., 1992). Plant growth simulation processes of both ALMANAC and SWAT include light interception, leaf area development and conversion of intercepted light into biomass (Kiniry *et al*., 2008; Neitsch *et al*., 2011; Kiniry *et al*., 2012). Biomass is calculated based on light interception using Beer's law (Monsi & Saeki, 1953) with species-specific radiant use efficiency (BIO_E, amount of dry biomass produced per unit of intercepted light) values (Kiniry *et al*., 1999; Kiniry *et al*., 2007; Guo *et al*., 2015). A summary of plant growth algorithms and parameters in SWAT is included in Data A.1.

SWAT has been used to assess the influence of land use management and requires various input parameters for plants (Arnold *et al*., 2012). Some researchers have investigated parameterization and improvement of the plant dataset in the SWAT model. For example, Raj (2013) developed and improved the parameters of switchgrass (*Panicum virgatum* L.) and giant miscanthus (*Miscanthus* × *giganteus*) in the SWAT plant dataset, and validated and analyzed the range of parameters for these two grasses. The parameters representing perennial rhizomatous grasses, switchgrass and miscanthus, were used for simulating bioenergy crop growth and hydrologic impact in SWAT (Boles, 2013; Raj, 2013). The parameters in the SWAT plant dataset representing tree growth were developed based on personal communication and need improvement based on data from the scientific literature (Arnold *et al*., 2012). Forest management was incorporated and modified in SWAT to better model water quantity and quality in watersheds in forested ecosystems (Li *et al*., 2008). However, the modification of forest management in the model is for mixed forest systems rather than a specific species (Li *et al*., 2008). Leaf area development in the model is a function of the growing season for mature plants, which can attain the stand maximum leaf area index (LAI) during the growing season (Arnold *et al*., 2011). The leaf area algorithm in the model was not applicable for tree growth before maturity, since LAI of young regenerations cannot reach stand maximum LAI before canopy closure (Guo *et al*., 2015). Thus, SWAT2012 (Revision 635) and prior versions can only be used for growth simulation for mature plants, and the ability to simulate tree biomass yields before maturity is limited (Arnold *et al*., 2011). Woody crops under SRIC systems are generally harvested before maturity or once they reach maturity (Hansen, 1983). Therefore, it is necessary to improve simulation of tree growth in SWAT.

Since sustainable, secure and environmentally friendly renewable energy sources are desired (Love & Nejadhashemi, 2011; Sarkar *et al*., 2011; Wu *et al*., 2012; Wu & Liu, 2012; Liu *et al*., 2014; Sarkar & Miller, 2014), it is necessary to study biofeedstock production, and hydrologic and water quality impacts modeling of *Populus*. This study focused on the improvement of the SWAT model to better model *Populus* biomass yields and effects on water quantity and quality. This study is the first to improve *Populus* growth algorithms and parameters in SWAT with published *Populus* growth and water quantity

and quality data. The objectives of this study were to: (1) improve the plant growth subroutine of SWAT based on new algorithms and growth parameters of hybrid poplar 'Tristis #1' (*Populus balsamifera* L. × P.*tristis* Fisch) and eastern cottonwood (*Populus deltoides* Bartr.) that were created in a prior study with ALMANAC; (2) perform sensitivity analysis and calculate relative sensitivity coefficients of plant growth parameters to model outputs to quantify the effect of *Populus* growth parameters on biomass yield, water yield, and plant uptake of N and P; (3) calibrate the model to match LAI and woody biomass of hybrid poplar in Wisconsin and aboveground biomass of cottonwood in Mississippi; and (4) test the modified model based on comparison of simulated LAI, biomass, runoff, sediment and nitrate-N results of *Populus* with published values.

3.3 Materials and Methods

3.3.1 Study Sites

This study was conducted in two study sites: a hybrid poplar site in Wisconsin and cottonwood site in Mississippi (Figure 3.1). The selected hybrid poplar study site was a SRIC system at the USDA Forest Service Harshaw Experimental Farm near Rhinelander, Wisconsin, USA (45.6° N, 89.5° W) (Hansen & Baker, 1979), on a loam soil of the Padus series with slope reaching at most 1% to provide a venue for experiments with planted *Populus* plantation (Nelson & Michael, 1982). Eight-inch hybrid poplar cuttings were planted in early June 1970, on a site in the Hugo Sauer Nursery near Rhinelander, Wisconsin (Ek & Dawson, 1976a). The site was sowed to rye, plowed and rototilled before planting. The nutrients in the stand were maintained as: pH 6.7-7.0; and P 213-224 kg ha^{-1}; N was maintained as 3.2% levels in new leaf tissue; soil moisture at 16-30% levels by irrigation; weeds were controlled using Linuron (Ek & Dawson, 1976a; Michael *et al.*, 1988).

The Tennessee Valley Authority (TVA) region, a 276 county area including all of Tennessee and portions of 10 contiguous states in the southeastern US, was shown to be viable for cost effective production of short-rotation woody crops based on economic analyses (Downing & Graham, 1993). The Delta Research and Extension Center at

Stoneville, Mississippi (33.34° N, 90.85°W) in the Tennessee Valley region was selected for cottonwood planting (Joslin & Schoenholtz, 1997). The cottonwood site was on agricultural land dominated by a Bostket silt loam soil. The site has a slope of 0.2-0.3%, and parent material of Riverine sediments. Soil physical property changes were determined at the site in 1995 prior to tree establishment and again in 1997 (the end of growing season) (Tolbert *et al.*, 1998). The site included six small 0.25-2 ha (0.0025-0.02 km^2) replicated watersheds with the same soil type, slope and land use (Joslin & Schoenholtz, 1997). The establishment of replicated watersheds was essential for the quantity, quality and timing of surface runoff comparison.

Eastern cottonwood (3-year rotation) is a frequently recommended woody species for SRIC systems in the southeastern U.S. (Downing & Graham, 1993). Cottonwood cuttings 20-30 cm long were planted with spacing of 1.2 × 3.6 m (population: 23 trees 100 m^{-2}) on February 3, 1995 (Thornton *et al.*, 1998). The artificial watersheds were formed using 0.5 m high berms to surround land areas (Joslin & Schoenholtz, 1997). Each point has a 0.5 meter H-shaped flume with a flow meter and an automated flow-proportional sampler, and a 2 meter flume section (Joslin & Schoenholtz, 1997). Four 91 cm length × 61 cm width × 8 cm depth pan lysimeters were installed in each plot at 80 cm depth to measure water flux and nutrients. Water samples were collected by the flow proportional sampler for sediment and nutrient concentration in runoff from May 1995 to June 1997 (Joslin & Schoenholtz, 1997).

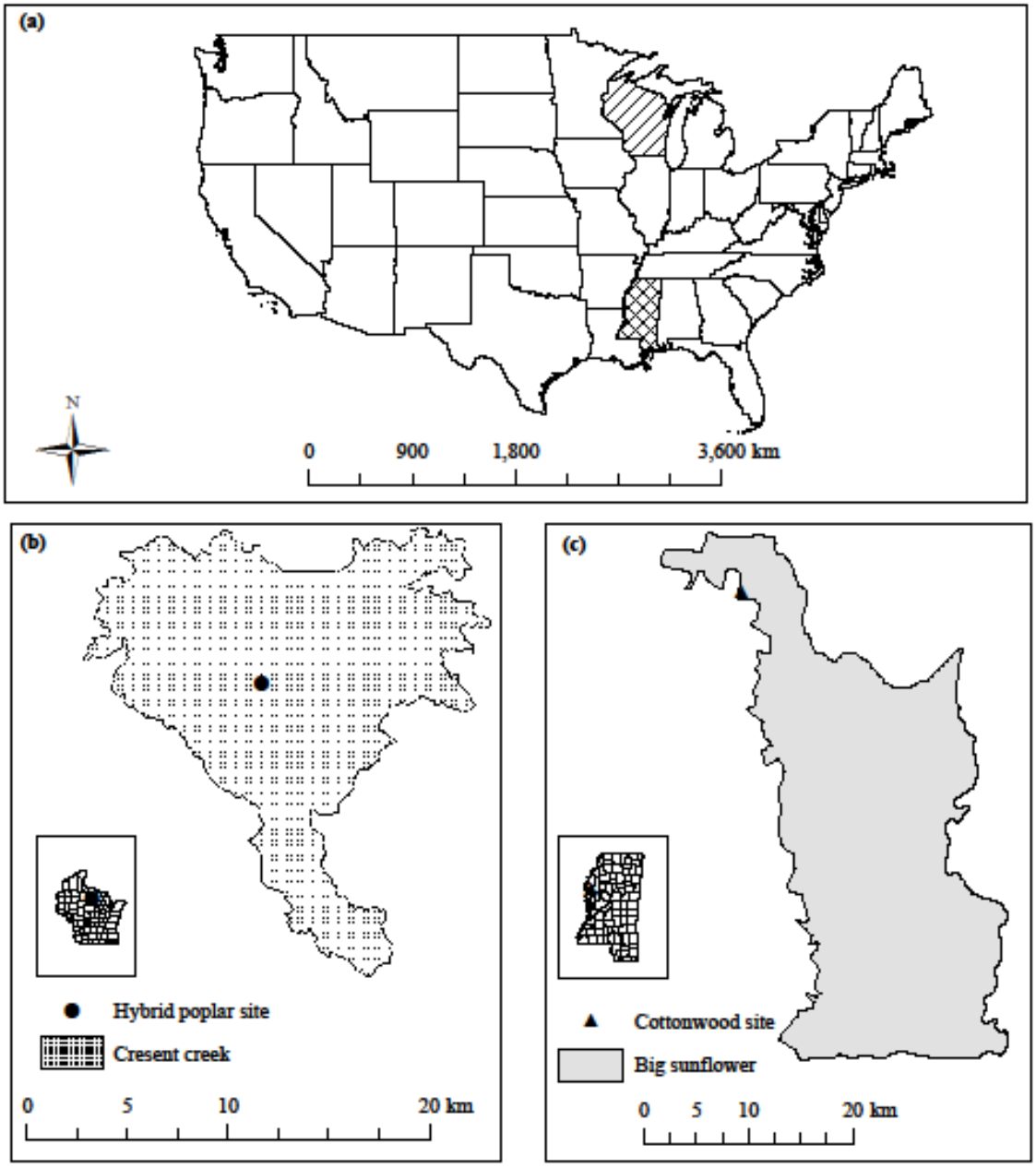

Figure 3.1 The hybrid poplar site in Crescent Creek-Wisconsin River Watershed in Wisconsin (b) and the cottonwood site in Big Sunflower River Watershed in Mississippi (c) in the continental U.S. (a)

3.3.2 Tree Growth Modification and Related Code changes in SWAT

The ALMANAC model was previously modified to simulate LAI and biomass yield of hybrid poplar in Wisconsin and cottonwood in Mississippi (Guo *et al.*, 2015). The functional components and parameters of hybrid poplar were determined, and related algorithms were changed in the model. Since SWAT and ALMANAC use similar plant algorithms (Kiniry *et al.*, 1992; Arnold *et al.*, 2012), tree growth modification in ALMANAC can also be used in SWAT. Thus, related source code on LAI and weight of dropping leaves algorithms (Guo *et al.*, 2015) were changed in SWAT2012 (revision 628). The SWAT2012 model with tree growth modification was called "modified SWAT" in this study.

3.3.3 The Modified SWAT Model Setup and Management Practices

The modified SWAT model was applied using data for Crescent Creek-Wisconsin River watershed in Wisconsin and Big Sunflower River watershed in Mississippi using ArcSWAT (Version 2012.10_1.13 released 1/7/14) in ArcGIS 10.1. Hydrologic Response Units (HRUs) were used to represent the hybrid poplar and cottonwood sites.

Daily precipitation and temperature data from 01/01/1965 to 12/31/1995 at Rhinelander WI US weather station (GHCND: USC00477113, Latitude: 45.63, Longitude: -89.42, Elevation: 476m) close to the hybrid poplar site were downloaded from National Climatic Data Center (NCDC). Daily precipitation and temperature data from 01/01/1995 to 12/31/1997 at Stoneville experimental station MS US (GHCND: USC00228445, Latitude: 33.4, Longitude: -90.92, Elevation: 39 m) close to the cottonwood site were also obtained from NCDC. These data were added into ArcSWAT for model setup. Other climate data, including solar radiation, relative humidity and wind speed were generated by the weather geodatabase (WGEN_US_COOP_1980_2010) within SWAT. The primary data required for SWAT model setup and simulation for these two sites came from a variety of sources (Tables 3.1 and 3.2).

Table 3.1 Data for hybrid poplar growth simulation in Wisconsin by SWAT

Data type	Source	Format	Date
Elevation	USGS National Map Viewer	30m Raster	
SSURGO	USDA Web Soil Survey	Polygon	
LULC	USGS The National Map Viewer	Raster	2006
Daily Precipitation	NCDC	Tabular data	1965 - 1995
Daily Temperature	NCDC	Tabular data	1965 - 1995
Aboveground Woody Biomass yields of hybrid poplar (mt ha^{-1})	Scientific literature*		1970 - 1980
Annual LAI of hybrid poplar	Scientific literature*		1970 - 1980

USGS U.S. Geological Survey, USDA U.S. Department of Agriculture, NCDC National Climate Data Center, SSURGO Soil Survey Geographic Database
* Hansen, 1983

Table 3.2 Data for simulation of water quantity and quality impacts of cottonwood growth in Mississippi by SWAT

Data type	Source	Format	Date
Elevation	USGS The National Map Viewer	30m Raster	
[4]SSURGO	USDA Web Soil Survey	Polygon Shapefile	
LULC	USGS The National Map Viewer	Raster	2006
Daily Precipitation	NCDC		1995 - 1997
Daily Temperature	NCDC		1995 - 1997
Aboveground Biomass yields of cottonwood (mt ha^{-1})	Unpublished report*		1995 - 1997
Mean runoff per event (m^3 ha^{-1}) for each season	Scientific literature†		1995- 1996
Mean sediment loss per event (kg ha^{-1}) for each season	Scientific literature†		1995- 1996
Seasonal total sediment loss (kg ha^{-1})	Scientific literature†		1995- 1996
Seasonal means of nutrient losses (nitrate-N) (kg ha^{-1})) per runoff event	Scientific literature†		1995- 1996
Seasonal total nutrient losses (nitrate-N) (kg ha^{-1})) in runoff	Scientific literature†		1995- 1996

* Pettry *et al*., 1997
† Thornton *et al*., 1998

The management operation schedules in SWAT include planting and end of schedule dates, tillage, nutrient and pesticide application rate and auto-irrigation. Management practices during the establishment year for each site included tillage and nutrient application data (Tables B.1 and B.2). Hybrid poplar growth from 1971 to 1980 also included the same N and P application as that in 1970 (Table B.1). Planting of hybrid poplar was on 22 May, 1970, and harvest and kill were on 1 May, 1980 (Ek, 1979; Hansen, 1983). Cottonwood

growth from 1996 to 1997 included the same N and P application as that in the establishment year (Table B.2). Planting of cottonwood was on 3 Feb, 1995, and harvest and kill were on 30 Nov, 1997 (Joslin & Schoenholtz, 1997). The management data from the field site did not include exact values for all the input data in SWAT. Thus, N, P, and auto-irrigation application included in model management practices were used to simulate an idealized condition under which *Populus* growth has little water or nutrient stress (Ek, 1979; Hansen, 1983; Guo *et al*., 2015).

3.3.4 Sensitivity Analysis for the Modified SWAT Model

Sensitivity analysis for tree growth parameters was performed based the one-at-a-time (OAT) (and global) approach (James & Burges, 1982) to identify the effect of hybrid poplar growth parameters on biomass yield, water yield, and plant uptake of N and P. Latin hypercube sampling (LHS) method was used to generate a sample of plausible collections (11 equally distributed samples) of parameter values (Helton & Davis, 2003). Relative sensitivity coefficient (James & Burges, 1982) of output values corresponding to ±10% of initial values of each tree growth parameter were also calculated, to mathematically compare each parameter influence on a predicted output and obtain the rank of sensitivity to different model outputs. The results of sensitivity analysis can provide guidance for determination of realistic values or potential ranges for parameters and model calibration.

3.3.5 Ranges and Values of Parameters Determined before Calibration of the Modified SWAT

Before calibrating the modified SWAT, values and ranges of some tree growth parameters were obtained from a previous study on *Populus* growth simulation by ALMANAC (Guo *et al*., 2015). Base temperature (T_BASE) and potential heat units (PHUs) were confirmed for hybrid poplar in Wisconsin and cottonwood in Mississippi (Guo *et al*., 2015) using daily temperature data downloaded from NCDC weather stations and the equation for PHU calculation included in the SWAT Theoretical Documentation Version 2009 (Neitsch *et al*., 2011). Optimal temperature (T_OPT) value was assumed based on default value of T_OPT in the SWAT Input/Output Documentation Version 2012 (Arnold *et al*.,

2012).Values of radiation use efficiency are between 1.3 and 1.9 g MJ^{-1} intercepted photosynthetically active radiation for woody species generally (Kiniry *et al*., 1989), and between 2.4 and 3.4 for intensively cultured poplar in Scotland (Cannell *et al*., 1988). BIO_E (kg ha^{-1})/(MJ m^{-2}) in SWAT is radiant use efficiency value (g MJ^{-1}) multiplied by 10 (Arnold *et al*., 2011). Ranges of BIO_E, EXT_COEF, BLAI, ALAI_MIN, FRGRW1, FRGRW2, CNYLD and CPYLD for model calibration were derived from previous hybrid poplar site studies in Wisconsin (Zavitkovski, 1981; Hansen, 1983; McLaughlin *et al*., 1987; Landsberg & Wright, 1989; Black *et al*., 2002).

Default values were used for the following *Populus* growth parameters: plant N fraction at emergence (PLTNFR1), 50% maturity (PLTNFR2), and maturity (PLTNFR3); P fraction at emergence (PLTPFR1), 50% maturity (PLTPFR2) and maturity (PLTPFR3); rate of decline in RUE per unit increase in vapor pressure deficit (WAVP) and maximum rooting depth (RDMX), have been used for boreal forest (MacDonald *et al*., 2008), eastern red cedar (Juniperus virginiana) and honey mesquite (Prosopis glandulosa) growth simulation (Kiniry, 1998) by ALMANAC and resulted in reasonable modeled biomass values. Thus, default values of PLTNFR1, PLTNFR2, PLTNFR3, PLTPFR1, PLTPFR2, PLTPFR3, WAVP and RDMX in the SWAT plant database (0.0060, 0.0020, 0.0015, 0.0007, 0.0004, 0.0003, 8.00 and 3.5) were used for hybrid poplar and cottonwood growth simulation (Guo *et al*., 2015).

Ranges of harvest index in optimal growing conditions (HVSTI) for hybrid poplar and cottonwood were derived as 0.45-0.70 and 0.40-0.65, respectively. Values of HVSTI for hybrid poplar and cottonwood for this study were derived as 0.65 and 0.60, respectively (Michael *et al*., 1990; Arnold *et al*., 2011). Ranges of maximum canopy height (CHTMX) for hybrid poplar and cottonwood were assumed as 7-15 and 10-15, respectively. Values of CHTMX for hybrid poplar and cottonwood were assumed to be 7.5 and 10, respectively (J. Kiniry, personal communication). Ranges and value of maximum stomatal conductance (GSI) for *Populus* were assumed as 0.004-0.007 and 0.007, respectively (J. Kiniry, personal communication).

3.3.6 Calibration of the Modified SWAT and Parameterization

Hybrid poplar growth parameters were adjusted manually, and LAI and woody biomass data of hybrid poplar in Wisconsin with high density (population: 278 trees 100 m^{-2}) and low density (population: 17 trees 100 m^{-2}), and woody biomass data of hybrid poplar with medium density (population: 69 trees 100 m^{-2}) were compared with observed data for calibration of the modified SWAT. *Populus* populations and densities used for model calibration and validation were similar with Guo *et al.* (2015)'s study.

PHU, BIO_E, EXT_COEF, BLAI, ALAI_MIN, FRGRW1, FRGRW2, CNYLD and CPYLD were modified manually within derived ranges to match well with published LAI and aboveground root biomass values for hybrid poplar with various populations during calibration of the modified SWAT.

3.3.7 Validation of the modified SWAT after Calibration

Woody biomass and LAI of hybrid poplar in Wisconsin with high density (population: 83 trees 100 m^{-2}) and medium density (population: 25 trees 100 m^{-2}), and woody biomass data of hybrid poplar with high density (population: 1111 trees 100 m^{-2}) and low density (population: 8 trees 100 m^{-2}) were compared with observed data for validation of the modified SWAT after calibration.

Aboveground biomass, seasonal mean runoff per runoff event, seasonal mean sediment per runoff event, seasonal total sediment, seasonal mean nitrate-N in runoff and seasonal total nitrate-N in runoff for cottonwood with a population of 23 trees 100 m^{-2} (medium density) in Mississippi modeled by the modified SWAT model after calibration were compared with observed data for validation. Coefficient of determination (R^2), Nash-Sutcliffe model efficiency coefficient (NSE) and percent bias/percent error (PBIAS [%]) were used to evaluate model performance (Kumar & Merwade, 2009). The R^2 value can represent the strength of the linear relationship between simulated and measured data. The NSE value (Nash & Sutcliffe, 1970) can indicate how well the measured data versus simulated data fits the 1:1 line. An R^2 or NSE value of greater than 0.5 is considered reasonable model performance (Moriasi *et al.*, 2007). Percent bias (Gupta *et al.*, 1999) measures the tendency

of the simulated data to be larger or smaller than the measured data. Negative values represent model overestimation bias. If P_{BIAS} ± 25% for streamflow, ± 55% for sediment, and ± 70% for N and P, model simulation results can be considered as satisfactory (Moriasi *et al.*, 2007).

3.4 Results and Discussion

3.4.1 Changes to the SWAT Code

A new leaf area algorithm was added in SWAT and used for maximum seasonal LAI calculation. This is useful for simulating tree growth prior to maturity (Guo *et al.*, 2015). A new tree leaf area parameter, TreeD, was added in the plant database. The parameter describes how LAI increases to the maximum potential LAI (BLAI) with varying densities. An algorithm used for calculating dropping leaves weight was added (Guo *et al.*, 2015). BIO_LEAF (fraction of tree biomass accumulated each year converted to residue during dormant period), a stable value, was removed from the plant dataset. Tree growth algorithm and parameter to simulate leaf area development and leaf biomass were improved (Data B.2), and related code was changed in the subroutines (Table B.3).

3.4.2 Sensitivity Analysis of Hybrid Poplar Growth Parameters to Selected Outputs by the Modified SWAT Model of Hybrid Poplar Site in Wisconsin

The effects of hybrid poplar growth parameters on the selected SWAT model outputs (annual biomass yield, water yield, plant uptake of N and P) were analyzed. The "water yield" is the water leaving the HRU representing the hybrid poplar site and entering the main channel. Sensitive parameters and the selected model outputs were plotted (Figure B.1).

Relative sensitivity coefficient (Table B.4) was also calculated for each tree growth parameter to obtain the rank of sensitivity to different model outputs. Hybrid poplar biomass yield was most sensitive to BIO_E, number of years required for tree species to reach full development (MAT_YRS), T_BASE, T_OPT, light extinction coefficient (EXT_COEF), TREED and other leaf area development parameters (minimum LAI for

plant during dormancy (ALAI_MIN), BLAI, fraction of BLAI corresponding to the second point on optimal leaf development curve (LAIMX2), and fraction of growing season coinciding with LAIMX2 (FRGRW2)). Annual water yield output was sensitive to MAT_YRS, GSI, and BIO_E. Plant uptake of N was most sensitive to PLTNFR2, BIO_E, EXT_COEF and PLTNFR1. Plant uptake of P was sensitive to MAT_YRS, BIO_E, T_OPT, EXT_COEF, and TREED. All hybrid poplar biomass yield, water yield and plant uptake of N and P were highly sensitive to MAT_YRS and BIO_E (Figure B.1), which is consistent with sensitivity analysis of switchgrass growth parameters in SWAT (Trybula *et al*., 2014).

3.4.3 Calibration of the Modified SWAT for Hybrid Poplar Growth in Wisconsin

The simulated annual LAI values by the modified SWAT after calibration compared favorably with published values for hybrid poplar with population of 278 trees 100 m^{-2} (high density) and 17 trees 100 m^{-2} (low density) (Figure 3.2). Simulated annual aboveground woody biomass values by the modified SWAT were compared with published values for hybrid poplar with populations of 278 tree 100 m^{-2} (high density), 69 trees 100 m^{-2} (medium density), and 17 trees 100 m^{-2} (low density) (Figure 3.3).

Projected annual LAI of hybrid poplar with populations of 278 and 17 trees 100 m^{-2} by the modified SWAT fit the measured values reasonably well, except that the projected LAI values at years 8 and 9 were slightly higher than the measured values (population of 17 trees 100 m^{-2}) (Figure 3.2b).

Projected annual aboveground woody biomass of hybrid poplar with populations of 278, 69, and 17 trees 100 m^{-2} by the modified SWAT model reasonably matched measured values, except that projected annual aboveground woody biomass values at years 2 and 3 were higher than observed values (population of 278 trees 100 m^{-2}) (Figure 3.3a). Projected aboveground woody biomass values from years 8 to 10 were slightly higher than measured values (population of 17 trees 100 m^{-2}) (Figure 3.3c).

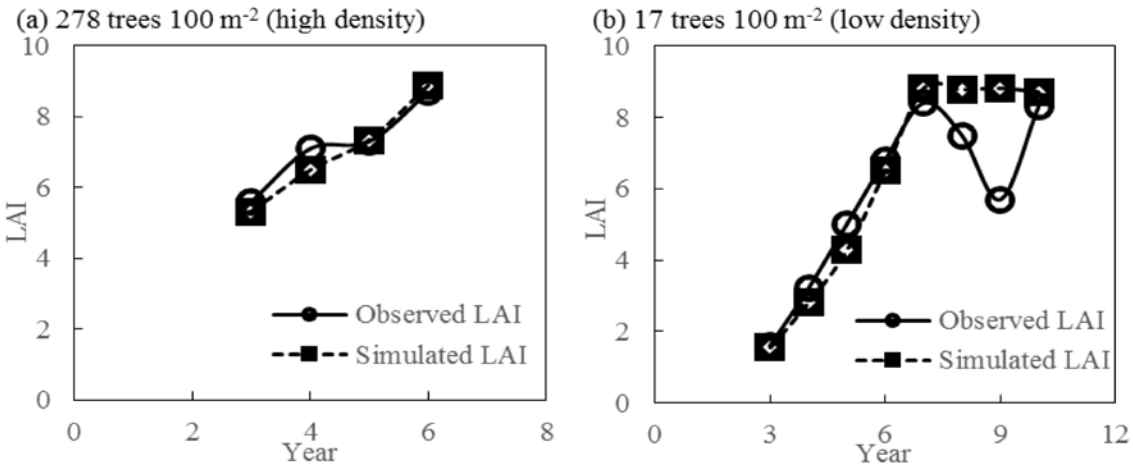

Figure 3.2 Yearly observed and calibrated LAI of hybrid poplar with populations of 278 (a) and 17 (b) trees 100 m^{-2} for the modified SWAT during calibration

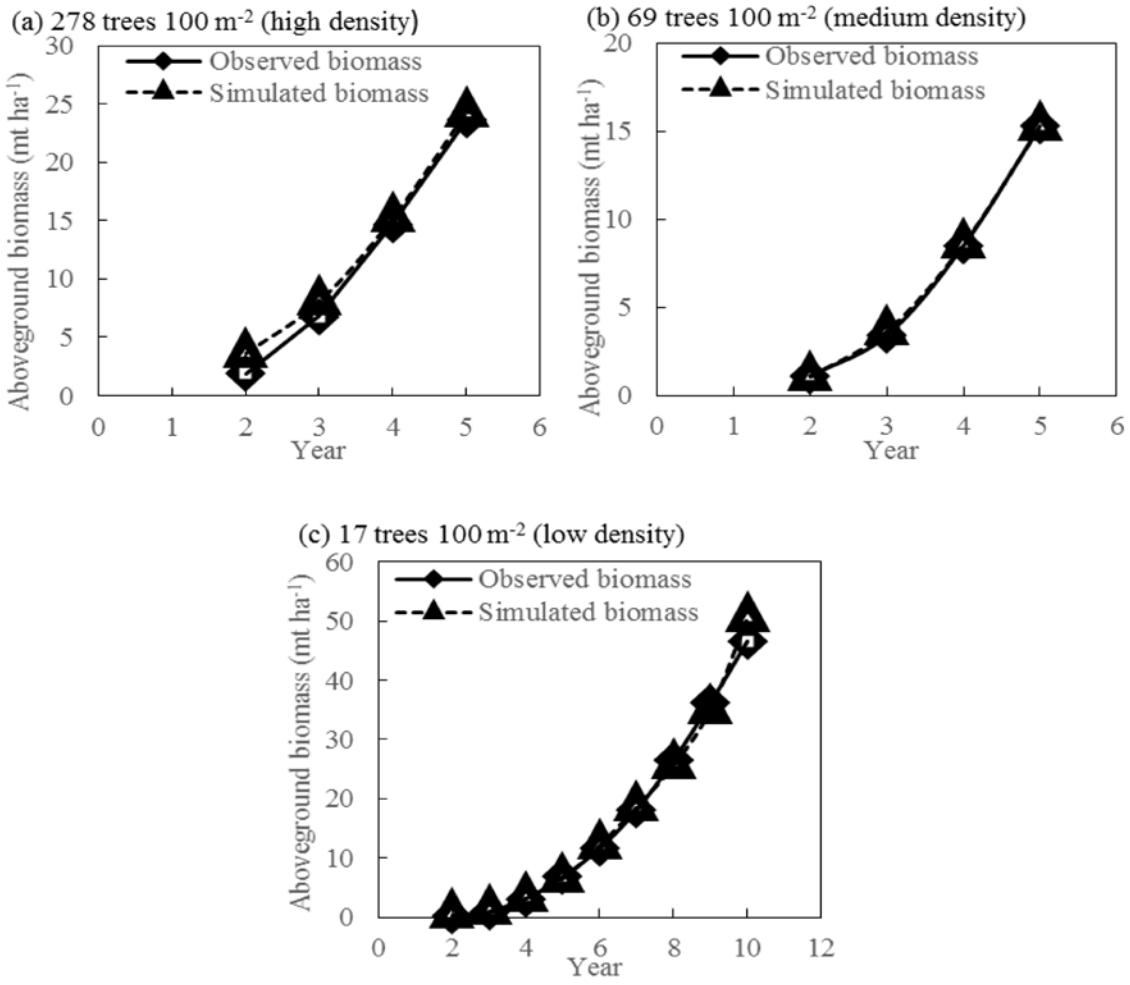

Figure 3.3 Yearly observed and calibrated aboveground woody biomass of hybrid poplar with populations of 278 (a), 69 (b) and 17 (c) trees 100 m^{-2} for the modified SWAT during calibration

3.4.4 Values and Potential Parameter Range for *Populus* Growth in the Modified SWAT

The calibrated modified SWAT reasonably simulated annual LAI and aboveground woody biomass yield of hybrid poplar with various spacings. During calibration, values and potential parameter ranges for *Populus* were determined (Table 3) (Zavitkovski, 1981; Hansen, 1983; McLaughlin *et al.*, 1987; Michael *et al.*, 1988; Landsberg & Wright, 1989; Kiniry *et al.*, 1999; Black *et al.*, 2002; MacDonald *et al.*, 2008; Arnold *et al.*, 2011; Guo *et*

al., 2015). Since obtaining enough detailed data about the phenological and physiological characteristics of the vegetation is difficult and time consuming, globally approximated plant parameter ranges are often used in ecological models (Neitsch *et al*., 2011; Arnold *et al*., 2012). Values and potential parameter ranges of hybrid poplar and cottonwood (Table 3.3) can be adjusted when applied to specific regions. These values and ranges also provide guidance for determination of growth parameters for other *Populus* clones or other woody species in process based models.

Table 3.3 Values and potential parameter ranges for hybrid poplar (*Populus balsamifera* L. × *P.tristis* Fisch) and cottonwood (*Populus deltoides* Bartr.) compared to current parameters for *Populus* in SWAT2012 plant database

Acronym	Parameter	Hybrid poplar		Cottonwood		*Populus*
		Value	Range	Value	Range	Database value
T_BASE*	Base Temperature (℃)	4	0-6	8	7-15	10
[PHU] *	Heat Units to Maturity	[1750]	[2150-1500]	[2818]	[2900-2200]	-
T_OPT†	Optimal Temperature (℃)	25	25-30	25	25-30	30
BIO_E‡·§	Radiation Use Efficiency in ambient CO_2 (kg ha^{-1})/(MJ m^{-2})	20	20-35	41	30-58	30
EXT_COEF‡·§	Light Extinction Coefficient	0.3	0.2-0.6	0.6	0.2-0.6	0.45
BLAI‡·¶·**	Maximum LAI	9.5	5-9.5	9.5	5-9.5	5
LAIMX2‡·¶·**	Fraction of BLAI corresponding to 2nd point	0.95	0.95-0.98	0.95	0.95-0.98	0.95
DLAI‡·¶·**	Point in growing season when LAI declines	0.99	0.99	0.99	0.99	0.99
BIO_LEAF	Fraction of tree biomass converted to residue during dormancy	0.3	0.1-0.5	0.3	0.1-0.5	0.3
TREED‡·¶·††	Tree leaf area factor	0.5-4.5	0.5-4.5	0.5-4.5	0.5-4.5	-
FRGRW2‡·¶·**	Fraction of growing season coinciding with LAIMX2	0.4	0.4-0.45	0.4	0.4-0.45	0.4

Table 3.3 Continued.

ALAI_MIN‡,¶,**	Minimum LAI for plant during dormancy	0	0-0.75	0	0-0.75	0.75
FRGRW1‡,¶,**	Fraction of growing season coinciding with LAIMX1	0.05	0.05-0.07	0.05	0.05-0.07	0.05
LAIMX1‡,¶,**	Fraction of BLAI corresponding to 1st point	0.05	0.05-0.3	0.05	0.05-0.3	0.05
PLTPFR1††,‡‡	Plant P fraction at emergence (whole plant)	Existing value	Existing value	Existing value	Existing value	0.0007
GSI†	Maximum stomatal conductance	0.007	0.004-0.007	0.007	0.004-0.007	0.004
CHTMX†	Maximum canopy height (m)	Existing value	7-15	10	10-15	7.5
FRGMAX†	Fraction of GSI corresponding to the 2nd point of stomatal conductance curve	Existing value	Existing value	Existing value	Existing value	0.75
VPDFR†	Vapor pressure deficit (kPa) corresponding to 2nd point of stomatal conductance curve	Existing value	Existing value	Existing value	Existing value	4
PLTNFR1††,‡‡	Plant N fraction at emergence (whole plant)	Existing value	Existing value	Existing value	Existing value	0.006
PLTNFR3††,‡‡	Plant N fraction at maturity (whole plant)	Existing value	Existing value	Existing value	Existing value	0.0015
PLTNFR2††,‡‡	Plant N fraction at 50% maturity (whole plant)	Existing value	Existing value	Existing value	Existing value	0.002
RSDCO_PL†	Plant residue decomposition coefficient	Existing value	Existing value	Existing value	Existing value	0.05
RDMX††,‡‡	Maximum rooting depth (m)	Existing value	Existing value	Existing value	Existing value	3.5
CNYLD‡,§§,¶¶	Plant N fraction in harvested biomass	0.0005	0.0005-0.0015	0.0005	0.0005-0.0015	0.0015
CPYLD‡,§§,¶¶	Plant P fraction in harvested biomass	0.0002	0.0002-0.0003	0.0002	0.0002-0.0003	0.0003
PLTPFR2††,‡‡	Plant P fraction at 50% maturity (whole plant)	Existing value	Existing value	Existing value	Existing value	0.0004

Table 3.3 Continued.

PLTPFR3††,‡‡	Plant P fraction at maturity (whole plant)	Existing value	Existing value	Existing value	Existing value	0.0003
USLE_C†	Minimum crop factor for water erosion	Existing value	Existing value	Existing value	Existing value	0.001
WAVP††,‡‡	Rate of decline in radiation use efficiency per unit increase in vapor pressure deficit	Existing value	Existing value	Existing value	Existing value	8
CO2HI†	Elevated CO_2 atmospheric concentration (µL CO_2 L^{-1} air) corresponding the 2nd point	Existing value	Existing value	Existing value	Existing value	660
BIOHI†	Biomass-energy ratio corresponding to 2nd point	Existing value	Existing value	Existing value	Existing value	31
WSYF‡	Lower limit of harvest index ((kg ha^{-1})/(kg ha^{-1}))	0	0	0	0	0.01
MAT_YRS¶,**	Number of years required for tree species to reach full development (years)	6-9	6-9	6-9	6-9	10
BMX_TREES†,‡‡	Maximum biomass for a forest (mt ha^{-1})	Existing value	Existing value	Existing value	Existing value	200
BM_DIEOFF†	Biomass dieoff fraction	Existing value	Existing value	Existing value	Existing value	0.1
HVSTI†††,‡‡‡	Harvest index for optimal growing conditions	0.65	0.45-0.7	0.6	0.4-0.65	0.76

* Calculated based on maximum and minimum daily temperature from NCDC weather stations.
† Assumption.
‡ Modified value after calibration.
§ Landsberg and Wright, 1989
¶ Hansen, 1983
** Zavitkovski, 1981
†† Kiniry *et al.*, 1999
‡‡ MacDonald *et al.*, 2008
§§ Black *et al.*, 2002
¶¶ McLaughlin *et al.*, 1987
*** J. Kiniry, personal communication.
††† Michael *et al.*, 1988
‡‡‡ Arnold *et al.*, 2011

3.4.5 The Modified SWAT Model Validation for Hybrid Poplar Growth in Wisconsin

Annual LAI values modeled by modified SWAT were compared with published values for hybrid poplar with populations of 83 trees 100 m^{-2} (high density) and 25 trees 100 m^{-2} (medium density) (Figure 3.4). Annual aboveground woody biomass values modeled by the modified SWAT were compared with published values for hybrid poplar with populations of 1111 and 83 trees 100 m^{-2} (high density), 25 trees 100 m^{-2} (medium density), and 8 trees 100 m^{-2} (low density) (Figure 3.5). Modeled outputs of the modified SWAT for the hybrid poplar site in Wisconsin were evaluated (Table 3.4). Simulated yields by the modified SWAT were compared with observed values and projected values from the original SWAT, FOREST and modified FOREST models for hybrid poplar growth in Wisconsin (Table 3.5). Annual evapotranspiration and water yield (1970-1979) of the hybrid poplar site in Wisconsin were also simulated by the modified SWAT (Figure A.2).

Overall performance of the modeled LAI of hybrid poplar with populations of 83 and 25 trees 100 m^{-2} was satisfactory (NSE > 0.5 and R^2 > 0.5). Simulated annual LAI of hybrid poplar (83 and 25 trees 100 m^{-2}) by the modified SWAT model fit measured values well (Figure 3.4), except that simulated LAI value at year 4 was slightly lower than the observed value (population of 83 trees 100 m^{-2}) (Figure 3.4a) . P_{BIAS} values of hybrid poplar with populations of 83 and 25 trees 100 m^{-2} were 7% and -8% respectively, indicating accurate model simulation. NSE (R^2) values for modeled LAI of hybrid poplar with populations of 83 and 25 trees 100 m^{-2} were 0.94 (0.74) and 0.98 (0.98), respectively (Table 3.4).

Overall performance of the modeled aboveground woody biomass yields of hybrid poplar with populations of 1111, 83, 25 and 8 trees 100 m^{-2} was acceptable (NSE > 0.5 and R^2 > 0.5). Simulated annual aboveground woody biomass of hybrid poplar (1111, 83, 25 and 8 trees 100 m^{-2}) by the modified SWAT model had a good match with measured values (Fig. 5). P_{BIAS} values were -57% (1111 trees 100 m^{-2}), -14% (83 trees 100 m^{-2}) and -26% (25 trees 100 m^{-2}), indicating that modeled annual aboveground woody biomass results by the modified SWAT were overestimated. Aboveground woody biomass values were calculated based on simulated total biomass and fraction of total biomass partitioned to tree stems and

branches. Overestimation of percentage of hybrid poplar aboveground biomass partitioned to woody biomass would result in larger than observed aboveground woody biomass values.

For aboveground woody biomass from year 2 to 5 of 1111 trees 100 m^{-2} hybrid poplar (Figure 3.5a), from year 2 to 4 of 83 trees 100 m^{-2} hybrid poplar (Figure 3.5b), and years 3 and 4 of 25 trees 100 m^{-2} hybrid poplar (Figure 3.5c), simulated values by the modified SWAT were higher than observed values. P_{BIAS} values of hybrid poplar with populations of 8 trees 100 m^{-2} was 4%, representing accurate model simulation (Figure 3.5d). NSE (R^2) values for modeled aboveground woody biomass of hybrid poplar with populations of 1111, 83, 25, and 8 trees 100 m^{-2} are 0.95 (0.86), 0.96 (0.88), 0.96 (0.99), and 0.99 (0.99), respectively (Table 3.4).

Projected woody biomass by the modified SWAT model was improved relative to simulations by original SWAT, FOREST, and modified FOREST models (Table 3.5). Biomass yield simulation from FOREST and modified FOREST was based on estimated tree height, diameter and survival, thus projected biomass was much higher than the observed value (Ek & Dawson, 1976a, 1976b). Observed mean annual biomass increment (MABI) of 5-year old 69 trees 100 m^{-2} hybrid poplar was 7.6 mt ha^{-1} $year^{-1}$ (Isebrands *et al.*, 1979) (Table 3.5). Simulated values by FOREST, SWAT, and the modified SWAT models were 42% higher (10.8 mt ha^{-1} $year^{-1}$ (Ek & Dawson, 1976a, 1976b)), 34% (10.2 mt ha^{-1} $year^{-1}$) higher, and 4% (7.3 mt ha^{-1} $year^{-1}$) lower than observed value (Table 3.5). Additionally, observed MABI value of 10-year old 17 trees 100 m^{-2} hybrid poplar was 10.4 mt ha^{-1} $year^{-1}$ (Hansen, 1983) (Table 3.5). Projected values by FOREST, modified FOREST, SWAT, and modified SWAT models were 96% (20.4 mt ha^{-1} $year^{-1}$) higher (Ek & Dawson, 1976a, 1976b), 81% (18.8 mt ha^{-1} $year^{-1}$) higher (Meldahl, 1979), 86% (1.5 mt ha^{-1} $year^{-1}$) lower, and 12% (9.2 mt ha^{-1} $year^{-1}$) lower than observed value (Table 3.5). Observed MABI value of 9-year old 8 trees 100 m^{-2} hybrid poplar was 6.2 mt ha^{-1} $year^{-1}$ (Hansen, 1983) (Table 3.5). Modeled values by FOREST, SWAT, and modified SWAT were 182% (17.5 mt ha^{-1} $year^{-1}$) higher, 76% (1.51 mt ha^{-1} $year^{-1}$) lower (Ek & Dawson, 1976a, 1976b), and 19% (7.4 mt ha^{-1} $year^{-1}$) higher, respectively, than the observed value (Table 3.5).

Mean (median) values of annual evapotranspiration and water yield at the hybrid poplar site from 1970 to 1979 were 527 (518) mm, and 603 (587) mm, respectively (Figure B.2).

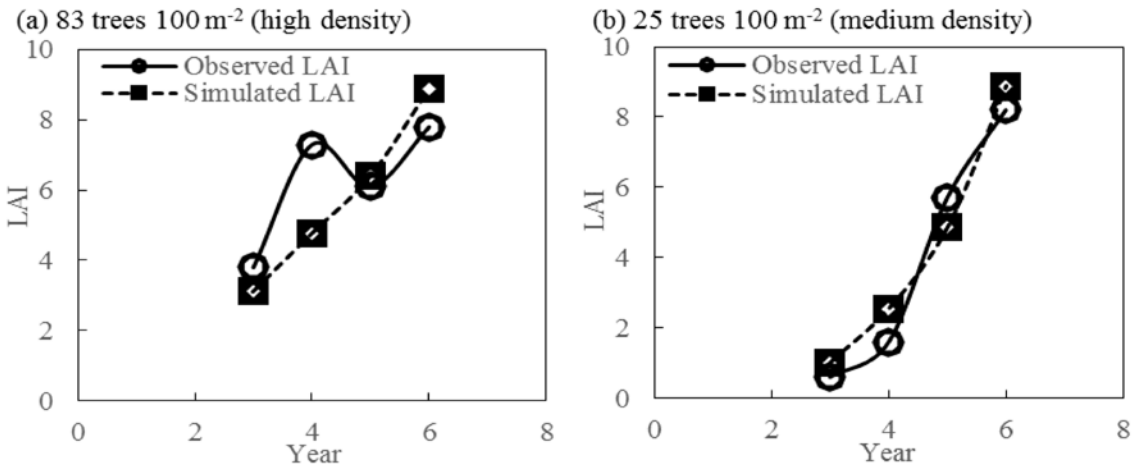

Figure 3.4 Yearly observed and calibrated LAI of hybrid poplar with populations of 83 (a) and 25 (b) trees 100 m^{-2} for the modified SWAT during validation

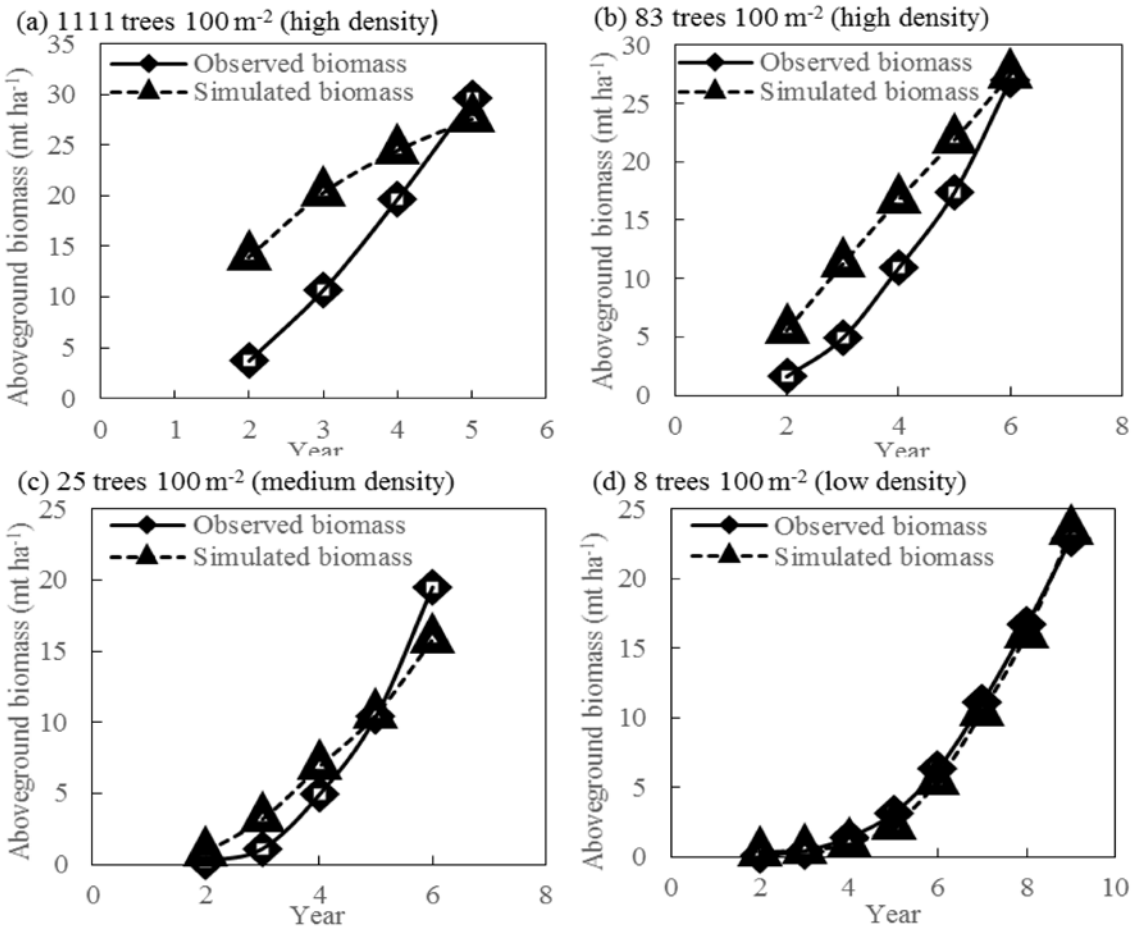

Figure 3.5 Yearly observed and calibrated aboveground woody biomass of hybrid poplar with populations of 1111 (a), 83 (b), 25 (c) and 8 (d) trees 100 m^{-2} for the modified SWAT during validation

Table 3.4 Evaluation of model outputs with various populations for the modified SWAT

Tree population (trees 100 m^{-2})	Density level	Outputs (Annual aboveground woody biomass (AWB) and LAI)	P_{BIAS} (%)	NSE	R^2
1111	high	AWB (mt ha^{-1})	-57	0.95	0.86
83	high	LAI	7	0.94	0.74
		AWB (mt ha^{-1})	-14	0.96	0.88
25	medium	LAI	-8	0.98	0.98
		AWB (mt ha^{-1})	-26	0.96	0.99
8	low	AWB (mt ha^{-1})	4	0.99	0.99

Table 3.5 Comparison of projected and observed mean annual biomass increment (MABI) of 5-, 9- and 10-year-old short rotation intensively cultured hybrid poplar grown with various populations in Wisconsin (number in parentheses represents rate of increase/decrease of simulated results to related observed results)

Age (yr)	Spacing (m×m)	Population (trees 100 m^{-2})	Observed MABI (mt ha^{-1})	Modeled MABI (mt ha^{-1})			
				Modified SWAT	SWAT	FOREST	Modified FOREST
5	1.2×1.2	69	7.6*	7.3† (-4%)	10.2† (34%)	10.8‡,§ (42%)	-
10	2.4×2.4	17	10.4¶	9.2† (-12%)	1.5† (-86%)	20.4‡,§ (96%)	18.8** (81%)
9	3.6 ×3.6	8	6.2¶	7.4† (19%)	1.51† (-76%)	17.5‡,§ (182%)	-

* Isebrands *et al*., 1979
† Present study.
‡ Ek and Dawson, 1976a
§ Ek and Dawson, 1976b
¶ Hansen, 1983
** Meldahl, 1979

3.4.6 The Modified SWAT Model Validation for Cottonwood Growth and Hydrologic and Water Quality Responses in Mississippi

Modeled aboveground biomass, seasonal mean runoff per runoff event, seasonal mean sediment per runoff event, seasonal total sediment, seasonal mean nitrate-N in runoff and seasonal total nitrate-N in runoff values by modified SWAT were compared with observed values for 23 trees 100 m^{-2} (medium density) cottonwood in Mississippi (Figure 3.6). Values of hydrologic and water quality input parameters were obtained based on manual calibration, and the ranges, default values, and modified values for calibrated parameters in the modified SWAT are shown in Table 6 (Wischmeier & Smith, 1978; Longabucco & Rafferty, 1998; Neitsch *et al*., 2002; Neitsch *et al*., 2011; Arnold *et al*., 2012). Simulated outputs of the modified SWAT model for the cottonwood site in Mississippi were evaluated (Table 7). Annual evapotranspiration and water yield (1995-1997) of the cottonwood site in Mississippi were also simulated by the modified SWAT (Figure B.3).

Overall performance of the modeled annual aboveground biomass, seasonal mean runoff per runoff event, seasonal mean sediment per runoff event, seasonal mean nitrate-N in runoff per runoff event, and seasonal total nitrate-N in runoff of cottonwood growth were satisfactory (NSE $\geq$ 0.5 and $R^2 \geq$ 0.5). The calibrated results of annual aboveground

biomass (Figure 3.6a), seasonal mean runoff per runoff event (Figure 3.6b), seasonal mean sediment per runoff event (Figure 3.6c), seasonal mean nitrate-N in runoff per runoff event (Figure 3.6e), and seasonal total nitrate-N in runoff (Figure 3.6f) of cottonwood growth from the modified SWAT model had a good match with observed values. NSE (R^2) values for modeled annual aboveground biomass, seasonal mean runoff per runoff event, seasonal mean sediment per runoff event, seasonal mean nitrate-N in runoff per runoff event, and seasonal total nitrate-N in runoff of 23 trees 100 m^{-2} cottonwood were 0.99 (0.99), 0.91 (0.93), 0.98 (0.99), 0.86 (0.98), and 0.97 (0.98), respectively (Table 7). Additionally, P_{BIAS} = 0.8% (close to 0) for the modeled annual aboveground biomass and seasonal total nitrate-N in runoff (Table 7) indicated that simulated biomass yield and seasonal total nitrate-N in runoff values by the modified SWAT were accurate. P_{BIAS} values of the modeled seasonal mean runoff per runoff event, seasonal mean sediment per runoff event, and seasonal mean nitrate-N in runoff per runoff event of cottonwood growth were -12% (P_{BIAS} > - 25%), 11% (P_{BIAS} < 55%), -39% (P_{BIAS} > - 70%), representing accurate model simulation. P_{BIAS}= -12% and -39% indicate modeled results were overestimated generally and modeled mean runoff during the fall and winter of 1995 (Figure 3.6b) and mean nitrate-N in runoff during the winter of 1995 and the spring of 1996 (Figure 3.6e) were higher than the observed values. P_{BIAS} = 11% indicating seasonal mean sediment per runoff event was slightly underestimated and simulated mean sediment during the spring of 1996 was slightly lower than the observed value (Figure 3.6c). Simulated seasonal total sediment by modified SWAT did not fit observed values well, except that modeled total sediment during the fall of 1995 was close to the observed value (Figure 3.6d). NSE and R^2 values of modeled seasonal total sediment are -0.15 and 0.42 (NSE < 0.5, R^2 < 0.5), which were not satisfactory (Table 3.7). NSE and R^2 were slightly lower than acceptable limits. P_{BIAS} = 60% (P_{BIAS} > 55%) indicating seasonal mean runoff was underestimated. Simulated total sediment values during the winter of 1995 and the spring of 1996 were lower than the observed values as shown in Figure 3.6d.

Mean (median) values of annual evapotranspiration and water yield at the cottonwood site from 1995 to 1997 were 602 (611) mm, and 594 (568) mm, respectively (Figure B.3).

Table 3.6 Parameters for hydrologic and water quality results calibration

File	Parameter	Definition	Modified value	Default value	Parameter range
.mgt	CN2	Initial SCS CN II value	91	85	0-100*
.hru	SLSUBBSN	Average slope length [m]	201	122	-
.hru	LAT_SED	Sediment concentration in lateral flow and groundwater flow [mg l^{-1}]	30	0	0-30†
.bsn	ADJ_PKR	Peak rate adjustment factor for sediment routing in the subbasin (tributary channels)	2	1	0.5-2.0*
.bsn	RCN	Concentration of nitrogen in rainfall [mg N l^{-1}]	4	0	0.0-4.0‡
.sol	USLE_K	USLE equation soil credibility (K) factor [0.013 (mt m^2 hr)/(m^3-mt cm)]	0.60	0.37	0.01-0.99§
crop.dat	USLE_C	Minimum value of USLE C factor for water erosion applicable to the land cover/plant	0.009	0.001	0.001-0.009¶

* Neitsch *et al.*, 2002
† Longabucco and Rafferty, 1998
‡ Cary Institute of Ecosystem Studies
§ Neitsch *et al.*, 2011
¶ Wischmeier and Smith, 1978

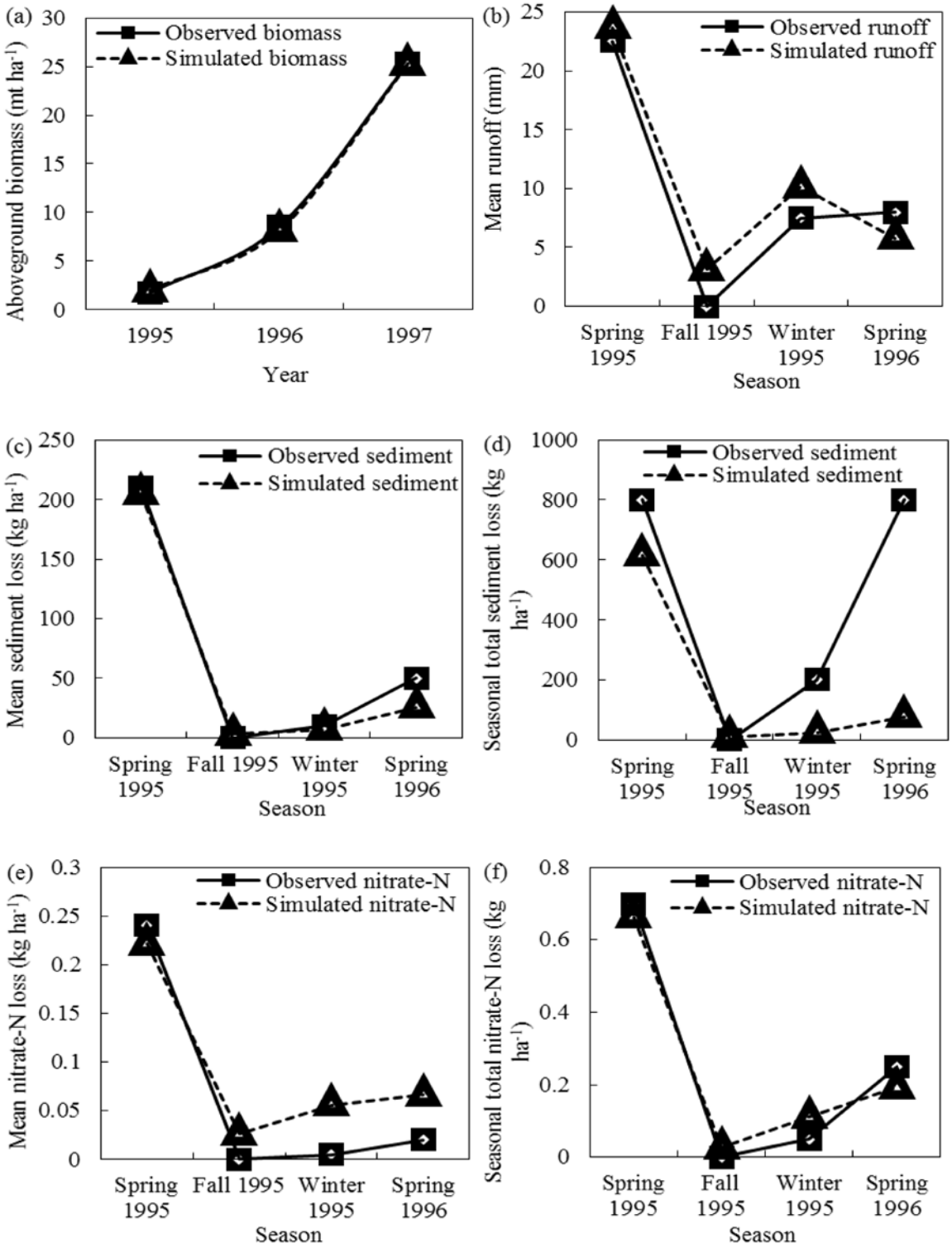

Figure 3.6 Observed and calibrated aboveground biomass (a), runoff (b), sediment (c, d) and nitrate-N in runoff (e, f) of cottonwood with population of 23 trees 100 m^{-2} for the modified SWAT during validation

Table 3.7 Validation of model outputs in cottonwood site in Mississippi by the modified SWAT

Tree population (trees 100 m^{-2})	Density level	Model outputs	P_{BIAS} (%)	NSE	R^2
23	medium	Annual aboveground biomass (mt ha^{-1})	0.8	0.99	0.99
		Mean runoff per runoff event (mm)	-12	0.91	0.93
		Mean sediment loss per runoff event (kg ha^{-1})	11	0.98	0.99
		Seasonal total sediment loss (kg ha^{-1})	60	-0.15	0.42
		Seasonal means of nitrate-N loss per runoff event (kg ha^{-1})	-39	0.86	0.98
		Seasonal total nitrate-N loss in runoff (kg ha^{-1})	0.8	0.97	0.98

Only three or four yearly/seasonal data were available for some tree populations. More continuous *Populus* growth, hydrology and water quality field data have the potential to improve determination of values and ranges for tree growth parameters in process based model and thus improve biomass yields and water quantity and quality response modeling of short rotation woody crops. Additionally, current SWAT outputs only include plant total biomass, but aboveground woody biomass (stem and branch) is used as biofeedstock. Thus, it is desirable to improve the model to include root biomass, aboveground biomass and aboveground woody biomass in model outputs.

3.5 Conclusions

Populus has the potential to provide large quantities of biofeedstock masses for energy production, and it is important to quantify water quantity and water quality responses to *Populus* growth when it is planted in large areas as a biomass feedstock. Tree growth algorithms and parameters were previously improved in ALMANAC and reasonably simulated LAI and biomass yield of juvenile and mature *Populus*. The functional components and parameters of *Populus* are also useful for SWAT. In this study, SWAT was modified and used to simulate *Populus* growth and its impacts on runoff, sediment and nitrate-N losses. Sensitivity analysis was used to determine ranges and values of growth parameters of *Populus*. The modified SWAT with tree growth modification was used to simulate *Populus* LAI and biomass yield, runoff, sediment and nutrient loading to *Populus*

growth at a hybrid poplar site in Wisconsin and cottonwood site in Mississippi. The simulated values were compared with observed data to calibrate and validate the modified SWAT.

Populus biomass yield was sensitive to 10 of 35 plant growth parameters: BIO_E, MAT_YRS, T_BASE, T_OPT, EXT_COEF, TREED, and other leaf area development parameters (ALAI_MIN, BLAI, LAIMX2, FRGRW2) in the SWAT plant dataset. The results of sensitivity analysis can provide guidance for determination of values or potential ranges for parameters and model calibration.

Modeled aboveground woody biomass and LAI values from the modified SWAT for hybrid poplar in Wisconsin were satisfactory (P_{BIAS}: -57 ~ 7%, NSE: 0.94 ~ 0.99, and R^2: 0.74 ~ 0.99). Performance of aboveground woody biomass simulation from the modified SWAT was superior to SWAT, FOREST, and modified FOREST models. Additionally, modeled aboveground biomass, seasonal mean runoff, seasonal mean sediment, seasonal mean nitrate-N in runoff and seasonal total nitrate-N in runoff results from the modified SWAT model for the cottonwood site in Mississippi were good (P_{BIAS}: -39 ~ 11%, NSE: 0.86 ~ 0.99, and R^2: 0.93 ~ 0.99).

Thus, tree growth algorithms and parameters added in the modified SWAT and related changes in source code were acceptable. Values and potential ranges for hybrid poplar and cottonwood growth parameters were reasonable. The modified SWAT model can be used for biofeedstock production modeling for *Populus* (before and after maturity), and hydrologic and water quality response to its growth at landscape scales. The improved algorithms and parameters for tree growth, and values and ranges for *Populus* should also be useful for other process based models, such as EPIC and APEX.

3.6 References

Aditya, S., & William, F. R. (2010). Evaluation of Best Management Practices in Millsboro Pond Watershed Using Soil and Water Assessment Tool (SWAT) Model. *Journal of Water Resource and Protection, 2*(5), 403-412.

Amichev, B. Y., Hangs, R. D., & Van Rees, K. C. (2011). A novel approach to simulate growth of multi-stem willow in bioenergy production systems with a simple process-based model (3PG). *Biomass and Bioenergy, 35*(1), 473-488.

Amichev, B. Y., Johnston, M., & Van Rees, K. C. (2010). Hybrid poplar growth in bioenergy production systems: biomass prediction with a simple process-based model (3PG). *Biomass and Bioenergy, 34*(5), 687-702.

Anderson, H., Papadopol, C., & Zsuffa, L. (1983). Wood energy plantations in temperate climates. *Forest Ecology and Management, 6*(3), 281-306.

Arnold, J., Kiniry, J., Srinivasan, R., Williams, J., Haney, E., & Neitsch, S. (2011). Soil and water assessment tool input/output file documentation version 2009. Texas Water Resources Institute Technical Report. (365).

Arnold, J., Kiniry, J., Srinivasan, R., Williams, J., Haney, E., & Neitsch, S. (2012). Soil and Water Assessment Tool input/output file documentation: Version 2012. Texas Water Resources Institute Technical Report (Vol. 436).

Black, B. L., Fuchigami, L. H., & Coleman, G. D. (2002). Partitioning of nitrate assimilation among leaves, stems and roots of poplar. *Tree Physiology, 22*(10), 717-724.

Boles, C. M. (2013). *SWAT model simulation of bioenergy crop impacts in a tile-drained watershed* (Master Thesis), Purdue University.

Cannell, M., Sheppard, L., & Milne, R. (1988). Light use efficiency and woody biomass production of poplar and willow. *Forestry, 61*(2), 125-136.

Cannell, M., & Smith, R. (1980). Yields of minirotation closely spaced hardwoods in temperate regions: review and appraisal. *Forest Science, 26*(3), 415-428.

Ceulemans, R. (1990). Genetic variation in functional and structural productivity determinants in poplar. Amsterdam: Thesis Publishers.

Clendenen, G. W. (1996). Use of harmonized equations to estimate above-ground woody biomass for two hybrid poplar clones in the Pacific Northwest. *Biomass and Bioenergy, 11*(6), 475-482.

Deckmyn, G., Laureysens, I., Garcia, J., Muys, B., & Ceulemans, R. (2004). Poplar growth and yield in short rotation coppice: model simulations using the process model SECRETS. *Biomass and Bioenergy, 26*(3), 221-227.

Downing, M., & Graham, R. L. (1993). Evaluating a biomass resource: The TVA region-wide biomass resource assessment model. Oak Ridge National Lab., TN (United States). Funding organization: USDOE, Washington, DC (United States).

Ek, A. R. (1979). Notes: A model for estimating branch weight and branch leaf weight in biomass studies. *Forest Science, 25*(2), 303-306.

Ek, A. R., & Dawson, D. H. (1976a). Actual and projected growth and yields of *Populus*' Tristis# 1'under intensive culture. *Canadian Journal of Forest Research, 6*(2), 132-144.

Ek, A. R., & Dawson, D. H. (1976b). Yields of intensively grown *Populus*: actual and projected. USDA Forest Service General Technical Report NC, 21: 5-9.

Fege, A. S., Inman, R. E., & Salo, D. J. (1979). Energy farms for the future. *Journal of Forestry, 77*(6), 358-361.

Gassman, P. W., Secchi, S., & Jha, M. (2008). Assessment of bioenergy-related scenarios for the Boone River Watershed in North Central Iowa. In *21st Century Watershed Technology: Improving Water Quality and Environment Conference Proceedings, 29 March-3 April 2008, Concepcion, Chile* (p. 61). American Society of Agricultural and Biological Engineers.

Guest, G., Cherubini, F., & Strømman, A. H. (2013). The role of forest residues in the accounting for the global warming potential of bioenergy. *Global Change Biology Bioenergy, 5*(4), 459-466.

Guo, T., Engel, B. A., Shao, G., Arnold, J. G., Srinivasan, R., & Kiniry, J. R. (2015). Functional approach to simulating short-rotation woody crops in process-based models. *BioEnergy Research*, *8*(4), 1598-1613.

Gupta, H. V., Sorooshian, S., & Yapo, P. O. (1999). Status of automatic calibration for hydrologic models: Comparison with multilevel expert calibration. *Journal of Hydrologic Engineering, 4*(2), 135-143.

Haissig, B. E., Nelson, N. D., & Kidd, G. H. (1987). Trends in the use of tissue culture in forest improvement. *Nature Biotechnology, 5*(1), 52-59.

Hansen, E., & Baker, J. (1979). *Biomass and nutrient removal in short rotation intensively cultured plantations*. Paper presented at the Impact of intensive harvesting on forest nutrient cycling, State University of New York, College of Environmental Science and Forestry.

Hansen, E. A. (1983). Intensive plantation culture: 12 years research. General Technical Report, North Central Forest Experiment Station, USDA Forest Service (NC-91).

Helton, J. C., & Davis, F. J. (2003). Latin hypercube sampling and the propagation of uncertainty in analyses of complex systems. *Reliability Engineering & System Safety, 81*(1), 23-69.

Host, G. E., Rauscher, H. M., Isebrands, J., Dickmann, D. I., Dickson, R. E., Crow, T. R., & Michael, D. (1990). The microcomputer scientific software series 6. The ECOPHYS user's manual. General Technical Report-North Central Forest Experiment Station, USDA Forest Service.

Isebrands, J., Ek, A., & Meldahl, R. (1982). Comparison of growth model and harvest yields of short rotation intensively cultured *Populus*: a case study. *Canadian Journal of Forest Research, 12*(1), 58-63.

Isebrands, J., Sturos, J., & Crist, J. (1979). Integrated utilization of biomass: A case study of short-rotation intensively cultured *Populus* raw material. Technical Association of the Pulp and Paper Industry (USA), *62*(7): 67-70.

James, L. D., & Burges, S. J. (1982). Selection, calibration, and testing of hydrologic models, Hydrologic Modeling of Small Watersheds CT Haan, HP Johnson, DL Brakensiek, 437–472, American Society of Agricultural Engineers, St. *Joseph, Mich.*

Johansson, D. J. A., & Azar, C. (2007). A scenario based analysis of land competition between food and bioenergy production in the US. *Climatic Change, 82*(3-4), 267-291. doi: 10.1007/s10584-006-9208-1

Joslin, J., & Schoenholtz, S. (1997). Measuring the environmental effects of converting cropland to short-rotation woody crops: A research approach. *Biomass and Bioenergy, 13*(4), 301-311.

Kiniry, J. (1998). Biomass accumulation and radiation use efficiency of honey mesquite and eastern red cedar. *Biomass and Bioenergy, 15*(6), 467-473.

Kiniry, J., Burson, B., Evers, G., Williams, J., Sanchez, H., Wade, C., Featherston, J., & Greenwade, J. (2007). Coastal bermudagrass, bahiagrass, and native range simulation at diverse sites in Texas. *Agronomy Journal, 99*(2), 450-461.

Kiniry, J., Jones, C., O'toole, J., Blanchet, R., Cabelguenne, M., & Spanel, D. (1989). Radiation-use efficiency in biomass accumulation prior to grain-filling for five grain-crop species. *Field Crops Research, 20*(1), 51-64.

Kiniry, J., MacDonald, J., Kemanian, A. R., Watson, B., Putz, G., & Prepas, E. E. (2008). Plant growth simulation for landscape-scale hydrological modelling. *Hydrological Sciences Journal, 53*(5), 1030-1042.

Kiniry, J., Tischler, C., & Van Esbroeck, G. (1999). Radiation use efficiency and leaf CO_2 exchange for diverse C_4 grasses. *Biomass and Bioenergy, 17*(2), 95-112.

Kiniry, J. R., Johnson, M.-V. V., Bruckerhoff, S. B., Kaiser, J. U., Cordsiemon, R., & Harmel, R. D. (2012). Clash of the titans: comparing productivity via radiation use efficiency for two grass giants of the biofuel field. *BioEnergy Research, 5*(1), 41-48.

Kiniry, J. R., Williams, J. R., Gassman, P. W., & Debaeke, P. (1992). A general, process-oriented model for two competing plant species. *Trans. ASAE*, *35*(3), 801-810.

Kumar, S., & Merwade, V. (2009). Impact of watershed subdivision and soil data resolution on SWAT model calibration and parameter uncertainty1. *Journal of the American Water Resources Association, 45*(5), 1179-1196.

Landsberg, J., & Wright, L. (1989). Comparisons among *Populus* clones and intensive culture conditions, using an energy-conservation model. *Forest Ecology and Management, 27*(2), 129-147.

Li, X., Nour, M. H., Smith, D. W., Prepas, E. E., Putz, G., & Watson, B. M. (2008). Incorporating water quantity and quality modelling into forest management. *The Forestry Chronicle, 84*(3), 338-348.

Liski, J., Kaasalainen, S., Raumonen, P., Akujärvi, A., Krooks, A., Repo, A., & Kaasalainen, M. (2014). Indirect emissions of forest bioenergy: detailed modeling of stump-root systems. *Global Change Biology Bioenergy, 6*(6), 777-784.

Liu, W., Mi, J., Song, Z., Yan, J., Li, J., & Sang, T. (2014). Long-term water balance and sustainable production of Miscanthus energy crops in the Loess Plateau of China. *Biomass and Bioenergy, 62*, 47-57.

Longabucco, P., & Rafferty, M. R. (1998). Analysis of material loading to Cannonsville Reservoir: advantages of event-based sampling. *Lake and Reservoir Management, 14*(2-3), 197-212.

Love, B. J., & Nejadhashemi, A. P. (2011). Water quality impact assessment of large-scale biofuel crops expansion in agricultural regions of Michigan. *Biomass and Bioenergy, 35*(5), 2200-2216.

MacDonald, J. D., Kiniry, J., Putz, G., & Prepas, E. (2008). A multi-species, process based vegetation simulation module to simulate successional forest regrowth after forest disturbance in daily time step hydrological transport models *Journal of Environmental Engineering and Science, 7*(S1), 127-143.

Manning, P., Taylor, G., & Hanley, M. (2014). Bioenergy, food production and biodiversity-an unlikely alliance? *Global Change Biology Bioenergy*, 1-18.

McLaughlin, R. A., Hansen, E. A., & Pope, P. E. (1987). Biomass and nitrogen dynamics in an irrigated hybrid poplar plantation. *Forest Ecology and Management, 18*(3), 169-188.

Meldahl, R. S. (1979). *Yield projection methodology and analysis of hybrid poplars based on multispacial plots.* (PhD Thesis), University of Wisconsin, Madison. ((University Microfilm No 80-0506))

Michael, D., Dickmann, D., Isebrands, J., & Nelson, N. (1990). Photosynthesis patterns during the establishment year within two *Populus* clones with contrasting morphology and phenology. *Tree Physiology, 6*(1), 11-27.

Michael, D., Isebrands, J., Dickmann, D., & Nelson, N. (1988). Growth and development during the establishment year of two *Populus* clones with contrasting morphology and phenology. *Tree Physiology, 4*(2), 139-152.

Monsi, M., & Saeki, T. (1953). The light factor in plant communities and its significance for dry matter production. *Japanese Journal of Botany, 14*, 22-52.

Moriasi, D., Arnold, J., Van Liew, M., Bingner, R., Harmel, R., & Veith, T. (2007). *Model evaluation guidelines for systematic quantification of accuracy in watershed simulations*. Paper presented at the Trans. ASABE.

Nair, S. S., King, K. W., Witter, J. D., Sohngen, B. L., & Fausey, N. R. (2011). Importance of Crop Yield in Calibrating Watershed Water Quality Simulation Tools. *Journal of the American Water Resource Association*(47), 1285-1297.

Nash, J., & Sutcliffe, J. (1970). River flow forecasting through conceptual models part I—A discussion of principles. *Journal of hydrology, 10*(3), 282-290.

Neitsch, S., Arnold, J., Kiniry, J., & Williams, J. (2011). Soil and water assessment tool theoretical documentation version 2009. Texas Water Resources Institute Technical Report.

Neitsch, S., Arnold, J., Kiniry, J., Williams, J., & King, K. (2002). Soil and Water Assessment Tool (Version 2000)—theoretical documentation. Texas Water Research Institute Technical Report.

Nelson, N. D., & Michael, D. (1982). Photosynthesis, leaf conductance, and specific leaf weight in long and short shoots of *Populus* 'Tristis# 1' grown under intensive culture. *Forest Science, 28*(4), 737-744.

Parajuli, P. B., & Duffy, S. E. (2013). Quantifying Hydrologic and Water Quality Responses to Bioenergy Crops in Town Creek Watershed in Mississippi. *Journal of Sustainable Bioenergy Systems, 3*(03), 202.

Pettry, D., Schoenholtz, S., Dewey, J., Switzer, R., & Mitchell, B. (1997). *Environmental impacts of conversion of cropland to short rotation woody biomass plantations*. Annual Progress Report, Mississippi State University, submitted to Tennessee Valley Authority, Muscle Shoals, AL and Oak Ridge National Laboratory, Oak Ridge, TN.

Powers, S., Ascough, J., Nelson, R., & Larocque, G. (2011). Modeling water and soil quality environmental impacts associated with bioenergy crop production and biomass removal in the Midwest USA. *Ecological Modelling, 222*(14), 2430-2447.

Raj, C. (2013). *Optimal land use planning on selection and placement of energy crops for sustainable biofuel production.* (Doctoral dissertation), Purdue University.

Rauscher, H., Isebrands, J., Host, G., Dickson, R., Dickmann, D., Crow, T., & Michael, D. (1990). ECOPHYS: an ecophysiological growth process model for juvenile poplar. *Tree Physiology, 7*(1-2-3-4), 255-281.

Sarkar, S., & Miller, S. A. (2014). Water quality impacts of converting intensively-managed agricultural lands to switchgrass. *Biomass and Bioenergy, 68*, 32-43.

Sarkar, S., Miller, S. A., Frederick, J. R., & Chamberlain, J. F. (2011). Modeling nitrogen loss from switchgrass agricultural systems. *Biomass and Bioenergy, 35*(10), 4381-4389.

Sixto, H., Gil, P., Ciria, P., Camps, F., Sánchez, M., Cañellas, I., & Voltas, J. (2014). Performance of hybrid poplar clones in short rotation coppice in Mediterranean environments: analysis of genotypic stability. *Global Change Biology Bioenergy, 6*(6), 661-671.

Stettler, R., & Bradshaw, H. (1994). The choice of genetic material for mechanistic studies of adaptation in forest trees. *Tree Physiology, 14*(7-8-9), 781-796.

Strand, S. E., Newman, L., & Ruszaj, M. (1995). Removal of trichloroethylene from aquifers using trees. In R. D. Vidic & F. G. Pohland (Eds.), *National Conference of the Environmental Engineering Division of the American Society of Civil Engineers* New York, NY (USA).

Strong, T., & Hansen, E. (1993). Hybrid poplar spacing/productivity relations in short rotation intensive culture plantations. *Biomass and Bioenergy, 4*(4), 255-261.

Thornton, F. C., Dev Joslin, J., Bock, B. R., Houston, A., Green, T., Schoenholtz, S., Pettry, D., & Tyler, D. D. (1998). Environmental effects of growing woody crops on agricultural land: first year effects on erosion, and water quality. *Biomass and Bioenergy, 15*(1), 57-69.

Tolbert, V. R., Lindberg, J., & Green, T. (1997). Soil and water quality implications of production of herbaceous and woody energy crops. Oak Ridge National Lab, TN (USA).

Tolbert, Virginia R., Frank C. Thornton, J. Dev Joslin, Bert R. Bock, Wije E. Bandaranayake, Don D. Tyler, David Pettry et al. "Soil and water quality aspects of herbaceous and woody energy crop production: lessons from research-scale comparisons with agricultural crops." In *Proceedings, BioEnergy*, vol. 98, pp. 1272-1281. 1998.Trybula, E. M., Cibin, R., Burks, J. L., Chaubey, I., Brouder, S. M., & Volenec, J. J. (2014). Perennial rhizomatous grasses as bioenergy feedstock in SWAT: parameter development and model improvement. *Global Change Biology Bioenergy*. doi: 10.1111/gcbb.12210

U. S. Department of Agriculture, F. S. (1980). Energy & wood from intensively cultured plantations: research and development program. Gen. Tech. Rep. St. Paul, MN. North Central Forest Experiment Station, (NC-58), 28. http://www.nrs.fs.fed.us/pubs/gtr/gtr_nc058.pdf. Accessed 1 July 2014.

Wang, D., LeBauer, D., & Dietze, M. (2013). Predicting yields of short-rotation hybrid poplar (*Populus* spp.) for the United States through model-data synthesis. *Ecological Applications, 23*(4), 944-958.

Williams, J., Jones, C., & Dyke, P. (1984). *Modeling approach to determining the relationship between erosion and soil productivity*. Paper presented at the *Trans. ASAE.*

Williams, J. R., Jones, C. A., Kiniry, J. R., & Spanel, D. A. (1989). The EPIC crop growth model. *Trans. ASAE*, *32*(2), 497-0511.

Wischmeier, W. H., & Smith, D. D. (1978). Predicting rainfall erosion losses-A guide to conservation planning. U.S. Department of Agricultural, Agricultural Handbook No. 537, 62.

Wolf, J., Bindraban, P., Luijten, J., & Vleeshouwers, L. (2003). Exploratory study on the land area required for global food supply and the potential global production of bioenergy. *Agricultural systems, 76*(3), 841-861.

Wu, M., Demissie, Y., & Yan, E. (2012). Simulated impact of future biofuel production on water quality and water cycle dynamics in the Upper Mississippi river basin. *Biomass and Bioenergy, 41*, 44-56.

Wu, Y., & Liu, S. (2012). Impacts of biofuels production alternatives on water quantity and quality in the Iowa River Basin. *Biomass and Bioenergy, 36*, 182-191.

Zavitkovski, J. (1978). *Biomass farms for energy production: biological considerations*. Paper presented at the SAF/CIF Annual Meeting, St. Louis, MO.

Zavitkovski, J. (1981). Characterization of light climate under canopies of intensively-cultured hybrid poplar plantations. *Agricultural Meteorology, 25*, 245-255.

CHAPTER 4. COMPARISON OF PERFORMANCE OF TILE DRAINAGE ROUTINES IN SWAT 2009 AND 2012 IN THE LITTLE VERMILLION RIVER WATERSHED

4.1 Abstract

Subsurface tile drainage systems are widely used in agricultural watersheds in the Midwestern U.S. Tile drainage systems enable the Midwest area to become highly productive agricultural lands, but also create environmental problems like nitrate-N contamination of the water drained. Soil and Water Assessment Tool (SWAT) has been used to model watersheds with tile drainage. However, SWAT2012 revision 615 and 645 provide new tile drainage routines, and only a few research have studied tile drainage impacts at both field and watershed scales. Moreover, SWAT2012 revision 645 improved the curve number calculation method based on soil moisture, which has not been fully tested. This study used long-term (1991-2003) field site and river station data from the LVR watershed to evaluate performance of tile drainage routines in SWAT2009 revision 528 (the old routine) and SWAT2012 revision 615 and 645 (the new routine). Both routines provided reasonable but not satisfactory uncalibrated flow and nitrate loss results. Calibrated monthly tile flow, surface flow, nitrate-N in tile and surface flow, sediment and annual corn and soybean yield results from SWAT with the old and new tile drainage routines were compared with observed values. Generally, the new routine provide acceptable simulated tile flow (NSE = 0.50 ~ 0.68), and nitrate in tile flow (NSE = 0.50 ~ 0.77) for both field sites with random pattern tile and constant tile spacing, while the old routine simulated tile flow (NSE = -0.77~ -0.20) and nitrate in tile flow results (NSE = -0.99 ~ 0.21) for the field site with constant tile spacing were unacceptable. The new modified curve number calculation method in revision 645 (NSE = 0.56 ~ 0.82) better simulated surface runoff than revision 615 (NSE = -5.95 ~ 0.5). Calibration provided reasonable parameter sets for the old and new routines in LVR watershed, and the

validation results showed that the new routine has the potential to accurately simulate hydrologic processes in mildly-sloped watersheds.

4.2 Introduction

Subsurface drainage systems are common practices in agricultural watersheds in the Midwest area of the US. With subsurface drainage systems, the soil horizontal hydraulic conductivity is greater and makes water drainage from soils to ditches or subsurface drains effective; the soil vertical hydraulic conductivity is large enough to usually prevent crop damage from flooding (Mitchell *et al*., 2003). In this way, subsurface drainage systems enable large regions of the Midwestern US to become some of the most productive agricultural lands. However, intensive tile drainage systems also create environmental problems, due to contaminants like nitrate-N and pesticides in the water they transport. Thus, it is important to accurately simulate tile drains in hydrological models to correctly predict the hydrologic processes and simulate the impacts of land cover and conservation practice changes at the watershed scale. Study on tile drainage simulation at a watershed scale using the new tile drainage routine in SWAT is limited. More information about application of realistic parameters for SWAT2012 tile drainage are needed.

4.2.1 Tile Drainage in the Midwest Area in the US

The Midwestern United States, including Illinois, Iowa, Indiana, Minnesota, Ohio, Michigan, Wisconsin and Missouri, have uneven drainage systems and poorly drained soils. These soils remain wet after rainfall events, preventing proper field management. Plant roots cannot obtain enough aeration in saturated soils, plant growth is under stress, and thus yields decrease. Consequently, extensive drainage networks have been built up since 1870 in the Midwest to alleviate the damage caused by uneven drainage (Jaynes and James, 2007). Subsurface drainage can allow excess water to leave the soil profile through a network of perforated tubes installed below the soil surface. Subsurface drainage plays an important role in water balance in the poorly drained soils of agriculture land, especially in the Midwest area of the USA. Water flows into the tubing through holes in the tube or the cracks between adjacent clay tiles and drains away when the water table in the soil is higher

than the tile. Tile drainage removes surplus water from fields, allows flexible field management and enhances crop production (U.S. Environmental Protection Agency). Tile drainage is widely used in much of the Upper Midwest area. For instance, over 40,468 km^2 (10 million acres) in Illinois have been tiled (University of Illinois Extension, 2014). Indiana is estimated to have more than 2.2 million hectares of land with tile drainage (Sugg, 2007).

4.2.1 Impacts of Tile Drainage on Hydrology and Water Quality

Drainage improvements today are usually aimed at increasing production of agricultural land. In many fields more tiles are have often been added in recent years to improve drainage efficiency (U.S. Environmental Protection Agency, 2014). For instance, the Little Vermilion River (LVR) watershed has altered hydrology from an extensive subsurface drainage system network, in which the soil vertical hydraulic conductivity is very high and can prevent plant damage from flooding. Additionally, Algoazany *et al.* (2007) assessed the transport of soluble P through subsurface drainage and surface runoff and found that crop, discharge and the interactions between sites had significant effects on soluble P concentrations in subsurface flow, and annual average soluble P mass loads in subsurface flow was substantially greater than that in surface runoff.

Subsurface tile drainage systems could increase nitrate and pesticide transport, because they move out of the soil surface and convey soluble nitrate-N from the crop root zone. Nitrate coming from tile drains has been considered as the main sources of nitrate in rivers and streams in the Midwestern US. Some studies have shown that artificial subsurface drainage could affect surface water and groundwater negatively (Fausey *et al.*, 1995; Shirmohammadi *et al.*, 1995; Gentry *el al.*, 2000; Kladivko *et al.*, 2001). An average of 23.2% of annual precipitation was drained to tiles on plots with corn and soybean in Indiana (Hernandez-Ramirez *et al.*, 2011). Additionally, 89%-95% of nitrate losses in a ditch catchment were transported by the tile drainage system of the catchment (Tiemeyer *et al.*, 2008).

Subsurface drainage plays a significant role in water balance in the poorly drained soils of agriculture land, especially in the Midwestern USA. For example, at the field scale, Lal *et al.* (1989) studied tillage-caused alterations in water infiltration, surface runoff, subsurface flow and sediment transport in surface and subsurface flow for a corn-soybean rotation in northwestern Ohio, and the results demonstrated that the percentage of annual precipitation drained by tiles in plowed conditions and on no-till plots are 33% to 58% and 28% to 59%, respectively. In terms of water quality, in-stream nitrate loading is particularly influenced by tile drainage. Generally, agricultural land with good subsurface drainage would reduce surface runoff, soil erosion and P loss, while increasing nitrate loss. Nitrate flows easily through the soil and into tile lines because of its high solubility and nitrite concentrations in subsurface drains are usually high (10-40 mg/L) (U.S. Environmental Protection Agency, 2014).

Oversupply of nutrients from multiple sources has become an increasing concern around the globe, which impacts shallow coastal areas. The impacts include aquatic habitat loss, reduced light penetration and hypoxia. The northern Gulf of Mexico, the largest zone of oxygen-depleted coastal waters in the U.S, is affected by the water discharge and nutrient loads of the Mississippi River (Diaz and Solow, 1999; Rabalais *et al.*, 1999).

4.2.2 Tile Drainage Routine Development in SWAT

Tile drainage has been simulated in SWAT since its early versions. Arnold *et al.* (1999) enhanced SWAT2000 with a subsurface tile flow component and tested the enhanced model at a field scale with satisfactory results. However, because pothole impacts had not been included in SWAT2002 and the tile drainage routines were old, the SWAT2002 tile drainage method was not adequate to simulate subsurface flow and stream discharge at a watershed scale (Arnold *et al.*, 1999; Du *et al.*, 2005). Equation (4.1) (Neitsch *et al.*, 2002) used for tile drainage simulation in SWAT2002 is:

$$tile_{wtr} = \left(SW_{ly} - FC_{ly}\right) \times \left(1 - exp\left[\frac{-24}{t_{drain}}\right]\right) \quad if\ SW_{ly} > FC_{ly} \quad (4.1)$$

where $tile_{wtr}$ is the amount of water removed from the layer on a given day by tile drainage (mm H_2O), SW_{ly} is the water content of the layer on a given day (mm H_2O), FC_{ly} is the field capacity water content of the layer (mm H_2O), and t_{drain} is the time required to drain the soil to field capacity (hrs) (Neitsch *et al.*, 2002).

Du *et al.* (2005) created an impervious layer and improved the simulation of water table dynamics, and monthly flow and subsurface tile drainage simulated by SWAT2005 are much better than those simulated by SWAT2000. The time to drain soils to field capacity (TDRAIN) was used to determine the flow rate. Additionally, a new coefficient GDRAIN, the drain tile lag time was introduced and used as the portion of the flow from tile drains into the streams on a daily basis (Du *et al.*, 2006). Some studies have shown that the tile drainage routine in SWAT2005 could simulate the influence of subsurface drainage on hydrology at a watershed scale (Sui and Frankenburger, 2008; Koch *et al.*, 2013). However, using only a drawdown time (TDRAIN) method to simulate tile drains is simplified and limited. Equation (4.2) (Neitsch *et al.*, 2005) used for tile drainage simulation in SWAT2005 is:

$$tile_{wtr} = \left(\frac{h_{wtbl}-h_{drain}}{h_{wtbl}}\right) \times (SW - FC) \times \left(1 - exp\left[\frac{-24}{t_{drain}}\right]\right) \quad if\ h_{wtbl} > h_{drain} \quad (4.2)$$

where $tile_{wtr}$ is the amount of water removed from the layer on a given day by tile drainage (mm H_2O), h_{wtbl} is the height of the water table above the impervious zone (mm), h_{drain} is the height of the tile drain above the impervious zone (mm), SW is the water content of the profile on a given day (mm H_2O), FC is the field capacity water content of the profile (mm H_2O), and t_{drain} is the time required to drain the soil to field capacity (hrs) (Neitsch *et al.*, 2005).

A new drainage routine which includes the use of the Hooghoudt and Kirkham drainage equations was developed by Moriasi to simulate real-world drainage systems more accurately (Moriasi *et al.* 2007a; Moriasi *et al.* 2012). Based on measured flow data from the South Fork Watershed in Iowa, the capability of SWAT with the new tile drain equations was evaluated. The water balance components were simulated, and the results

showed that the modified SWAT with the Hooghoudt steady-state and Kirkham tile drain equations simulated flow well (Moriasi *et al.* 2012). The new tile drainage routines (Equation (4.3), (4.4) (4.5)) incorporated into SWAT2005 are shown below.

When the water table is below the surface and ponded depressional depths are below a threshold, the Hooghoudt steady state equation is used to compute drainage flux:

$$q = \frac{8K_e d_e m + 4K_e m^2}{L^2} \quad (4.3)$$

where q is the drainage flux (mm/h), m is the midpoint water table height above the drain (mm), K_e is the effective lateral saturated hydraulic conductivity (mm/h), L is the distance between drains (mm), and d_e is the equivalent depth of the impermeable layer below the tile drains (Moriasi *et al.*, 2012; Moriasi *et al.*, 2013).

When the water table completely fills the surface and the ponded water remains at the surface for long periods of time, drainage flux is computed using the Kirkham equation (Moriasi *et al.* 2012; Moriasi *et al.*, 2013):

$$\mathrm{q} = \frac{4\pi K_e (t + b - r)}{\delta L} \quad (4.4)$$

where t is the average depressional storage depth (mm), b is the depth of the tile drain from the soil surface (mm), r is the radius of the tile drain (mm), and δ is a dimensionless factor, determined by an equation developed by Kirkham (1957).

When predicted drainage flux is greater than the drainage coefficient, then the drainage flux is set equal to the drainage coefficient:

$$q = DC \quad (4.5)$$

where q is the drainage flux (mm/h) and DC is drainage coefficient (mm/d) (Moriasi *et al.* 2012; Moriasi *et al.*, 2013).

Additionally, the drainage coefficient (DRAIN_CO) has been included in the new tile drainage routine in SWAT2012 to control peak drain flow. However, research on

simulation of tile flow by the new tile drainage routine is limited. Boles (2013) parameterized the new tile drainage simulation method in SWAT2012 and found that peak tile flow could decrease when moving from SWAT2009 to SWAT2012, because the peaks decreased and the tiles flowed for a longer period of time. Thus, it is necessary to test and calibrate the new drainage routines in a tile-drained watershed and compare the modeled results by the new tile drainage routines with those by the old routines. Thus, realistic parameters can be selected based on the physical condition and the impacts of tile drainage on water balance and nutrient loading can be predicted realistically.

4.2.3 Tile Drainage Simulation at the Watershed Scale by SWAT

SWAT can be used to simulate tile drains since early versions, but studies on simulation of tile drainage impact at the watershed scale are few (Arnold *et al*., 1998). For instance, Macrae *et al*. (2007) examined seasonal variability in the contribution of tile drains to hydrologic discharge and P export within a basin over a period of one year and found that 42% of annual flow and 43% of total P originated from tile drainage system in a watershed near Maryhill, Ontario. Additionally, Sui and Frankenburger (2008) quantified the impact of tile drains on nitrate loss in a heavily drained watershed, Sugar Creek watershed in Indiana, and showed that modeled nitrate loss results by SWAT2005 could be used for simulation of potential nitrate reductions at the watershed level. Moreover, Moriasi *et al*. (2012) used new tile drain equations in SWAT to evaluate hydrology of the South Fork Watershed in Iowa and determined a range of values for the new tile drain parameters, finding that Hooghoudt steady-state and Kirkham tile drain equations could be alternative tile drain simulation methods in SWAT. Boles (2013) tested a new tile drainage routine in the St. Joseph watershed in Indiana using SWAT and found that the new tile drainage routine in SWAT2012 has the potential to predict tile flow and nitrate transported by tiles. Since tile drainage has impacts on hydrology and nutrient loads at the watershed scale, it is important to accurately simulate tile drains in hydrological models to correctly predict the hydrologic processes and simulate the impacts of land cover and conservation practices changes at the watershed scale. More information about application of realistic parameters for SWAT2012 tile drainage are needed.

4.2.4 Goal of the Work

This goal of this study is to compare simulated flow, tile flow, runoff, nitrate in tile flow and sediment load results for the new tile drainage routines in SWAT2012 and the old one in SWAT2009 in the Little Vermilion River (LVR) watershed and determine which routine provides a better model fit with observed values. This can allow selection of the most appropriate tile drainage routine suitable for modeling mildly-sloped watersheds in the Midwest with subsurface drainage systems.

4.3 Materials and Methods

4.3.1 Study Area

The LVR watershed is located in east-central Illinois and drains approximately 518 km^2, and the dominant crops are corn and soybeans (Illinois Environmental Protection Agency, 2008). Eighty five percent of watershed area is in eastern Vermilion County, 13% of the watershed is in Champaign County, and 2% of the watershed is in Edgar County. The LVR watershed consists of flat topography, with elevations ranging from 235 meters in the headwaters to 174 meters at the outlet of the watershed and with average slope reaching at most 1% (Zanardo *et al.*, 2012) (Figure 4.1).

The watershed was subdivided into two subwatersheds based on their respective Illinois water body segment identification, corresponding to the upstream contributing areas of Georgetown Lake and the Little Vermilion River. Ninety percent of the LVR watershed is agricultural land used for corn and soybean production, and the remainder consists of grassland, forest land, roadways and farmsteads (Kalita *et al.*, 2006) (Figure 4.2). Annual area planted to soybeans is equal to the area for corn planting (Algoazany *et al.*, 2007). The dominant soil associations in the LVR watershed are Drummer silty clay loam and Flanagan silt loam (Zanardo *et al.*, 2012; Keefer, 2003), and the dominant hydrologic soil groups are B and C.

The LVR watershed is a typical tile-drained watershed in Illinois (Figure 4.3). Based on years of field observation data from the LVR watershed in Illinois, Mitchell *et al.* (2003) and Kalita *et al.* (2006) studied hydrology of flat upland watersheds in Illinois and

demonstrated that the water could remain ponded on the soil surface until it would evaporate, seep or flow to the subsurface when the rainfall rate exceeds the infiltration rate of rainfall events, and surface runoff could flow into the streams directly during extremely large rainfall events.

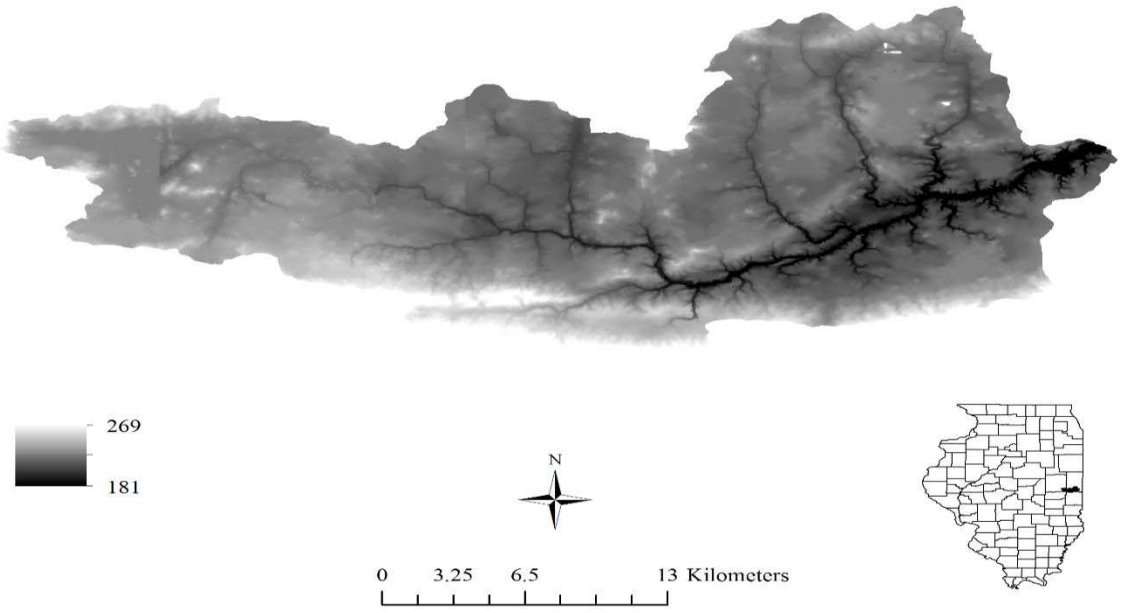

Figure 4.1 Elevation of the LVR watershed

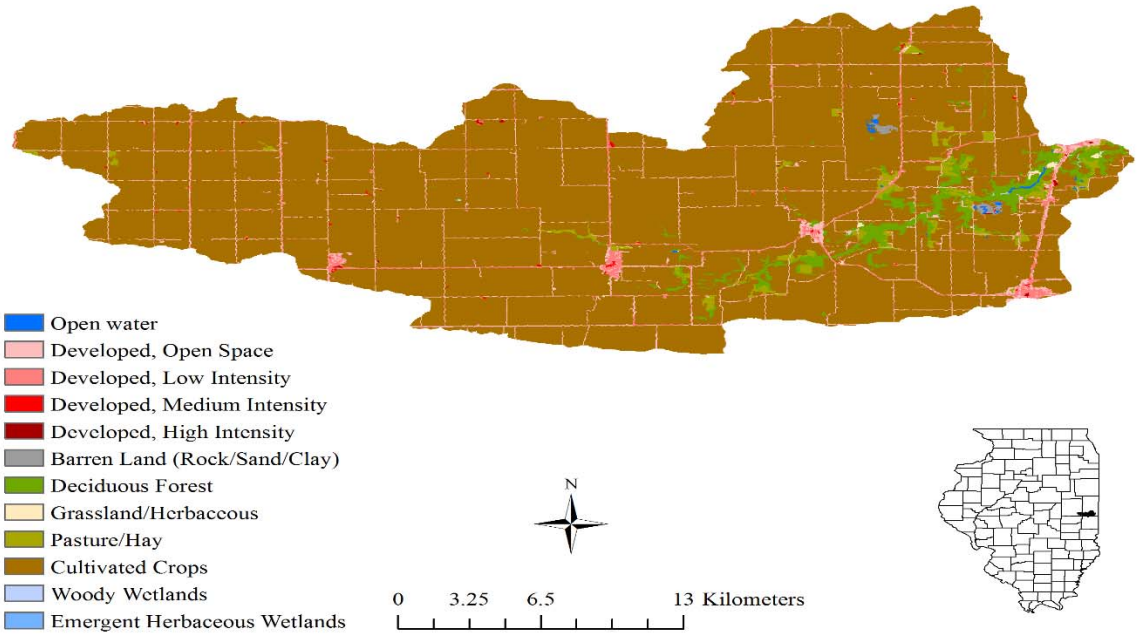

Figure 4.2 Land cover of the LVR watershed

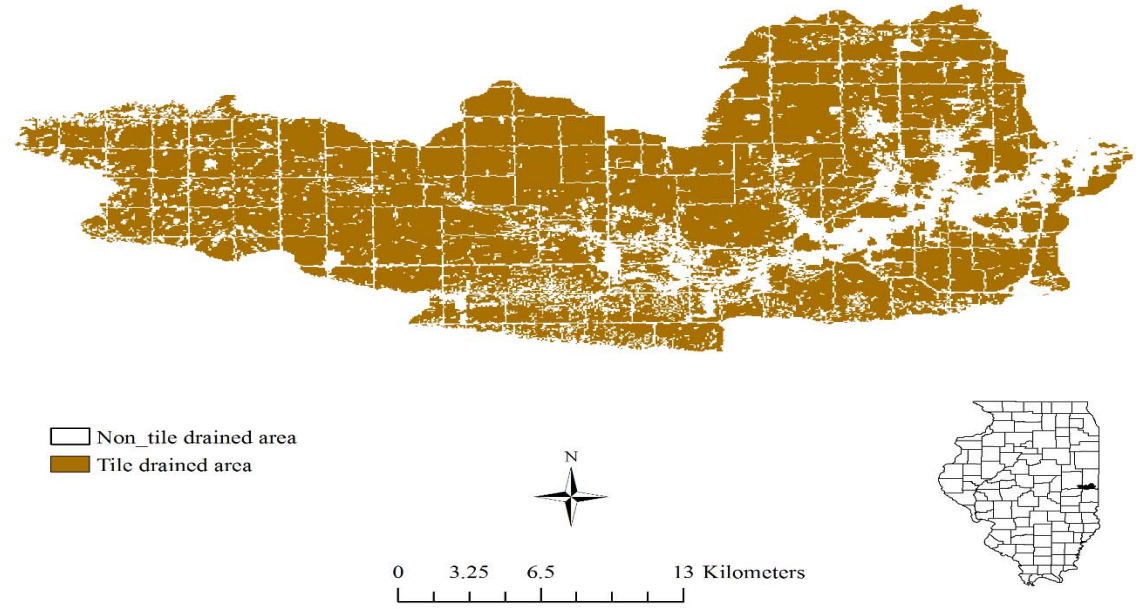

Figure 4.3 Tile drained area in the LVR watershed

4.3.2 Monitored Sites and Data for Model Setup

A long-term (1991-2003) monitoring project was conducted, and water quantity and quality data were collected from several subsurface stations, surface stations, river stations and wetland sites in the LVR watershed (Mitchell *et al.*, 2003; Kalita *et al.*, 2006). Two subsurface stations, B and E, two surface runoff stations, Bs and Es, and one river station, R5, with drainage areas of 0.03, 0.076, 0.03, 0.023, and 69 km^2, were selected for this study (Figure 4.4 and Table 4.1) Subsurface sites B and E were close to surface station Bs and Es, respectively. B and E had similar land use, cropping system and tile drainage systems with Bs and Es, respectively (Table 4.1). Elevation, soil, land use and weather data were used for SWAT model setup (Table 4.2). Daily water discharge data were monitored at subsurface, surface runoff, and river stations. Water samples were obtained bi-weekly, and additional samples were taken by pump samplers during increased flow (Kalita *et al.*, 2006). Daily nitrate and sediment load was computed by multiplying water discharges with nitrate concentration (Yuan *et al.*, 2000). Nitrate and sediment concentrations were not measured every day that water discharge occurred, and collected data contained more water discharge measurements than nitrate and sediment concentration. Nitrate and sediment load during a time period was computed by multiplying the concentration at a specific time by half the flow volume since the last concentration measurement plus half the flow volume from the concentration measurement to the next concentration measurement (Kalita *et al.*, 2006).

Daily tile flow, surface runoff, nitrate load in tile flow, surface runoff, and streamflow, and sediment load in surface runoff and streamflow were aggregated into monthly data and adopted in this study for model calibration and validation (Table 4.2). Other stations were not considered due to the quality of their data (Zanatdo *et al.*, 2012). Corn and soybean planting, harvest and tillage practice data were collected from landowners (Table 4.3).

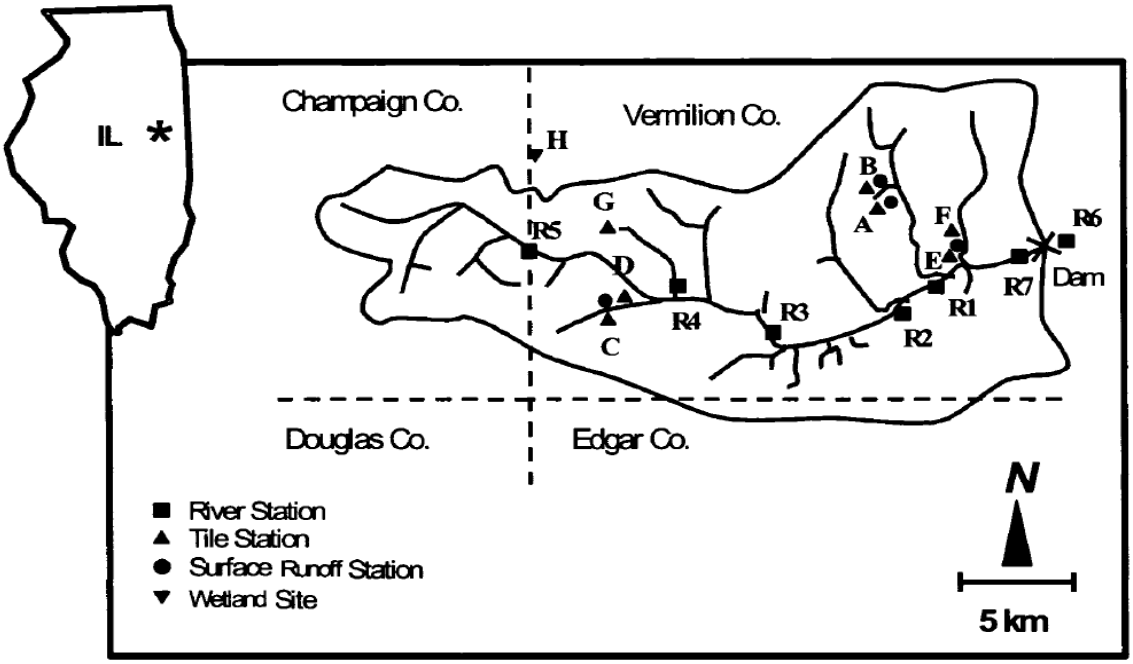

Figure 4.4 Monitored subsurface, surface and river stations in the LVR watershed (adapted from Algoazany et al., 2006)

Table 4.1 Monitored subsurface, surface and river stations in the LVR watershed

Site	Soils	Station	Drainage system	Cropping
B	Drummer silt clay loam	Subsurface	Random tile drainage tubing systems in depressional areas	Reduced-Tillage
Bs	Flanagan silt loam	Surface		Beans-Corn
E	Sabina silt loam	Subsurface	Complete tile drainage system at 28-m spacing	No-Tillage
Es	Xenia silt loam	Surface		Corn-Beans
R5	-	River	Random tile systems	

Table 4.2 Data for tile drainage simulation by SWAT

Data type	Source	Format	Date
Elevation	[1]USGS The National Map Viewer	30m Raster	
[2]SSURGO	[3]USDA Web Soil Survey	Polygon Shapefile	
LULC	[1]USGS The National Map Viewer	Raster	2006
Temperature, solar radiation, relative humidity and wind speed	[4]ISWS	Tabular data	1991 - 2003
Precipitation	[5]UIUC	Tabular data	1991 - 2003
Corn and soybean yield, planting, harvest, fertilization and tillage for sites B and E	[5]UIUC	Tabular data	1991- 2003
Tile flow, nitrate in tile flow, site B	[5]UIUC		1992 – 2003*
Tile flow, nitrate in tile flow, site E	[5]UIUC		1991 - 2002
Surface runoff, sediment and NO3 in runoff for sites Bs and Es	[5]UIUC		1993 - 2003
Flow, and sediment and NO3 in flow for site R5	[5]UIUC		1993 - 2003

[1]USGS: U.S. Geological Survey
[2]SSURGO: Soil Survey Geographic Database
[3]USDA: U.S. Department of Agriculture
[4]ISWS: Illinois State Water Survey
[5]UIUC: University of Illinois at Urbana Champaign, USA
* Tile flow data during 2000 for site B was corrupted and was not used in this study.

Table 4.3 Cropping and tillage practices for sites B and E in the LVR watershed

Year	Crop	Planting date	Harvest date	Tillage type
Site B				
1991	Soybean	05/08	09/21	Reduced tillage-chisel plowed, disked, or field cultivated
1992	Corn	04/30	10/06	
1993	Soybean	05/17	09/30	
1994	Corn	04/21	09/13	
1995	Soybean	06/04	10/02	
1996	Corn	04/18	09/19	
1997	Soybean	04/29	09/26	
1998	Corn	04/26	09/23	
1999	Soybean	05/07	09/19	
2000	Corn	04/13	09/19	
2001	Soybean	04/30	09/27	
2002	Corn	05/21	10/01	
2003	Soybean	05/22	10/01	

Table 4.3 Continued.

Site E				
1991	Corn	04/26	10/08	No tillage
1992	Soybean	05/16	10/06	
1993	Corn	05/17	11/08	
1994	Soybean	06/03	10/06	
1995	Corn	05/05	10/17	
1996	Soybean	06/25	10/17	
1997	Corn	04/23	10/15	
1998	Soybean	05/29	09/28	
1999	Corn	04/29	11/09	
2000	Soybean	05/16	10/04	
2001	Corn	04/24	10/29	
2002	Soybean	06/04	10/01	
2003	Corn	04/24	10/27	

4.3.3 Modification to the Soil Moisture Retention Parameter Calculation Method

The tile drainage routine based on drawdown time in SWAT2009 Revision 528 (Rev.528) was called the "old routine" in this study. The tile drainage routine based on the Hooghoudt and Kirkham equations with a drainage coefficient in SWAT2012 Revision 615 (Rev.615) was called the "new routine" in this study. SWAT Revision 645 (Rev.645) added a retention parameter adjustment factor (R2ADJ) to Rev.615 to modify the soil moisture retention parameter calculation method (Equations (4.6) and (4.7)) (Neitsch *et al.*, 2011).

$$S = 25.4\left(\frac{1000}{CN} - 10\right) \quad (4.6)$$

$$S = S_{max}\left(1 - \frac{SW}{[SW + exp(w_1 - w_2 * SW)]}\right) \quad (4.7)$$

Where S is the retention parameter for a given day (mm), CN is the curve number for the day, S_{max} is the maximum value the retention parameter can achieve on any given day (mm), SW is the soil water content of the entire profile excluding the amount of water held in the profile at wilting point (mm H_2O), and w_1 and w_2 are shape coefficients.

$$w_2 = \frac{\left(Log\left(\frac{SW_{fc}}{rto3} - SW_{fc}\right) - Log\left(\frac{SW_{sa}}{rtos} - SW_{sa}\right)\right)}{(SW_{sa} - SW_{fc})} \quad (4.8)$$

$$w_1 = Log\left(\frac{SW_{fc}}{rto3} - SW_{fc}\right) + (SW_{fc} \times w_2) \quad (4.9)$$

rto3 is the fraction difference between CN III and CN I retention parameters, rtos is the fraction difference between CN=99 (CN_{max}) and CN I retention parameters, SW_{fc} is amount of water held in soil profile at field capacity, SW_{sa} is amount of water held in the soil profile at saturation.

In Rev.645, R2ADJ was used to modify shape coefficients, w1 and w2, to increase S and thus decrease CN. R2ADJ ranges from 0 to 1. When R2ADJ is 0, CN II is calculated as soil at field capacity. When R2ADJ is 1, CN II is calculated as soil saturation (Figure 4.5). In this case, CN is decreased gradually based on soil from capacity to saturation, which is more reasonable than decreasing CN directly. This modification is suitable for surface runoff simulation at mildly-sloped watersheds.

$$MSW_{fc} = SW_{fc} + R2ADJ \times (SW_{sa} - SW_{fc}) \quad (4.10)$$

$$w_2 = \frac{\left(Log\left(\frac{MSW_{fc}}{rto3} - MSW_{fc}\right) - Log\left(\frac{SW_{sa}}{rtos} - SW_{sa}\right)\right)}{(SW_{sa} - MSW_{fc})} \quad (4.11)$$

$$w_1 = Log\left(\frac{MSW_{fc}}{rto3} - MSW_{fc}\right) + (MSW_{fc} \times w_2) \quad (4.12)$$

MSW_{fc} is the modified amount of water held in the soil profile at field capacity, and R2ADJ is the newly added retention parameter adjustment factor.

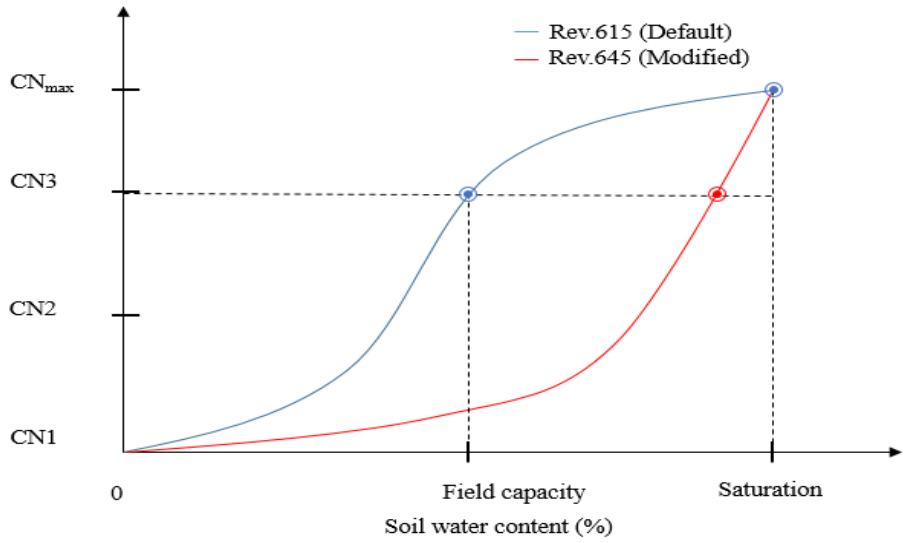

Figure 4.5 Curve number calculation methods based on soil moisture retention curve

4.3.4 Model Setup

SWAT2012 in conjunction with ArcGIS10.1 was used to simulate the LVR watershed. The 30 m National Hydrography Dataset (NHD) was used to burn a clipped stream layer for the LVR watershed into the simulation and subbasins in the LVR watershed were delineated. Landuse data (NLCD 2006) for the study area was obtained from USGS. The National Map Viewer and SSURGO from USDA Web Soil Survey was added into ArcSWAT (Table 4.2). HRUs were defined using the following thresholds: 0% landuse, 10% soil and 0% slope.

Daily precipitation data from rain gauge station at sites B, E and 6 km southeast of site R5 were added in ArcSWAT and used for simulation at sites B and Bs, sites E and Es, and site R5, respectively (Table 4.2). Daily temperature, solar radiation, wind speed and relative humidity data from a station closest to the LVR watershed were used (Table 4.2).

Management operation data for corn and soybean growth at sties B and E were collected (Table 4.3). 218 kg/ha Anhydrous ammonia and 67 kg/ha P_2O_5 fertilizer were applied 10 days before planting, and 2.2 kg/ha Atrazine was applied three days before planting during corn growing years. 56 kg/ha P_2O_5 fertilizer was applied 14 days before planting during soybean production years.

Tile drainage was assumed in HRUs where corn or soybeans were the current land use, slope lower than 5%, and soil drainage was somewhat poorly drained, poorly drained, or very poorly drained (Sugg, 2007; Sui and Frankenberger, 2008; Boles *et al.*, 2015), and 75% of the watershed was tile drained (Figure 4.3).

4.3.5 Parameter Adjustments before Model Calibration

Plant growth parameters for corn and soybean growth simulation at sites B and E were adjusted. BIO_E and HVSTI values for corn growth ranged from 32 to 39, and from 0.41 to 0.54, respectively, from various studies (Kiniry *et al.*, 1998; Linquist *et al.*, 2005; Edwards *et al.*, 2005; Ciampitti *et al.*, 2012). BIO_E and HVSTI values for soybean growth ranged from 13.2 to 25.2, and from 0.44 to 0.59, respectively (Sinclair and Muchow 1999; Edwards and Purcell, 2005; Mastrodomenico and Purcell, 2012).

The plant growth parameters for corn and soybean growth simulation of sites B and E were adjusted (Table 4.3). Cibin *et al* (2015) adjusted radiation use efficiency (BIO_E) and potential heat units (PHU) for corn growth, and PHU, minimum temperature for plant growth (T_BASE), harvest index (HVSTI), normal fraction of phosphorus in yield (CPYLD) for soybean growth (Table 4.4) to compare with county level yield data for two watersheds in the Midwest USA. This study adopted the same adjustment for corn and soybean growth simulation.

Table 4.4 Adjusted parameter values for corn and soybean growth simulation

Parameter	Description	Initial value	Adjusted value Rev. 615
BIO_E	Radiation-use efficiency ((kg/ha)/(MJ/m^2))	39 (corn) 25 (soybean)	36 (corn) 25 (soybean)
PHU	Potential heat units	1556 (corn) 1556 (soybean)	1500 (corn) 1250 (soybean)
T_BASE	Minimum temperature for plant growth (°C)	8 (corn) 10 (soybean)	8 (corn) 8 (soybean)
HVSTI	Harvest index for optimal growing conditions	0.5 (corn) 0.31 (soybean)	0.5 (corn) 0.40 (soybean)
CPYLD	Normal fraction of phosphorus in yield (kg P/kg yield)	0.0016 (corn) 0.0091 (soybean)	0.0016 (corn) 0.0067 (soybean)

Tile drainage simulation parameters were adjusted for the new routine. For Rev.615 and Rev.645, tile depth ranged from 1.05 m to 1.1 m at various sites (Drablos *et al.*, 1988, Singh *et al.*, 2001), and tile depth (DDRAIN) was set as 1.075 m in the model. The maximum depressional storage selection flag/code ISAMX was used to control the method used to calculate the static maximum depressional storage parameter (SSTMAXD), representing the surface storage. When ISMAX is 0, SSTMAXD is allowed to be defined by the user while when ISMAX is 1, SSTAMXD is dynamically calculated based on rainfall and tillage practices (Moriasi *et al.*, 2007a; 2012). In this study, ISMAX was set as 0 and SSTMAXD was set as 12mm, based on previous DRAINMOD (Skaggs *et al.*, 2012) and SWAT studies (Boles *et al.*, 2015). Drainage coefficient (DRAIN_CO), the amount of water drains in 24 hours, was set as 20 mm/day, describing the size of the main collector drain pipes and the outlet (Sui and Frankenberger, 2008).

4.3.6 Model Calibration and Validation

Rev.528, Rev.615 and Rev.645 simulated tile flow at sites B and E were compared with the observed values to evaluate tile drainage simulation performance of the old and new routine and the new routine with modified curve number calculation method. Rev.528 and Rev.615 simulated nitrate in tile flow at sites B and E were compared with the observed values to evaluate nitrate in tile flow simulation performance of the old and the new routines. Rev.615 and Rev.645 simulated surface runoff at site Bs and Es were compared with the observed values to evaluate surface runoff simulation performance of the default soil moisture based curve number calculation method and modified curve number calculation method. Rev.528 and Rev.645 simulated flow at site R5 were compared with the observed values to evaluate flow simulation performance of the old and new routine. Rev.645 was not used for flow simulation at river station R5, because Rev.645 could not run successfully for the mainly tile drained river station R5. DEP_IMP values were too low and impervious layer was too close to the soil profile, may have influence on functionality of Rev.645 in simulating ground water and tile flow, and it has been debugging so far.

The model was run for a total of 19 years (1985-2003). The first five years (1985-1990) were for model warm-up. Model outputs, annual corn and soybean yield from 1991 to

1997, and from 1998 to 2003 at sites B and E were compared with the observed values for model calibration and validation, respectively. Monthly tile flow and nitrate in tile flow from 1992 to 1997 and from 1998 to 2003 at site B were compared with the observed values for model calibration and validation, respectively. Monthly tile flow and nitrate in tile flow from 1991 to 1997 and from 1998 to 2002 at site E were compared with the observed values for model calibration and validation, respectively. Monthly surface runoff, sediment and nitrate in surface runoff at sites Bs and Es, and monthly flow, sediment and nitrate in flow at site R5 from 1993 to 1997 and from 1998 to 2003 were compared with the observed values for model calibration and validation, respectively.

The model was autocalibrated using SWATCUP_5.1.6.2 (SUFI-2). Parameters related to surface runoff, tile drainage, evapotranspiration (ET), snow, ground water, soil water, sediment losses, and nitrate loss processes were selected during model calibration (Table 4.5). Ranges of parameters (Table 4.6) were determined based on previous DRAINMOD studies in LVR watershed (Singh *et al.*, 2001) and several tile drain studies in Iowa (Singh *et al.*, 2006; Singh *et al.*, 2007; Schilling and Helmers, 2008; Singh and Helmers, 2008; Moriasi *et al.*, 2012; Moriasi *et al.*, 2014) and Indiana (Boles, 2013).

For Rev.528, calibrated values for tile flow simulation parameters at site B, TDRIAN, GDRIAN, and DEP_IMP were used for flow simulation at site R5. For Rev.615, calibrated values for tile flow simulation parameters at site B, DEP_IMP, LATKSATF and SDRAIN were modified at site R5, to accurately simulate flow and obtain reasonable water budget results (Table 4.6).

Table 4.5 Parameters used for various processes during model calibration

Parameter	Description	Process
ICN	CN method flag: 0 use traditional SWAT method, which bases CN on soil moisture, 1 use method which bases CN on plant ET	Surface runoff
CN2	Soil moisture condition II curve number	
CNCOEF	Plant ET curve number coefficient	
R2ADJ	Curve number retention parameter adjust factor	
SURLAG	Surface runoff lag coefficient	

Table 4.5 Continued.

TDRAIN	Time to drain soil to field capacity (hours)	Tile drains
GDRAIN	Drain tile lag time (hours)	
DEP_IMP	Depth to impervious layer (mm)	
LATKSATF	Multiplication factor to determine lateral saturated hydraulic conductivity	
SDRAIN	Tile spacing (mm)	
SOL_K(1)	Saturated hydraulic conductivity (mm/hr)	
ESCO	Soil evaporation compensation factor	Evapotranspiration
SFTMP	Snowfall temperature (℃)	Snow
SMTMP	Snow melt base temperature (℃)	
GW_DELAY	Groundwater delay time (days)	Groundwater
RCHRG_DP	Deep aquifer percolation fraction	
SOL_AWC(1)	Available water capacity of the soil layer (mm H_20/ mm soil)	Soil water
ADJ_PKR	Peak rate adjustment factor for sediment routing in the subbasin (tributary channels)	Sediment losses
SPEXP	Exponent parameter for calculating sediment reentrained in channel sediment routing	
CH_COV1	Channel erodibility factor	
HRU_SLP	Average slope steepness (m/m)	
SLSUBBSN	Average slope length (m)	
USLE_K	USLE equation soil erodibility (K) factor (0.013 (metric ton m^2 hr)/(m3-metric ton cm))	
USLE_C	Minimum value of USLE C factor for water erosion applicable to plant	
CMN	Rate factor for mineralization for the humus active organic nutrients (N)	Nitrate losses
RCN	Concentration of nitrogen in rainfall (mg N/L)	
NPERCO	Nitrogen concentration reduction coefficient	
SDNCO	Denitrification threshold water content	
CDN	Denitrification exponential rate coefficient	

4.3.7 Model Performance Evaluation

Model outputs, annual corn and soybean yield, monthly tile flow and nitrate in tile flow at sites B and E, monthly surface runoff, sediment and nitrate in surface runoff at sites Bs and Es, and monthly flow, sediment and nitrate in flow at site R5 from the old and new routines were compared with observed values for model calibration and validation. Comparison between simulated results from the old and new routine and observed values were plotted. The differences between simulated tile flow results at sites B and E and flow results at site R5 with observed values were plotted. The statistical methods used for verifying the model performance included Percent bias/Percent error (P_{BIAS} (%)), the coefficient of

determination (R^2), the Nash-Sutcliffe model efficiency coefficient (NSE), the modified NSE (MSE) and the Kling-Gupta efficiency (KGE) (Equations (4.13), (4.14), (4.15), (4.16) and (4.17)).

$$P_{BIAS}\ [\%]\ =\ \frac{\sum_{i=1}^{n}(Observed\ data-Simulated\ data)}{\sum_{i=1}^{n}Observed\ data}\times 100 \quad (4.13)$$

$$\mathrm{NSE}\ =1-\frac{\sum_{i=1}^{n}(Observed\ data-Simulated\ data)^2}{\sum_{i=1}^{n}(Observed\ data-\overline{Observed\ data})^2} \quad (4.14)$$

$$R^2=\frac{\left[\sum_{i=1}^{n}(\mathrm{Observed\ data}-\overline{\mathrm{Observed\ data}})(\mathrm{Simulated\ data}-\overline{\mathrm{Simulated\ data}})\right]^2}{\sum_{i=1}^{n}(\mathrm{Observed\ data}-\overline{\mathrm{Observed\ data}})^2\sum_{i=1}^{n}(\mathrm{Simulated\ data}-\overline{\mathrm{Simulated\ data}})^2} \quad (4.15)$$

$$\mathrm{MSE}\ =1-\frac{\sum_{i=1}^{n}(Observed\ data-Simulated\ data)^2}{\sum_{i=1}^{n}(Observed\ data-\overline{Observed\ data})^2} \quad (4.16)$$

$$\mathrm{KGE}\ =\ 1-\sqrt{(r-1)^2+(\alpha-1)^2+(\beta-1)^2} \quad (4.17)$$

Where $\alpha=\frac{\sigma_{Simulated\ data}}{\sigma_{Observed\ data}}$, and $\beta=\frac{\mu_{Simulated\ data}}{\mu_{Observed\ data}}$, and r is the linear regression coefficient between simulated and observed data (Equation (4.15)).

Percent bias (Gupta *et al*., 1999) can measure the average tendency of the simulated data to deviate from the observed data. A value of 0.0 is the optimal for P_{BIAS}, representing accurate model simulation. Negative values represent model overestimation bias and positive values indicate model underestimation bias. If P_{BIAS} ± 25% for streamflow, ± 55% for sediment, and ± 70% for N and P, model simulation results can be considered satisfactory (Moriasi *et al*., 2007b). The R^2 value can indicate the strength of the linear relationship between the observed and simulated data. A R^2 value of greater than 0.5 is considered reasonable model performance (Moriasi *et al*., 2007b). The NSE (Nash and Sutcliff, 1970) can represent how well the plot of observed versus simulated data fits the 1:1 line. The NSE value ranges from -∞ to 1, and the optimal value is 1. A NSE value of greater than 0.5 is considered satisfactory model performance (Moriasi *et al*., 2007b). A NSE value of 0 means that the simulated values are as accurate as the mean of the observed data, and a negative NSE value indicates that the mean observed value is a better predictor

than the simulated value, meaning unacceptable performance (Moriasi *et al*., 2007b). 0.36 $\leq$ NSE $\leq$ 0.72 and NSE $\geq$ 0.75 also have been considered as satisfactory and good simulated results, respectively (Larose *et al*., 2007; Van Liew and Garbrecht, 2003). A modified form of the NSE (Equation (4.12)) could decrease the oversensitivity of the NSE to extreme values (Krause *et al*., 2005), and is sensitive to chronic over- or under predictions. The KGE computes the Euclidian distance of the correlation, the bias, and a measure of variability. The use of KGE (Equation (4.13)) improves the bias and the variability measure considerably and decreases the correlation slightly to the NSE (Gupta *et al*., 2009). The KGE value ranges from -∞ to 1. Essentially, the closer to 1, the more accurate the model is. A KGE value of greater than 0.5 is considered satisfactory model performance (Gupta *et al*., 2009).

4.4 Results and Discussion

4.4.1 Calibrated Parameter Values

Parameter ranges and calibrated parameter values for tile flow and nitrate in tile flow simulation at subsurface sites B and E, runoff, sediment and nitrate in runoff simulation at surface sites Bs and Es, and flow, sediment and nitrate in flow simulation at river station R5 (Table 4.6).Curve number calculation based on soil moisture (ICN=0) and plant ET (ICN=1) methods were included in model calibration. For Rev.528 and Rev.615, calibrated Curve number (CN2) values ranged from 60 to 65 to accurately simulate surface runoff at field sites, and were reduced by 20% to accurately simulate streamflow at the river station, which were reasonable for a watershed dominated by agricultural land. For Rev.645, calibrated values of newly added curve number calculation retention parameter adjustment factor (R2ADJ) ranged from 0.81 to 0.97 at field sites. In this case and CN2 value was set as soil water content near saturation (Equation (4.8) and Figure 4.5), which was reasonable for mildly-sloped watershed with low runoff. The calibrated parameter sets provide guidance for accurate simulation of tile drainage systems in hydrologic process at field and watershed scales, and can be used for tile flow, runoff, and sediment and nitrate losses simulation of mildly-sloped watersheds in the Midwest.

Table 4.6 Calibrated values of adjusted parameters for tile flow and nitrate-N calibration of SWAT at sites B, E, Bs, Es and R5

Parameter	Range	Calibrated value											
		Site B			Site E			Site Bs		Site Es		Site R5	
		528	615	645	528	615	645	615	645	615	645	528	615
ICN		1	1	0	0	0	0	0	0	0	0	1	0
CN2	-0.2~-0.1	61	63	-	64	65	-	60	-	60	-	-0.2	-0.2
CNCOEF	0.5~2	0.83	0.98	-	-	-	-	-	-	-	-	0.58	-
R2ADJ	0~1	-	-	0.96	-	-	0.97	-	0.88	-	0.81	-	-
SURLAG	0.5~2	1.91	1.62	0.97	0.61	1.59	0.73	1.78	1.80	1.82	1.83	0.77	1.03
TDRAIN (hrs)	24~48	26	-	-	25	-	-	-	-	-	-	26	-
GDRAIN	24~48	25	-	-	26	-	-	-	-	-	-	25	-
DEP_IMP	1200~3500	3400	2300	2600	2100	1200	1500	3400	2000	3100	1900	3600	2700
LATKSATF	0.01~4	-	2.2	1.02	-	0.07	0.26	1.68	0.48	1.89	0.28	-	1.05
SDRAIN	25000~50000	-	33000	37000	-	28000	28000	36000	29000	29000	41000	-	38000
SOL_K(1)	-0.8~0.8	-0.24	0.68	-0.79	0.32	-0.62	0.62	0.03	0.52	-0.17	0.36	-0.26	0.07
ESCO	0.8~0.99	0.94	0.95	0.86	0.82	0.88	0.91	0.85	0.85	0.90	0.95	0.93	0.98
SFTMP	-5~5	-1.79	2.77	-4.47	-1.99	1.34	3.35	-4.96	4.37	4.53	3.97	0.58	-4.25
SMTMP	-5~5	-2.28	2.59	-3.78	3.39	0.86	-1.52	-1.4	4.8	0.11	1.57	0.99	2.08
GW_DELAY	10~40	16	29	22	27	21	20	12	16	32	19	37	25
RCHRG_DP	0~0.3	0.05	0.09	0.28	0.04	0.11	0.03	0.08	0.20	0.21	0.28	0.72	0.56
SOL_AWC(1)	-0.2~0.2	0.05	-0.19	0.18	0.04	-0.09	-0.03	0.03	-0.16	0.19	0.15	0.06	-0.03
ADJ_PKR	0.5~2	-	-	-	-	-	-	-	1.75	-	0.74	1.10	1.16
SPEXP	1~2	-	-	-	-	-	-	-		-	-	1.50	1.94
CH_COV1	0~1	-	-	-	-	-	-	-		-	-	0.38	0.31
HRU_SLP	0~0.02	-	-	-	-	-	-	-	0	-	0.02	0.02	0
SLSUBBSN	-0.1~0.1	-	-	-	-	-	-	-		-		0.08	0.03
USLE_K(1)	-0.1~0.1	-	-	-	-	-	-	-	0.07	-	0.1	0.1	-0.06
USLE_C{19}	-0.25~0.25	-	-	-	-	-	-	-	0.00	-	0.24	0.23	0.15
USLE_C{56}	-0.25~0.25	-	-	-	-	-	-	-	-0.17	-	-0.12	0.15	0.07
CMN	0.0003~0.03	0.02	0.02	-	0.0003	0.02	-	-	0.01	-	0.02	0.0003	0.03
RCN	0~15	11	15	-	10	11	-	-	6	-	5	11	0.1
NPERCO	0~1	0.84	0.01	-	0.53	0.48	-	-	0.99	-	1	0.99	0.99
SDNCO	0~1.5	1.25	1.26	-	1.02	1.39	-	-	1.30	-	0.93	1	1.46
CDN	0~1	0.01	0.02	-	0.33	0.28	-	-	1	-	1	0.06	0

Negative value for CN2, and value for SOL_K(1), SOL_AWC(1), USLE_K(1), USLE_C{19}, and USLE_C{56} is relative change to default value. (1) indicates the first soil layer. {19} and {56} represent corn and soybean, respectively.

4.4.2 Calibration and Validation Results for Subsurface Stations

This section outlines calibration and validation performance for monthly tile flow and nitrate-nitrogen losses for subsurface sites B and E.

4.4.2.1 Calibration and validation results at site B

Simulated annual corn and soybean yields, monthly tile flow, and nitrate in tile flow were compared with observed values during calibration and validation periods at site B (Figures 4.6, 4.7 and 4.9). Differences between simulated tile flow and observed values were plotted (Figure 4.8). Model performance in simulating crop yield, tile flow and nitrate in tile flow at site B were evaluated (Table 4.7).

Performance of the simulated corn and soybean yields from Rev.615 at site B during calibration and validation was satisfactory. Simulated annual corn and soybean yields fit observed values well (Figure 4.6). P_{BIAS} values of corn and soybean yields during calibration and validation periods were 13% and 2%, respectively, indicating accurate model simulation. During the calibration period, R^2, NSE, MSE and KGE values for corn and soybean yields were 0.99, 0.91, 0.77 and 0.75, respectively. During the validation period, R^2, NSE, MSE and KGE values for corn and soybean yields were 0.92, 0.91, 0.76 and 0.89, respectively (Table 4.7). Adjusted crop growth parameters (Table 4.4) in Rev.615 provided good predictions of corn and soybean yields.

Performance of the simulated monthly tile flow from Rev.528, Rev.615 and Rev.645 at site B during calibration and validation was satisfactory. Generally, simulated tile flow results for the old routine from Rev.528 were better than those for the new routine from Rev.615 and Rev.645. The modified curve number calculation method in Rev.645 improved surface runoff simulation and then improved tile flow simulation to default curve number calculation method based on soil moisture in Rev.615. Simulated monthly tile flow was similar to observed values, except that Rev.615 simulated tile flow could not capture tile flow peaks well in May of 1996 and February of 1997 (Figure 4.7). Since annual precipitation was 745 mm during 1995 at site B, soil moisture was reduced resulting in long dry periods. Subsurface tile drains can lower the water table (Sui, 2007), and long-

term water depletion may drop the water table lower than the depth of tiles (1075 mm). For long-term water table depth simulation (19 years in this study), the computed water table depth may gradually drop as profile soil water decreased due to higher ET, which made it harder for the water table to rise to the surface after rain events (Moriasi *et al.*, 2013). When water storage was higher than the height of the surface storage threshold (20% of the static maximum depressional storage (SSTMAXD)) and water table was near the bottom of the soil surface, the Kirkham equation will be used to calculate drainage flux (Boles, 2013). Thus, overestimation of water table depth may cause the new routine not to trigger the Kirkham equation to calculate tile flow drainage even though 1996 was a wet year (annual precipitation was 1008 mm). The new routine in Rev.615 resulted in decreased tile flow peaks and longer storage time (Boles, 2013). The new routine in Rev.645 could capture tile flow peaks well, and difference between simulated and observed tile flow values were big in May 1996 and February 1997 (Figures 4.7 and 4.8). The newly added curve number calculation retention parameter adjustment factor in Rev.645 can calculate curve number reasonably based on the soil moisture retention curve from field capacity to saturation, and can partition surface runoff and tile flow well. Thus, simulated tile flow results from Rev.645 can capture peaks well, and difference between simulated and observed tile flow values were small after long dry periods (Figures 4.7 and 4.8). P_{BIAS} values of tile flow results were 3% and 4% from Rev.528, 14% and 3% from Rev.615, and -19% and -18% from Rev.645 during calibration and validation periods, respectively, indicating accurate model simulation. Generally, R^2, NSE, MSE and KGE values for tile flow from three versions were satisfactory (>0.5), except that R^2 (0.49) from Rev.615 during calibration period and MSE (0.48) from Rev.645 during validation period were slightly under the acceptable limit (Table 4.7).

Performance of the modeled monthly nitrate in tile flow from Rev.528 and Rev.615 at site B during calibration and validation was satisfactory. Generally, simulated nitrate in tile flow results by the old routine from Rev.528 were better than those by the new routine from Rev.615. Simulated monthly nitrate in tile flow matched observed values well, except that Rev.615 simulated nitrate in tile flow could not capture peaks well in May 1996 and February 1997 (Figure 4.9), which was caused by the failure to predict tile flow correctly

during these periods (Figures 4.7 and 4.8). P_{BIAS} values of nitrate in tile flow results were 8% and 23% from Rev.528, and 33% and 18% from Rev.615 during calibration and validation periods, respectively, indicating accurate model simulation (Table 4.7). Generally, R^2, NSE, MSE and KGE values for simulated nitrate in tile flow were satisfactory (>0.5). However, R^2 (0.37) and NSE (0.22) from Rev.615 during the calibration period were unacceptable, and MSE (0.43) and KGE (0.48) from Rev.615 during the calibration period were slightly under the acceptable limit (Table 4.7), which was due to underestimated nitrate in tile flow values after long dry periods (Figure 4.9).

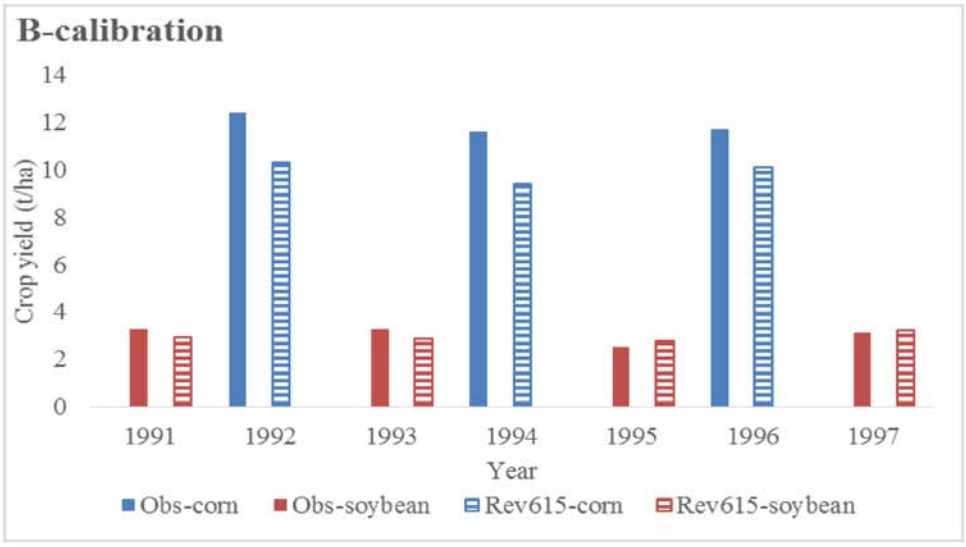

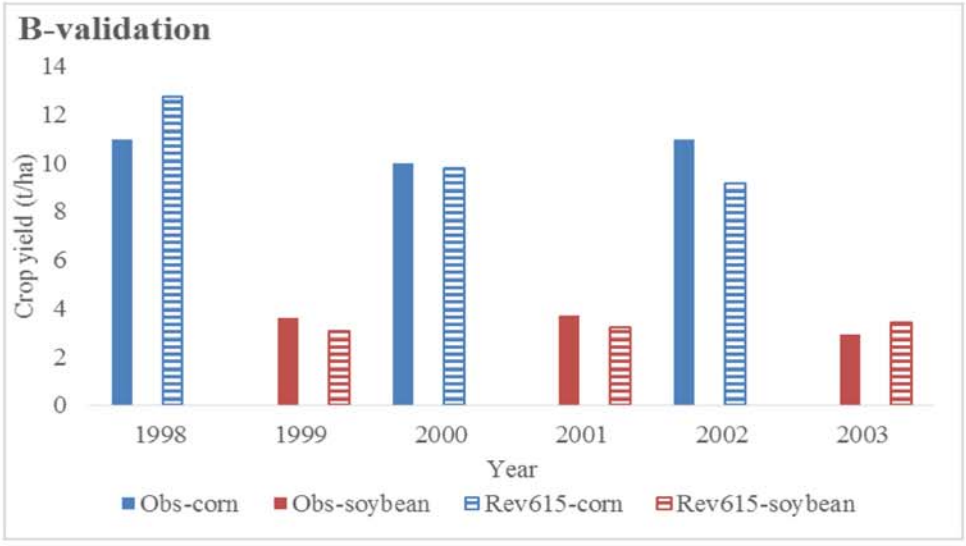

Figure 4.6 Calibration and validation results for annual crop yields at site B

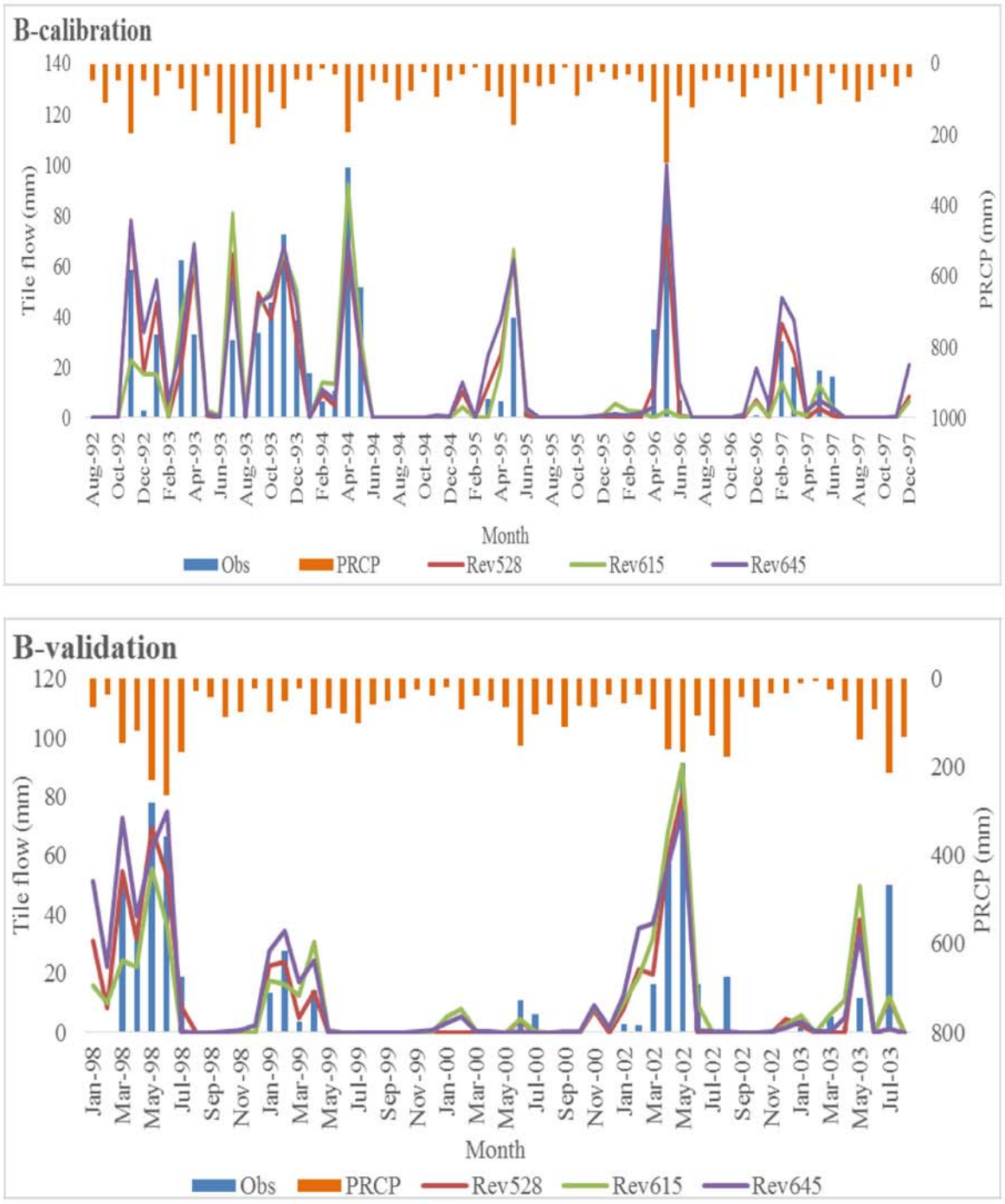

Figure 4.7 Calibration and validation results for monthly tile flow at site B

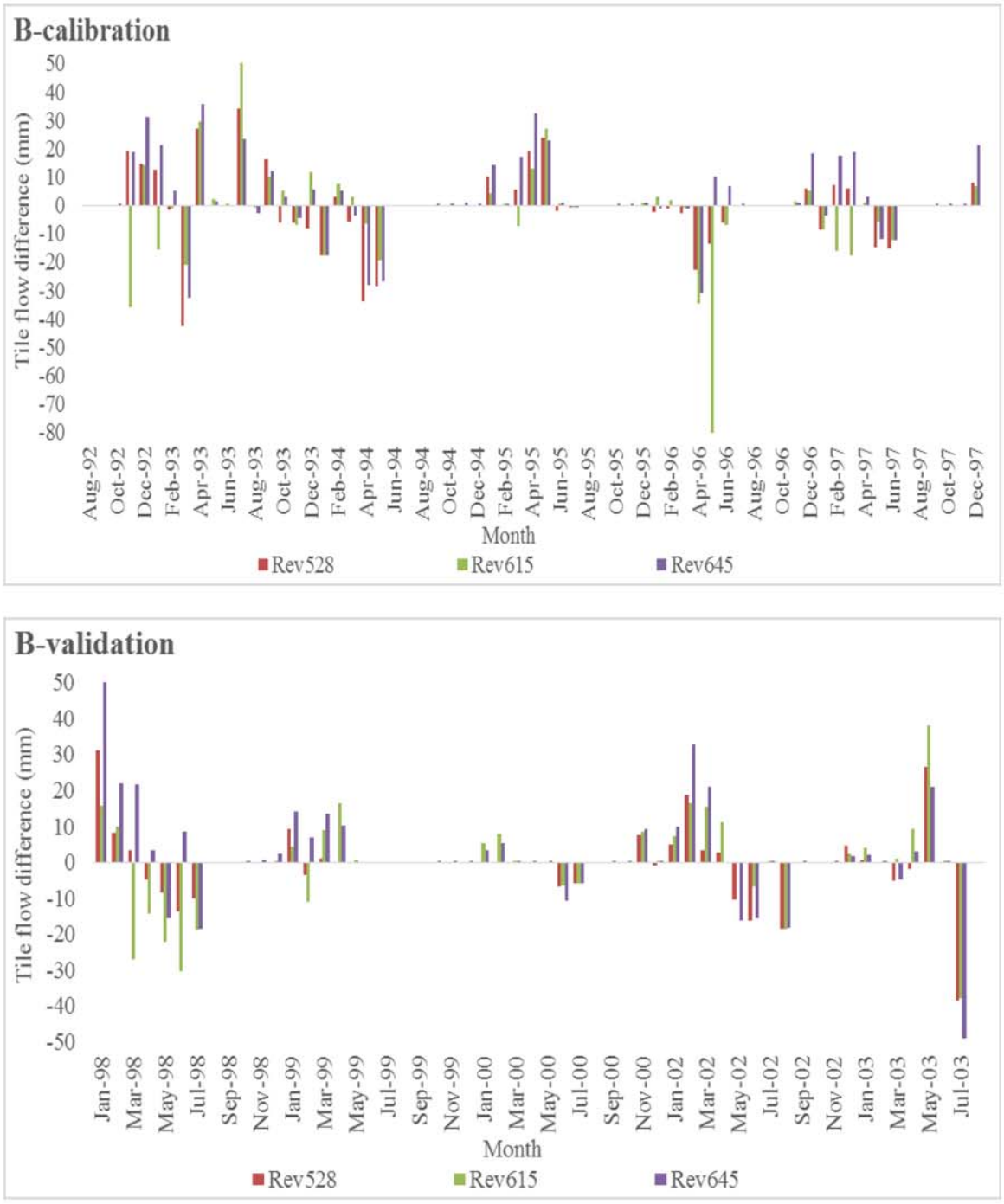

Figure 4.8 Difference between simulated monthly tile flow with observed values at site B

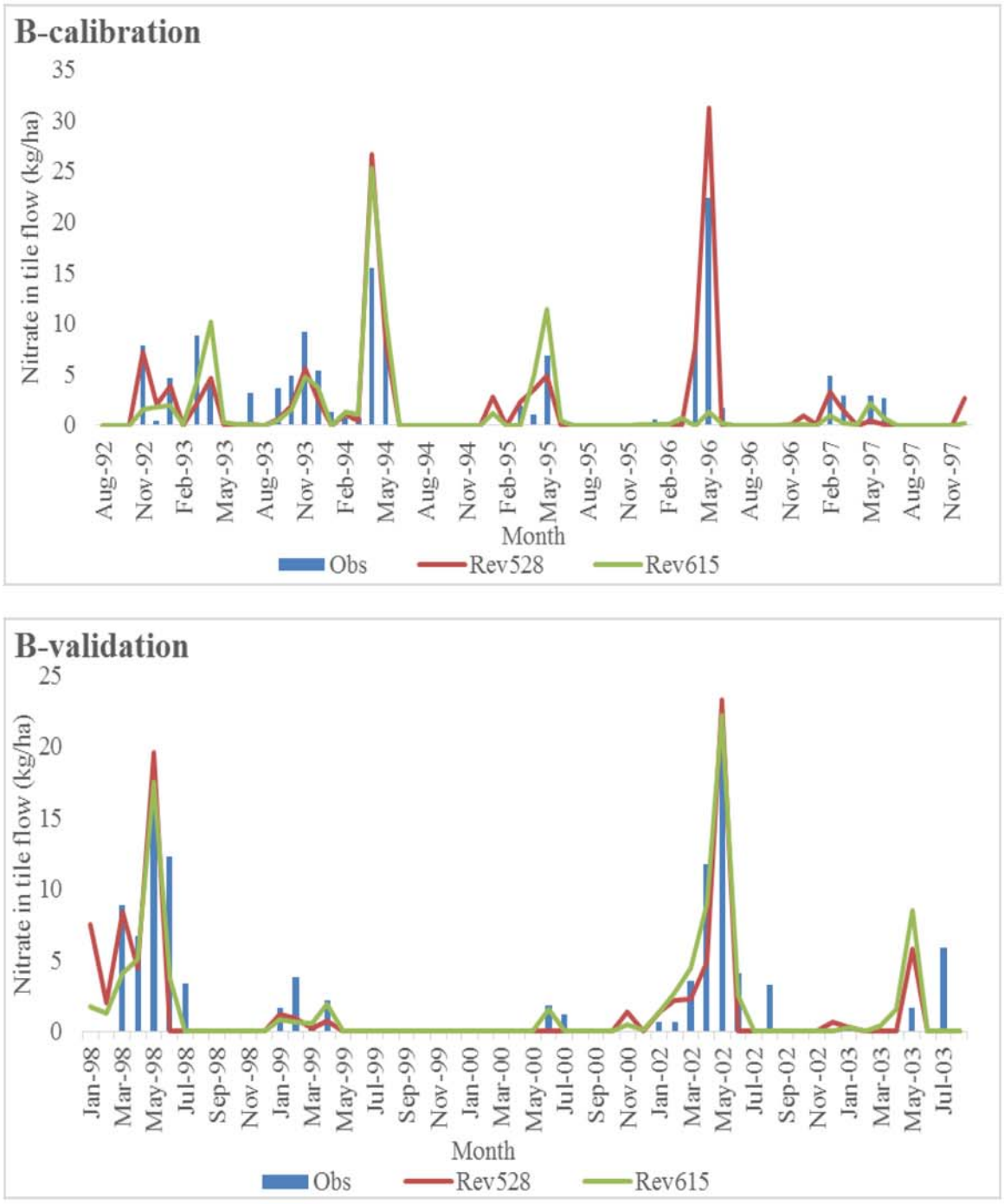

Figure 4.9 Calibration and validation results for monthly nitrate-nitrogen losses in tile flow at site B

Table 4.7 Performance evaluation of calibrated crop yield, tile flow and nitrate in tile flow results at site B

Site B	Annual Crop yield (t/ha)		Monthly Tile flow (mm)						Monthly NO3-N in tile flow (kg/ha)			
	Cali	Vali	Cali			Vali			Cali		Vali	
Revision	615	615	528	615	645	528	615	645	528	615	528	615
P_{BIAS} (%)	13	2	3	14	-19	4	3	-18	8	33	23	18
R^2	0.99	0.92	0.73	0.49	0.72	0.80	0.69	0.64	0.65	0.37	0.67	0.78
NSE	0.91	0.91	0.71	0.54	0.66	0.80	0.68	0.58	0.66	0.22	0.63	0.77
MSE	0.77	0.76	0.60	0.54	0.53	0.67	0.53	0.48	0.59	0.43	0.55	0.64
KGE	0.75	0.89	0.85	0.70	0.75	0.86	0.78	0.73	0.68	0.48	0.71	0.78

Cali and Vali are abbreviations for Calibration and Validation, respectively.

4.4.2.2 Calibration and validation results at site E

Simulated annual corn and soybean yields, monthly tile flow, and nitrate in tile flow were compared with observed values during calibration and validation periods at site E (Figures 4.10, 4.11 and 4.13). Differences between simulated tile flow and observed values were plotted (Figure 4.12). Model performance of simulating crop yield, tile flow and nitrate in tile flow at site E were evaluated (Table 4.8).

Performance of modeled corn and soybean yields from Rev.615 at site E during calibration and validation was satisfactory. Simulated annual corn and soybean yields were similar to observed values (Figure 4.10). P_{BIAS} values of corn and soybean yields during calibration and validation periods were -2% and 5%, respectively, indicating accurate model simulation. During the calibration period, R^2, NSE, MSE and KGE values for corn and soybean yields were 0.95, 0.95, 0.80 and 0.95, respectively. During the validation period, R^2, NSE, MSE and KGE values for corn and soybean yields were 0.92, 0.88, 0.71 and 0.91, respectively (Table 4.8). Adjusted crop growth parameters (Table 4.4) in Rev.615 provided good predictions of corn and soybean yields.

Performance of the modeled monthly tile flow from Rev.615 and Rev.645 at site E during calibration and validation was satisfactory. Generally, simulated tile flow results for the new routine from Rev.615 and Rev.645 were better than those from the old routine from Rev.528. Simulated monthly tile flow from Rev.615 and Rev.645 fit observed values well (Figure 4.11), and the difference between simulated and observed tile flow was small

(Figure 4.12). However, Rev.528 simulated tile flow was overestimated at tile flow peaks in November 1992, May 1996, March 1997, May and June of 1998, December 2001, and the February, April and May of 2002 (Figure 4.11), and the differences between simulated and observed tile flow during these periods were big (Figure 4.12). Rev.528 simulated tile flows were underestimated from May to October in 1992, from June to November in 1994, from July in 1995 to March in 1996, from May in 1999 to February in 2000, from May to August in 2001, and from July to December in 2002 (Figure 4.11), and the differences between simulated and observed tile flow during these periods were large (Figure 4.12). Simulated tile flow by the old routine in Rev.528 was controlled by a simple drawdown time parameter (TDRIAN), and tiles were allowed to carry an unlimited maximum of water no matter how intense the rainfall. Thus, the old routine overestimated tile flow peaks for site E (Figure 4.10).

The new routine in Rev.615 and Rev.645 incorporates the drainage coefficient (DRAIN_CO), and tile flow peaks can be limited by the radius of the tile. In this case, the tiles could flow for a slightly longer period of time, and simulated tile flow matched well with observed values (Figure 4.11). The old routine was used to simulate tile flow on days when the simulated height of the water table exceeded the height of the tile drain (Neitsch *et al.*, 2011). Tile drainage systems can cause water table recession in tile-drained soil. Water table was lower when respiratory activity was highest in summer (Muhr *et al.*, 2011), which may be lower than the depth of subsurface tiles during long dry summer periods. Water table depth calculation based on change in the soil water for the whole soil profile tended to overestimate the distance between water table and the soil surface when long-term simulations were performed, most commonly in cases where days without rainfall dominated (Moriasi *et al.*, 2013). Thus, Rev.528 simulated tile flow was zero during long dry summer periods. Overall, more physically-based equations and drainage coefficient in the new routine in Rev.615 and Rev.645 can reduce the flashiness of the tile flow simulation and result in lower tile flow peak and longer recession. The new routine in Rev.615 and Rev.645 provided more reasonable tile flow simulation for site E (Figure 4.11). P_{BIAS} values of tile flow results were -6% and 12% from Rev.615 and -17% and -2% from Rev.645 during calibration and validation periods, respectively, indicating accurate

model simulation. R^2, NSE, and KGE values for tile flow from Rev.615 and Rev.645 were satisfactory (>0.5). However, MSE from Rev.615 (0.28) and from Rev.645 (0.27) during calibration period, and MSE from Rev.615 (0.31) and from Rev.645 (0.34) during validation period were under the generally acceptable limit (Table 4.6). P_{BIAS} value of tile flow results from Rev.528 during calibration period was -37%, indicating overestimated model values. NSE, MSE and KGE values from Rev.528 during calibration and validation periods were unacceptable (< 0.5) (Table 4.8).

Performance of the simulated monthly nitrate in tile flow from Rev.615 at site E during calibration and validation was satisfactory. Generally, simulated nitrate in tile flow results for the new routine from Rev.615 were better than those for the old routine from Rev.528. Simulated monthly nitrate in tile flow matched with observed values well, except that Rev.615 simulated nitrate in tile flow was underestimated in May 2002 (Figure 4.13), which is caused by the underestimation of tile flow during this period (Figures 4.11 and 4.12). Performance of the modeled monthly nitrate in tile flow from Rev.528 for site E during calibration and validation was unsatisfactory, which is likely caused by the failure to predict accurate tile flow (Figures 4.11 and 4.12). P_{BIAS} values of nitrate in tile flow results from Rev.615 during calibration and validation periods were 26% and 20%, respectively, indicating accurate model simulation. R^2, NSE, and KGE values for simulated nitrate in tile flow from Rev.615 during calibration and validation periods were satisfactory (>0.5), but MSE values during calibration (0.30) and validation (0.34) periods were under the acceptable limit (< 0.5) (Table 4.8). P_{BIAS} values of nitrate in tile flow results from Rev.528 during the validation period was 36%, indicating underestimated model simulation. NSE, MSE, and KGE values for simulated nitrate in tile flow from Rev.528 during calibration and validation periods were unsatisfactory (<0.5) (Table 4.8).

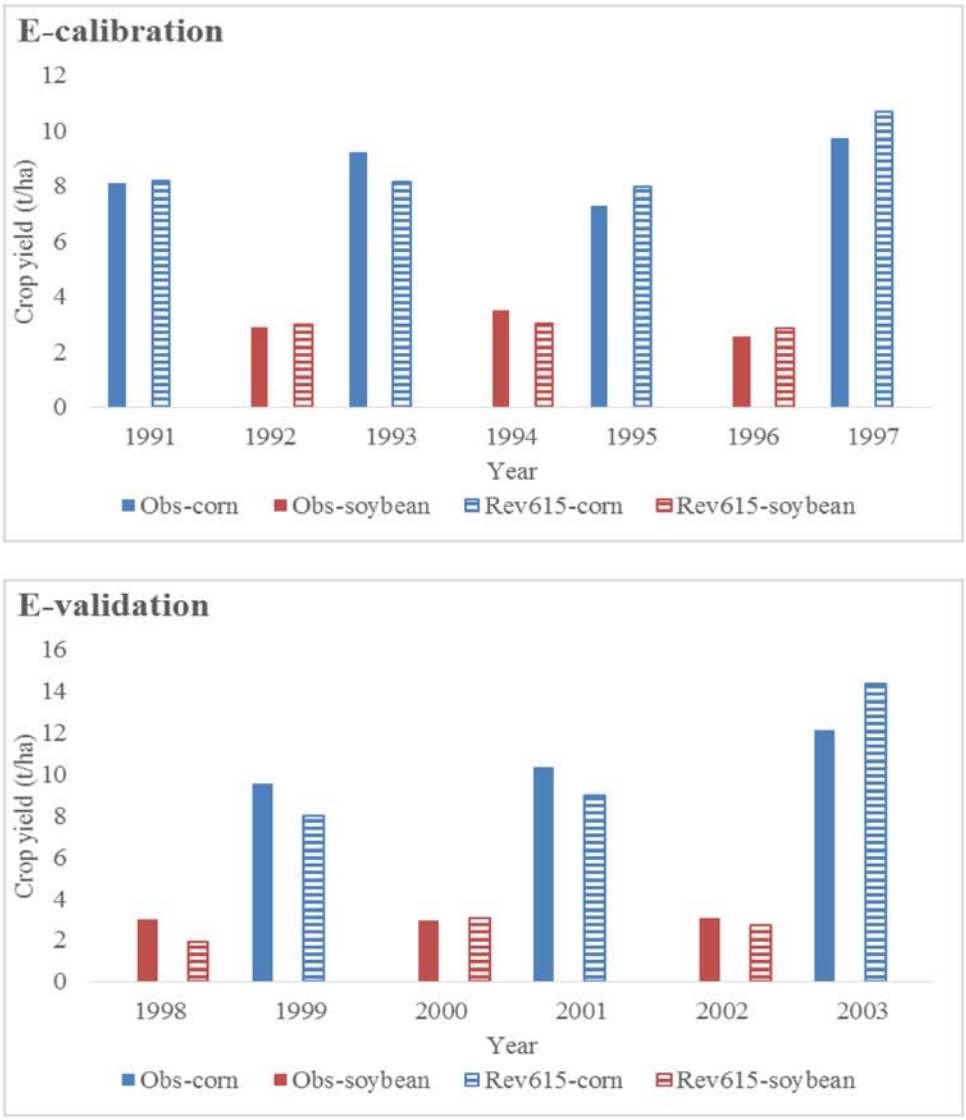

Figure 4.10 Calibration and validation results for annual crop yields at site E

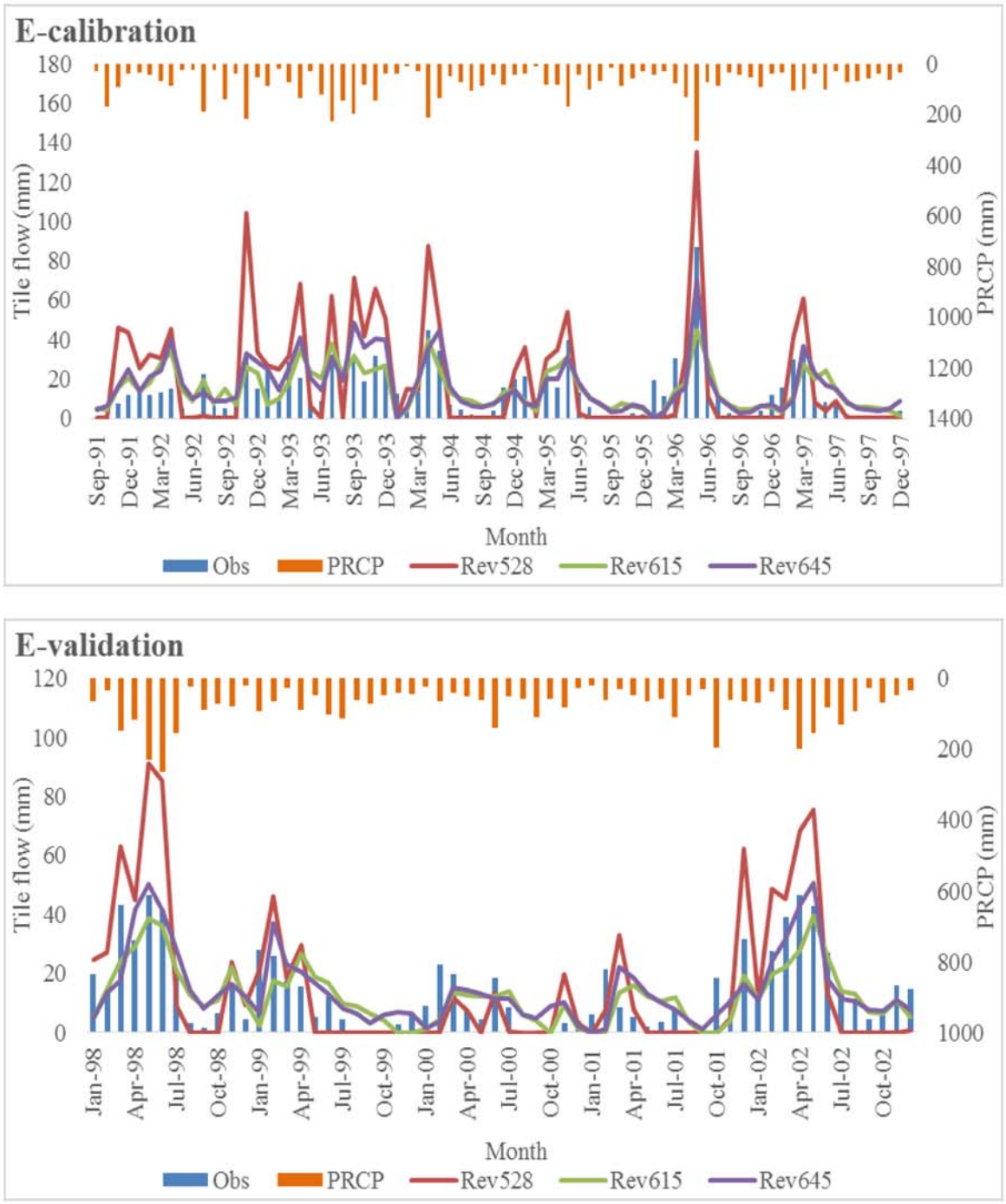

Figure 4.11 Calibration and validation results for monthly tile flow at site E

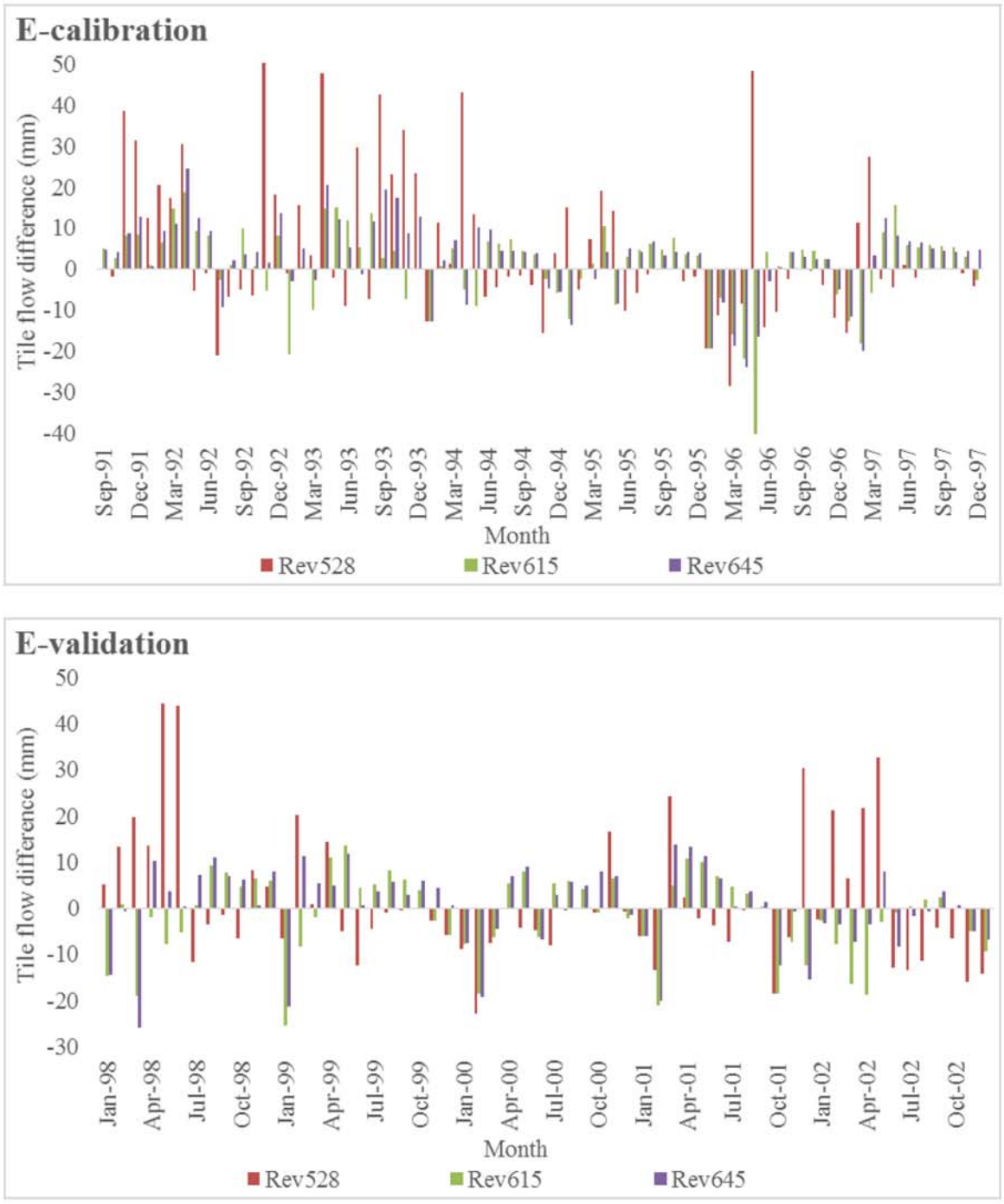

Figure 4.12 Difference between simulated monthly tile flow with observed values at site E

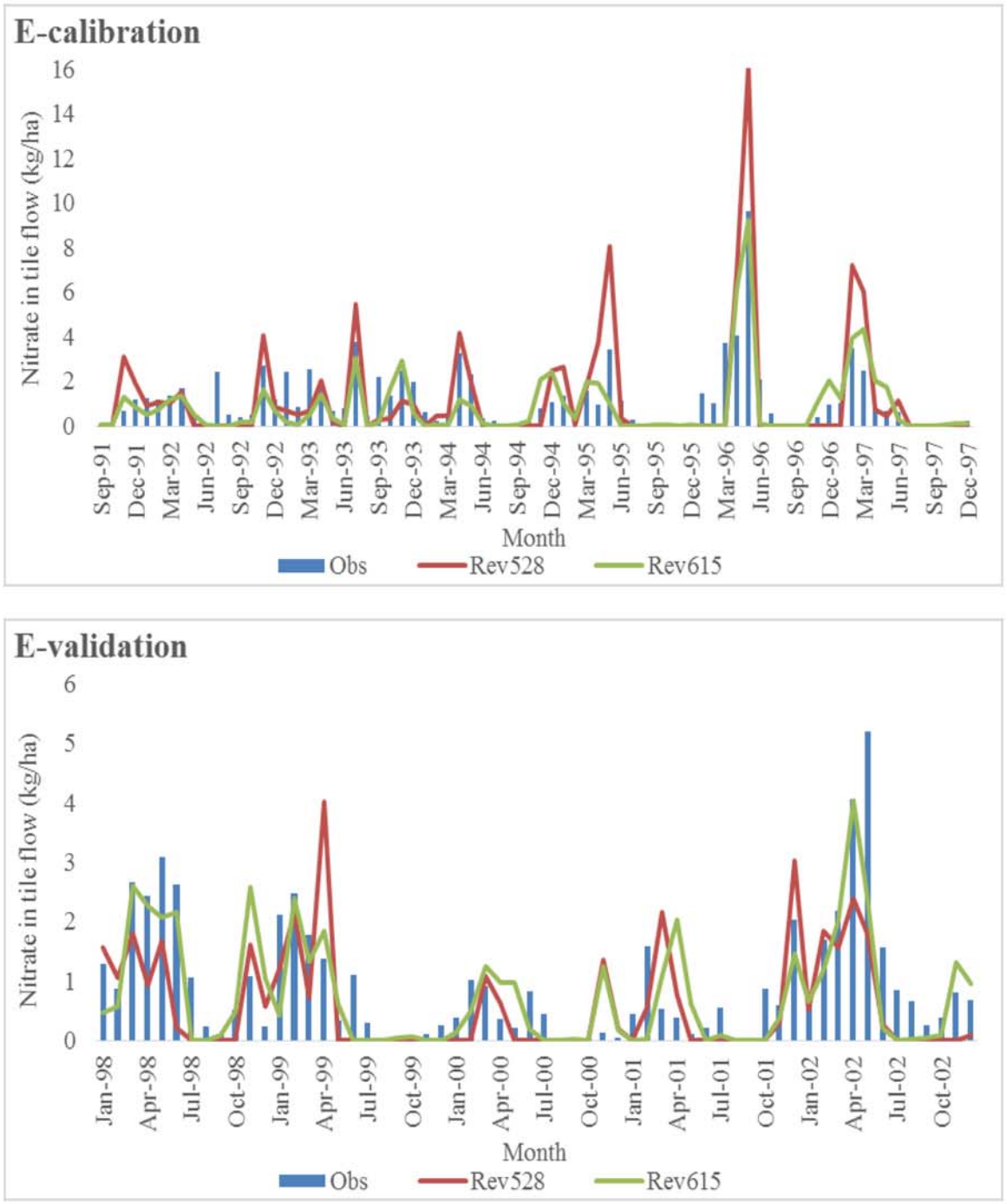

Figure 4.13 Calibration and validation results for monthly nitrate-nitrogen losses in tile flow at site E

Table 4.8 Performance evaluation of calibrated tile flow and nitrate in tile flow results at site E

Site E	Annual Crop yield (t/ha)		Monthly Tile flow (mm)						Monthly NO3-N in tile flow (kg/ha)			
	Cali	Vali	Cali			Vali			Cali		Vali	
Revision	615	615	528	615	645	528	615	645	528	615	528	615
P_{BIAS} (%)	-2	5	-37	-6	-17	-10	12	-2	-1	26	36	20
R^2	0.95	0.92	0.68	0.51	0.6	0.75	0.52	0.56	0.72	0.61	0.38	0.55
NSE	0.95	0.88	-0.77	0.5	0.54	-0.2	0.5	0.53	-0.09	0.5	0.21	0.5
MSE	0.80	0.71	-0.20	0.28	0.27	0.04	0.31	0.34	0.08	0.3	0.18	0.34
KGE	0.95	0.91	-0.05	0.6	0.71	0.15	0.60	0.74	0.24	0.66	0.45	0.65

Cali and Vali are abbreviations for Calibration and Validation, respectively.

Simulated monthly tile flow results for Rev.615 at sites B and E were better than previous DRAINMOD and Root Zone Water Quality Model (RZWQM) simulated results (Singh *et al.*, 2001), since both DRAINMOD and RZWQM models overestimated daily tile flow at these sites to obtain the acceptable R^2 value (>0.5) and predicted peak tile flows, but they did not match well with the observed values generally from 1993 to 1998. Simulated monthly tile flow results for Rev.615 at sites B and E were similar to the observed values, and obtained acceptable P_{BIAS}, R^2, NSE, MNS and KGE generally from 1991 to 2003.

4.4.3 Calibration and Validation Results for Surface Stations

This section describes calibration and validation performance for monthly surface runoff, sediment and nitrate-nitrogen losses at surface sites Bs and Es. The LVR watershed is dominated by agricultural land with extensive tile drainage system. Surface runoff was a small percentage (⩽15%) of stream flow from 1993 and 1998, and was nearly zero for years 1995 and 1997 (Mitchell *et al.*, 2001). Thus, it is challenging to simulate surface runoff, sediment load, and nutrient load in runoff in the LVR watershed.

4.4.3.1 Calibration and validation results at site Bs

Performance of the modeled monthly surface runoff from Rev.645 at site Bs during calibration and validation was satisfactory. Modeled monthly surface runoff from Rev.615 at site Bs during calibration and validation was unsatisfactory. Generally, simulated surface runoff results from Rev.645 with the improved curve number calculation method were better than those from Rev.615 with the default soil moisture based curve number

calculation method. Simulated surface runoff results from Rev.645 were better than those from Rev.615 for site Bs. Generally, simulated monthly surface runoff from Rev.645 was similar to observed values (Figure 4.14). Rev.615 simulated surface runoff results were higher than observed values (Figure 4.14). For Rev. 615, calibration ranges of CN2 (-20%~-10%) and calibrated CN2 value (60.1) were realistic for a watershed dominated by agricultural land (Table 4.4), and simulated surface runoff was overestimated. P_{BIAS} values of surface runoff results from Rev.615 during calibration and validation periods were -614% and -475%, respectively, representing overestimated simulation results. P_{BIAS} values of surface runoff results from Rev.645 during calibration and validation periods were -26% and -74%, indicating slightly overestimated and overestimated simulation results, respectively. Generally, R^2, NSE, MSE and KGE values for simulated surface runoff results from Rev.615 were unacceptable (<0.5) (Table 4.7). R^2, NSE, MSE and KGE values for simulated surface runoff results from Rev.645 were acceptable (>0.5) (Table 4.9), except that MSE during calibration (0.48) and validation (0.41) periods were slightly under the acceptable limit, and KGE value during validation period (0.18) was unacceptable (Table 4.9). In this watershed with a flat topography and dominated by tile drainage, surface runoff was small for surface station Bs and nearly zero from 1994 May to 1996 March and from 1999 March to 2002 April.

Performance of the modeled monthly sediment load in flow from Rev.645 for site Bs was satisfactory during calibration and reasonable during validation. Simulated monthly sediment load from Rev.645 was similar to observed values, except that simulated sediment load was lower than the observed value for March 1999 (Figure 4.15). P_{BIAS} values of sediment load results were -5% and 37% from Rev.645, during calibration and validation periods, respectively, indicating accurate simulation results (Table 4.9). R^2, NSE, MSE and KGE values for simulated sediment during the calibration period were satisfactory (>0.5) (Table 4.9). R^2, NSE, MSE and KGE values for simulated sediment during validation period were unsatisfactory (<0.5) (Table 4.9), which was because the simulated sediment could not capture the sediment peak well for March 1999, and performance evaluation methods are sensitive to high values. The magnitude of sediment

load for site Bs was small, thus simulated results were reasonable even though simulated sediment load was underestimated for March 1999.

Performance of the modeled monthly nitrate load in surface runoff from Rev.645 for site Bs during calibration and validation was reasonable. Simulated monthly nitrate load was similar to observed values, except that simulated nitrate load values were lower than the observed values in the May of 1996 and 1998, and January 1999 (Figure 4.16). P_{BIAS} values of nitrate load results were 79% and 53% during calibration and validation periods, indicating underestimated model simulation. Generally, R^2, NSE, MSE and KGE values for simulated nitrate load were unsatisfactory (<0.5) (Table 4.9). However, Rev.645 simulated nitrate in surface flow was reasonable, as nitrate in surface runoff was low given the watershed was dominated by tile flow.

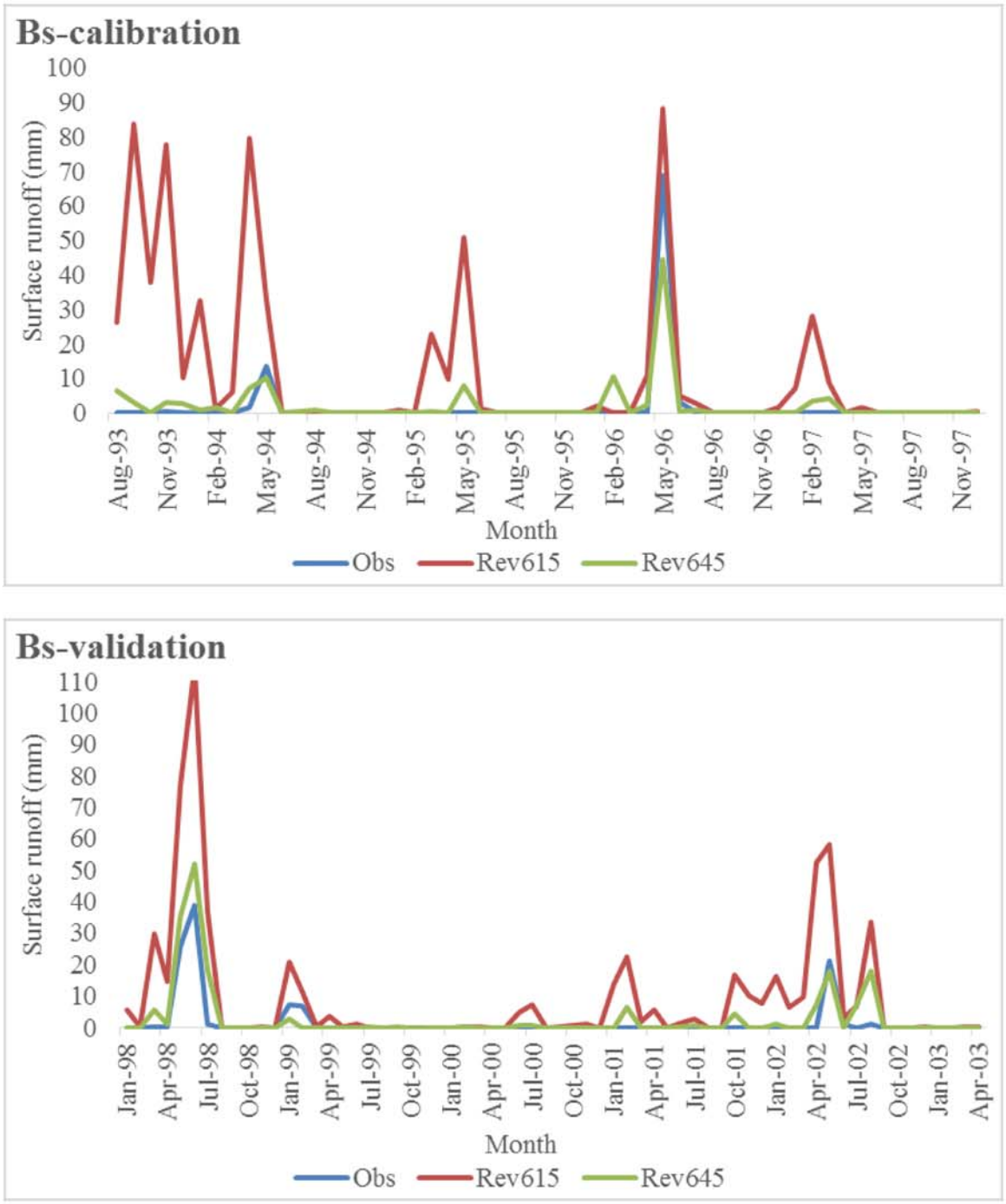

Figure 4.14 Calibration and validation results for monthly nitrate in surface runoff at site Bs

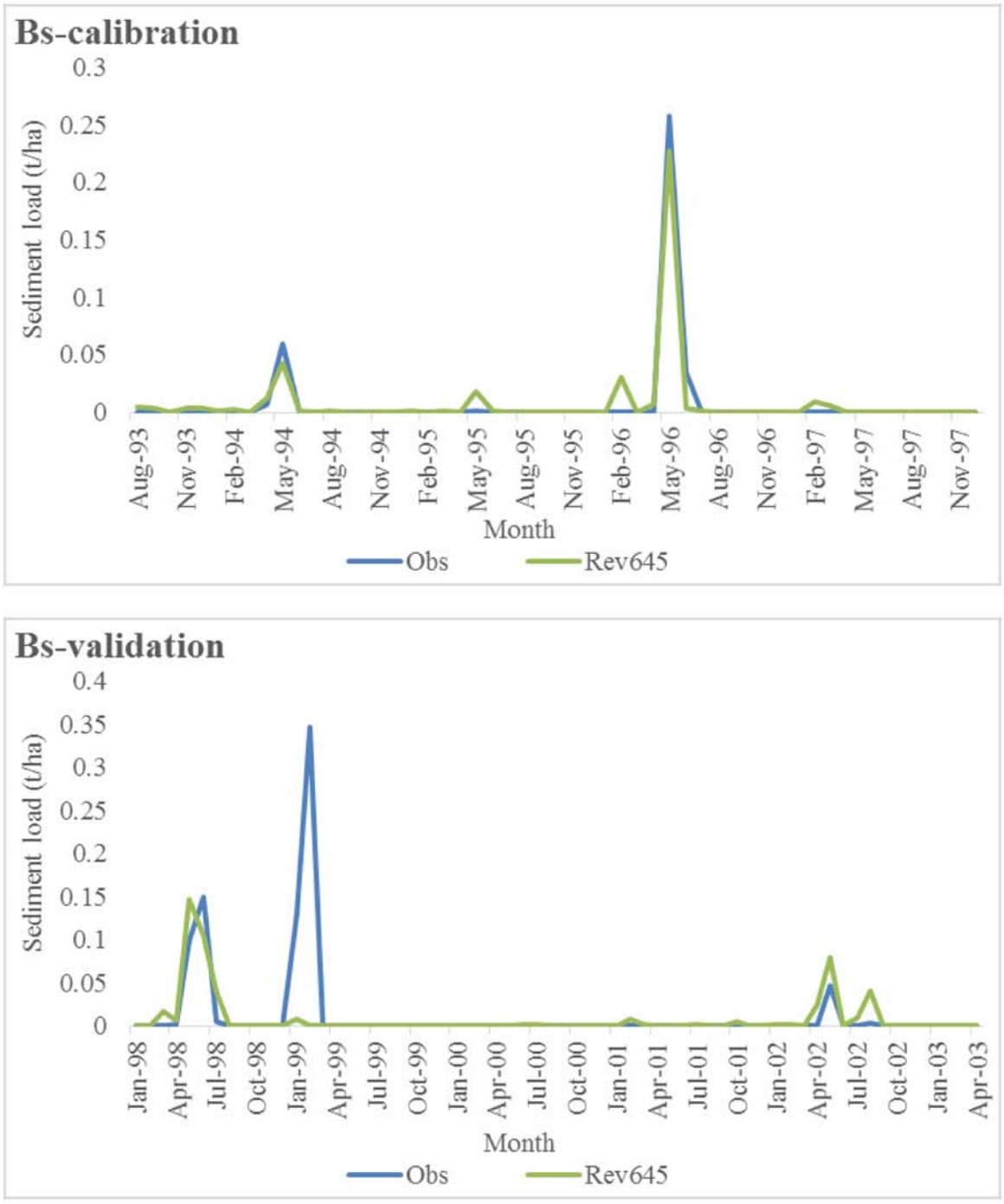

Figure 4.14 Calibration and validation results for monthly sediment in surface runoff at site Bs

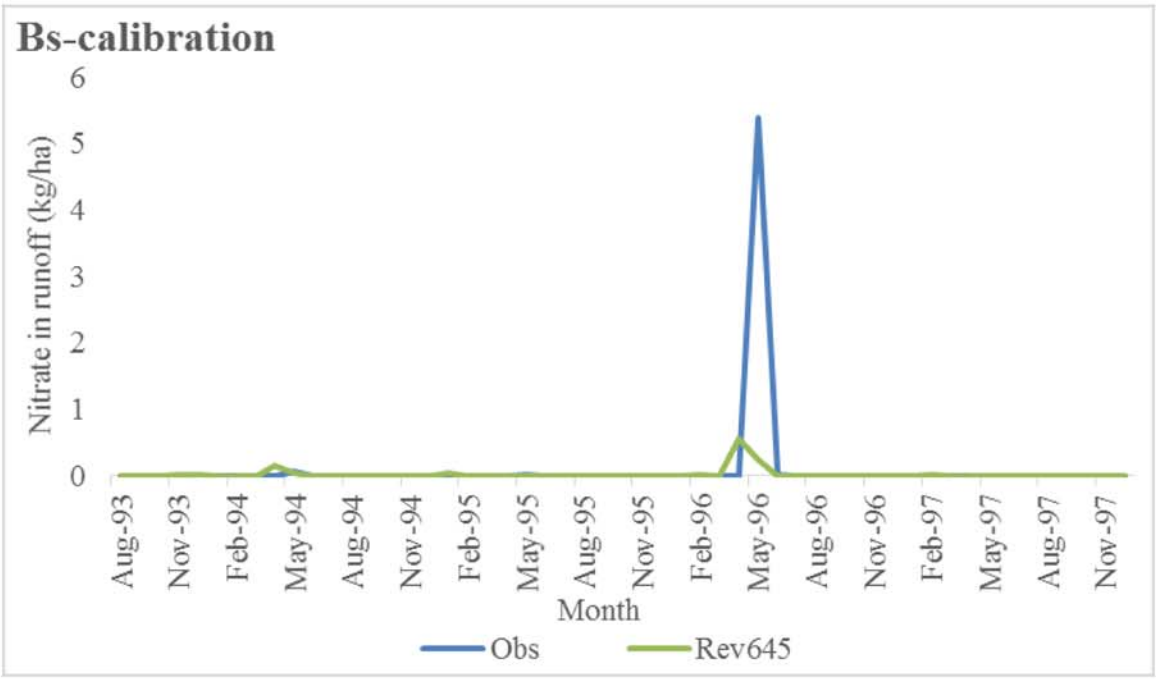

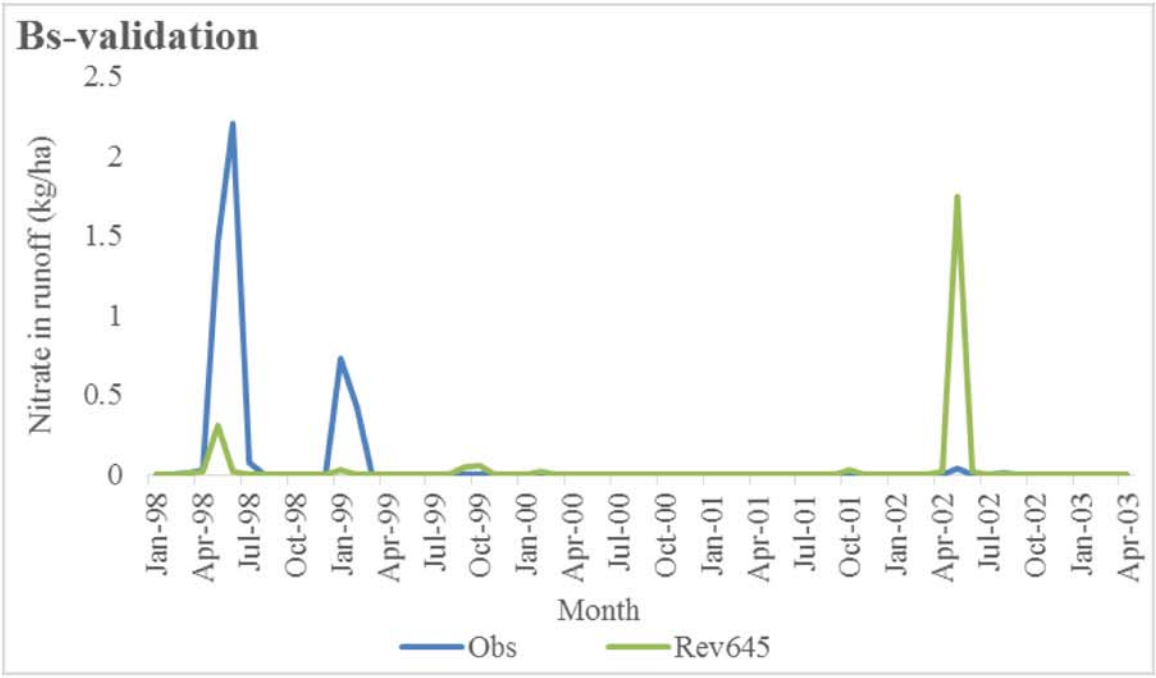

Figure 4.15 Calibration and validation results for monthly nitrate in surface runoff at site Bs

Table 4.9 Performance evaluation of calibrated surface runoff and nitrate in surface runoff results at site Bs

Site Bs	Monthly Surface runoff (mm)				Monthly Sediment (t/ha)		Monthly Nitrate in runoff (kg/ha)	
	Cali		Vali		Cali	Vali	Cali	Vali
Revision	615	645	615	645	645		645	
P_{BIAS} (%)	-614	-26	-475	-74	-5	37	79	53
R^2	0.23	0.88	0.76	0.80	0.96	0.13	0.14	0.01
NSE	-4.7	0.81	-5.95	0.56	0.95	0.11	0.06	-0.32
MSE	-2.36	0.48	-1.70	0.41	0.74	0.48	0.43	0.29
KGE	-5.33	0.58	-4.22	0.18	0.86	0.10	-0.34	-0.11

Cali and Vali are abbreviation of Calibration and Validation, respectively.

4.4.3.2 Calibration and validation results at site Es

Performance of the modeled monthly surface runoff results from Rev.615 and Rev.645 at site Es was satisfactory during the calibration period and unsatisfactory during the validation period. Simulated surface runoff results from Rev.645 were better than those from Rev.615 for site Es. Generally, simulated monthly surface runoff from Rev.615 and Rev.645 fit observed values well during the calibration period, and provided higher than observed values during the validation period (Figure 4.17). For Rev. 615, calibrated CN2 value (60.1) was realistic for watersheds dominated by agricultural land (Table 4.6), and simulated surface runoff was overestimated. P_{BIAS} values of surface runoff results from Rev.615 during calibration and validation periods were -107% and -143%, respectively (Table 4.10), representing overestimated simulation results. P_{BIAS} values of surface runoff results from Rev.645 during calibration and validation periods were -18% and -99% (Table 4.10), indicating slightly overestimated and overestimated simulation results, respectively. Generally, R^2, NSE, MSE and KGE values for simulated surface runoff results from Rev.615 were unacceptable (<0.5), except that R^2 values were 0.71 and 0.55 during calibration and validation periods, respectively, and NSE value was 0.50 during calibration period (Table 4.10). R^2, NSE, MSE and KGE values for simulated surface runoff results from Rev.645 were acceptable during the calibration period (>0.5) and unacceptable during the validation period (Table 4.10). In this mildly-sloped watershed with extensive tile drainage systems, surface runoff was small for surface station Es and nearly zero from 1994 June to 1995 April and from 1998 July to 2002 March.

Performance of the modeled monthly sediment load in flow from Rev.645 for site Es was satisfactory during calibration and reasonable during validation. Simulated monthly sediment load from Rev.645 was similar to observed values during the calibration period, except that simulated sediment load was lower than the observed value for May 1996 (Figure 4.18). Simulated monthly sediment load from Rev.645 did not match observed values well during the validation period, and had difficulty in capturing sediment load peaks well (Figure 4.18). P_{BIAS} values of sediment load results were 32% and 22% from Rev.645 during calibration and validation periods, respectively, indicating accurate simulation results (Table 4.8). R^2, NSE, MSE and KGE values for simulated sediment during calibration and validation periods were unsatisfactory (<0.5) (Table 4.10), except that R^2 (0.79) was acceptable and NSE (0.46) was slightly under the acceptable limit during the calibration period (Table 4.10). Simulated results from Rev.645 were reasonable, even though evaluation statistics were unsatisfactory, as the magnitude of sediment load was small for the mildly-sloped site.

Performance of the modeled monthly nitrate load in surface runoff from Rev.645 for site Es during calibration and validation was reasonable. Simulated monthly nitrate load was similar to observed values during the calibration period, except that simulated nitrate load values were lower than the observed values in May 1996 (Figure 4.19). Simulated nitrate load in surface runoff could not capture nitrate load peaks well during the validation period (Figure 4.19). P_{BIAS} values of nitrate load results were 25% and 83% during calibration and validation periods, indicating accurate and underestimated model simulation, respectively. Generally, R^2, NSE, MSE and KGE values for simulated nitrate load were unsatisfactory (<0.5) (Table 4.10). Rev.645 simulated nitrate in surface flow for site Es was reasonable, as nitrate in surface runoff was small as surface runoff rarely occurred.

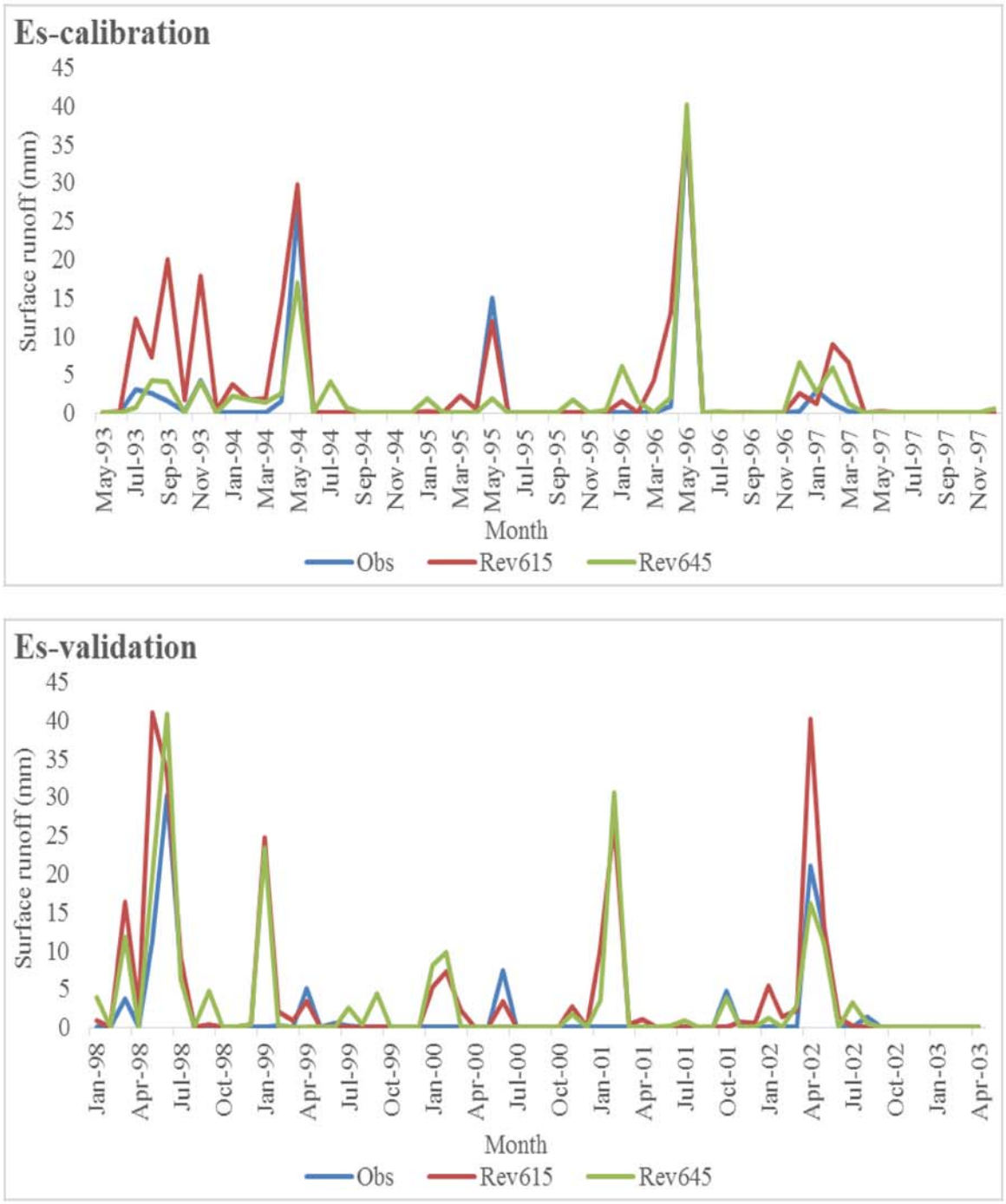

Figure 4.16 Calibration and validation results for monthly surface runoff at site Es

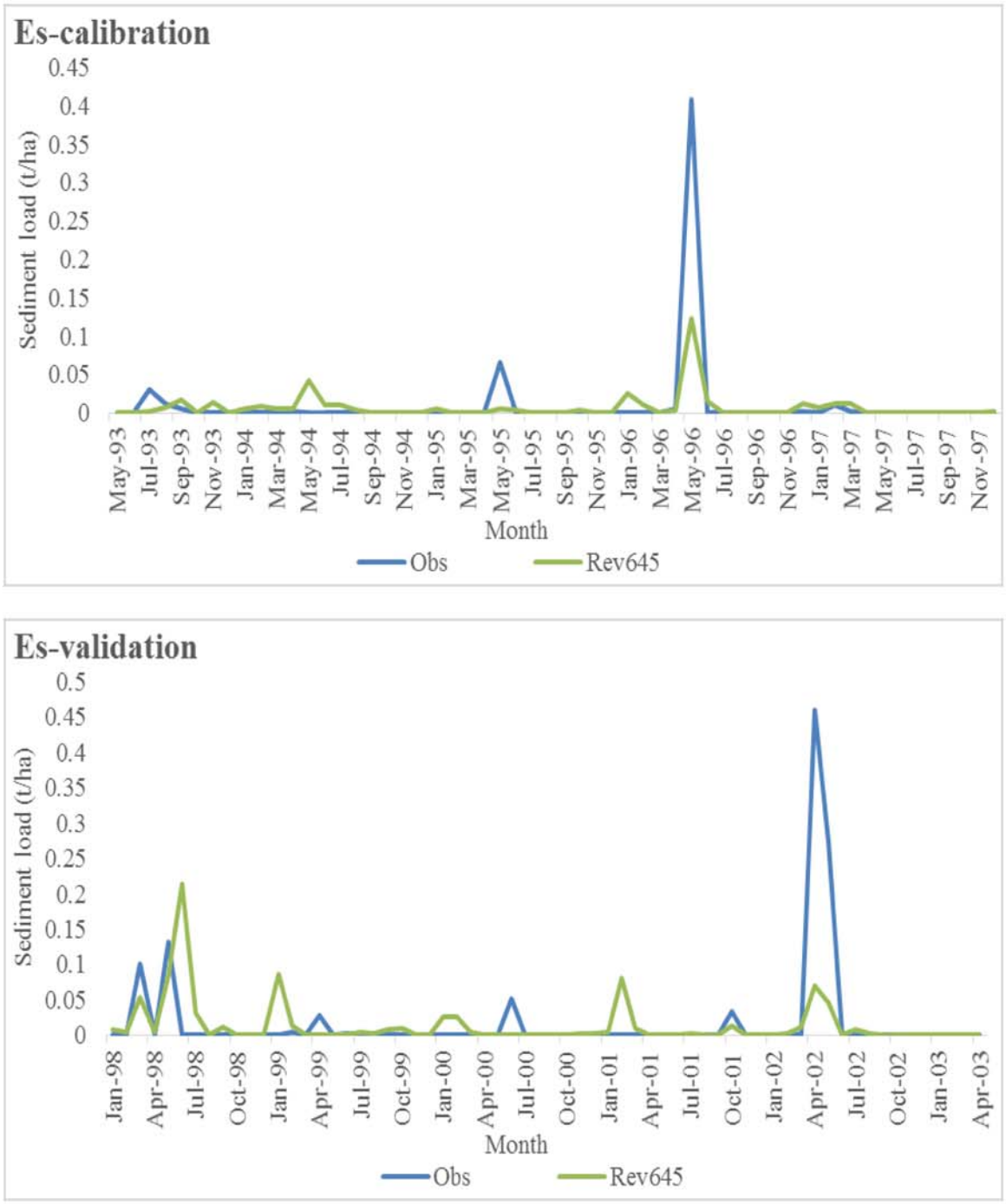

Figure 4.17 Calibration and validation results for monthly sediment in surface runoff at site Es

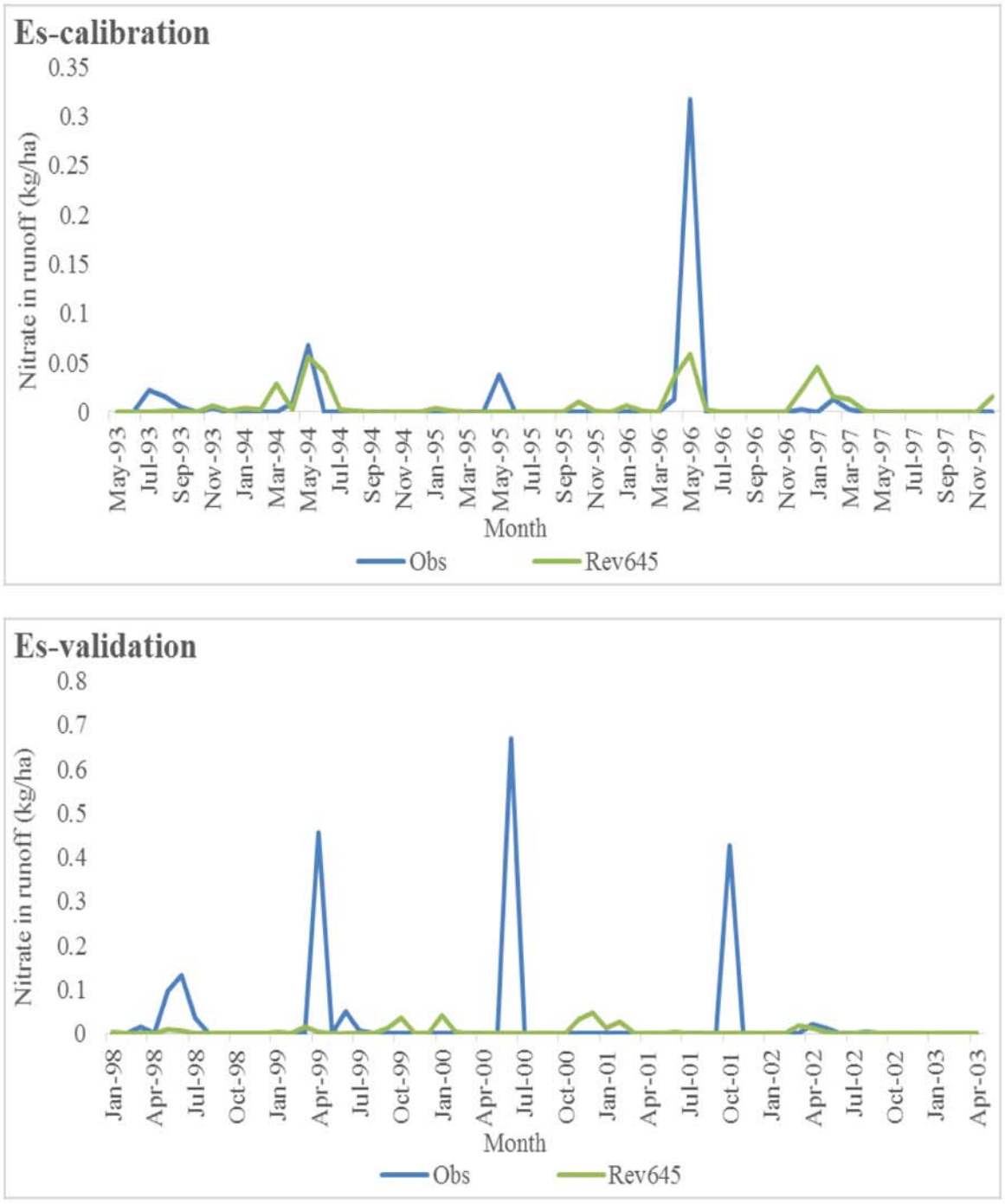

Figure 4.18 Calibration and validation results for monthly nitrate in surface runoff at site Es

Table 4.10 Performance evaluation of calibrated surface runoff and nitrate in surface runoff results for site Es

Site Es	Monthly Surface runoff (mm)				Monthly Sediment (t/ha)		Monthly Nitrate in runoff (kg/ha)	
	Cali		Vali		Cali	Vali	Cali	Vali
Revision	615	645	615	645	645		645	
P_{BIAS} (%)	-107	-18	-143	-99	32	22	25	83
R^2	0.71	0.82	0.55	0.48	0.79	0.11	0.33	0.005
NSE	0.50	0.82	-0.85	-0.28	0.46	0.08	0.27	-0.07
MSE	0.28	0.57	0.01	0.15	0.39	0.27	0.31	0.35
KGE	-0.10	0.78	-0.67	-0.15	0.24	0.12	0.17	-0.54

4.4.4 Calibration and Validation Results for River Station

Simulated monthly flow, sediment and nitrate load from Rev.528 and Rev.615 were compared with observed values during calibration and validation periods for site R5 (Figures 4.20, 4.23 and 4.24). Differences between simulated flow and observed values were plotted (Figure 4.21). Water budgets of simulated results from Rev.528 and Rev.615 were plotted (Figure 4.22). Model performance of simulating flow, sediment, and nitrate load for site R5 were evaluated (Table 4.11).

Performance of the modeled monthly flow from Rev.528 and Rev.615 at site R5 during calibration and validation was satisfactory. Simulated monthly flow results from Rev.528 were slightly better than those from Rev.615 at site R5. Generally, simulated monthly flow was similar to observed values (Figure 4.20). However, Rev.528 simulated flow values were higher than observed values in May 1996 and December 1997 (Figure 4.20), and the differences between simulated and observed flow values were large during these periods (Figure 4.21), which was mainly caused by overestimation of tile flow during these periods. Simulated tile flow by the old routine in Rev.528 was controlled by a simple drawdown time parameter (TDRIAN), no matter how intense the rainfall. Thus, Rev.528 had potential to simulate overestimated tile flow peaks. Rev.528 and Rev.615 simulated flow values were slightly higher than observed values from June to November of 1994, 1996 and 1998 (Figure 4.20), which was mainly because of the overestimation of surface runoff during these periods. Calibration ranges of CN2 (-20%~-10%) and CNCOEF (0.5~2) were realistic for a watershed dominated by agricultural land (Table 4.6), and simulated surface

runoff was overestimated. Rev.528 and Rev.615 simulated flow values were lower than observed values from January 2000 to February 2001 (Figure 4.20), and the differences between simulated and observed flow values were large during these periods (Figure 4.21), which was mainly caused by underestimation of tile flow. The old routine in Rev.528 could not simulate tile flow, and the new routine in Rev.615 could not use the Kirkham equation to calculate tile drainage flux when the water table was lower than tiles after the long dry period in 1999. P_{BIAS} values of flow results from Rev.528 and Rev.615 during the calibration period were -36% and -48% respectively, representing overestimated simulation results. P_{BIAS} values of flow results from Rev.528 and Rev.615 during the validation period were -1% and -11%, respectively, indicating accurate simulation results. Generally, R^2, NSE and KGE values for simulated flow results from Rev.528 and Rev.615 were satisfactory (>0.5), except that NSE (0.48) from Rev.615 during validation period was slightly under the acceptable limit (Table 4.11). MSE from Rev.615 during the calibration period (0.43) was slightly under the acceptable limit, and MSE from Rev.528 (0.36) and Rev.615 (0.26) during the validation period was unacceptable (Table 4.11). Simulated flow results from Rev.528 and Rev.615 during the calibration period had a better match with observed values (Figures 4.20 and 4.21) and better P_{BIAS}, R^2, NSE, MSE, and KGE values than those during the validation period. The long dry period during 1999 affected water table depth calculation and then simulation of tile flow from Rev.528 and Rev.615 during 2000 and 2001.

Annual flow partitioning from Rev.528 and Rev.615 for site R5 during simulation period was plotted (Figure 4.22). Simulated average annual tile flow values from Rev.528 (128 mm) and Rev.615 (129 mm) were 14% and 15% of total precipitation over the period from 1992 to 2003. Simulated average annual ET values from Rev.528 (585 mm) and Rev.615 (571 mm) were 71% and 69% of total precipitation. Simulated average annual water yield values from Rev.528 (248 mm) and Rev.615 (265 mm) were 27% and 29% of total precipitation. Flow partitioning appeared reasonable for simulated results from Rev.528 and Rev.615. Major flow paths are important in determining sediment and nitrate loads.

Performance of the modeled monthly sediment load in flow from Rev.528 and Rev.615 at site R5 during calibration and validation was reasonable. Simulated monthly sediment load in flow results from Rev.615 were better than those from Rev.528 at site R5. Simulated monthly sediment load from Rev.528 and Rev.615 matched observed values fairly well, except that both routines could not capture sediment load peaks well (Figure 4.23), which was caused by the failure of predicting surface runoff. P_{BIAS} values of sediment load results were 62% and -141% from Rev.528, and 10% and -474% from Rev.615 during calibration and validation periods, respectively, indicating underestimated model simulation during calibration and overestimated model simulation during validation (Table 4.11). Generally, R^2, NSE, MSE and KGE values for simulated sediment were unsatisfactory (< 0.5), except that for KGE (0.56) from Rev.615 during the calibration period, and R^2 (0.76) from Rev.615 during validation was acceptable (Table 4.9). However, for watersheds dominated by tile flow, surface runoff is low and it was challenging to simulate sediment load accurately. Rev.528 and Rev.615 simulated sediment load had difficulty in simulating sediment load peaks (Figure 4.23), and performance evaluation results were unacceptable generally (Table 4.11), but simulated sediment load can still be considered reasonable, since the magnitude of sediment load in mildly-sloped watershed was small (Figure 4.23).

Performance of the modeled monthly nitrate load in flow from Rev.528 and Rev.615 at site R5 during calibration and validation was satisfactory. Simulated monthly nitrate loads in flow results from Rev.615 were better than those from Rev.528 at site R5. Simulated monthly nitrate load was similar to observed values, except that Rev.528 simulated nitrate load values were higher than observed values in May 1996, December 1997, and May 2002 (Figure 4.24), which was mainly caused by overestimation of tile flow during these periods. Rev.528 and Rev.615 simulated nitrate load values were lower than observed values during June 1997, and May and June of 2002 (Figure 4.24), which was mainly caused by underestimation of tile flow during these periods. P_{BIAS} values of nitrate load results were 11% and 31% from Rev.528 during calibration and validation periods, and 17% and 37% from Rev.615 during calibration and validation periods, indicating accurate model simulation. Generally, R^2, NSE, MSE and KGE values for simulated nitrate load were satisfactory (>0.5). However, NSE (0.33) and MSE (0.40) from Rev.528 during the

calibration period were unacceptable, and KGE (0.48) from Rev.615 during the validation period were slightly under the acceptable limit (Table 4.11). R^2, NSE and MSE values from Rev.615 were 0.63, 0.48 and 0.26 for simulated flow, and 0.67, 0.58 and 0.50 for simulated nitrate load during the validation period (Table 4.11), which may be because simulated nitrate load results could capture peaks better than simulated flow results during May 2000 and February 2001 (Figures 4.20 and 4.24).

The new tile drainage routine in Rev.615 was improved compared to the old routine in Rev.528. Capacity of water that can be drained by tiles was unlimited by the old routine in Rev.528, and the old routine overestimated tile flow peaks and resulted in overestimated flow results during the calibration period (Figure 4.20). While simulation of tile flow from the new routine in Rev.615 incorporated drainage coefficient to control peak drain flow (Figure 4.20). Rev.528 could not simulate tile flow once the water table was lower than tile depth, while Rev.615 could simulate tile flow by the Hooghoudt equation once the water table dropped after a long dry period during validation (Figure 4.21). Rev.615 incorporated more realistic tile parameters, such as drainage coefficient, tile depth, multiplication factor to determine lateral saturated hydraulic conductivity, effective radius and tile spacing to represent characteristics of tile drainage system, which can simulate tile flow more realistically. Some processes in Rev.615 could be improved. For instance, DEP_IMP can represent depth to impervious layer and soil permeability and can be separated in the model. Water table depth calculation can determine which equation will be used for tile flow simulation, and water table depth calculation during long dry period can be improved to better simulate tile flow.

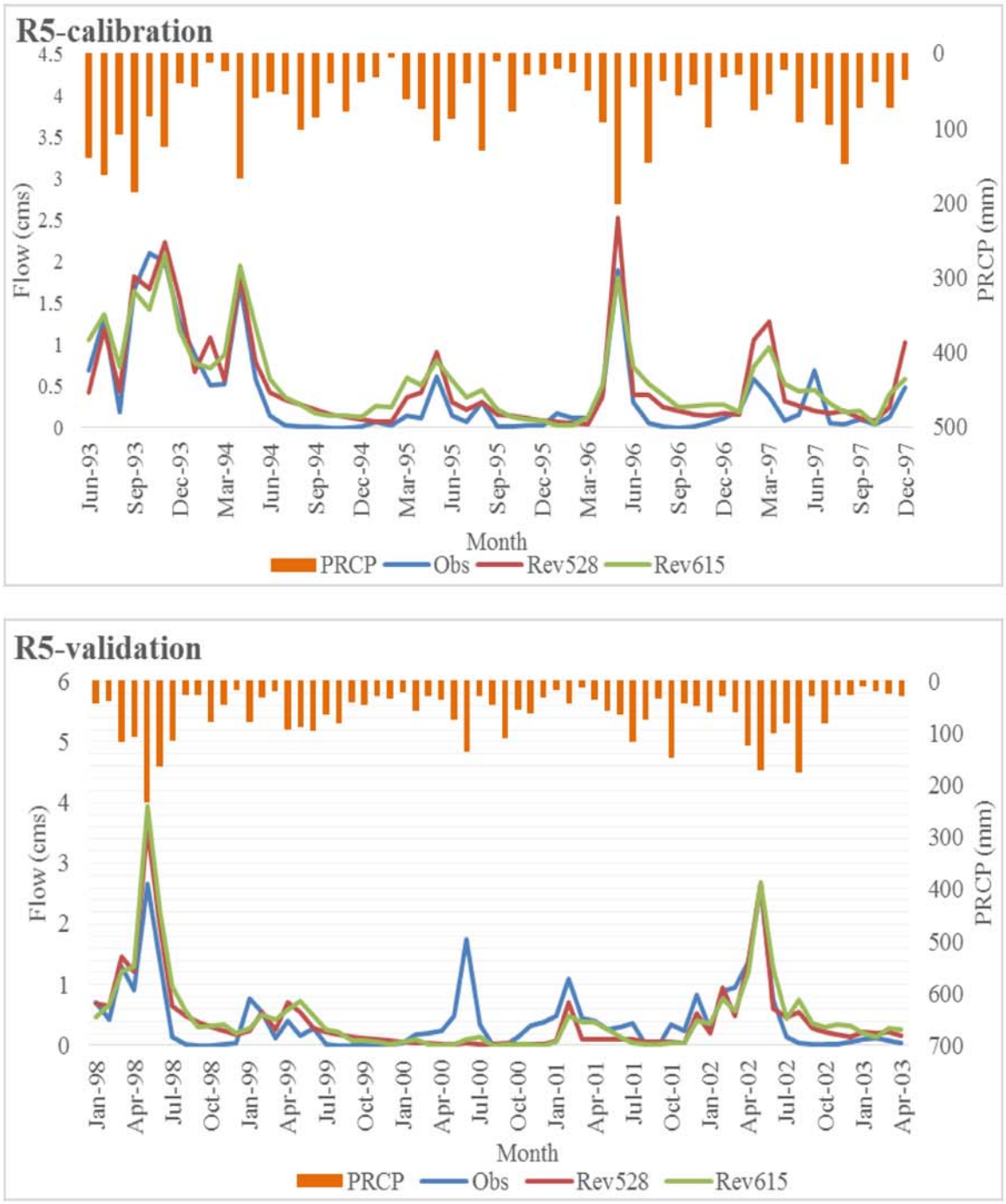

Figure 4.19 Calibration and validation results for monthly flow at site R5

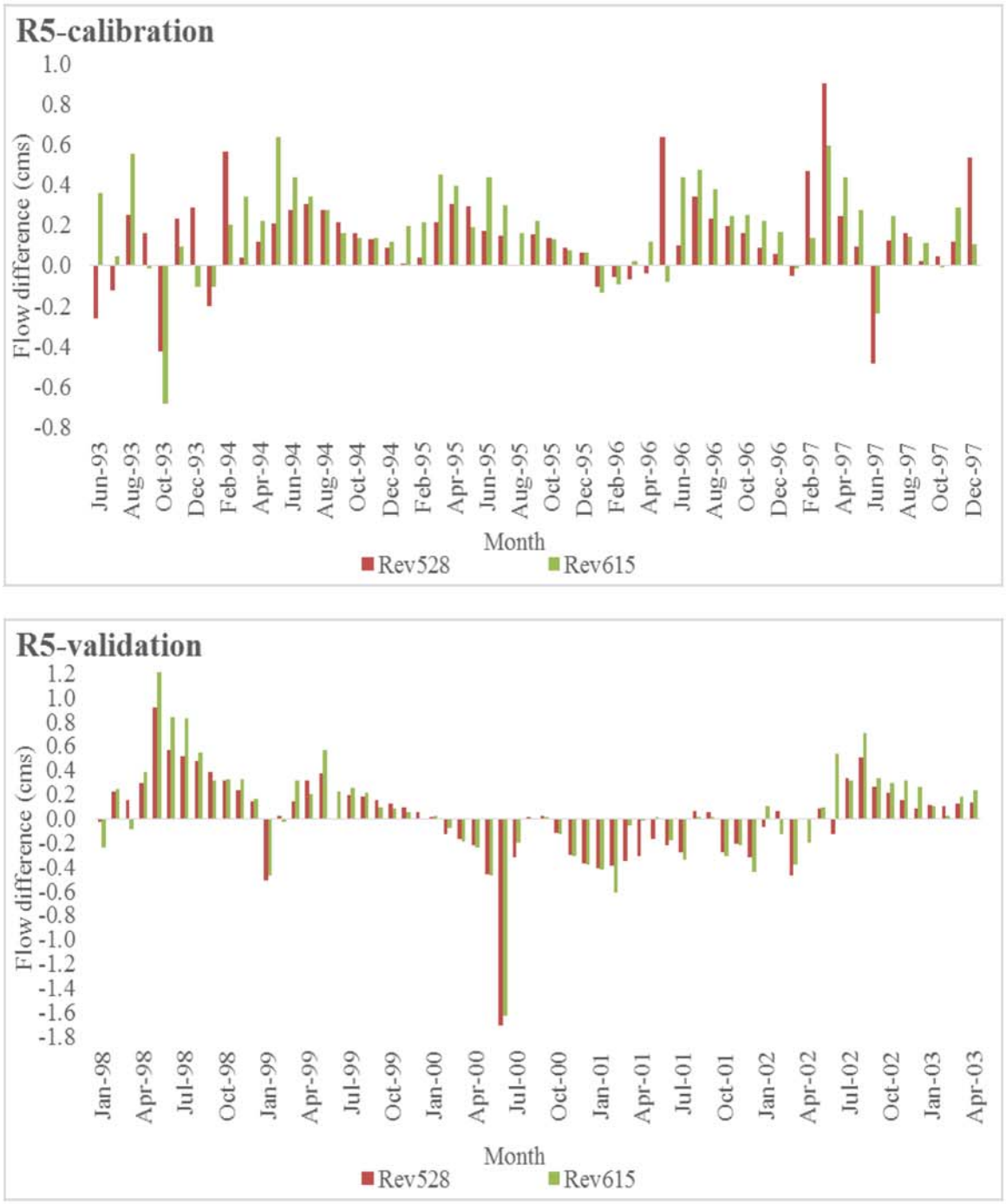

Figure 4.20 Difference between simulated monthly flow with observed values at site R5

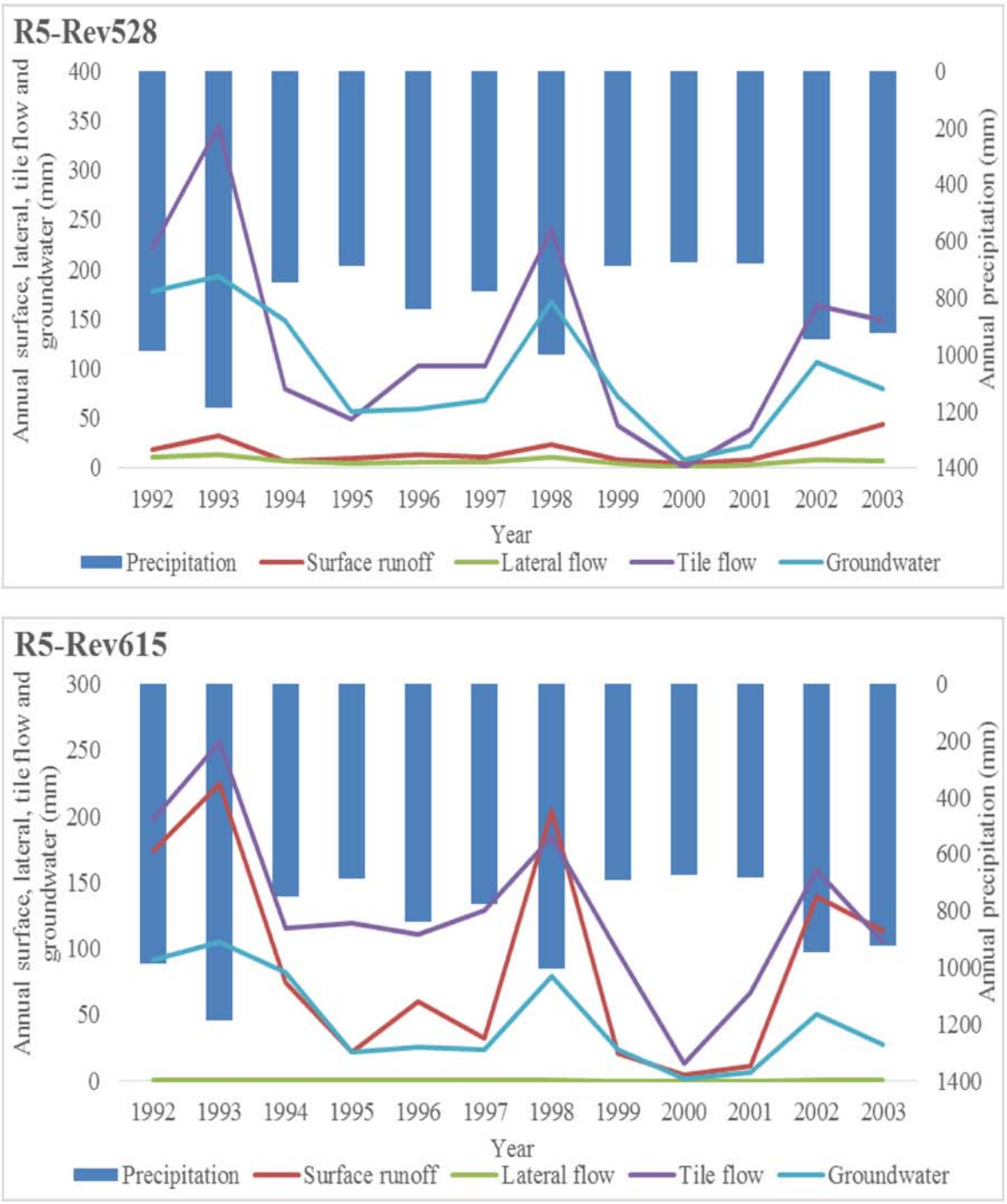

Figure 4.21 Annual flow partitioning from Rev.528 and Rev.615 at site R5

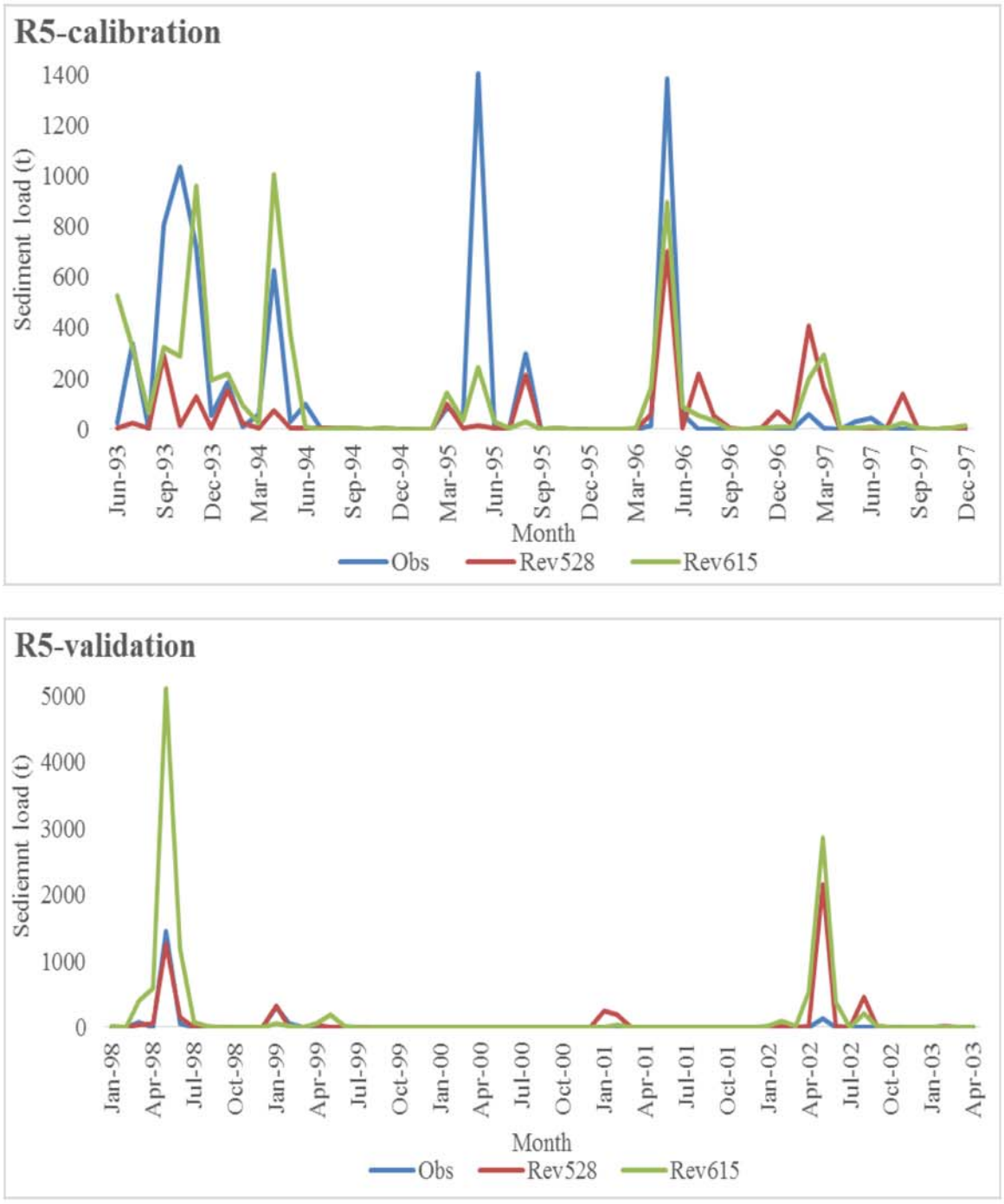

Figure 4.22 Calibration and validation results for monthly sediment load at site R5

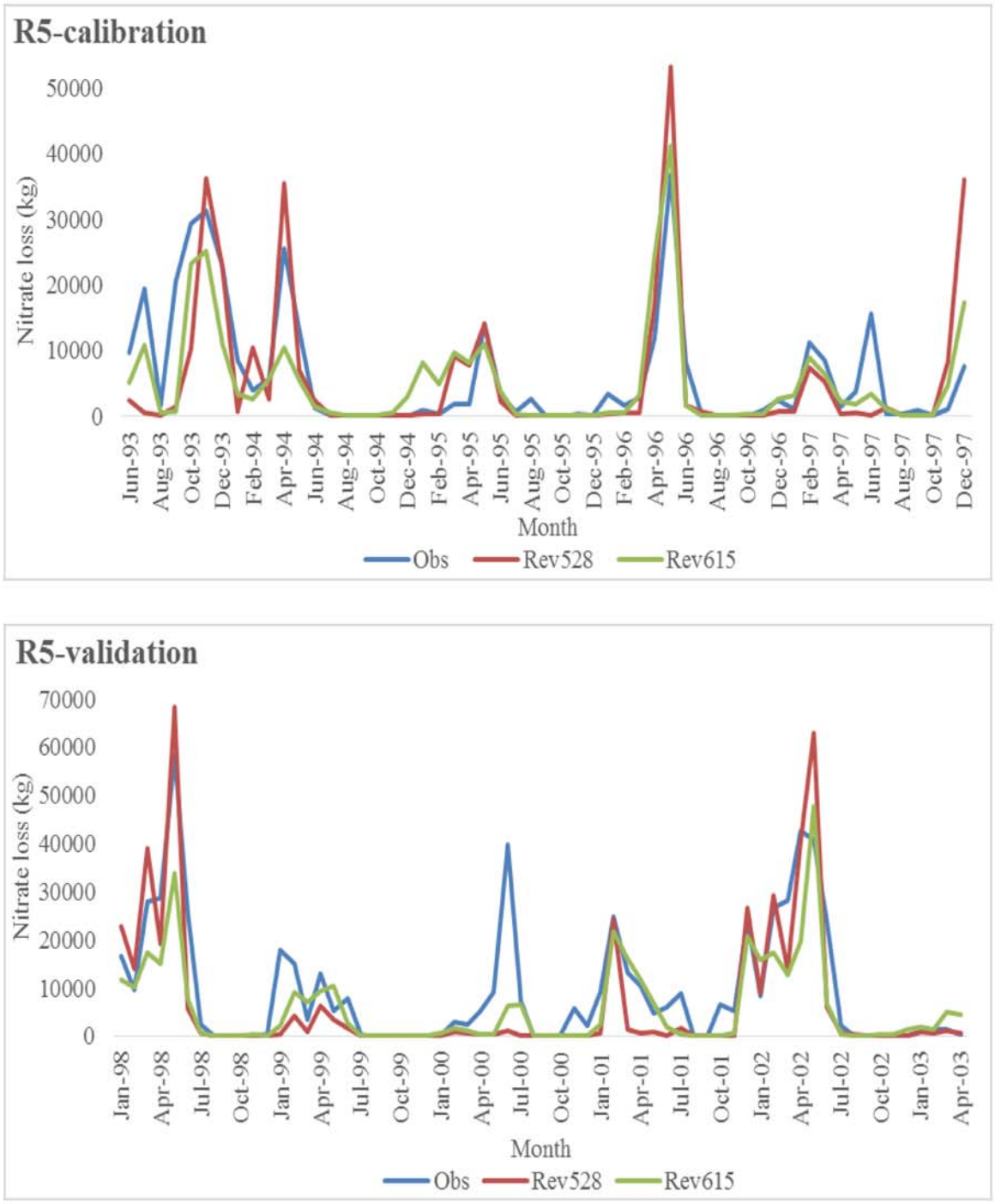

Figure 4.23 Calibration and validation results for monthly nitrate load at site R5

Table 4.11 Performance evaluation of calibrated tile flow and nitrate in tile flow results at site R5

Site R5	Monthly Flow (cms)				Monthly Sediment (t)				Monthly Nitrate (kg)			
	Cali		Vali		Cali		Vali		Cali		Vali	
Revision	528	615	528	615	528	615	528	615	528	615	528	615
P_{BIAS} (%)	-36	-48	-1	-11	62	10	-141	-474	11	17	31	37
R^2	0.85	0.84	0.68	0.63	0.27	0.45	0.31	0.76	0.56	0.63	0.70	0.67
NSE	0.77	0.73	0.60	0.48	0.18	0.45	-1.05	-9.67	0.33	0.61	0.57	0.58
MSE	0.50	0.43	0.36	0.26	0.40	0.46	0.07	-1.77	0.40	0.50	0.51	0.50
KGE	0.63	0.50	0.80	0.71	0.001	0.56	-0.63	-4.61	0.65	0.71	0.64	0.48

Cali and Vali are abbreviations for Calibration and Validation, respectively.

4.5 Conclusions

The old tile drainage routine in SWAT2009 (Rev.528) and the new tile drainage routine in SWAT2012 (Rev.615 and Rev.645) were used to simulate monthly tile flow, nitrate in tile flow, surface runoff, and sediment and nitrate in surface runoff at field sites, and monthly flow, sediment and nitrate in flow at a river station. Performance of both routines was evaluated and compared with observed values.

The results showed that Rev.615 satisfactorily simulated corn and soybean yield results at field sites, and both routines provided satisfactory tile flow and nitrate in tile flow results at subsurface sites, satisfactory flow and nitrate load in flow, and reasonable sediment load in flow results at the river station after model calibration. Rev.645 with an improved curve number calculation method provided satisfactory surface runoff, and reasonable sediment and nitrate load in surface runoff results at surface stations.

Generally, simulated tile flow results by the old routine were better than those for the new routine at site B, while simulated tile flow results from the new routine were better than those from the old routine at site E. Nitrate in tile flow results from the new routine were better than those from the old routine at both sites. Simulated flow and nitrate in flow results from the new routine were better than those from the old routine at site R5. The new routine provided more realistic and accurate simulation of tile drainage, and the new curve number retention parameter adjustment factor in Rev.645 improved surface runoff simulation, and is suitable for surface runoff simulation in mildly-sloped watersheds.

Limitations of this work include limited observed rainfall data for site R5, water table depth calculation after long dry periods, and difficulty in simulating surface runoff, sediment, and nitrate in surface runoff from this extensively tile drained, mildly-sloped watershed. Observed rainfall data for site R5 was from the closest rain gauge station located 6 km southeast of site R5, which may impact the accuracy of flow simulation at site R5. There is an opportunity to improve the representation of tile drainage systems in SWAT, and improve Rev.645 functionality at watershed scales. The new routine and the improved curve number calculation method can be tested in more individual tiles and watersheds.

4.6 References

Alexander, R. B., Smith, R. A., Schwarz, G. E., Boyer, E. W., Nolan, J. V., & Brakebill, J. W. (2007). Differences in phosphorus and nitrogen delivery to the Gulf of Mexico from the Mississippi River Basin. *Environmental Science & Technology*, *42*(3), 822-830.

Algoazany, A. S. (2006). Long-term effects of agricultural chemicals and management practices on water quality in a subsurface drained watershed (Doctoral dissertation, University of Illinois at Urbana-Champaign).

Algoazany, A. S., Kalita, P. K., Czapar, G. F., & Mitchell, J. K. (2007). Phosphorus transport through subsurface drainage and surface runoff from a flat watershed in east central Illinois, USA. *Journal of Environmental Quality*, *36*(3), 681-693.

Arnold, J.G., Kiniry, J.R., Srinivasan, R., Williams, J.R., Hansey, E.B., & Neitsch, S.L. (2014). Soil and Water Assessment Tool Input/Output Documentation Version 2012. *USDA Agricultural Research Service and Texas A&M Blackland Research Center, Temple, Texas*.

Arnold, J. G., P. W. Gassman, K. W. King, A. Saleh, and U. Sunday.(1999). Validation of the subsurface tile flow component in the SWAT model. Presented at the ASAE/CSAE-SCGR Annual International Meeting. ASAE Paper No. 992138. St. Joseph, Mich.: ASAE.

Arnold, J. G., Srinivasan, R., Muttiah, R. S., & Williams, J. R. (1998). Large area hydrologic modeling and assessment part I: Model development1. *JAWRA Journal of the American Water Resources Association*, *34*(1), 73-89.

Boles, C. M. (2013). *SWAT model simulation of bioenergy crop impacts in a tile-drained watershed* (Master thesis), Purdue University.

Boles, C. M., Frankenberger, J. R., & Moriasi, D. N. (2015). Tile Drainage Simulation in SWAT2012: Parameterization and Evaluation in an Indiana Watershed. *Trans. ASABE*, *58*(5), 1201-1213.

Diaz, Robert J. and Solow, Andrew (1999) *Ecological and economic consequences of hypoxia: Topic 2 Report for the Integrated Assessment on Hypoxia in the Gulf of Mexico.* Silver Spring, MD , NOAA/National Centers for Coastal Ocean Science , 45pp. (NOAA Coastal Ocean Program Decision Analysis Series, 16)

Drablos, C. J. W., Konyha, K. D., Simmons, F. W., & Hirschi, M. C. (1988). Estimating soil parameters used in DRAINMOD for artificially drained soils in Illinois. *American Society of Agricultural Engineers (Microfiche collection)(USA)*.

Du, B., Arnold, J. G., Saleh, A., & Jaynes, D. B. (2005). Development and application of SWAT to landscapes with tiles and potholes. *Trans. ASAE*, *48*(3), 1121-1133.

Du, B., Saleh, A., Jaynes, D. B., & Arnold, J. G. (2006). Evaluation of SWAT in simulating nitrate nitrogen and atrazine fates in a watershed with tiles and potholes. *Trans. ASAE*, *49*(4), 949-959.

Edwards, J. T., & Purcell, L. C. (2005). Soybean yield and biomass responses to increasing plant population among diverse maturity groups. *Crop Science*, *45*(5), 1770-1777.

Edwards, J. T.; Purcell, L. C.; Vories, E. D (2005). Light Interception and Yield Potential of Short-Season Maize (Zea mays L.) Hybrids in the Midsouth. *Agronomy J. 97*(1), 225-234.

Fausey, N. R., Brown, L. C., Belcher, H. W., & Kanwar, R. S. (1995). Drainage and water quality in Great Lakes and cornbelt states. *Journal of Irrigation and Drainage Engineering*, *121*(4), 283-288.

Gentry, L. E., David, M. B., Smith-Starks, K. M., & Kovacic, D. A. (2000). Nitrogen fertilizer and herbicide transport from tile drained fields. *Journal of Environmental Quality*, *29*(1), 232-240.

Gupta, H. V., Sorooshian, S., & Yapo, P. O. (1999). Status of automatic calibration for hydrologic models: Comparison with multilevel expert calibration. *Journal of Hydrologic Engineering*, *4*(2), 135-143.

Hernandez-Ramirez, G., Brouder, S. M., Ruark, M. D., & Turco, R. F. (2011). Nitrate, phosphate, and ammonium loads at subsurface drains: Agroecosystems and nitrogen management. *Journal of Environmental Quality*, *40*(4), 1229-1240.

Illinois Environmental Protection Agency: Bureau of Water. (2008). Little Vermilion River Lake Georgetown Watershed TMDL Report. Springfield, IL., 2008 June.

James, L. D., & Burges, S. J. (1982). Selection, calibration, and testing of hydrologic models. *Hydrologic Modeling of Small Watersheds*, (5), 435-472.

Jaynes, D.B., and D.E. James. 2007. The extent of farm drainage in the United States. In *Proceedings of the Annual Meeting of the Soil and Water Conservation Society*, Tampa, Florida, July 21, 2007. Ankeny, IA: Soil and Water Conservation Society.

Kalita, P. K., Algoazany, A. S., Mitchell, J. K., Cooke, R. A. C., & Hirschi, M. C. (2006). Subsurface water quality from a flat tile-drained watershed in Illinois, USA. *Agriculture, Ecosystems & Environment*, *115*(1), 183-193.

Keefer, L. (2003). *Sediment and Water Quality Monitoring for the Vermilion River and Little Vermilion River Watersheds*. Illinois State Water Survey. 2003, April.

Kiniry, J.R.; Landivar, J.A.; Witt, M.; Gerik, T.J.; Cavero, J.; Wade. L.J. (1989). Radiation-use efficiency response to vapor pressure deficit for maize and sorghum. *Field Crops Research. 56: 265–270.*

Kirkham, D. (1957). Theory of land drainage. *Drainage of agricultural lands. Agron. Monogr*, *7*, 139-181.

Kladivko, E. J., Brown, L. C., & Baker, J. L. (2001). Pesticide transport to subsurface tile drains in humid regions of North America. *Critical Reviews in Environmental Science and Technology*, *31*(1), 1-62.

Koch, S., Bauwe, A., & Lennartz, B. (2013). Application of the SWAT model for a tile-drained lowland catchment in North-Eastern Germany on subbasin scale. *Water Resources Management*, *27*(3), 791-805.

Krause, P., Boyle, D. P., & Bäse, F. (2005). Comparison of different efficiency criteria for hydrological model assessment. *Advances in Geosciences*, *5*, 89-97.

Lal, R., Logan, T. J., & Fausey, N. R. (1989). Long-term tillage and wheel traffic effects on a poorly drained Mollic Ochraqualf in northwest Ohio. 1. Soil physical properties, root distribution and grain yield of corn and soybean. *Soil and Tillage Research*, *14*(4), 341-358.

Larose, M., Heathman, G. C., Norton, L. D., & Engel, B. (2007). Hydrologic and atrazine simulation of the Cedar Creek watershed using the SWAT model. *Journal of Environmental Quality*, *36*(2), 521-531.

Lindquist, J. L.; Arkebauer, T. J.; Walters, D. T.; Cassman, K. G.; Dobermann, A (2005). Maize Radiation Use Efficiency under Optimal Growth Conditions. *Agronomy Journal*, *97*(1), 72-78.

Macrae, M. L., English, M. C., Schiff, S. L., & Stone, M. (2007). Intra-annual variability in the contribution of tile drains to basin discharge and phosphorus export in a first-order agricultural catchment. *Agricultural Water Management*, *92*(3), 171-182.

Mastrodomenico, A. T.; Purcell, L. C. (2012). Soybean Nitrogen Fixation and Nitrogen Remobilization during Reproductive Development. *Crop Sciec.*, *52*(3), 1281-1289.

Mitchell, J. K., McIsaac, G. F., Walker, S. E., & Hirschi, M. C. (2000). Nitrate in river and subsurface drainage flows from an east central Illinois watershed. *Trans. ASAE*, *43*(2), 337-342.

Mitchell, J. K., Kalita, P. K., Hirschi, M. C., & Cooke, R. A. C. (2003). Upland drainage–watershed hydrology is different. In *AWRA 2003 Spring Specialty Conf. Agricultural Hydrology and Water Quality* (Vol. 1214), 12-14 May 2003, Kansas City, MO.

Moriasi, D. N., Arnold, J. G., & Green, C. H. (2007a, July). Incorporation of Hooghoudt and Kirkham tile drain equations into SWAT2005. In *Proc. 4th Intl. SWAT Conf* (pp. 139-147).

Moriasi, D. N., Arnold, J. G., Van Liew, M. W., Bingner, R. L., Harmel, R. D., & Veith, T. L. (2007b). Model evaluation guidelines for systematic quantification of accuracy in watershed simulations. *Trans. of ASABE*, *50*(3), 885-900.

Moriasi, D. N., Rossi, C. G., Arnold, J. G., & Tomer, M. D. (2012). Evaluating hydrology of the Soil and Water Assessment Tool (SWAT) with new tile drain equations. *Journal of Soil and Water Conservation*, *67*(6), 513-524.

Moriasi, D. N., Gowda, P. H., Arnold, J. G., Mulla, D. J., Ale, S., Steiner, J. L., & Tomer, M. D. (2013). Evaluation of the Hooghoudt and Kirkham tile drain equations in the Soil and Water Assessment Tool to simulate tile flow and nitrate-nitrogen. *Journal of Environmental Quality*, *42*(6), 1699-1710.

Muhr, J., Höhle, J., Otieno, D. O., & Borken, W. (2011). Manipulative lowering of the water table during summer does not affect CO2 emissions and uptake in a fen in Germany. *Ecological Applications*, *21*(2), 391-401

Nash, J., & Sutcliffe, J. V. (1970). River flow forecasting through conceptual models part I—A discussion of principles. *Journal of Hydrology*, *10*(3), 282-290.

Neitsch, S.L, Arnold, J.G., Kiniry, J.R., & Williams, J.R. (2011). Soil and Water Assessment Tool Theoretical Documentation Version 2009. *USDA Agricultural Research Service and Texas A&M Blackland Research Center, Temple, Texas*.

Neitsch, S. L., Arnold, J. G., Kiniry, J. R., and Williams, J. R. (2005). *Soil and Water Assessment Tool theoretical documentation: Version 2005*, USDA Agricultural Research Service and Texas A&M Blackland Research Center, Temple, Texas.

Neitsch, S. L., Arnold, J. G., Kiniry, J. R., and Williams, J. R. (2002). *Soil and Water Assessment Tool theoretical documentation: Version 2000*, USDA Agricultural Research Service and Texas A&M Blackland Research Center, Temple, Texas.

Rabalais, N. N., Turner, R. E., Justic, D., Dortch, Q., & Wiseman Jr, W. J. (1999). *Characterization of hypoxia: Topic 1 Report for the Integrated Assessment of Hypoxia in the Gulf of Mexico*. NOAA Coastal Ocean Program, 46-47.

Schilling, K. E., & Helmers, M. (2008). Effects of subsurface drainage tiles on streamflow in Iowa agricultural watersheds: Exploratory hydrograph analysis. *Hydrological Processes*, *22*(23), 4497-4506.

Schroeder, J. W. (2004). *Silage fermentation and preservation*. Fargo, North Dakota: North Dakota State University Extension Service.

Shirmohammadi, A., Wenberg, R. D., Ritter, W. F., & Wright, F. S. (1995). Effect of agricultural drainage on water quality in Mid-Atlantic States. *Journal of Irrigation and Drainage Engineering*, *121*(4), 302-306.

Sinclair, T. R., & Muchow, R. C. (1999). Radiation use efficiency. *Advances in agronomy*, *65*(21), 5-265.

Singh, R., Helmers, M. J., & Qi, Z. (2006). Calibration and validation of DRAINMOD to design subsurface drainage systems for Iowa's tile landscapes. *Agricultural Water Management*, *85*(3), 221-232.

Singh, R., Helmers, M. J., Crumpton, W. G., & Lemke, D. W. (2007). Predicting effects of drainage water management in Iowa's subsurface drained landscapes. *Agricultural Water Management*, *92*(3), 162-170.

Singh, R., & Helmers, M. J. (2008). Improving Crop Growth Simulation in the Hydrologic Model DRAINMOD to Simulate Corn Yields in Subsurface Drained Landscapes. In *2008 Providence, Rhode Island, June 29–July 2, 2008* (p. 1). American Society of Agricultural and Biological Engineers.

Singh, J., P. K. Kalita, J. K. Mitchell, R. A. C. Cooke, and M. C. Hirschi. "Simulation of tile flow for a flat tile drained watershed in east central Illinois." In *2001 ASAE Annual Meeting*, p. 1. American Society of Agricultural and Biological Engineers, July 29- August 1, 2001, Sacramento, California, USA.

Skaggs, R. W., Youssef, M. A., & Chescheir, G. M. (2012). DRAINMOD: Model use, calibration, and validation. *Trans. ASABE*, *55*(4), 1509-1522.

Sugg, Z. (2007). Assessing US farm drainage: Can GIS lead to better estimates of subsurface drainage extent. *World Resources Institute, Washington, DC20002*.

Sui, Y. (2007). *Potential impact of controlled drainage in Indiana watersheds*. ProQuest.

Sui, Y., & Frankenberger, J. R. (2008). Nitrate loss from subsurface drains in an agricultural watershed using SWAT2005. *Trans. ASABE*, *51*(4), 1263-1272.

Tiemeyer, B., Lennartz, B., & Kahle, P. (2008). Analysing nitrate losses from an artificially drained lowland catchment (North-Eastern Germany) with a mixing model. *Agriculture, Ecosystems & Environment*, *123*(1), 125-136.

U.S. Environmental Protection Agency, National Agriculture Compliance Assistance Center. (2014). Drainage. Retrieved from website: http://www.epa.gov/oecaagct/ag101/cropdrainage.html.

University of Illinois Extension. Bioreactor, Water Table Management, and Water Quality: Brief History of Tilling. (2014). Retrieved from website: http://web.extension.illinois.edu/bioreactors/history.cfm.

Van Liew, M. W., Arnold, J. G., & Garbrecht, J. D. (2003). Hydrologic simulation on agricultural watersheds: Choosing between two models. *Tran. ASAE*, *46*(6), 1539-1551.

Yuan, Y., Mitchell, J. K., Walker, S. E., Hirschi, M. C., & Cooke, R. A. C. (2000). Atrazine losses from corn fields in the Little Vermilion River watershed in east central Illinois. *Applied Engineering in Agriculture*, *16*(1), 51.

Zanardo, S., Basu, N. B., Botter, G., Rinaldo, A., & Rao, P. S. C. (2012). Dominant controls on pesticide transport from tile to catchment scale: Lessons from a minimalist model. *Water Resources Research*, *48*(4), 1-17.

CHAPTER 5. EVALUATION OF BIOENERGY CROP GROWTH AND THE IMPACTS OF BIOENERGY CROPS ON STREAMFLOW, TILE DRAIN FLOW AND NUTRIENT LOSSES IN THE LITTLE VERMILLION WATERSHED USING SWAT

5.1 Abstract

Large quantities of biofuel production are expected from bioenergy crops at a national scale to meet US biofuel goals. It is important to study biomass production of bioenergy crops and the impacts of these crops on water quantity and quality to identify environment-friendly and productive biofeedstocks. In this study, SWAT2012 (Revision 615) with a new tile drainage routine (DRAINMOD routine) and improved perennial grass and tree growth simulation was used to model long-term annual biomass yields, streamflow, tile flow, sediment load, total nitrogen, nitrate load in flow, nitrate in tile flow, soluble nitrogen, organic nitrogen, total phosphorus, mineral phosphorus and organic phosphorus under various bioenergy scenarios in an extensively agricultural watershed in the Midwestern US. Simulated results from different bioenergy crop scenarios were compared with those from the baseline. The results showed that simulated annual crop yields were similar to observed county level values for corn and soybeans, and were reasonable for *Miscanthus*, switchgrass and hybrid poplar. Removal of 38% of corn stover (66,439 Mg/yr) with *Miscanthus* production on highly erodible areas and marginal land (19,039 Mg/yr) provided the highest biofeedstock production. Streamflow, tile flow, erosion and nutrient losses were reduced under bioenergy crop scenarios of *Miscanthus*, switchgrass, and hybrid poplar on highly erodible areas, marginal land and marginal land with forest. Corn stover removal did not result in significant water quality changes. The increase in sediment load and nutrient losses under corn stover removal could be offset with production of other bioenergy crops in other portions of the watershed. Potential areas for bioenergy crop production when meeting the criteria above were small, thus the ability to produce biomass and improve water quality was not substantial. The study showed that corn stover removal

with bioenergy crops both on highly erodible areas and marginal land could provide more biofuel production relative to the baseline, and was beneficial to hydrology and water quality at the watershed scale, providing guidance for further research on evaluation of bioenergy crop scenarios in a typical extensively tile-drained watershed in the Midwestern U.S.

5.2 Introduction

One of the grand challenges in meeting the US biofuel goal is supplying large quantities of cellulosic materials for biofuel production at a national scale. Based on productivity and adaptability in different regions, the selection of biofeedstocks will vary geographically. Land cover change, management practices and climate change have impacts on water quantity, sediment and nutrient losses. Thus, it is challenging to take advantage of the opportunity bioenergy crops offer, while safeguarding against their potential environmental disadvantages. The study of the effects of bioenergy crop growth and intensive tile drainage systems on tile drain flow and nutrient loading in subsurface flow is of great significance.

5.2.1 Nutrient Loadings in Watersheds in Midwest and Hypoxia in Mississippi River and Gulf of Mexico

The Mississippi River system encompasses 41% of the conterminous US and contributes an average 580 km^3 of fresh water along with 210×10^6 Mg sediment, 1.6×10^6 Mg nitrogen and 0.1×10^6 Mg phosphorus to the Gulf of Mexico yearly (Rabalais *et al.*, 1999). Nutrient loading from the Mississippi River to the adjacent continental shelf has doubled from the 1950s to the 1960s. The Gulf of Mexico has undergone eutrophication as a result of increasing nutrients that has worsened hypoxia (Brezonik *et al.*, 1999). Tile drainage of agricultural fields in the Midwestern U.S. provides the majority of the nitrate that enters the Mississippi River and contributes to hypoxia in the northern Gulf of Mexico (Jaynes and James, 2007). Kalita *et al.* (2007) estimated that 15% of Mississippi river nitrogen loading and 10% of phosphorus loading comes from Illinois. Numerous studies have demonstrated that the application of agrochemicals in watersheds in the Midwestern US

not only impact water quality at the watershed scale, but also affect receiving water bodies and drive coastal hypoxia in the Gulf of Mexico (Rabalais *et al*., 2002; Phillips *et al*., 2006; Blann *et al*., 2009). Models that link Mississippi River discharge with Gulf of Mexico hypoxia have shown that a reduction in oxygen demand would result from nitrogen reduction, meaning that a decrease of nutrient loading can alleviate hypoxia in the Gulf of Mexico (Rabalais *et al*., 1999).

5.2.2 Biofeedstock Yield under Different Bioenergy Crop Scenarios

Bioenergy crops, such as corn (*Zea mays* L.), corn stover, Shawnee switchgrass (*Panicum virgatum L.*), *Miscanthus* (*Miscanthus* × *giganteus*) and *Populus* 'Tristis #1' (*Populus balsamifera* L. × *P.tristis* Fisch), are biofeedstock sources for biofuel production (McIsaac *et al*., 2010; Kiniry *et al*., 2012; Thomas *et al*., 2014; Cibin *et al*., 2015; Guo *et al*., 2015; Kiniry *et al*., 2015). Bioenergy crops can have different levels of potential crop yield under different scenarios. For example, Parajuli and Duffy (2013) modeled and compared biomass yields of bioenergy crops in the Town Creek watershed, and the results showed that growing *Miscanthus* could obtain the greatest long-term average annual feedstock yield followed by switchgrass, corn, and soybeans. Additionally, biomass yields of five forest scenario (clear cutting at 10%, 20%, 30%, 55% and 75% of the total forest area) yields were evaluated using SWAT and showed that with an increase in the forest area clearcut percentage, crop yield also increased (Khanal and Parajuli, 2013). Moreover, biofuel production from corn residue could be economically viable with government support, and may cause more continuous corn planting (Cibin *et al*., 2012). Annual average biomass yields for corn stover with 38%, 52% and 70% removal rates were modeled as 4.1 Mg/ha, 5.6 Mg/ha and 7.5 Mg/ha by SWAT (Cibin *et al*., 2012).

5.2.3 The Impacts of Bioenergy Crop Growth on Hydrology and Water Quality under Different Scenarios

Bioenergy crop planting in large areas can potentially create problems like land competition with food crops and higher food prices. Numerous studies have been conducted on the influence of bioenergy crop scenarios on water quantity and quality.

5.2.3.1 Hydrologic and water quality responses to corn stover removal

Some researchers have studied water quantity and quality responses to removal of corn stover. For instance, streamflow was reduced, sediment loading was increased, nitrate and mineral phosphorus loading were reduced, and organic nitrogen loading was increased at the watershed outlet with three corn stover removal rates (38%, 52% and 70%) in watersheds in Indiana (Thomas *et al.*, 2011; Cibin *et al.*, 2012). Some researchers have found that 30 to 50% of corn stover could be removed without significantly impacting soil erosion and crop production (Lindstrom, 1986; Kim and Dale, 2004; Graham *et al.*, 2007). The influence of land use and land cover change on the water balance of the Raccoon River watershed in west-central Iowa was explored with SWAT, and the results showed that with the increase of corn production, annual evapotranspiration decreased and losses of sediment, nitrate and phosphorus and water yield increased (Jha *et al.*, 2007). Additionally, corn stover removal can accelerate soil cover losses, and have adverse impacts to soil and water conservation (Delgado, 2010). Corn stover removal can reduce organic carbon and total nitrogen and increase erosion, and additional fertilizer was recommended to compensate for nutrient reduction by corn stover removal (Karlen *et al.*, 1994; Kim and Dale, 2004; Graham *et al.*, 2007; Hoskinson *et al.*, 2007; Brechbill and Tyner, 2008; Cibin *et al.*, 2012).

5.2.3.2 Hydrologic and water quality responses to perennial grass growth

Some studies have quantified water quantity and quality responses to perennial grass growth at a watershed scale. For example, Hickman *et al.* (2010) found that switchgrass could increase evapotranspiration by 25% during the growing season compared with corn. The annual tile flow component change was small under perennial scenarios in the Raccoon River watershed in west-central Iowa simulated by SWAT (Jha *et al.*, 2007). Hydrologic responses to bioenergy crops in the Town Creek Watershed were estimated and the results predicted the lowest sediment yield from switchgrass and *Miscanthus* scenarios (Parajuli and Duffy, 2013). Moreover, Raj (2013) studied the environmental impacts of 13 plausible biofuel scenarios with perennial grasses, including agricultural marginal areas, which provided guidance for development of watershed management, such as slope, timing and

amount of fertilizer applied. Love and Nejadhashemi (2011) assessed water quality impacts of biofuel crops in four watersheds in Michigan and suggested that perennial grass species were the most suitable for implementation at large scales, the majority of which could reduce sediment and total phosphorus loadings. Additionally, Boles (2013) studied simulation of switchgrass growth and its impacts on tile flow and nutrient losses under different scenarios in Matson Ditch watershed, IN, and demonstrated that switchgrass growth can reduce nutrient and sediment export at the watershed outlet.

5.2.3.3 Hydrologic and water quality responses to hybrid poplar tree growth

Some researchers have studied water quantity and quality impacts of tree growth. For instance, the potential impacts of five forest scenarios (clear cutting at 10%, 20%, 30%, 55% and 75% of the total forest area) on water and sediment yields were explored in the Upper Pearl River Watershed located in east-central Mississippi, and the results demonstrated that with an increase in the forest area clearcut area from 10% to 75%, water and sediment yield changed between 17% to 96% and 33% to 250% (Khanal and Parajuli, 2013). Additionally, sediment loss from a *Populus* tree field site was lower than that from a conventional cotton field site in Mississippi (Thornton *et al*., 1998), and nutrient movement from woody crops was less than agricultural crops after the establishment year (Tolbert *et al*., 1997; Thornton *et al*., 1998). Moreover, fast growing hybrid poplar trees were also found to decrease total nitrogen and phosphorus loading in the Millsboro Pond Watershed (Aditya and William, 2010).

It is important to compare benefits of biofeedstock production of bioenergy crops, and water quantity and quality responses to bioenergy crops, to determine bioenergy crop scenarios with high biomass yield and low environmental impact.

5.2.4 Influence of Tile Drainage on Hydrology in the Little Vermilion River (LVR) Watershed

The 489 km^2 LVR watershed is a typical tile-drained flat watershed with altered hydrology from subsurface drainage systems in east central Illinois, USA. Generally, subsurface

drainage systems are laid out in an irregular fashion in east central Illinois. Tile drainage can increase infiltration and subsequently decrease surface runoff (Kladivko *et al.*, 2001). Based on long-term data from the LVR watershed, surface runoff rarely occurs in the LVR, and the removal of water from soils was mainly by subsurface drainage systems (Kalita *et al.*, 2006). In the upper Midwest of the US, subsurface drainage systems drain near-surface perched water tables, which lie above groundwater aquifers (Kalita *et al.*, 2006). In the perched water table zones, water and nutrients within it can discharge through the tile drainage to surface water or move downward to groundwater aquifers.

The hydrology of Midwestern landscapes has been extensively modified to promote rapid drainage by artificial surface ditches and subsurface tile drain construction (Schilling and Helmers, 2008; Basu *et al.*, 2010; Guan *et al.*, 2011). The subsurface drainage system increase hydrological connectivity to the channels and lead to quick responses to rainfall and exponential recession curves which dominate flow in the tile drainage and the streams (Evans and Fausey, 1999; Basu *et al.*, 2010).

5.2.5 Influence of Tile Drainage on Nutrient Loadings in the LVR Watershed

In agricultural watersheds with intensive artificial subsurface drainage networks, fertilizer and pesticide application has significantly affected the natural biogeochemical regime (Guan *et al.*, 2011). Water quality studies have been completed in the LVR watershed, including sediment transport (Mitchell *et al.*, 2000a), nitrate transport (Mitchell *et al.*, 2000b), model evaluation (Northcott *et al.*, 2001; Ye *et al.*, 2012; Yu *et al.*, 2001; Yuan *et al.*, 2001; Zanardo *et al.*, 2012) and Best Management Practices (BMPs) performance (Cooke *et al.*, 2001). Subsurface drainage systems can enhance water transport through soils and serve as major transport pathways for soluble chemicals such as nitrate-N and atrazine (Buhler *et al.*, 1993; Randall and Iragavarapu, 1995; Kalita *et al.*, 1998). Nutrient transport in subsurface systems has an influence on plant growth.

Kalita *et al.* (2006) studied surface water quality from the LVR watershed and demonstrated that the concentrations of nitrate-N in tile drains varied depending on fertilizer application methods. The contribution of pre-planting application to nitrate-N

concentrations was higher than the Drinking Water Standard of the US Environmental Protection Agency for nitrate-N (10 mg/L) in subsurface drainage water. Atrazine concentrations were lower than the Drinking Water Standard of the US Environmental Protection Agency (3 µg/L) in most water samples. Moreover, the LVR watershed was monitored by researchers, and the results demonstrated that nitrate-N concentrations in the river followed a seasonal cycle with no big differences along the river length. Nitrate-N concentrations in tile drains were higher from fields with more N fertilization, particularly when fertilization occurred prior to planting (Mitchell *et al.*, 2000b; Borah *et al.*, 2003).The solution to reducing nutrient loading from the LVR watershed in Illinois not only could improve water quality and meet the requirements of TMDLs in LVR watershed, but also could provide guidance for nutrient loading management in typical tile-drained watersheds in corn-belt states, and thus can decrease nutrient loading of the Mississippi River and alleviate hypoxia conditions in the Gulf of Mexico.

5.2.6 Goal of the Study

The objective of this study was to quantify biomass yields of bioenergy crops and their impacts on streamflow, tile drain flow and nutrient losses under different bioenergy crop scenarios in a typical tile drained watershed. The results of this study can help determine optimal bioenergy scenarios with high biomass yields, and water balance and water quality benefits in the LVR watershed and even the Mississippi River system and Gulf of Mexico.

5.3 Materials and Methods

5.3.1 Study Area

The LVR watershed is a typical flat upland watershed in east-central Illinois and drains approximately 518 km^2, at the boundary of Champaign and Vermilion counties. The LVR watershed has an average slope reaching at most 1%, with elevation ranging from approximately 235 meters in the headwaters to 174 meters at the outlet of the watershed (Zanardo *et al.*, 2012) (Figure 5.1). About 90% of the LVR watershed is agricultural land used for corn and soybean production, and the remainder consists of grassland, forest land, roadways and farmsteads (Kalita *et al.*, 2006) (Figure 5.2). Based on agricultural statistical

data for the LVR watershed, the cropland was equally subdivided between corn and soybeans (Algoazany *et al.*, 2007). The dominant soil associations are Drummer silty clay loam and Flanagan silt loam (Zanardo *et al.*, 2012; Keefer, 2003). The LVR watershed has altered hydrology from an extensive subsurface drainage system network (Algoazany *et al.*, 2007)

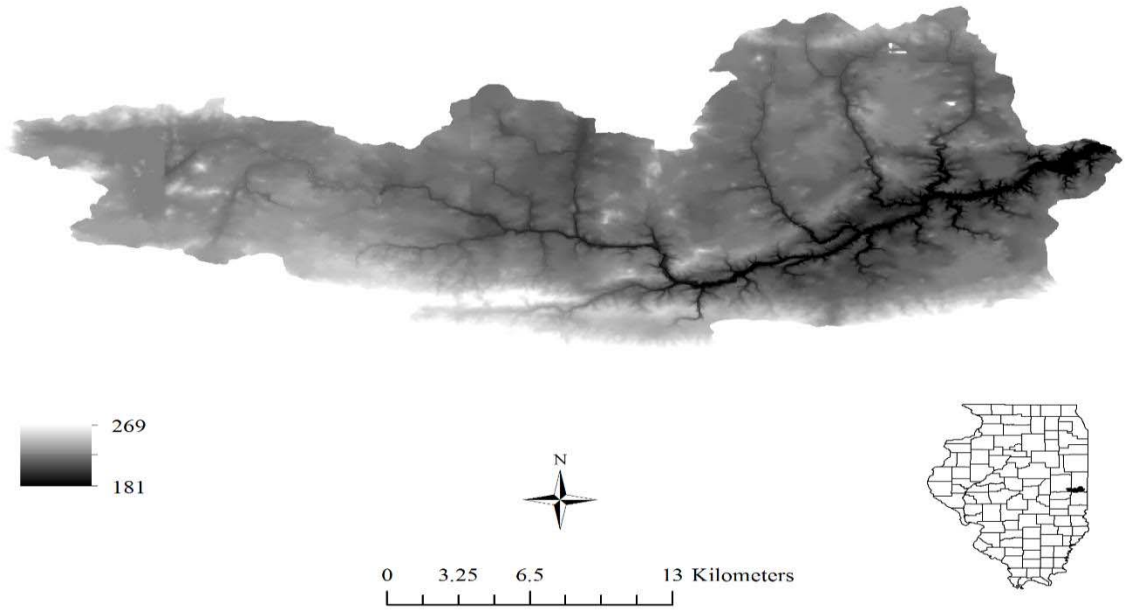

Figure 5.1 Elevation of the LVR watershed

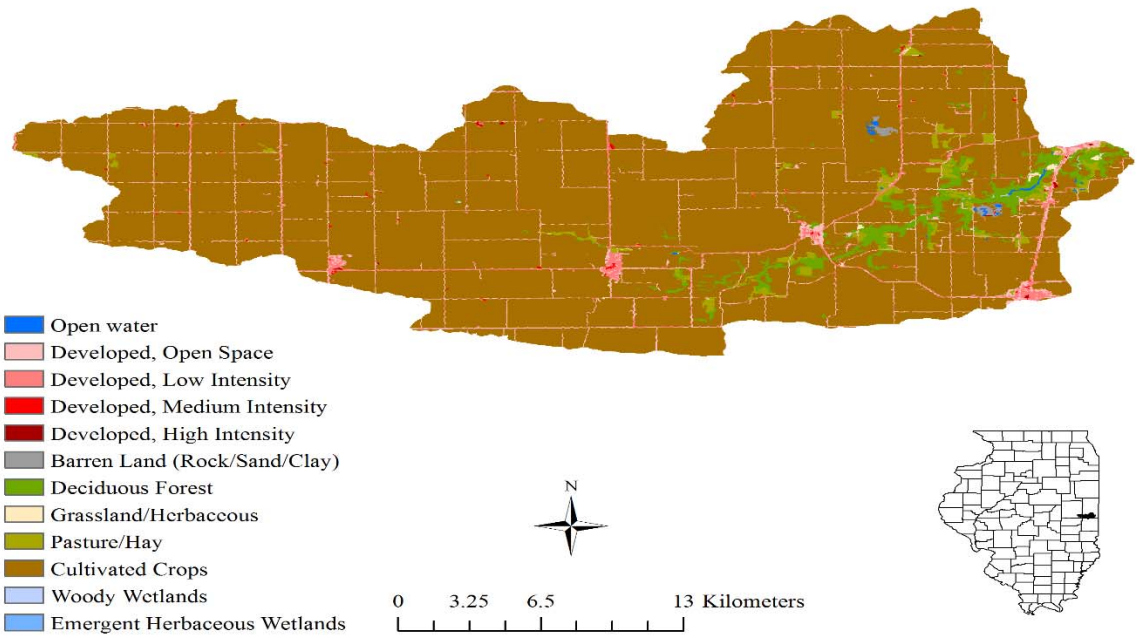

Figure 5.2 Land cover of the LVR watershed

5.3.2 Bioenergy Crop Scenarios

In the current study, the primary goal was to estimate biofeedstock production of plausible bioenergy scenarios and their impacts on watershed hydrology and water quality. The purpose of scenario planning was to place bioenergy crops with high biomass yields on the LVR watershed and explore hydrologic and water quality impacts. Thus, there were several concerns about bioenergy scenario planning (Peterson *et al.*, 2003):

1. It was significant to design bioenergy scenarios favoring the growth of high yielding bioenergy crops (switchgrass, *Miscanthus* and hybrid poplar), and also have minimal impacts on food production (grain production of corn and soybean).

2. Marginal lands with high slope, low soil productivity or not suited for cash crop growth, which has low crop productivity could be chosen for bioenergy crop placement.

3. Minimal nutrient or sediment export to the outlet of the LVR watershed should also be taken into consideration.

To meet the above goals of bioenergy crop scenario planning, biofuel crop scenarios were formulated and simulated on highly erodible soils, agriculturally marginal land, and pasture areas in the LVR watershed (Figure 5.3). The corn and soybean areas with greater than 5% slope were considered as potential highly erodible areas. The areas with soil non-irrigated unit capability class of 3 and 4 (may be more profitable used for grasses or trees), 6 (excess or lack of water), 7 (soil damage) and 8 (soil and climatic limitations) were considered as agricultural marginal land (Table 5.1) (Klingebiel & Montgomery 1961). Based on these criteria, areas for bioenergy crop scenarios were small (Table 5.1).

Nineteen bioenergy crop scenarios were formulated (Table 5.2) considering bioenergy crop production on highly erodible areas (Scenarios 1, 2 and 3), on marginal land (Scenarios 4, 5, 6 and 7), with stover removal with various nutrient replacement amounts (Scenarios 8, 9 and 10), combination of stover removal and bioenergy crop production on highly erodible areas (Scenarios 11, 12 and 13), combination of stover removal and bioenergy crop production on marginal land (Scenarios 14, 15 and 16), and combination of stover removal and bioenergy crop production on highly erodible areas and marginal land (Scenarios 17, 18 and 19).

Shawnee switchgrass (*Panicum virgatum L.*), *Miscanthus* (*Miscanthus* × *giganteus*) and *Populus* 'Tristis #1' (*Populus balsamifera* L. × *P.tristis* Fisch) were included as high yielding bioenergy crops and corn stover as crop residue for biofuel production due to high productivity, availability and adaptability (Hansen 1991; Tilman *et al.*, 2009; Casler 2010; Cortese *et al.*, 2010; Schmer *et al.*, 2010; Thomas 2011; Thomas *et al.*, 2011; Boles 2013; Kiniry *et al.*, 2013; Behrman *et al.*, 2014; Thomas *et al.*, 2014; Trybula *et al.*, 2014). The stover removal rate of 38% proposed by Brechbill and Tyner (2008) was used for the study, representing potential corn stover that can be collected from baling a windrow (Brechbill and Tyner, 2008).

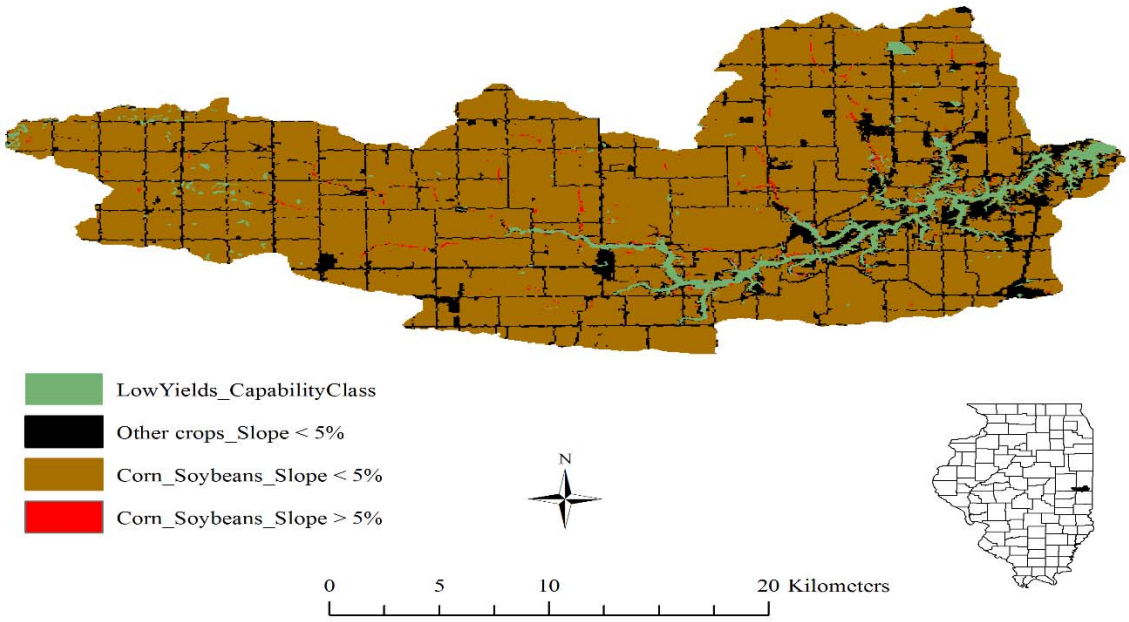

Figure 5.3 Potential lands for bioenergy crop scenarios in the LVR watershed

Table 5.1 Potential area for bioenergy crop scenarios

Potential lands	Land use	Slope	Soil (Non-Irrigation Unit class)	Area (km^2)	Percent of the watershed (%)
Corn stover	Corn soybean	< 5%	-	177.53	43
Highly erodible areas	Corn soybean	> 5%	-	2.10	0.50
Land capability	-	-	3, 4, 6, 7, 8	8.78	2.11
Land capability classification with forest	Forest	-	3, 4, 6, 7, 8	8.31	1.99

Table 5.2 Description of biofuel scenarios evaluated in this study

Name	<5% slope area	>5% slope area	Land capability	Land capability with forest
Baseline	-	-	-	-
Scenario1	-	*Miscanthus*	-	-
Scenario2	-	Switchgrass	-	-
Scenario3	-	*Populus*	-	-
Scenario4	-	-	*Miscanthus*	-
Scenario5	-	-	Switchgrass	-
Scenario6	-	-	*Populus*	-
Scenario7			*Populus*	*Populus*
Scenario8	38% stover (no nutrient replacement)	-	-	-
Scenario9	38% stover (more nutrient replacement)	-	-	-
Scenario10	38% stover (less nutrient replacement)	-	-	-
Scenario11	38% stover	*Miscanthus*	-	-
Scenario12	38% stover	Switchgrass	-	-
Scenario13	38% stover	*Populus*	-	-
Scenario14	38% stover	-	*Miscanthus*	-
Scenario15	38% stover	-	Switchgrass	-
Scenario16	38% stover	-	*Populus*	-
Scenario17	38% stover	*Miscanthus*	*Miscanthus*	-
Scenario18	38% stover	Switchgrass	Switchgrass	-
Scenario19	38% stover	*Populus*	*Populus*	-

Note: Baseline scenario represents the current land use in the watershed and the developed scenarios changing corresponding land use from the baseline. No, more and less nutrient replacement for corn stover removal of scenario 8, 9 and 10 represent no nutrient replacement, 32 kg/ha additional Anhydrous Ammonia and 11 kg/ha P_20_5, and 16 kg/ha additional Anhydrous Ammonia and 5 kg/ha P_20_5 applied to corn stover removal relative to corn growth (Table 5.6).

5.3.3 SWAT Model Setup

SWAT2012 (Rev.615) with improved tree growth simulation was used for modeling. The 30 m National Hydrography Dataset (NHD) was used to create a clipped stream layer for the LVR watershed into the simulation and subbasins in LVR watershed were delineated. Crop data layer (CDL 2014) for the study area was obtained from USDA National Agricultural Statistics Service (NASS). The National Map Viewer and SSURGO from USDA Web Soil Survey were also added into ArcSWAT. The delineated 17 sub-basins

yielded 990 total hydrologic response units (HRUs) based on the following thresholds: 0% land, 10% soil, and 0% slope. Tile drainage was assumed in areas where corn or soybean were the current land use, slope lower than 5%, and soil drainage was somewhat poorly drained, poorly drained, or very poorly drained (Sugg, 2007; Sui and Frankenberger, 2008; Boles *et al*., 2015), and 75% of the watershed was tile drained.

Daily precipitation data from 01/01/1985 to 12/31/2008 of SIDELL 4 N IL US weather station (GHCND: USC00117952, Latitude: 39.98°, Longitude: -87.88°, Elevation: 206 m) weather station in the watershed was downloaded from National Climatic Data Center (NCDC CDO) and added into ArcSWAT. Annual average precipitation used in simulation at the watershed outlet was 1016 mm from 1985 to 2008. Other climate data, including daily temperature, solar radiation, wind speed and relative humidity data was obtained from a station closest to the LVR watershed (Table 5.3). The model ran for a total of 23 years (1985-2008) to allow for sufficient warm-up (1985-1989) before reaching the simulation years (1990-2008).

The SWAT model (Rev.615) was calibrated/validated for monthly tile flow and surface runoff, sediment in surface runoff, and nitrate in tile flow and surface runoff, at field sites, and flow, sediment and nitrate in flow at a river site (See Chapter 4). Calibrated parameter sets can be used to model hydrology and water quality results reasonably at field site and river basin levels in the LVR watershed (Table 5.4). Tile depth (DDRAIN) was set as 1.075m in the model (Singh *et al*., 2001). The maximum depressional storage selection flag/code ISAMX was set as 0, and static maximum depressional storage (SSTMAXD) was defined as 12mm, based on previous DRAINMOD (Skaggs *et al*., 2012) and SWAT studies (Boles *et al*., 2015). The calibrated/validated model representing the current land cover was considered the baseline scenario. Bioenergy crop scenarios (Table 5.2) were represented in the calibrated model.

Nineteen-year average simulated flow, sediment, nitrate, total nitrogen, soluble nitrogen, organic nitrogen, total phosphorus, mineral phosphorus, and organic phosphorus results at the watershed outlet, and tile flow and nitrate in tile flow across the whole watershed from year 1990 to year 2008 were compared with the baseline scenario, and percentage changes

were calculated to determine biofeedstock production of bioenergy crop scenarios and their hydrologic and water quality impacts.

Table 5.3 Data for bioenergy crop scenario simulation by SWAT

Data type	Source	Format	Date
Elevation	[1]USGS The National Map Viewer	30m Raster	
[2]SSURGO	[3]USDA Web Soil Survey	Polygon Shapefile	
[4]CDL	[5]USDA NASS	Raster	2014
Temperature, solar radiation, relative humidity and wind speed	[6]ISWS	Tabular data	1985-2008
Precipitation	[7]NCDC	Tabular data	1985-2008

[1]USGS: U.S. Geological Survey
[2]SSURGO: Soil Survey Geographic Database
[3]USDA: U.S. Department of Agriculture
[4]CDL: Cropland Data Layer
[5]USDA NASS: United States Department of Agriculture National Agricultural Statistics Service
[6]ISWS: Illinois State Water Survey
[7] NCDC: National Climatic Data Center

Table 5.4 Description of calibrated parameter values for water quantity and quality processes in the LVR watershed

Parameter	Description	Calibrated values	Process
ICN	CN method flag: 0 use traditional SWAT method, which bases CN on soil moisture, 1 use method which bases CN on plant ET	0	Surface runoff
CN2	Soil moisture condition II curve number	-0.20	
SURLAG	Surface runoff lag coefficient	1.03	
DEP_IMP	Depth to impervious layer (mm)	2700	Tile drains
DRAIN_CO	Drainage coefficient (mm/d)	20	
LATKSATF	Multiplication factor to determine lateral saturated hydraulic conductivity	1.05	
SDRAIN	Tile spacing (mm)	38000	
ESCO	Soil evaporation compensation factor	0.98	Evapotranspiration

Table 5.4 Continued.

SFTMP	Snowfall temperature (℃)	-4.25	Snow
SMTMP	Snow melt base temperature (℃)	2.08	
GW_DELAY	Groundwater delay time (days)	25	Groundwater
RCHRG_DP	Deep aquifer percolation fraction	0.56	
ADJ_PKR	Peak rate adjustment factor for sediment routing in the subbasin (tributary channels)	1.16	Sediment losses
SPEXP	Exponent parameter for calculating sediment reentrained in channel sediment routing	1.94	
CH_COV1	Channel erodibility factor	0.31	
CMN	Rate factor for mineralization for the humus active organic nutrients (N)	0.03	Nitrate losses
RCN	Concentration of nitrogen in rainfall (mg N/L)	0.10	
NPERCO	Nitrogen concentration reduction coefficient	0.99	
SDNCO	Denitrification threshold water content	1.46	
CDN	Denitrification exponential rate coefficient	0.00	

5.3.4 Bioenergy Crop Scenarios Representation in the Model

The plant growth parameters for corn (*Zea mays* L.), soybean (*Glycine max* L. *Merril*), Shawnee switchgrass (*Panicum virgatum L.*), *Miscanthus* (*Miscanthus* × *giganteus*) and *Populus* 'Tristis #1' (*Populus balsamifera* L. × *P.tristis* Fisch) were adjusted in the model (Table 5.5). Cibin *et al.* (2015) adjusted radiation use efficiency (BIO_E) and potential heat units (PHU) for corn growth, and PHU, minimum temperature for plant growth (T_BASE), harvest index (HVSTI), normal fraction of phosphorus in yield (CPYLD) for soybean growth (Table 5.5) to compare with county level yield data for two watersheds in the Midwest USA. This study adopted the same adjustment for corn and soybean growth simulation. Trybula *et al.* (2014) collected growth data for *Miscanthus* and Shawnee switchgrass at the Purdue Water Quality Field Station in Indiana near the LVR watershed and improved perennial grass growth simulation in SWAT to accurately model biofeedstock production, nutrient uptake, and water quantity and water quality impacts of perennial grasses. Guo *et al.* (2015) improved leaf area index and biomass yield simulation of *Populus* tree growth simulation in SWAT, and determined reasonable parameter sets for

hybrid poplar growth, which can be used to accurately model biofeedstock production of hybrid poplar growth and its impacts on hydrology and water quality since planting. This study used SWAT version (Rev.615), incorporating modification of perennial grasses (Trybula *et al.*, 2014; Cibin *et al.* (2015) and hybrid poplar tree growth (Guo *et al.*, 2015) with calibrated growth parameter values (Table 5.5).

Planting and harvest date, rotation, tillage practice, and fertilization and pesticide application of corn, soybean, corn stover, Tall Fescue, switchgrass, *Miscanthus*, and hybrid poplar in the LVR watershed varied (Table 5.6). Rotation years for switchgrass, *Miscanthus*, and hybrid poplar were set as 10, 10 and 14 years, respectively, since perennial grasses would produce biomass yield once established with proper management, and poplar trees could resprout vigorously after harvest for a period longer than 10 years (Hansen *et al.*, 1991; Pyter *et al.*, 2007). Hybrid poplar with population of 500 trees/100 m^2 was selected as short-rotation woody crops, which could reach maturity at the 6th year since planting (Hansen, 1983).Corn stover removal was set as 38% stover biomass removal after corn grain harvest in the model, including no (218 kg/ha Anhydrous Ammonia and 67 kg/ha P_20_5) more (250 kg/ha Anhydrous Ammonia and 78 kg/ha P_20_5) and less (234 kg/ha Anhydrous Ammonia and 72 kg/ha P_20_5) additional fertilizer application to account for nutrient replacement (Table 5.6) (Brechbill and Tyner, 2008). Tall Fescue (*Schedonorus arundinaceus* (Schreb.) Dumort) with hay cut and rotational gazing (Table 5.6) was selected for pasture area crop in this study. Consumed and trampled biomass were both considered as 37 kg/ha/day during grazing, and 60% of the consumed biomass was considered as the manure deposited back in field (Cibin *et al.*, 2015). Kentucky bluegrass (*Poa pratensis*) was selected as the grass in urban areas for this study. IGRO in .mgt file was set as 1, and the grass was set as growing at the beginning of simulation with initial biomass of 2 Mg/ha in the model. Auto-fertilization and auto-irrigation were set for Kentucky bluegrass growth management. Biweekly lawn mowing was set from Mid-April to Mid-July and monthly lawn mowing was set from Mid-July to Mid-October, with 40% of aboveground biomass clipped each time. Additional detailed information about simulation of Tall Fescue and Kentucky bluegrass are provided in Cibin *et al.* (2015).

Table 5.5 Adjusted parameter value of corn, soybean, switchgrass, *Miscanthus* and hybrid poplar growth simulation in SWAT

Acronym	Parameter	Corn	Soybean	Switchgrass	*Miscanthus*	Hybrid poplar
T_BASE	Base Temperature (°C)	8	8	10	8	4
[PHU]	Heat Units to Maturity	[1500]	[1250]	[1400]	[1830]	[1750]
T_OPT	Optimal Temperature (°C)	25	25	25	25	25
BIO_E	Radiation Use Efficiency in ambient CO_2 (kg ha^{-1})/(MJ m^{-2})	36	25	17	41	20
EXT_COEF	Light Extinction Coefficient	0.65	0.45	0.5	0.55	0.3
BLAI	Maximum LAI	6	3	8	11	9.5
LAIMX2	Fraction of BLAI corresponding to 2nd point	0.5	0.5	0.4	0.45	0.4
DLAI	Point in growing season when LAI declines	0.7	0.6	1	1.1	0.99
BIO_LEAF	Fraction of tree biomass converted to residue during dormancy	-	-	-	-	0.3
TREED	Tree leaf area factor	-	-	-	-	0.6
FRGRW2	Fraction of growing season coinciding with LAIMX2	0.95	0.95	0.85	0.85	0.95
ALAI_MIN	Minimum LAI for plant during dormancy	0	0	0	0	0
FRGRW1	Fraction of growing season coinciding with LAIMX1	0.05	0.05	0.1	0.1	0.05
LAIMX1	Fraction of BLAI corresponding to 1st point	0.15	0.15	0.1	0.1	0.05
PLTPFR1	Plant P fraction at emergence (whole plant)	0.047	0.0074	0.0073	0.01	0.0007
GSI	Maximum stomatal conductance	0.007	0.007	0.005	0.005	0.007
CHTMX	Maximum canopy height (m)	2.5	0.8	2	3.5	7.5
FRGMAX	Fraction of GSI corresponding to the 2nd point of stomatal conductance curve	0.75	0.75	0.75	0.75	0.75
VPDFR	Vapor pressure deficit (kPa) corresponding to 2nd point of stomatal conductance curve	4	4	4	4	4
PLTNFR1	Plant N fraction at emergence (whole plant)	0.047	0.0524	0.0073	0.01	0.006
PLTNFR3	Plant N fraction at maturity (whole plant)	0.0138	0.0258	0.0053	0.0057	0.0015
PLTNFR2	Plant N fraction at 50% maturity (whole plant)	0.0177	0.0265	0.0068	0.0065	0.002
RSDCO_PL	Plant residue decomposition coefficient	0.05	0.05	0.05	0.05	0.05

Table 5.5 Continued.

RDMX	Maximum rooting depth (m)	2	1.7	3	3	3.5
CNYLD	Plant N fraction in harvested biomass	0.014	0.065	0.0054	0.0035	0.0005
CPYLD	Plant P fraction in harvested biomass	0.0016	0.0067	0.001	0.0003	0.0002
PLTPFR2	Plant P fraction at 50% maturity (whole plant)	0.0018	0.0037	0.0068	0.0065	0.0004
PLTPFR3	Plant P fraction at maturity (whole plant)	0.0014	0.0035	0.0053	0.0057	0.0003
USLE_C	Minimum crop factor for water erosion	0.2	0.2	0.003	0.003	0.001
WAVP	Rate of decline in radiation use efficiency per unit increase in vapor pressure deficit	7.2	8	7.2	7.2	8
CO2HI	Elevated CO_2 atmospheric concentration ($\mu L\ CO_2\ L^{-1}$ air) corresponding the 2nd point	660	660	660	660	660
BIOHI	Biomass-energy ratio corresponding to 2nd point	45	34	35	54	31
WSYF	Lower limit of harvest index ((kg ha^{-1})/(kg ha^{-1}))	0.3	0.01	1	1	0
MAT_YRS	Number of years required for tree species to reach full development (years)	-	-	-	-	6-9
BMX_TREES	Maximum biomass for a forest (mt ha^{-1})	-	-	-	-	200
BM_DIEOFF	Biomass dieoff fraction	-	-	-	-	0.1
HVSTI	Harvest index for optimal growing conditions	0.5	0.4	1	1	0.65

Table 5.6 SWAT management practices for corn, soybean, pasture crop, lawn grass, corn stover, switchgrass, *Miscanthus* and hybrid poplar in the LVR watershed

Management operations	Corn (Corn stover)	Soybean	Tall Fescue (pasture crop)	Switchgrass (*Miscanthus*)	Hybrid poplar
Planting date	May 5	May 24	Mar 1	Apr 1	May 22
Harvesting date	Oct14	Oct 7	May 30 (Hay cut)	Oct 30	Dec 30 (7th, 14th years)
Rotation (year)	2	2	1	10	14
Tillage	Apr 15 Spring chisel plow May 5 Offset disk plow	Nov 1 Fall chisel plow	-	-	Apr1 Roto-Tiller (1st year)
Nitrogen fertilizer	Apr 22 Anhydrous Ammonia 218 kg/ha 250 kg/ha (more back) 234 kg/ha (less back)	-	May 1 & Aug 1 Urea 61 kg/ha	Apr 15 Urea 122 kg/ha	Apr1 Urea 110 kg/ha (every other year)
Phosphorus fertilizer	Apr 24 P_20_5 67 kg/ha 78 kg/ha (more nutrient) 72 kg/ha (less nutrient)	May 10 P_20_5 56 kg/ha	May 1 P_20_5 11 kg/ha	-	
Pesticide application	May 2 Atrazine 2.2 kg/ha	-	-	-	Apr1 Linuron 2.2 kg/ha (1st year)
Grazing	-	-	July 15, 14 days 1 cow/acre Sep 1, 14 days 2 cows/acre	-	-

5.4 Results and Discussion

5.4.1 Biofeedstock Production of Bioenergy Crop Scenarios

SWAT simulated annual corn and soybean yields were compared with measured National Agricultural Statistics Service (NASS) county level yield data (Figure 5.4). County level annual corn and soybean yield data for Vermilion, Champaign and Edgar County in Illinois from NASS statistics were area weighted to obtain watershed average yield data. Moisture

content for NASS corn and soybean yields were assumed as 15.5% and 13%, respectively (Schroeder, 2004). Simulated corn and soybean yields were similar to observed county level values (Figure 5.4), except that simulated values of corn and soybean yields for years 1996, 2002, 2005 and 2007 were lower than observed values. Precipitation was low in the growing season for corn and soybean during these years, which caused higher water stress during the growing season and underestimated crop yields.

Simulated yields of *Miscanthus*, switchgrass, and hybrid poplar on highly erodible areas (corn and soybean areas with slope greater than 5%) (Scenarios 1-3, and Scenarios 11-13) averaged 19.5, 9.4 and 8.2 Mg/ha/yr respectively (Table 5.7). Simulated *Miscanthus* and switchgrass yields on highly erodible areas were similar to measured yields of 25 and 10 Mg/ha/yr at the Purdue Water Quality Field Station (WQFS) near the LVR watershed (Burks, 2013). Simulated yields of *Miscanthus*, switchgrass, and hybrid poplar on marginal land (soil capability class as 3, 4, 6, 7 and 8) (Scenarios 4-6, and Scenarios 14-16) averaged 17.0, 8.1, and 7.2 Mg/ha/yr, respectively (Table 5.7). Simulated yield of hybrid poplar on marginal land with forest (Scenario 7) averaged 7.4 Mg/ha/yr, respectively (Table 5.7). Simulated yields of *Miscanthus*, switchgrass, and hybrid poplar on highly erodible areas and marginal land (Scenario 17-19) averaged 17.5, 8.3 and 7.4 Mg/ha/yr, respectively (Table 5.7). Simulated *Miscanthus* and switchgrass yields on marginal land were lower than measured yields of 25 and 10 Mg/ha/yr at the Purdue WQFS near the LVR watershed (Burks, 2013), given that soil properties of marginal land in the LVR watershed were different than those from the WQFS. Simulated annual average *Miscanthus* and switchgrass yields on highly erodible areas and marginal land were within simulated ranges of *Miscanthus* (15-20 Mg/ha/yr) and switchgrass (8-11 Mg/ha/yr) yields by Feng (2016). Simulated hybrid poplar yields on highly erodible areas and marginal lands were lower than measured yield of 10 Mg/ha/yr at the USDA Forest Service Harshaw Experimental Farm (HEF) near Rhinelander, Wisconsin (Hansen, 1991), considering the soil, slope and climate differences between the HEF in Wisconsin and the LVR watershed in Illinois. Simulated yields of corn stover on highly erodible areas with no, more and less additional nutrient replacement (Scenarios 8-10) averaged 3.65, 3.81 and 3.74 Mg/ha/yr, respectively (Table 5.7). More nutrient replacement (Scenario 9) resulted in higher corn stover

production (3.81 Mg/ha/yr) and corn grain production (8.38 Mg/ha/yr), and no nutrient replacement (Scenario 8) resulted in lower corn stover production (3.65 Mg/ha/yr) and corn grain production (8.04 Mg/ha/yr). Average annual biofeedstock production for bioenergy areas varied for different scenarios, and quantity of potential biofeedstock production was not large (Table 5.7) since bioenergy areas were small (Table 5.1). Corn stover (66,000 Mg/yr) with combination of *Miscanthus* both on highly erodible areas and marginal land (19,000 Mg/yr) provided the highest biofeedstock production (Scenario 17) (Table 5.7).

Only one NOAA station with usable precipitation data was located in the LVR watershed. Corn and soybean management practice data for the whole watershed were represented by management data from several field sites. Limited precipitation and corn and soybean growth management data may influence the accuracy of biomass yield simulation for corn and soybean, as well as corn stover, switchgrass, *Miscanthus* and hybrid poplar.

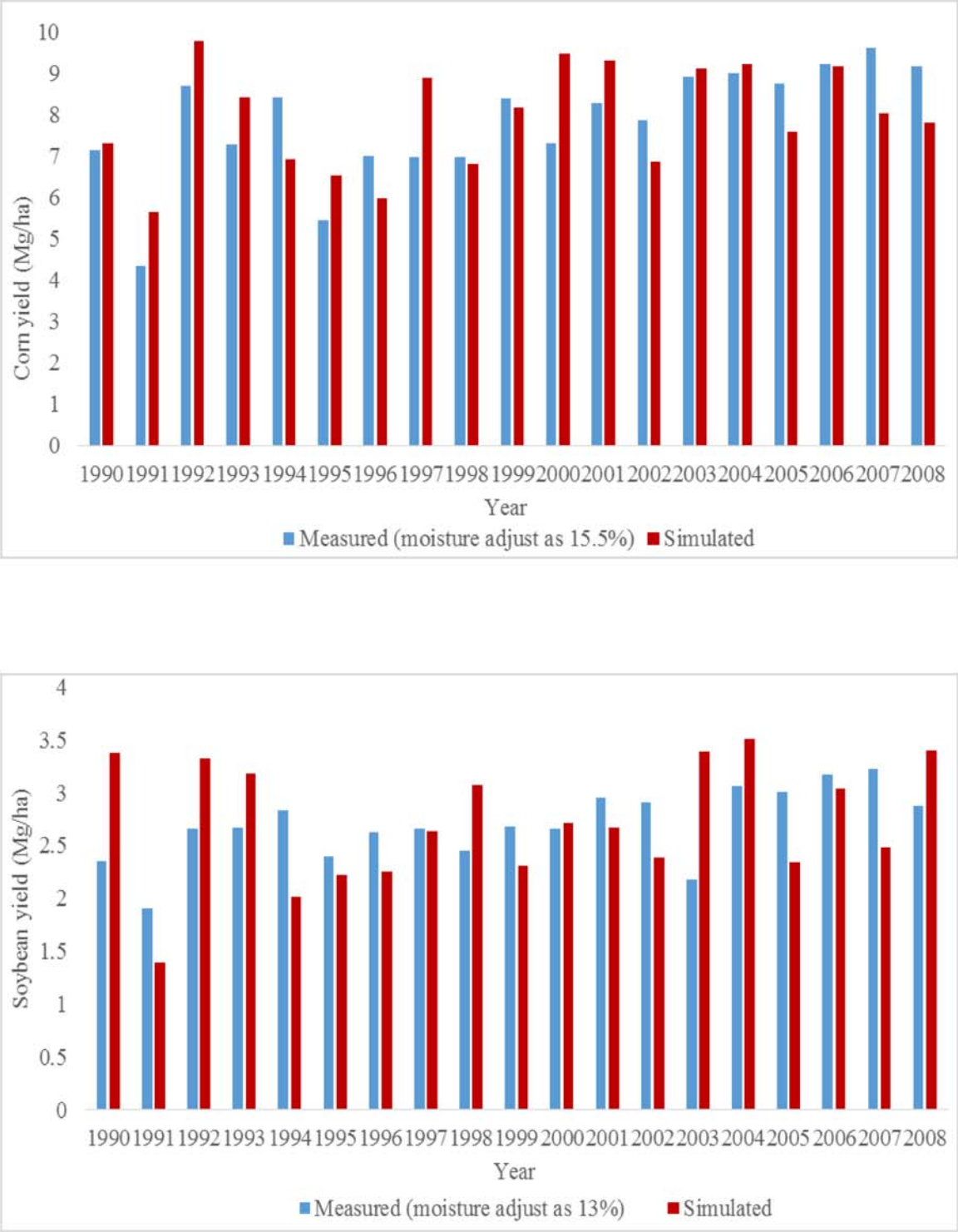

Figure 5.4 Comparison of simulated corn and soybean yields with measured data

Table 5.7 Potential grain and biomass production for bioenergy crop scenarios in the LVR watershed

Crop	Corn		Soybean		Corn stover		*Miscanthus*		Switchgrass		Hybrid poplar		Area of bioenergy crops (ha)
Yield	Mg/ ha/yr	Mg/yr	Mg/ ha/yr	Mg/yr	Mg/ ha/yr	Mg/yr	Mg/ ha/yr	Mg/yr	Mg/ ha/yr	Mg/yr	Mg/ ha/yr	Mg/yr	
Baseline	7.95	141,000	2.72	48,000									
Scenario 1	8.01	142,000	2.73	48,000			19.49	4,000					210
Scenario 2	8.01	142,000	2.73	48,000					9.39	2,000			210
Scenario 3	8.01	142,000	2.73	48,000							8.17	2,000	210
Scenario 4	7.95	141,000	2.72	48,000			17.01	15,000					878
Scenario 5	7.95	141,000	2.72	48,000					8.06	7,000			878
Scenario 6	7.95	141,000	2.72	48,000							7.16	6,000	878
Scenario 7	7.95	141,000	2.72	48,000							7.36	13,000	1708
Scenario 8	8.04	143,000	2.72	48,000	3.65	65,000							17753
Scenario 9	8.38	149,900	2.72	48,000	3.81	68,000							17753
Scenario 10	8.22	146,000	2.72	48,000	3.74	66,000							17753
Scenario 11	8.22	146,000	2.72	48,000	3.74	66,000	19.49	4,000					210
Scenario 12	8.22	146,000	2.72	48,000	3.74	66,000			9.39	2,000			210
Scenario 13	8.22	146,000	2.72	48,000	3.74	66,000					8.17	2,000	210
Scenario 14	8.22	146,000	2.72	48,000	3.74	66,000	17.01	15,000					878
Scenario 15	8.22	146,000	2.72	48,000	3.74	66,000			8.06	7,000			878
Scenario 16	8.22	146,000	2.72	48,000	3.74	66,000					7.16	6,000	878
Scenario 17	8.22	146,000	2.72	48,000	3.74	66,000	17.49	19,000					1088
Scenario 18	8.22	146,000	2.72	48,000	3.74	66,000			8.32	9,000			1088
Scenario 19	8.22	146,000	2.72	48,000	3.74	66,000					7.36	8,000	1088

5.4.2 Impacts of Bioenergy Crop Scenarios on Hydrology

Annual flow partitioning for the LVR watershed from 1990 to 2008 for the baseline was plotted (Figure 5.5). Simulated annual tile flow values ranged from 163 mm to 257 mm with an average value as 209 mm over the period from 1990 to 2008. Simulated tile flow fluctuated from 16% to 24% of total precipitation with an average 20% from 1990 to 2008. Percent of total precipitation as simulated average evapotranspiration values ranged from 41% to 62%, with an average of 51% from 1990 to 2008. Simulated water yield ranged from 34% to 59% of precipitation, with an average of 48% from 1990 to 2008. Flow partitioning was reasonable for simulated water quantity results at the LVR watershed for the baseline (Boles *et al.*, 2015).

Simulated annual average streamflow for the baseline and bioenergy crop scenarios at the LVR watershed outlet ranged from 3.79 to 3.82 m^3/s over the period from 1990 to 2008 (Figure 5.6). Streamflow was slightly reduced under bioenergy crop scenarios relative to the baseline (Figures 5.7 and 5.9). The percentage reduction in streamflow ranged from 0.05% (Scenario 3, hybrid poplar on highly erodible areas) to 0.76% (Scenario 17, stover with *Miscanthus* on highly erodible areas and marginal land) (Figure 5.6). Generally, streamflow reduction was slightly more under scenarios with corn stover with combination of bioenergy crops on marginal land (Scenarios 14-19) (Figure 5.8 (c)) than under scenarios on marginal land (Scenarios 4-6) (Figure 5.8 (a)), which had more streamflow reduction than scenarios on highly erodible areas (Scenarios 1-3) (Figures 5.6 and 5.9 (a)).

Simulated annual average tile flow for the baseline and bioenergy crop scenarios at the LVR watershed ranged from 204 to 206 mm over the period from 1990 to 2008 (Figure 5.7). Tile flow was slightly reduced under bioenergy crop scenarios (Figures 5.8 and 5.9). The percentage reduction in tile flow ranged from 0.01% (Scenario 6, hybrid poplar on marginal land) to 0.89% (Scenario 8, stover with no nutrient replacement) (Figure 5.7). Generally, tile flow reduction was slightly more under scenarios with corn stover (Scenarios 8-19) (Figure 5.8 (b) and (c)) than under scenarios without corn stover (Scenarios 1-7) (Figures 5.7 and 5.8 (a)).

Reduction of streamflow and tile flow under bioenergy crop scenarios may be because of higher infiltration, percolation, and evapotranspiration, and lower soil moisture under bioenergy crop scenarios (Hickman *et al.*, 2010; McIsaac *et al.*, 2010). Reduction in streamflow and tile flow under the scenario with corn stover may be due to increased evaporation from soil cover loss and reduced soil water holding capability caused by corn stover removal (Van Donk *et al.,* 2010; Cibin *et al.,* 2012). The impacts of corn stover, switchgrass, *Miscanthus*, and hybrid poplar scenarios on streamflow and tile flow were minimal, since potential area for bioenergy crop scenarios was small (Table 5.1). Corn stover removal (43 km^2) had a larger potential area than marginal land (2.11 km^2), which is slightly higher than that of highly erodible areas (0.5 km^2) (Table 5.1). The difference in potential area caused the difference in ability to reduce streamflow and tile flow for bioenergy crop scenarios. The larger the potential area for bioenergy scenarios, the higher the reduction in streamflow and tile flow. Thus, streamflow reduction was slightly more under scenarios with corn stover with combination of bioenergy crops on marginal land than under scenarios on marginal land, which had more streamflow reduction than scenarios on highly erodible areas. Streamflow reduction under scenarios with corn stover slightly more than that under scenarios without corn stover.

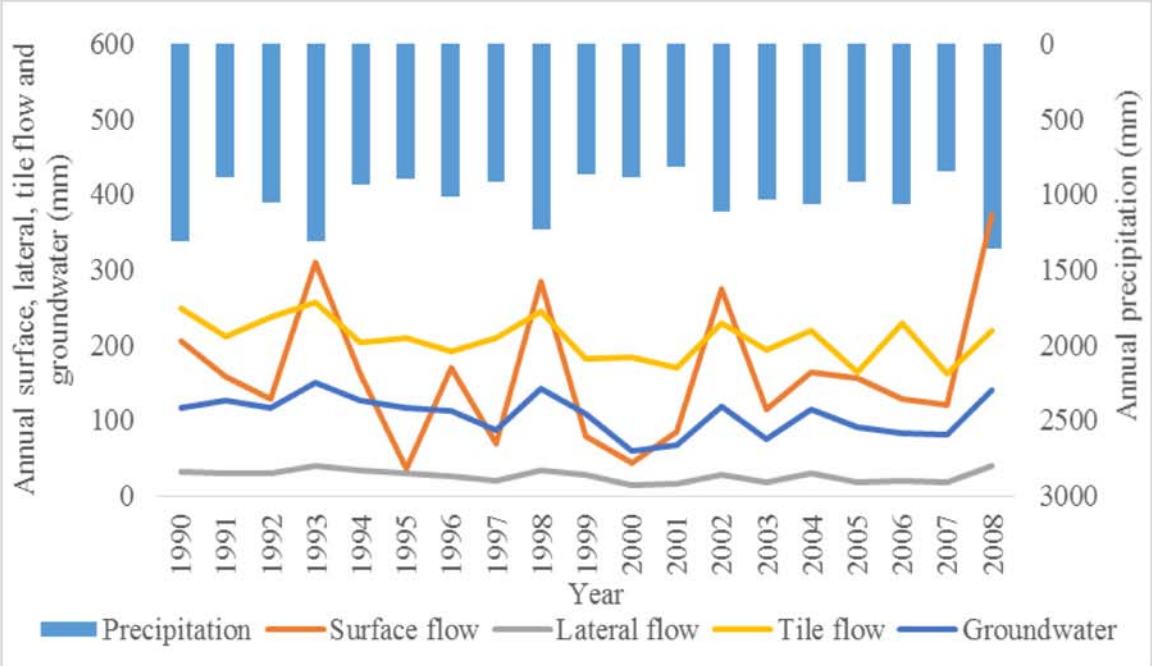

Figure 5.5 Simulated annual flow partitioning for baseline at the LVR watershed

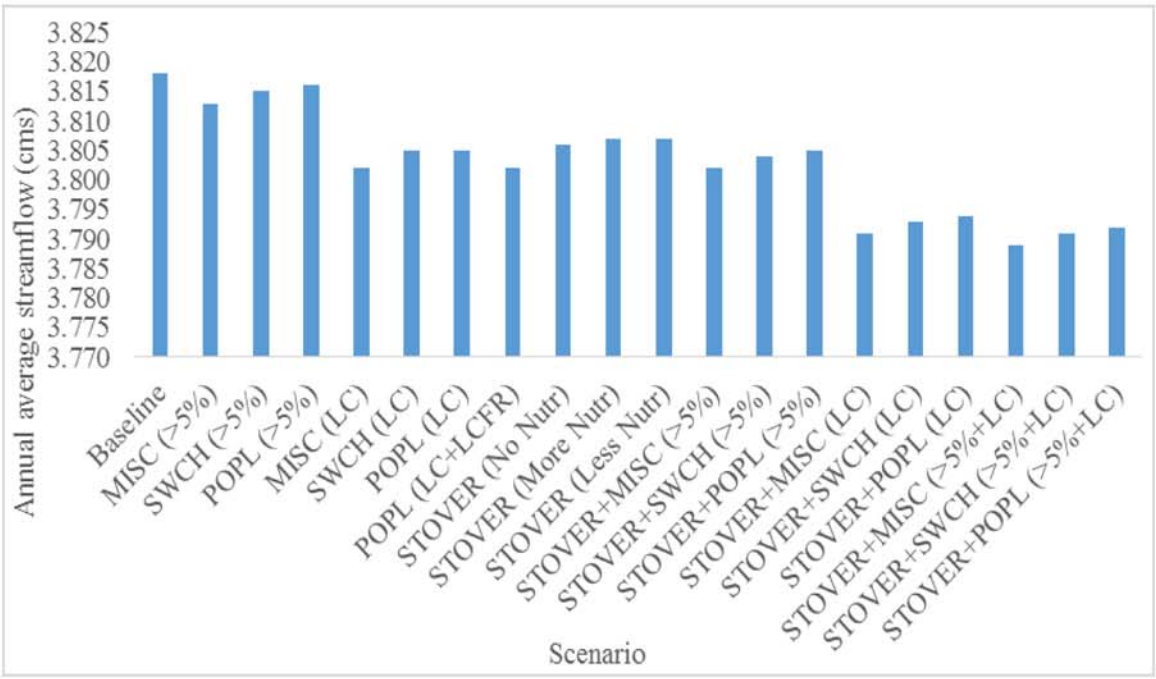

Figure 5.6 Simulated annual average streamflow at the LVR watershed outlet

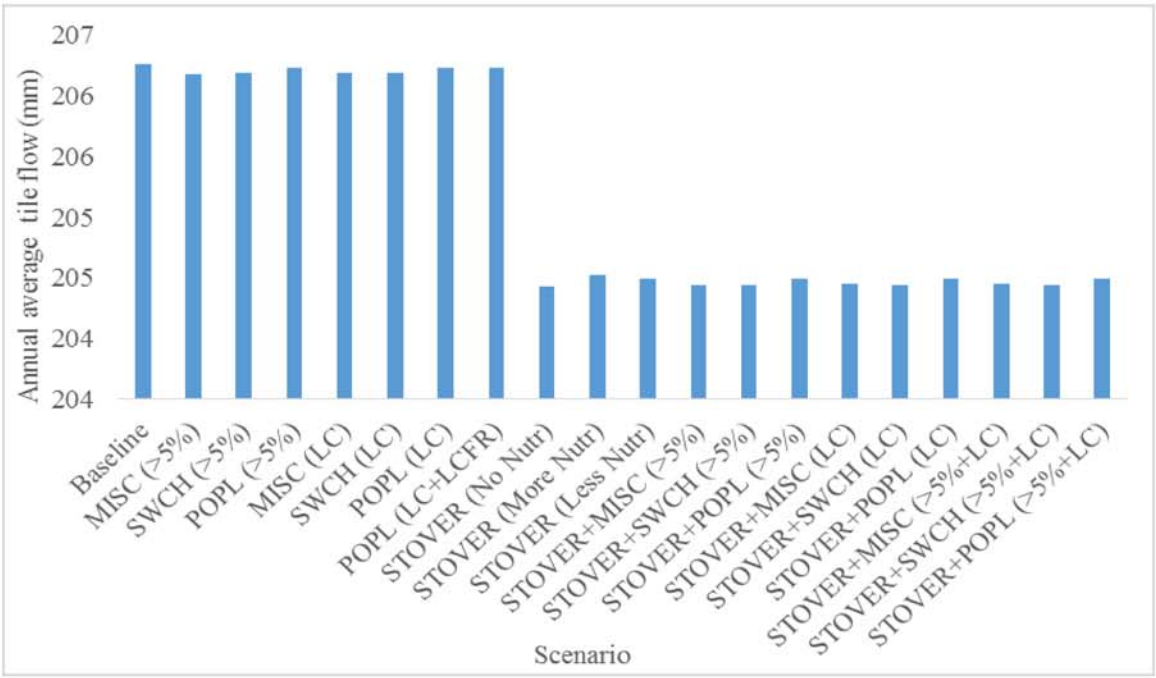

Figure 5.7 Simulated annual average tile flow in the LVR watershed

Note: MISC, SWCH, POPL, LC, LCFR and Nutr are abbreviation of *Miscanthus*, switchgrass, hybrid poplar, land capability, land capability with forest and nutrient, respectively.

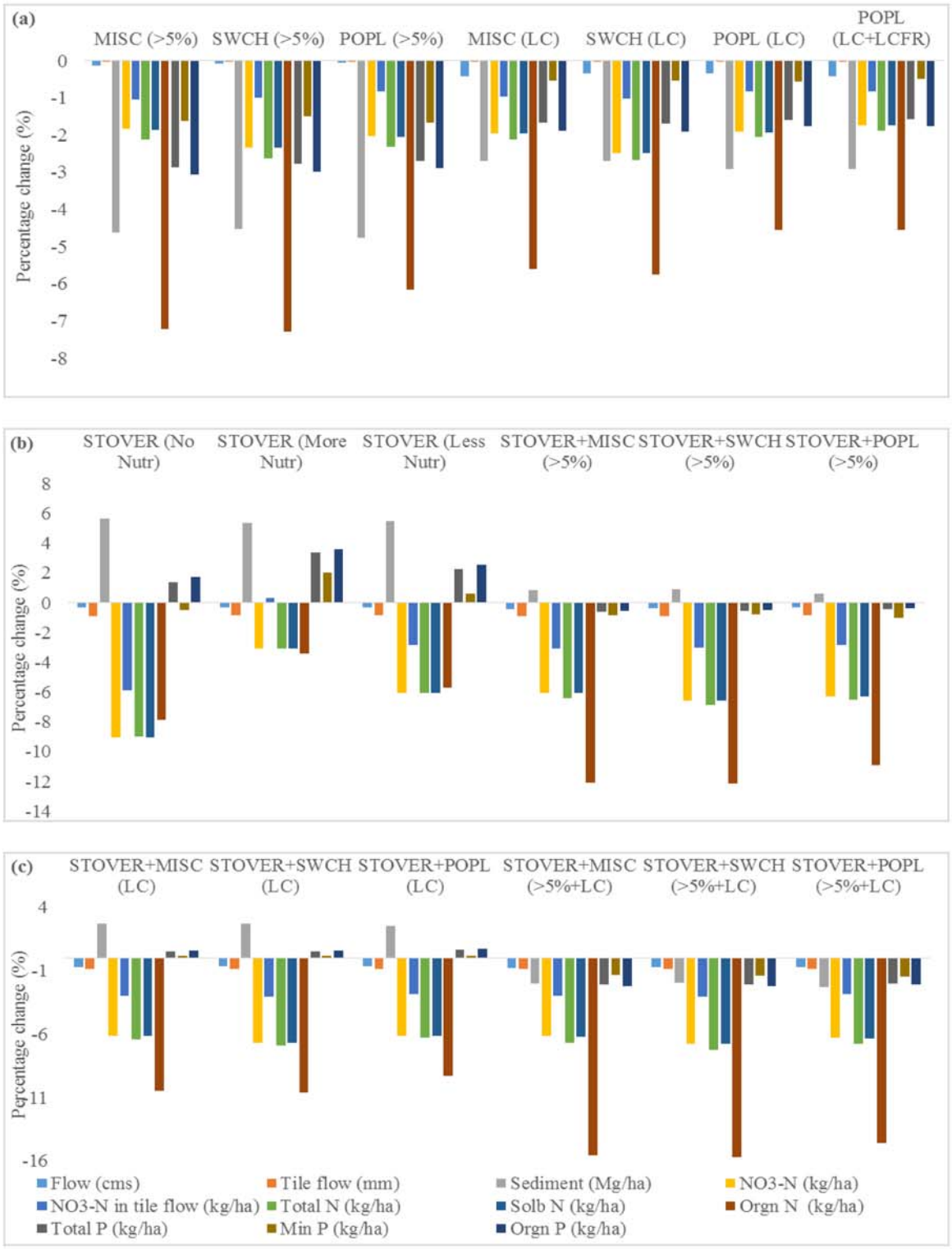

Figure 5.8 Average annual impacts of bioenergy crop scenarios on hydrology and water quality at the LVR watershed

5.4.3 Impacts of Bioenergy Crop Scenarios on Erosion

Simulated annual average sediment load for baseline and bioenergy crop scenarios at the LVR watershed outlet ranged from 0.95 to 1.05 Mg/ha over the period from 1990 to 2008 (Figure 5.9). Sediment was reduced under bioenergy crop scenarios of *Miscanthus*, switchgrass, and hybrid poplar on highly erodible areas, marginal land and marginal land with forest (Scenarios 1-7) (Figures 5.9 (a) and 5.10), with the percentage reduction in sediment load ranging from 2.69% (Scenarios 4 and 5, *Miscanthus* and Switchgrass on marginal land) to 4.76% (Scenario 3, hybrid poplar on high erodible land). Sediment load reduction was slightly more under bioenergy crop scenarios on highly erodible areas than scenarios on marginal land, and *Miscanthus* and switchgrass were equivalent in reducing sediment load (Figures 5.9 (a) and 5.10). Soil erosion and sediment loss were more severe on highly erodible areas, and bioenergy crops had the potential to reduce sediment load.

Corn stover removal scenarios increased sediment load and ranged from 5.34% for stover removal with more nutrient replacement (Scenario 9) to 5.65% for stover removal without nutrient replacement (Scenario 8) (Figures 5.9 (b) and 5.10). Corn stover removal may accelerate soil nutrient losses and intensify wind and water soil erosion (Kenney *et al.*, 2015). The increase in sediment load by corn stover removal could be offset under scenarios with corn stover removal with combination of *Miscanthus*, switchgrass and hybrid poplar (Scenarios 11-19) (Figures 5.9 (b), (c) and 5.10). With a combination of *Miscanthus*, switchgrass and hybrid poplar both on highly erodible areas and marginal land, corn stover scenarios reduced sediment load (Scenarios 17-19) (Figures 5.9 (c) and 5.10). Corn stover removal had the potential to increase soil erosion but not by a considerable amount, since soil erosion was small in the mildly-sloped watershed with flat topography (Figure 5.9). Perennial grasses and hybrid poplar trees in highly erodible areas and marginal land can reduce erosion slightly, since the area for bioenergy crops was small.

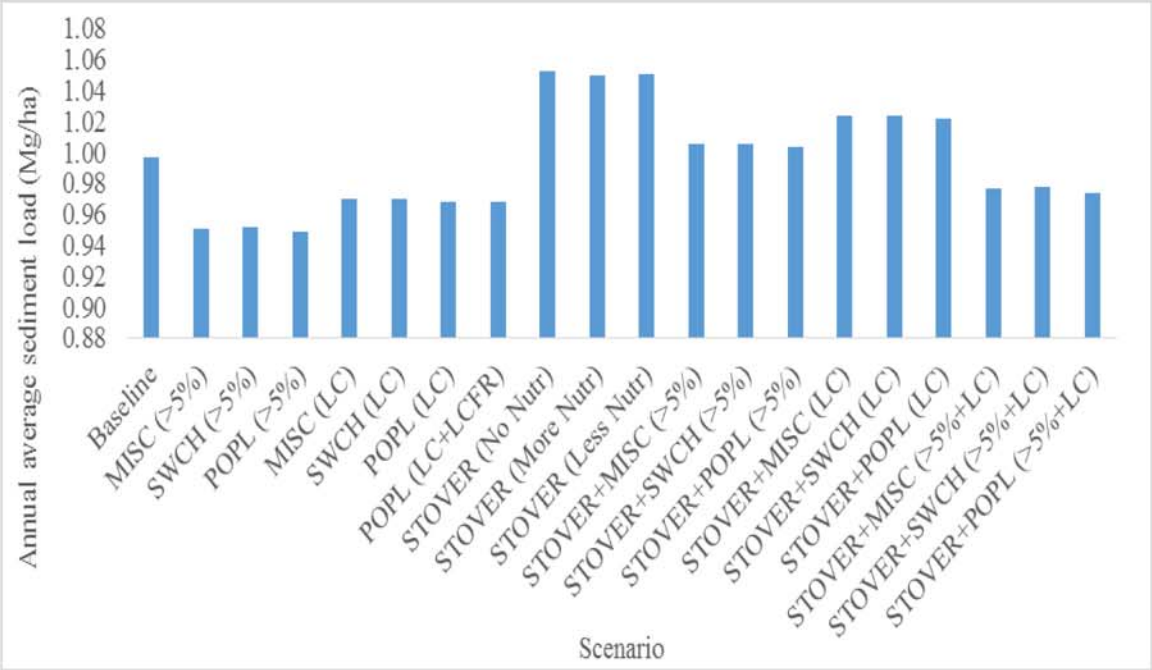

Figure 5.9 Simulated annual average sediment load at the LVR watershed outlet

5.4.4 Impacts of Bioenergy Crop Scenarios on Nutrient Losses

Simulated annual average nutrient load for baseline and bioenergy crop scenarios at the LVR watershed outlet ranged from 6.14 to 6.75 kg/ha for total nitrogen, from 5.81 to 6.38 kg/ha for nitrate load, from 4.32 to 4.60 kg/ha for nitrate in tile flow, and from 1.09 to 1.15 kg/ha for total phosphorus over the period from 1990 to 2008 (Figures 5.10, 5.11, 5.12, and 5.13). Simulated nitrate load at the watershed outlet was lower than nitrate load at the county line river station (10 kg/ha), since annual average precipitation used in simulation at the watershed outlet was higher than that for the county line river station inside the watershed, and annual average streamflow at watershed outlet may be higher than that for the county river station. Generally, nitrate load, nitrate in tile flow, total nitrogen, soluble nitrogen, and organic nitrogen load were reduced under bioenergy crop scenarios (Scenarios 1-19) (Figure 5.8), except that nitrate in tile flow was increased by corn stover removal without nutrient replacement (Scenarios 8) (Figure 5.8 (b)). The percentage reduction ranged from 1.73% (Scenario 7, hybrid poplar on marginal land and marginal land with forest) to 9.02% (Scenario 8,) for nitrate load, from -0.33% (Scenario 9, corn

stover removal with more nutrient replacement) to 5.88% (Scenario 8) for nitrate in tile flow, from 1.88% (Scenario 7) to 8.99% (Scenario 8) for total nitrogen, from 1.73% (Scenario 7) to 9.01% (Scenario 8) for soluble nitrogen, and from 3.43% (Scenario 9) to 15.7% (Scenario 18, corn stover removal with switchgrass on highly erodible areas and marginal land) for organic nitrogen (Figures 5.8, 5.10, 5.11 and 5.12). *Miscanthus*, switchgrass and hybrid poplar yielded more biomass than corn and soybean, and amount of belowground biomass of bioenergy crops are higher than that of cash crops, thus bioenergy crops are able to remobilize water and nutrients consistently (Burks, 2013). Moreover, belowground biomass can store nutrients and reduce nutrient requirements at the early growing stages for bioenergy crops, and less nutrient was applied to bioenergy crops than cash crops, which may cause less nutrient movement in drainage system for bioenergy crops than that for cash crops. Corn stover removal without nutrient replacement could accelerate soil cover loss and intensify soil erosion, and thus increase nitrate movement in subsurface drainage systems.

Total phosphorus, mineral phosphorus and organic phosphorus were reduced under bioenergy crop scenarios of *Miscanthus*, switchgrass, and hybrid poplar on highly erodible land, marginal land and marginal land with forest (Scenarios 1-7) (Figures 5.8 (a) and 5.13), and the percentage reduction ranged from 1.57% (Scenario 7) to 2.85% (Scenario 1, *Miscanthus* on high erodible land) for total phosphorus (Figures 5.8 (a) and 5.13), from 0.5% (Scenario 7) to 1.66% (Scenario 3, hybrid poplar on highly erodible areas) for mineral phosphorus (Figures 5.8 (a)), and from 1.77% (Scenarios 6 and 7, hybrid poplar on marginal land and marginal land with forest) to 3.1% (Scenario 1) for organic phosphorus (Figures 5.8 (a)). Reduction in total phosphorus, mineral phosphorus and organic phosphorus were slightly more under bioenergy crop scenarios on highly erodible areas than scenarios on marginal land (Figures 5.8 (a) and 5.9), since more phosphorus may move with sediment loss on highly erodible areas with steeper slopes (slope > 5%).

Generally, corn stover removal scenarios increased total phosphorus, mineral phosphorus and organic phosphorus load, except that stover removal with no replacement reduced mineral phosphorus load slightly (Figures 5.8 (b)). Increase in total phosphorus, mineral

phosphorus and organic phosphorus were slightly more under corn stover removal with more nutrient replacement than less nutrient replacement, which had more phosphorus increase than stover removal without nutrient replacement (Figures 5.8 (a)). The increase in total phosphorus, mineral phosphorus and organic phosphorus load for corn stover removal could be offset under scenarios with corn stover removal with combination of *Miscanthus*, switchgrass and hybrid poplar (Scenarios 11-19) (Figures 5.8 (b) and (c)). With combination of *Miscanthus*, switchgrass and hybrid poplar both on highly erodible areas and marginal land, corn stover scenarios reduced total phosphorus, mineral phosphorus and organic phosphorus load (Scenarios 17-19) (Figures 5.8 (c) and 5.13). Corn stover removal with nutrient replacement had potential to increase nutrient loss, and perennial grasses and hybrid poplar trees on highly erodible area and marginal land could reduce nutrient losses slightly (Figure 5.8). *Miscanthus*, switchgrass, and hybrid poplar yielded higher biomass yields than corn and soybean and they can store nutrients in belowground biomass, and nutrient requirements for bioenergy crops were lower than those for cash crops, thus bioenergy crop scenarios can reduce nutrient losses in subsurface drainage system and at watershed outlet generally (Heaton *et al*., 2009; Cibin *et al*., 2015). Reduction of nutrient losses by bioenergy crop scenarios in this study was lower than reported values in previous studies (Gassman *et al*., 2008; Boles, 2013; Cibin *et al*., 2015; Feng, 2016), since the potential area for bioenergy crop scenarios was very small.

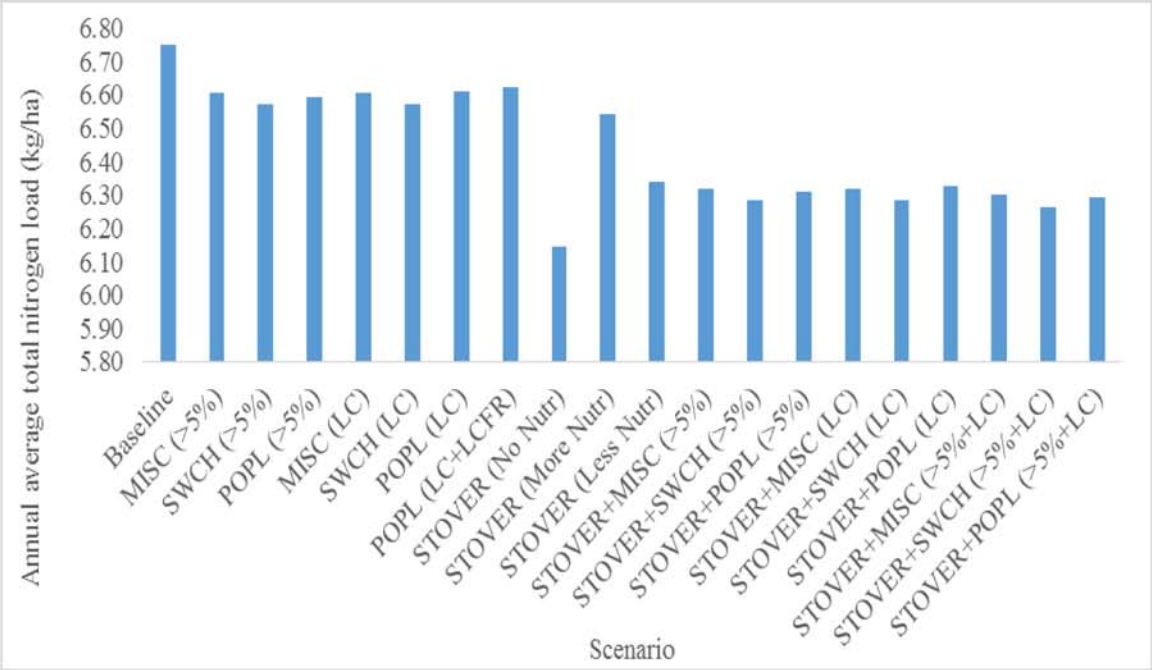

Figure 5.10 Simulated annual average total nitrogen load at the LVR watershed outlet

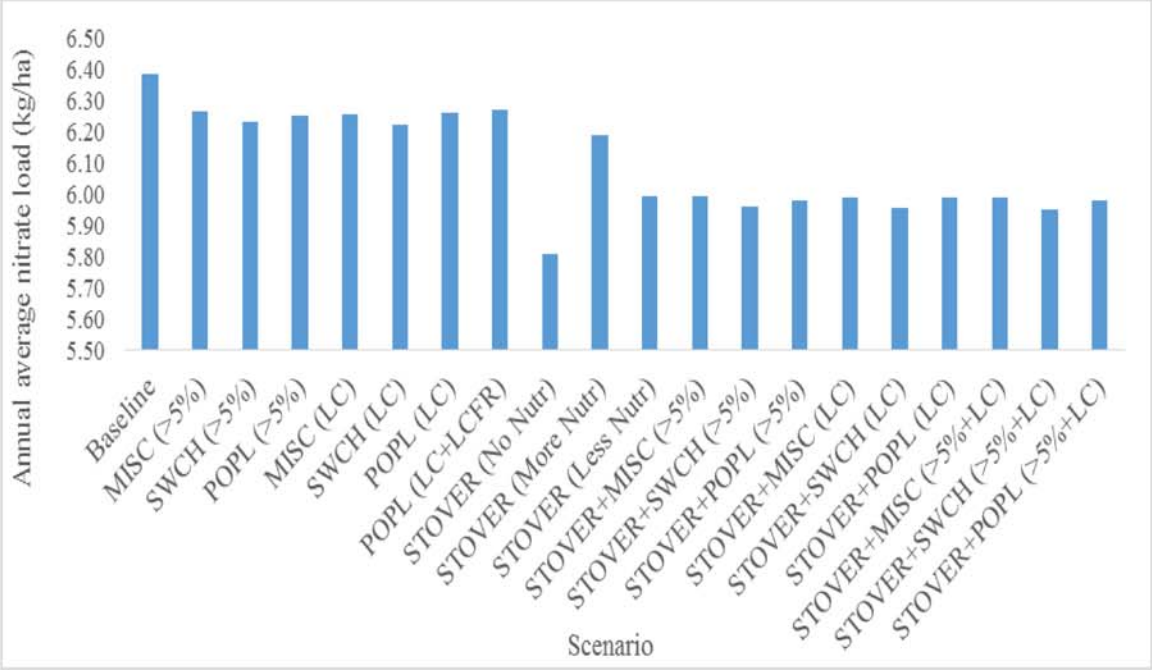

Figure 5.11 Simulated annual average nitrate load at the LVR watershed outlet

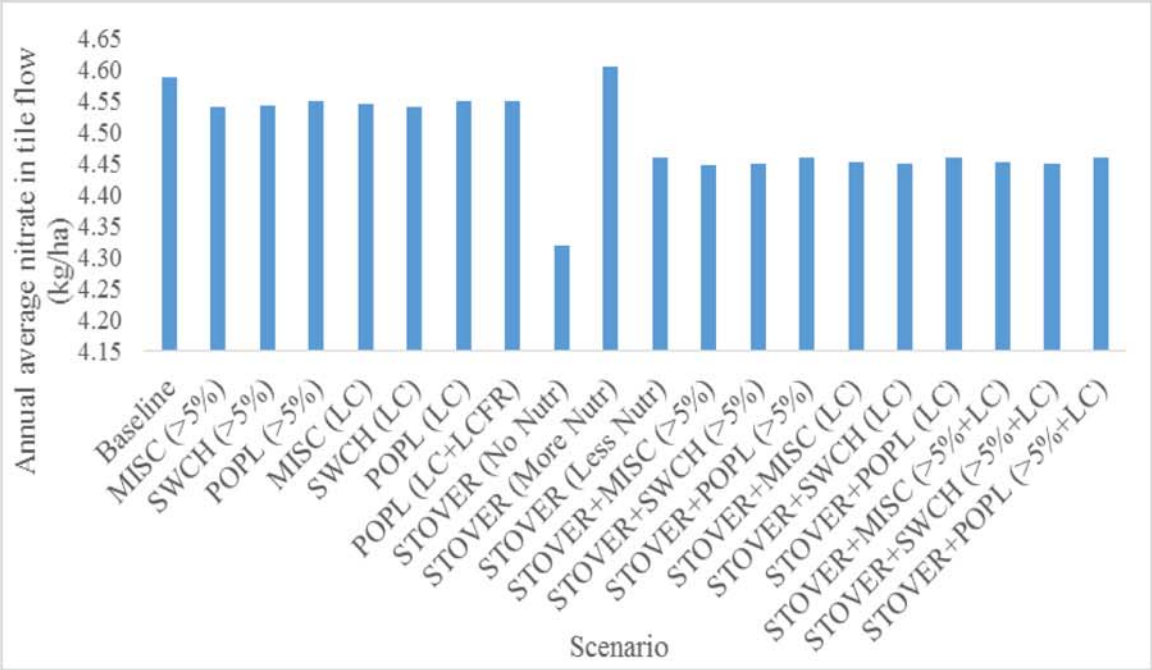

Figure 5.12 Simulated annual average nitrate in tile flow at the LVR watershed

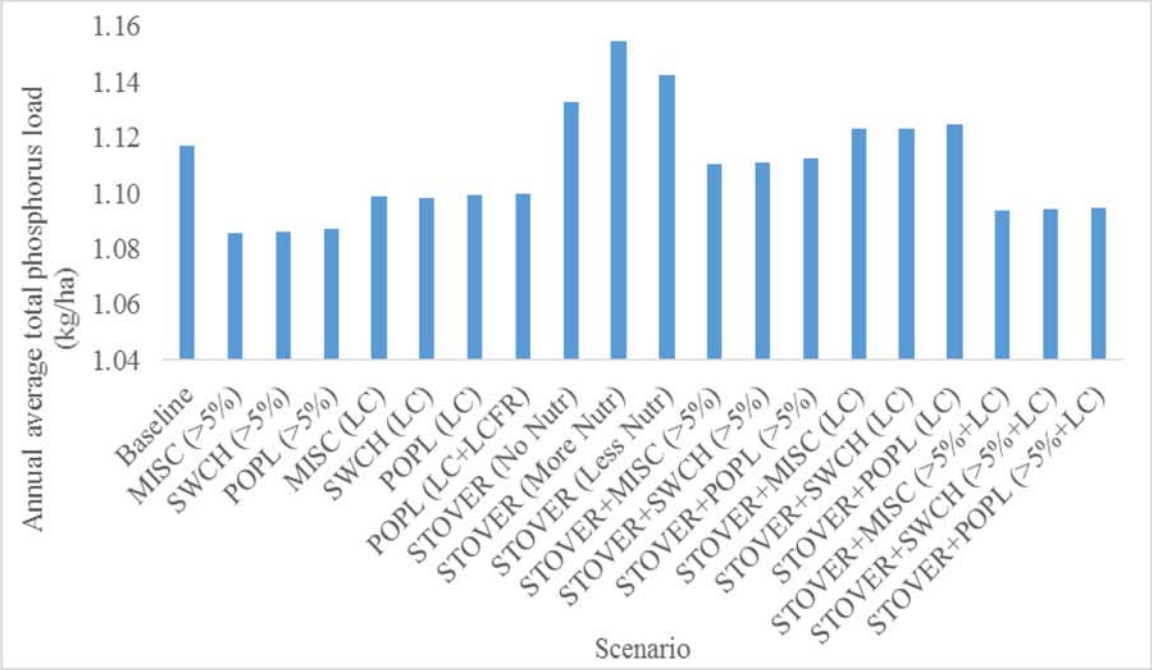

Figure 5.13 Simulated annual average phosphorus load at the LVR watershed outlet

5.5 Conclusions

SWAT2012 (Rev.615) with improved perennial grass and tree growth and the new tile drainage routine (DRAINMOD routine) was used to simulate annual biomass yields, streamflow, tile flow, sediment load, total nitrogen, nitrate load in flow, nitrate in tile flow, soluble nitrogen, organic nitrogen, total phosphorus, mineral phosphorus and organic phosphorus under various bioenergy scenarios from 1990 to 2008 for the LVR watershed. Simulated annual average results from different bioenergy crop scenarios were compared with those from the baseline.

The results showed that simulated annual corn and soybean yields for the baseline were similar to observed county level values. Simulated annual average yields for *Miscanthus*, switchgrass and hybrid poplar were reasonable compared to simulated results in the same region from previous studies. Annual average biofeedstock production for bioenergy areas varied for different bioenergy crop scenarios. 38% corn stover removal (66,000 Mg/yr) with combination of *Miscanthus* both on highly erodible areas and marginal land (19,000 Mg/yr) provided the highest biofeedstock production. Biofeedstock production was not considerable, since the potential area or bioenergy crop scenarios was very small.

Sediment load was reduced under bioenergy crop scenarios of *Miscanthus*, switchgrass, and hybrid poplar on high erodible land, marginal land and marginal land with forest. Corn stover removal scenarios increased sediment load, and the increase in sediment load by corn stover removal could be offset under scenarios with corn stover removal with combination of *Miscanthus*, switchgrass and hybrid poplar.

Generally, streamflow, tile flow, sediment load, nutrient losses were slightly reduced by switchgrass, *Miscanthus* and hybrid poplar under scenarios on highly erodible areas and marginal land. Corn stover removal did not result in significant water quality alterations. Adverse impacts of corn stover removal on sediment load and nutrient losses could be offset by bioenergy crop production in the watershed on highly erodible areas and marginal land. Corn stover removal with a combination of perennial grasses and hybrid poplar both on highly erodible areas and marginal land could slightly reduce streamflow and tile flow

and improve water quality. Stover removal could increase soil cover loss, and accelerate soil erosion and nutrient losses. Bioenergy crops could produce more biofeedstock than corn and soybeans, and store more nutrients in belowground biomass, and reduce sediment and nutrient losses in soil and drainage systems. Potential area for bioenergy crop scenarios was very small, and thus the ability to improve water quantity and quality in the LVR watershed was small and lower than reported values in previous studies.

Limitations of this work include limited observed precipitation data and crop management practices data, such as planting and harvest date and fertilizer application amount. Only one precipitation station could be used in the watershed, which may impact accuracy of crop growth, hydrology and water quality simulation. Potential area for bioenergy crop scenarios was small, thus the ability to produce biomass, and to improve water quantity and quality was not considerable. There is an opportunity to include more corn and soybean area as potential area for bioenergy crop scenarios at mildly-sloped watersheds, in further research on quantification of biofeedstock production of bioenergy crop growth, and its impacts on water quantity and quality.

5.6 References

Aditya, S., & William F, R. (2010). Evaluation of Best Management Practices in Millsboro Pond Watershed Using Soil and Water Assessment Tool (SWAT) Model. *Journal of Water Resource and Protection*, *2*, 403-412.

Algoazany, A. S., Kalita, P. K., Czapar, G. F., & Mitchell, J. K. (2007). Phosphorus transport through subsurface drainage and surface runoff from a flat watershed in east central Illinois, USA. *Journal of Environmental Quality*, *36*(3), 681-693.

Basu, N. B., Rao, P. S. C., Winzeler, H. E., Kumar, S., Owens, P., & Merwade, V. (2010). Parsimonious modeling of hydrologic responses in engineered watersheds: Structural heterogeneity versus functional homogeneity. *Water Resources Research*, *46*(4), 1-16.

Behrman, K. D., Keitt, T. H., & Kiniry, J. R. (2014). Modeling differential growth in switchgrass cultivars across the Central and Southern Great Plains. *BioEnergy Research*, *7*(4), 1165-1173.

Boles, C. M. (2013). *SWAT model simulation of bioenergy crop impacts in a tile-drained watershed* (Mater thesis), Purdue University.

Boles, C. M., Frankenberger, J. R., & Moriasi, D. N. (2015). Tile drainage simulation in swat2012: parameterization and evaluation in an Indiana watershed. *Trans. ASABE*, *58*(5), 1201-1213.

Borah, D. K., Bera, M., & Shaw, S. (2003). Water, sediment, nutrient, and pesticide measurements in an agricultural watershed in Illinois during storm events. *Trans. ASAE*, *46*(3), 657-674.

Blann, K. L., Anderson, J. L., Sands, G. R., & Vondracek, B. (2009). Effects of agricultural drainage on aquatic ecosystems: a review. *Critical Reviews in Environmental Science and Technology*, *39*(11), 909-1001.

Brechbill, S., & Tyner, W. E. (2008). *The economics of renewable energy: corn stover and switchgrass*. Purdue Extension ID-404-W, West Lafayette, IN.

Brezonik, P.L., Bierman Jr, V.J., Alexander, R., Anderson, J., Barko, J., Dortch, M., Hatch, L., Hitchcock, G.L., Keeney, D., Mulla, D. and Smith, V., 1999. Effects of reducing nutrient loads to surface waters within the Mississippi River Basin and the Gulf of Mexico: Topic 4 report for the integrated assessment on hypoxia in the Gulf of Mexico.

Buhler, D. D., Randall, G. W., Koskinen, W. C., & Wyse, D. L. (1993). Atrazine and alachlor losses from subsurface tile drainage of a clay loam soil. *Journal of Environmental Quality*, *22*(3), 583-588.

Burks, J. L. (2013). *Eco-physiology of three perennial bioenergy systems* (Doctoral dissertation), Purdue University.

Casler, M. D. (2010). Changes in mean and genetic variance during two cycles of within-family selection in switchgrass. *BioEnergy Research*, *3*(1), 47-54.

Cibin, R., Chaubey, I., & Engel, B. (2012). Simulated watershed scale impacts of corn stover removal for biofuel on hydrology and water quality. *Hydrological Processes*, *26*(11), 1629-1641.

Cibin, R., Trybula, E., Chaubey, I., Brouder, S. M., & Volenec, J. J. (2015). Watershed-scale impacts of bioenergy crops on hydrology and water quality using improved SWAT model. *GCB Bioenergy*.

Cooke, R. A., Doheny, A. M., & Hirschi, M. C. (1998). Bio-reactors for edge-of-field treatment of tile outflow. In *2001 ASAE Annual Meeting* (p. 1). American Society of Agricultural and Biological Engineers.

Cortese, L. M., Honig, J., Miller, C., & Bonos, S. A. (2010). Genetic diversity of twelve switchgrass populations using molecular and morphological markers. *Bioenergy Research*, *3*(3), 262-271.

Delgado, J. A. (2010). Crop residue is a key for sustaining maximum food production and for conservation of our biosphere. *Journal of Soil and Water Conservation*, *65*(5), 111A-116A.

Evans, R. O., Fausey, N. R., Skaggs, R. W., & Schilfgaarde, J. V. (1999). Effects of inadequate drainage on crop growth and yield. *Agricultural Drainage*, 13-54.

Feng, Q. (2016). *Hydrologic and water quality impacts from perennial crops production on marginal lands in the upper Mississippi river basin* (Doctoral dissertation), Purdue University.

Graham, R. L., Nelson, R., Sheehan, J., Perlack, R. D., & Wright, L. L. (2007). Current and potential US corn stover supplies. *Agronomy Journal*, *99*(1), 1-11.

Guan, K., Thompson, S. E., Harman, C. J., Basu, N. B., Rao, P. S. C., Sivapalan, M., & Kalita, P. K. (2011). Spatiotemporal scaling of hydrological and agrochemical export dynamics in a tile-drained Midwestern watershed. *Water Resources Research*, *47*(10).

Guo, T., Engel, B. A., Shao, G., Arnold, J. G., Srinivasan, R., & Kiniry, J. R. (2015). Functional approach to simulating short-rotation woody crops in process-based models. *BioEnergy Research*, *8*(4), 1598-1613.

Haan, C. T. (2002). Statistical methods in hydrology, 2nd Ed., Iowa State Press, Ames, Iowa.

Hansen, E. A. (1991). Poplar woody biomass yields: a look to the future. *Biomass and Bioenergy*, *1*(1), 1-7.

Heaton, E. A., Dohleman, F. G., & Long, S. P. (2009). Seasonal nitrogen dynamics of Miscanthus× giganteus and Panicum virgatum. *GCB Bioenergy*,*1*(4), 297-307.

Hickman, G. C., Vanloocke, A., Dohleman, F. G., & Bernacchi, C. J. (2010). A comparison of canopy evapotranspiration for maize and two perennial grasses identified as potential bioenergy crops. *Gcb Bioenergy*, *2*(4), 157-168.

Hoskinson, R. L., Karlen, D. L., Birrell, S. J., Radtke, C. W., & Wilhelm, W. W. (2007). Engineering, nutrient removal, and feedstock conversion evaluations of four corn stover harvest scenarios. *Biomass and Bioenergy*, *31*(2), 126-136.

Jaynes, D.B., and D.E. James. 2007. The extent of farm drainage in the United States. In *Proceedings of the Annual Meeting of the Soil and Water Conservation Society*, Tampa, Florida, July 21, 2007. Ankeny, IA: Soil and Water Conservation Society.

Jha, M. K., Gassman, P. W., & Arnold, J. G. (2007). Water quality modeling for the Raccoon River watershed using SWAT. *Trans. ASAE*, *50*(2), 479-493.

Joslin, J. D., & Schoenholtz, S. H. (1997). Measuring the environmental effects of converting cropland to short-rotation woody crops: A research approach. *Biomass and Bioenergy*, *13*(4), 301-311.

Kalita, P. K., Ward, A. D., Kanwar, R. S., & McCool, D. K. (1998). Simulation of pesticide concentrations in groundwater using Agricultural Drainage and Pesticide Transport (ADAPT) model. *Agricultural Water Management*, *36*(1), 23-44.

Kalita, P. K., Algoazany, A. S., Mitchell, J. K., Cooke, R. A. C., & Hirschi, M. C. (2006). Subsurface water quality from a flat tile-drained watershed in Illinois, USA. *Agriculture, Ecosystems & Environment*, *115*(1), 183-193.

Kalita, P. K., Cooke, R. A. C., Anderson, S. M., Hirschi, M. C., & Mitchell, J. K. (2007). Subsurface drainage and water quality: The Illinois experience. *Trans. ASABE*, *50*(5), 1651-1656.

Keefer, L. (2003). *Sediment and Water Quality Monitoring for the Vermilion River and Little Vermilion River Watersheds*. Illinois State Water Survey. 2003, April.

Kenney, I., Blanco-Canqui, H., Presley, D. R., Rice, C. W., Janssen, K., & Olson, B. (2015). Soil and crop response to stover removal from rainfed and irrigated corn. *GCB Bioenergy*, *7*(2), 219-230.

Khanal, S., & Parajuli, P. B. (2013). Evaluating the Impacts of Forest Clear Cutting on Water and Sediment Yields Using SWAT in Mississippi. *Journal of Water Resource and Protection*, *5*(04), 474.

Kim, S., & Dale, B. E. (2004). Global potential bioethanol production from wasted crops and crop residues. *Biomass and Bioenergy*, *26*(4), 361-375.

Kiniry, J. R., Johnson, M. V. V., Bruckerhoff, S. B., Kaiser, J. U., Cordsiemon, R. L., & Harmel, R. D. (2012). Clash of the titans: comparing productivity via radiation use efficiency for two grass giants of the biofuel field. *BioEnergy Research*, *5*(1), 41-48.

Kiniry, J. R., Anderson, L. C., Johnson, M. V., Behrman, K. D., Brakie, M., Burner, D., ... & Hawkes, C. (2013). Perennial biomass grasses and the mason–dixon line: comparative productivity across latitudes in the southern great plains. *BioEnergy Research*, *6*(1), 276-291.

Kladivko, E. J., Brown, L. C., & Baker, J. L. (2001). Pesticide transport to subsurface tile drains in humid regions of North America. *Critical Reviews in Environmental Science and Technology*, *31*(1), 1-62.

Klingebiel, A. A., & Montgomery, P. H. (1961). Land-capability classification. Agricultural Handbook. No. 210. Soil Conservation Service. *US Department of Agriculture, Washington DC*.

Lindstrom, M. J. (1986). Effects of residue harvesting on water runoff, soil erosion and nutrient loss. *Agriculture, Ecosystems & Environment*, *16*(2), 103-112.

Love, B. J., & Nejadhashemi, A. P. (2011). Water quality impact assessment of large-scale biofuel crops expansion in agricultural regions of Michigan. *Biomass and Bioenergy*, *35*(5), 2200-2216.

McIsaac, G. F., David, M. B., & Mitchell, C. A. (2010). Switchgrass Production in Central Illinois: Impacts on Hydrology and Inorganic Nitrogen Leaching. *Journal of Environmental Quality*, *39*(5), 1790-1799.

Mitchell, J. K., McIsaac, G. F., Walker, S. E., & Hirschi, M. C. (2000b). Nitrate in river and subsurface drainage flows from an east central Illinois watershed. *Trans. ASAE*, *43*(2), 337-342.

Mitchell, J. K., Banasik, K., Hirschi, M. C., Cooke, R. A. C., Kalita, P., & Flanagan, D. C. (2001). There is not always surface runoff and sediment transport. In *Soil erosion research for the 21st century. Proceedings of the International Symposium, Honolulu, Hawaii, USA, 3-5 January, 2001. American Society of Agricultural Engineers,* 575-578.

Mitchell, J. K., Kalita, P. K., Hirschi, M. C., & Cooke, R. A. C. (2003). Upland drainage–watershed hydrology is different. In *AWRA 2003 Spring Specialty Conf. Agricultural Hydrology and Water Quality* (Vol. 1214), 12-14 May 2003, Kansas City, MO.

Neitsch, S.L, Arnold, J.G., Kiniry, J.R., & Williams, J.R. (2011). Soil and Water Assessment Tool Theoretical Documentation Version 2009. *USDA Agricultural Research Service and Texas A&M Blackland Research Center, Temple, Texas*.

Northcott, W. J., Cooke, R. A., Walker, S. E., Mitchell, J. K., & Hirschi, M. C. (2001). Application of DRAINMOD-N to fields with irregular drainage systems. *Trans. ASAE*, *44*(2), 241-249.

Parajuli, P. B., & Duffy, S. E. (2013). Quantifying Hydrologic and Water Quality Responses to Bioenergy Crops in Town Creek Watershed in Mississippi. *Journal of Sustainable Bioenergy Systems*, *3*(03), 202.

Peterson, G. D., Cumming, G. S., & Carpenter, S. R. (2003). Scenario planning: a tool for conservation in an uncertain world. *Conservation Biology*, *17*(2), 358-366.

Phillips, B. M., Anderson, B. S., Hunt, J. W., Huntley, S. A., Tjeerdema, R. S., Kapellas, N., & Worcester, K. (2006). Solid-phase sediment toxicity identification evaluation in an agricultural stream. *Environmental Toxicology and Chemistry*, *25*(6), 1671-1676.

Purdue University Agricultural News (2015). Purdue study shows potential for growth in biofuels from corn stover. Available from: http://www.purdue.edu/newsroom/releases/2015/Q4/purdue-study-shows-potential-for-growth-in-biofuels-from-corn-stover.html.

Pyter, R., Voigt, T., Heaton, E., Dohleman, F., & Long, S. (2007). Giant miscanthus: biomass crop for Illinois. In *Proc. Sixth National Symposium. Issues in New Crops and New Uses, edited by J. Janick and A. Whipkey. ASHS Press. VA*.

Rabalais, N. N., Turner, R. E., Justic, D., Dortch, Q., & Wiseman Jr, W. J. (1999). *Characterization of hypoxia: Topic 1 Report for the Integrated Assessment of Hypoxia in the Gulf of Mexico.* NOAA Coastal Ocean Program, 46-47.

Rabalais, N. N., Turner, R. E., & Wiseman Jr, W. J. (2002). Gulf of Mexico hypoxia, AKA" The dead zone". *Annual Review of Ecology and Systematics*, 235-263.

Raj, C. (2013). *Optimal land use planning on selection and placement of energy crops for sustainable biofuel production* (Doctoral dissertation), Purdue University.

Randall, G. W., & Iragavarapu, T. K. (1995). Impact of long-term tillage systems for continuous corn on nitrate leaching to tile drainage. *Journal of Environmental Quality*, *24*(2), 360-366.

Schilling, K. E., & Helmers, M. (2008). Effects of subsurface drainage tiles on streamflow in Iowa agricultural watersheds: Exploratory hydrograph analysis. *Hydrological Processes*, *22*(23), 4497-4506.

Schmer, M. R., Mitchell, R. B., Vogel, K. P., Schacht, W. H., & Marx, D. B. (2010). Spatial and temporal effects on switchgrass stands and yield in the Great Plains. *BioEnergy Research*, *3*(2), 159-171.

Singh, J., P. K. Kalita, J. K. Mitchell, R. A. C. Cooke, and M. C. Hirschi. "Simulation of tile flow for a flat tile drained watershed in east central Illinois." In *2001 ASAE Annual Meeting*, p. 1. American Society of Agricultural and Biological Engineers, July 29- August 1, 2001, Sacramento, California, USA.

Skaggs, R. W., Youssef, M. A., & Chescheir, G. M. (2012). DRAINMOD: Model use, calibration, and validation. *Trans. ASABE*, *55*(4), 1509-1522.

Sugg, Z. (2007). Assessing US farm drainage: Can GIS lead to better estimates of subsurface drainage extent. *World Resources Institute, Washington, DC20002*.

Sui, Y., & Frankenberger, J. R. (2008). Nitrate loss from subsurface drains in an agricultural watershed using SWAT2005. *Trans. ASABE*, *51*(4), 1263-1272.

Thomas, M. A. (2011). *Environmental implications of feedstock production practices for bioenergy* (Doctoral dissertation), Purdue University.

Thomas, M. A., Engel, B. A., & Chaubey, I. (2011). Multiple corn stover removal rates for cellulosic biofuels and long-term water quality impacts. *Journal of Soil and Water Conservation*, *66*(6), 431-444.

Thomas, M. A., Ahiablame, L. M., Engel, B. A., & Chaubey, I. (2014). Modeling water quality impacts of growing corn, switchgrass, and Miscanthus on marginal soils. *Journal of Water Resource and Protection*, *6*(14), 1352.

Thornton, F. C., Dev Joslin, J., Bock, B. R., Houston, A., Green, T. H., Schoenholtz, S. & Tyler, D. D. (1998). Environmental effects of growing woody crops on agricultural land: first year effects on erosion, and water quality. *Biomass and Bioenergy*, *15*(1), 57-69.

Tilman, D., Socolow, R., Foley, J. A., Hill, J., Larson, E., Lynd, L., ... & Williams, R. (2009). Beneficial biofuels—the food, energy, and environment trilemma. *Science*, *325*(5938), 270-271.

Tolbert, V. R., Lindberg, J. E., & Green, T. H. (1997). *Soil and water quality implications of production of herbaceous and woody energy crops* (No. ORNL/CP--95956; CONF-9710174--). Oak Ridge National Lab., TN (United States).

Trybula, E. (2012). *Quantifying ecohydrologic impacts of perennial rhizomatous grasses on tile discharge: A plot level comparison of continuous corn, upland switchgrass, mixed prairie, and Miscanthus x giganteus* (Master thesis), Purdue University.

Trybula, E. M., Cibin, R., Burks, J. L., Chaubey, I., Brouder, S. M., & Volenec, J. J. (2015). Perennial rhizomatous grasses as bioenergy feedstock in SWAT: parameter development and model improvement. *GCB Bioenergy*,*7*(6), 1185-1202.

Van Donk, S. J., Martin, D. L., Irmak, S., Melvin, S. R., Petersen, J. L., & Davison, D. R. (2010). Crop residue cover effects on evaporation, soil water content, and yield of deficit-irrigated corn in west-central Nebraska. *Trans. ASABE*, *53*(6), 1787-1797.

Ye, S., Covino, T. P., Sivapalan, M., Basu, N. B., Li, H. Y., & Wang, S. W. (2012). Dissolved nutrient retention dynamics in river networks: A modeling investigation of transient flows and scale effects. *Water Resources Research*, *48*(6), 1-18.

Yu, C., Northcott, W. J., & McIsaac, G. F. (2004). Development of an artificial neural network for hydrologic and water quality modeling of agricultural watersheds. *Trans. ASAE*, *47*(1), 285-290.

Yuan, Y., Mitchell, J. K., Hirschi, M. C., & Cooke, R. A. C. (2001). Modified SCS curve number method for predicting subsurface drainage flow. *Trans. ASAE*, *44*(6), 1673-1682.

Zanardo, S., Basu, N. B., Botter, G., Rinaldo, A., & Rao, P. S. C. (2012). Dominant controls on pesticide transport from tile to catchment scale: Lessons from a minimalist model. *Water Resources Research*, *48*(4).

CHAPTER 6. SUMMARY, CONCLUSIONS, AND RECOMMENDATIONS FOR FUTURE RESEARCH

6.1 Research Overview

This set of four studies improved simulation of hybrid poplar tree growth in SWAT, compared performance of tile drainage routines in SWAT2009 and SWAT2012, and quantified biofeedstock production of bioenergy crop and the impacts of its growth on water quantity and quality at a watershed scale.

In the first study, the functional components and parameters of hybrid poplar and cottonwood were determined, and related algorithms improved in ALMANAC for leaf area, plant biomass, and biomass partitioning. The improved tree growth simulation in ALMANAC was applied to *Populus* plots in Wisconsin and Mississippi. The simulated LAI, total biomass, and biomass partitioning between above-ground and roots were compared with published data to modify and evaluate *Populus* growth parameters in ALMANAC.

In the second study, tree growth modification in ALMANAC was incorporated in SWAT. Sensitivity analysis was used to determine ranges and values of *Populus* growth parameters in the modified SWAT. SWAT with tree growth modification was used to simulate hybrid poplar LAI and biomass yield, runoff, sediment loss, and nitrate loss to hybrid poplar growth at a hybrid poplar site in Wisconsin and cottonwood biomass yield at a cottonwood in Mississippi. The simulated values were compared with observed data to calibrate and validate the modified SWAT.

In the third study, the old tile drainage routine in SWAT2009 (Rev.528) and the new tile drainage routine in SWAT2012 (Rev.615 and Rev.645) were used to simulate monthly tile flow, nitrate in tile flow, surface runoff, and sediment and nitrate in surface runoff at field

sites, and monthly flow, sediment and nitrate in flow at a river station in the LVR watershed. Performance of both routines were evaluated and compared with observed values.

In the fourth study, SWAT2012 (Rev.615) with improved perennial grass and tree growth modification and new tile drainage routine was used to simulate annual biomass yields, flow, tile flow, sediment load, total nitrogen, nitrate load in flow, nitrate in tile flow, soluble nitrogen, organic nitrogen, total phosphorus, mineral phosphorus and organic phosphorus under various bioenergy scenarios from 1990 to 2008 at the LVR watershed. Simulated results from different bioenergy crop scenarios were compared with those from the baseline.

Overall, studies improved SWAT to accurately simulate biomass production of hybrid poplar tree, determined reasonable parameter sets for the old and new tile drainage routines for tile drainage simulation, and provided guidance for further research on simulation of bioenergy crop growth and its hydrologic and water quality impacts.

6.2 Major Research Findings

Major research findings from the study are provided below:

(1) ALMANAC and SWAT simulated biomass and LAI were satisfactory, and improved relative to simulations by original SWAT, FOREST and modified FOREST models. SWAT simulated biomass, runoff, sediment, and Nitrate-N in runoff for cottonwood were reasonable. The new algorithm for estimating LAI and calculating falling leaves weight, suggested values and potential parameter range were reasonable. Modified ALMANAC and SWAT are able to accurately simulate biofeedstock production of *Populus* with various populations. Modified SWAT can be used to simulate hydrologic and water quality response to *Populus* growth at landscape scales. The improved algorithms of LAI and biomass simulation for tree growth could also be used in other process based models, such as Environmental Policy Integrated Climate (EPIC) and Agricultural Policy/Environmental eXtender (APEX).

(2) Both the old and new tile drainage routines provided satisfactory tile flow and nitrate in tile flow results at LVR subsurface sites (sites B and E), acceptable flow and nitrate load

in flow, and reasonable sediment load in flow results at the river station (site R5) after model calibration. Rev.645 with an improved curve number calculation method provided acceptable surface runoff, and reasonable sediment and nitrate load in surface runoff results at surface stations (sites Bs and Es). Generally, simulated tile flow results by the old routine were slightly better than those for the new routine at site B, while simulated tile flow results from the new routine were better than those from the old routine at site E. Nitrate in tile flow results from the new routine were better than those from the old routine at both sites B and E. Simulated flow and nitrate in flow results from the new routine were better than those from the old routine at site R5. The new routine provided more realistic and accurate simulation of tile drainage, and the new curve number retention parameter adjustment factor in Rev.645 improved surface runoff simulation.

(3) Simulated biomass production under the scenario with 38% corn stover removal (66,439 Mg/yr corn stover) combined *Miscanthus* both on highly erodible areas and marginal land (19,039 Mg/yr *Miscanthus*) was the highest relative to other bioenergy crop scenarios. Flow, tile flow, sediment load, nutrient losses were reduced by switchgrass, *Miscanthus* and hybrid poplar under scenarios on highly erodible areas and marginal land. Corn stover removal did not result in considerable sediment and nutrient alterations. Less nutrient replacement for corn stover removal could provide more improvements to water quality, but could result in lower corn and corn stover yield relative to more nutrient replacement. Corn stover removal scenarios increased sediment load and nutrient losses, and these adverse impacts by corn stover removal could be offset under scenarios with corn stover removal with combination of *Miscanthus*, switchgrass and hybrid poplar. Generally, corn stover removal with combination of perennial grasses and hybrid poplar both on highly erodible areas and marginal land was able to provide higher biomass yields than other bioenergy crop scenarios, and improve water quantity and water quality.

6.3 Limitations of Current Study and Recommendations for Future Research

A primary limitation of the tree growth simulation study is limited and old LAI and biomass yield data for *Populus* trees with various population during model calibration and validation periods. Only three or four annual LAI and aboveground biomass data were

obtained for some populations and tree planting techniques, and applied pesticide during 1970-1980 or 1995-1997 were different from those in recent hybrid poplar plots. Additionally, SWAT outputs only total biomass, but aboveground woody biomass (stem and branch) is used as biofeedstock.

Limitations of the tile drainage simulation study include limited observed precipitation data for the river station (site R5), water table depth calculation after long dry periods, and the challenge of simulating surface runoff, sediment, and nitrate in surface runoff from this extensively tile drained, flat watershed. For bioenergy crop scenario simulation, precipitation data and plant management practices data may affect the accuracy of simulated plant growth, hydrology and water quality results. Moreover, potential area for bioenergy crop production scenarios was small, thus the ability to produce biomass was not considerable, and water quantity and quality alterations were not significant.

Many avenues of future work could improve this study. For instance, additional continuous *Populus* growth, hydrology and water quality field data have the potential to improve tree growth parameters in process based models, and thus improve simulation of biomass production, and water quantity and quality impacts of *Populus* trees. Root biomass, aboveground biomass and aboveground woody biomass can be incorporated in SWAT outputs.

There is an opportunity to improve the representation of tile drainage system and water table depth calculation in SWAT, and improve Rev.645 functionality at watershed scales. The new tile drainage routine and the improved curve number calculation method can be tested for more individual tiles and watersheds. Additionally, field site experiments can be performed to detect water quality impacts of bioenergy crop scenarios. More corn and soybean areas can be considered as potential areas for bioenergy crop scenarios to evaluate biofeedstock production and water quantity and quality impacts in further research.

APPENDICIES

Appendix A Tree Growth Modification in ALMANAC

Data A.1 Hybrid Poplar Site in Northern Wisconsin

At Hybrid Poplar site, the rainless period is about 1-2 weeks per year. Severe droughts occur every 10-15 years (Strong and Hansen 1993). Phosphorus was applied prior to planting at 213-224 kg/ha. Nitrogen was maintained at 3.2% levels in new leaf tissue by adding ammonium nitrate to the soil every three weeks. Soil moisture at 16-30% levels by irrigation. Weeds were controlled using Linuron (Ek and Dawson 1976).

Plantings were made in 1970 and again in 1973 at spacings ranging from 0.23*0.23 to 2.4*2.4 m. Another planting was made at spacing of 3.6*3.6 m (Hansen 1983). The plot size ranging from 5 to 5.5 m on a side and each planting has three replicates (EK and Dawson 1976). 1.2 m spacing four-year old hybrid poplar was planted in 6 * 13.5 m plot, and each planting had two replicates (Strong and Zavitkovski 1983). In 1976/1977, hybrid poplar trees were planted in an area of 2500 m^2.

About 1/6 of the total planting area was designated for destructible sampling annually for biomass estimation. Hybrid poplar was cut at ground level and tree height was measured with a tape (Hansen 1983). Trees were separated into stem wood, stem bark, branch, branch bark, tips and leaves (EK and Dawson 1976). Dry weights were used to develop regression equations for biomass estimation of trees in a plot. Aboveground woody biomass included stem, branch with bark and foliage. Hybrid poplar biomass was estimated based on both the diameter at breast height (DBH) and height (Hansen 1983). Leaf area was measured by means of an electronic leaf area meter in each planting and LAI was estimated, based on destructive monthly sampling of one replicate (Zavitkovski 1981).

Data A.2 Cottonwood Site in Western Mississippi

The Cottonwood Site is located in the Tennessee Valley Authority (TVA) region, a 276 country area that includes all of Tennessee and portions of 10 contiguous states in the southeastern US, was shown to be viable for cost effective production of SRWCs based on

economic analyses (Downing and Graham 1993). Soils were expected to produce high yielding SRWCs. Cottonwood (3-year rotation) is one of the most frequently recommended SRWCs in the southeastern U.S (Joslin and Schoenholtz 1997).

Cottonwood cuttings were planted with spacing of 1.2 × 3.6 m in three plots (each plot is about 5000 m2). Cottonwood plantings had three replicates (Thornton et al. 1998). For cottonwood harvest, each row of trees was felled by chainsaw and spread out to decompose. In September of 1995, 1996 and November of 1997, aboveground part of three cottonwood trees from each plot were sampled destructively for estimation of aboveground biomass. Mean weight of tree sampled for each year was used to calculate dry-weight aboveground biomass of cottonwood. Tree root was lifted from the sampled trees to determine root biomass. (Pettry et al. 1997, unpublished annual progress report).

Yearly LAI and biomass data of hybrid poplar 'Tristis #1' were collected from Hansen (1983) and shown in Tables A.1 and A.2.

Table A 1 LAI of 3- to 10-year-old hybrid poplar with various spacings

Age	LAI					
Spacing (m)	0.3*0.3	0.6*0.6	1.1*1.1	1.2*1.2	2.0*2.0	2.4*2.4
Population (trees/100 m^2)	1111	278	83	69	25	17
3	6.0	5.6	3.8	4.9	0.6	1.6
4	6.9	7.1	7.3	5.9	1.6	3.2
5	-	7.3	6.1	-	5.7	-
6	8.6	8.7	7.8	-	8.2	6.8
7	-	-	-	-	-	8.4
8	-	-	-	-	-	7.5
9	-	-	-	-	-	5.7
10	-	-	-	-	-	8.3

Table A 2 Aboveground biomass production of 2- to 10-year-old hybrid poplar with various spacings

Age	Mean annual biomass production (mt/ha/year)						
Spacing (m)	0.3*0.3	0.6*0.6	1.1*1.1	1.2*1.2	2.0*2.0	2.4*2.4	3.6*3.6
Population (trees/100 m^2)	1111	278	83	69	25	17	8
2	3.7	1.9	1.6	1.1	0.2	0.2	0.1
3	7.0	4.9	3.3	2.3	0.9	0.6	0.3
4	9.0	7.9	6.0	5.1	3.8	2.3	1.0
5	9.9	8.9	6.5	6.8	5.5	3.7	1.7
6	-	-	9.6	-	9.1	4.8	3.2
7	-	-	-	-	-	6.5	4.8
8	-	-	-	-	-	8.4	5.6
9	-	-	-	-	-	9.7	6.2
10	-	-	-	-	-	10.4	-

Data A.3 ALMANAC Model Setup and Management Schedules

Daily precipitation and temperature data from 01/01/1970 to 12/31/1982 of Rhinelander WI US weather station (GHCND: USC00477113, Latitude: 45.63, Longitude: -89.42, Elevation: 476m) close to hybrid poplar site, and from 01/01/1995 to 12/31/1997 of Stoneville experimental station WI US (GHCND: USC00228445, Latitude: 33.4, Longitude: -90.92, Elevation: 38.7 m) were downloaded from National Climatic Data Center (NCDC CDO) and used for model setup, base temperature and PHU determination.

Data A.4 Algorithm and Parameter Changes in the Model

The ALMANAC model includes a function to calculate weight of dropping leaves, and then can be used for current aboveground biomass calculation

$$y = x_1 * (0.2 - 0.1 * \frac{yr-1}{x_2-1}) \quad \text{(A.1)}$$

where y is weight of dropping leaves, yr is current growth year, x_1 is aboveground biomass, x_2 is number of years to maximum height and maximum LAI of trees (CHTYR).

Data A.5 Values and Ranges of Parameters Determined before Model Calibration

Accumulation of heat unit (HU) for a given day was calculated with the equation:

$$HU = \overline{T}_{av} - T_{base} \text{ when } \overline{T}_{av} > T_{base} \text{ (A.2)}$$

$$PHU = \sum_{d=1}^{m} HU \text{ (A.3)}$$

where HU is the number of heat units accumulated on a given day, $\overline{T}_{av}$ (℃) is the average daily temperature, and T_{base} (℃) is the temperature from which *Populus* starts to growth (TG). PHU is the total heat units required for *Populus* maturity. The time that trees begin to develop buds and maturity of seeds are considered the beginning and end of the growing season, respectively (Neitsch *et al.* 2011).

Default values of RDMX, WAVP, BN_1 (BP_1), BN_2 (BP_2), and BN_3 (BP_3) in model are 3.5, 8.00, 0.0060 (0.0007), 0.0020 (0.0004) and 0.0015 (0.0003). These values have been used for simulation of forest growth (MacDonald *et al.* 2008) and biomass of honey mesquite and eastern red cedar (Kiniry 1998) and obtained reasonable simulation results. Thus, default values of RDMX, WAVP, BN_1 (BP_1), BN_2 (BP_2), and BN_3 (BP_3) were used for *Populus* growth simulation.

Ranges and values of GSI were assumed as 0.004-0.007 and 0.007 for *Populus* (Kiniry 2014, personal communication). Ranges and values of HMX for hybrid poplar and cottonwood were assumed as 7-15 (10-15) and 7.5 (10) (Kiniry 2014 personal communication).

HI ((leaf +stem dry weight)/total dry weight) of hybrid poplar is ranging from 0.4 to 0.6 (Michael *et al.* 1990). HI of *Populus* in model was calculated by dividing the weight of the harvest portion of the plant by the weight of the total aboveground biomass (Arnold *et al.* 2011). Thus, ranges of HI for hybrid poplar and cottonwood were calculated as 0.45-0.70 and 0.40-0.65. And 0.65 and 0.60 were determined as values of HI for hybrid poplar and cottonwood.

Data A.6 ALMANAC Model Calibration and Parameterization

Suggested ranges of WA and value of EXTINC for hybrid poplar were 58-64 and 0.6 from previous hybrid poplar biomass modeling research (Landsberg and Wright 1989). However,

since simulated aboveground biomass of hybrid poplar were higher than observed values (Landsberg and Wright 1989), the initial values of WA and EXTINC were assumed as 45 and 0.6.

Observed DMLA, 8.6, was considered as initial value of DMLA for calibration (Hansen, 1983). Default value of CNP, 0.003, was used as initial value of CNP for calibration (Kiniry 2014, personal communication). Suggested values of CNY, 0.001, was used as initial value of CNY for calibration (Black *et al*. 2002; McLaughlin *et al*. 1987). Based on condition of canopy during different periods of growing season, initial values of fraction of growing season coinciding with the first and second point on optimal leaf development curve, and fraction of DMLA corresponding to the first and second point were assumed as 0.05, 0.4, 0.05 and 0.95 (Zavitkovski 1981).

Appendix B Tree Growth Modification in SWAT

Data B.1 Summary of critical functions, parameters and processes for simulating leaf area index (LAI) and biomass in SWAT

The original SWAT (Rev.628) simulates light interception by Beer's law (Monsi & Saeki, 1953) and LAI (Equation (B.1)). With the increase of extinction coefficient values (k), a given LAI can intercept more light. The equation for calculation of fraction of intercepted incoming radiation by the leaf canopy is below:

$$Fraction = 1.0 - \exp(k * LAI) \quad \text{(B.1)}$$

Fraction is fractional light interception by the canopy of plant and k is extinction coefficient, depending upon the angle distribution of the leaves in the canopy and the angle of radiation. LAI is the area of green leaf per unit area of land.

A generic LAI calculation function is used to simulate leaf area of plant (Equation (B.2)). Seasonal LAI development curve ("S" curve) is determined by two input parameters: the percent of growing season and fraction of maximum LAI (Kiniry *et al.*, 1992).

$$F = X/(X + \exp(y_1 - y_2 * X)) \quad \text{(B.2)}$$

F is fractional change and is a function of a time dependent factor (X). F represents a percentage total leaf area and X means corresponding growth degree days. Variables y_1 and y_2 are generated by the model from these two points (Kiniry *et al.*, 1992). The model simulates leaf area loss with the LAI decline factor.

The model (Rev.628) includes a function to calculate weight of dropping leaves (Equation (B.3)).

$$FALF = STL * (0.2 - 0.1 * (current\ year - 1)/(CHTYR - 1.0)) \quad \text{(B.3)}$$

FALF is weight of dropping leaves, STL is aboveground biomass, CHTYR is number of years to maximum height of trees.

Base temperature is minimum temperature for plant growth which constrains leaf area growth initiation and dry matter accumulation. The higher the temperature, the more rapid the growth rate, when air temperature is higher than base temperature. However, the growth rate will slow when air temperature is higher than optimum temperature. Plant growth will cease when air temperature reaches maximum temperature of plant growth (Neitsch *et al.*, 2011). Both base temperature and optimal temperature are stable for cultivars within a plant species. All growth stages are assumed to have the same base and optimal temperature for a plant species. The potential heat units (PHUs) are a summation index used by ALMANAC. The growth rate is assumed proportional to temperature increase. Heat units are calculated from daily maximum and minimum temperatures. One heat unit is each degree of daily average temperature (Celsius) above base temperature (Neitsch *et al.*, 2011).

Table B 1 Management operations for hybrid poplar site in Rhinelander, Wisconsin in SWAT

Plant	Date	Management Operation	Rate
Hybrid poplar	30 May	Tillage, Roto-Tiller (mixing depth: 5 mm, mixing efficiency: 0.80)	
	1 June	Planting	
	1 June	Pesticide Application (as Linuron)	2.2 kg ha^{-1}*,†
	1 June	Nitrogen Application (as Anhydrous Ammonia)	200 kg ha^{-1}*,†
	1 June	Phosphorus Application(as Elemental Phosphorus)	50 kg ha^{-1}*,†
		Auto-irrigation	-
	31 Dec	The end of the operation scheduling for a year	

* Ek and Dawson, 1976
† R. Srinivasan & R. Cibin, personal communication.

Table B 2 Management operations for eastern cottonwood site in Stoneville, Mississippi in SWAT

Plant	Date	Management Operation	Rate
Cottonwood	3 Feb	Tillage, Roto-Tiller (mixing depth: 5 mm, mixing efficiency: 0.80)	
	3 Feb	Planting	
	3 Feb	Pesticide Application (as Linuron)	2.2 kg ha^{-1}*,†
	1 June	Nitrogen Application (as Anhydrous Ammonia)	200 kg ha^{-1}*,†
	1 June	Phosphorus Application (as Elemental Phosphorus)	30 kg ha^{-1}*,†
		Auto-irrigation	-
	31 Dec	The end of the operation scheduling for a year	

* Joslin and Schoenholtz, 1997); Thornton *et al.*, 1998
† R. Srinivasan & R. Cibin, personal communication.

Data B.2 Summary of tree growth algorithm and parameter improvements in SWAT

A leaf area development equation was generated to simulate leaf area development across years in prior research (Guo *et al*., 2015).

$$LAI_{current\ year} = LAI_{current\ year-1} \times 10^{RateTree}$$

$$RateTree = log_{10}(current\ year/CLAIYR) \times TreeD \quad \text{(B.4)}$$

CLAIYR is number of years until maximum LAI is attained (for any species), TreeD is tree parameter defining how LAI increases up to BLAI, and STL is aboveground biomass (mt ha^{-1}).

In this revision, leaf dropping is estimated as a user defined fraction of annual accumulated tree biomass instead of total aboveground biomass (Equation B.5).

$$FALF = BIO\_LEAF * TreeBioIni \quad \text{(B.5)}$$

FALF is weight of dropping leaves, $TreeBioIni$ is annual accumulated tree biomass, BIO_LEAF is a user defined fraction in plant.dat.

Table B 3 Changes to source code in SWAT

Subroutine	Code changes	Comment
modparm.f	real, dimension (:), allocatable :: rsr1, rsr2, tree_d real, dimension (:), allocatable :: TreeBioIni	Add new variable TreeD
readplant.f	read (104,777,iostat=eof) bioleaf, yrsmat, biomxtrees, extcoef, &bmdieoff, rsr1c, rsr2c, treed 777 format (f8.3,i5,6f8.3) tree_d (ic) =treed	Read new parameter TreeD from plant.dat
zero0.f	tree_d = 0	Initialize TreeD as 0
plantmod.f	sol_cov(j) = 0.8 * bio_ms(j) sol_cov(j) = (1-rwt(j)) * bio_ms(j) + sol_rsd(1,j)	Previously root ratio was hard coded as 0.8
allocate_parms.f	allocate (TreeBioIni(mhru)) allocate (tree_d(mcrdb))	Allocate the two new variables annual initial tree biomass and tree density
sim_inityr.f	TreeBioIni = bio_ms	Initialize initial tree biomass beginning of year
grow.f	!!laimax = rto * blai(idp) !! if (curyr_mat(j)==0) curyr_mat(j)=1 xx = 1. * curyr_mat(j) / mat_yrs(idp) xx = log10(xx) raretree=xx * tree_d(idp) laimax = blai (idp)* 10.**raretree	Maximum seasonal LAI each year with various densities is calculated based on a new leaf development algorithm rather than a function of fraction of growing season.
dormant.f	resnew = (bio_ms(j)-TreeBioIni(j)) * bio_leaf(idplt(j)) bio_ms(j) = bio_ms(j) - resnew	Leaf drop at dormancy as a fraction (bio_leaf) total annual accumulated biomass

harvestop.f	if (idplt(j) > 0) then
	if (idc(idplt(j)) == 7) then
	if (ff3 > 0.6) then
	curyr_mat(j) = 1
	curyr_mat(j) = Min(curyr_mat(j),&mat_yrs(idplt(j)))
	end if
	end if
	end if
		Reset the current year of maturity to one after harvest more than 60%

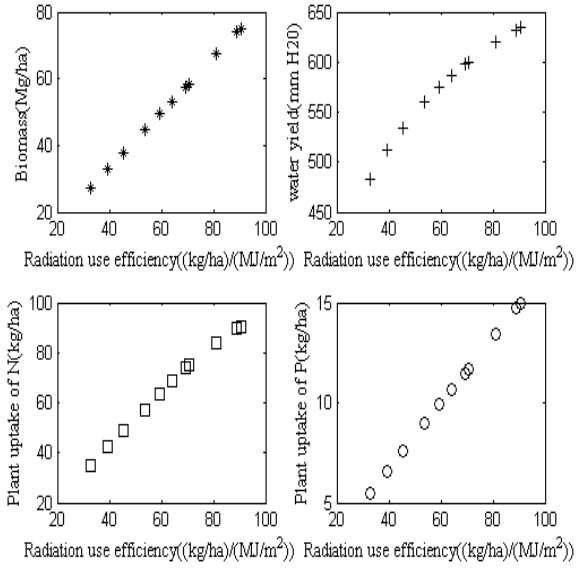

(a) Radiation use efficiency

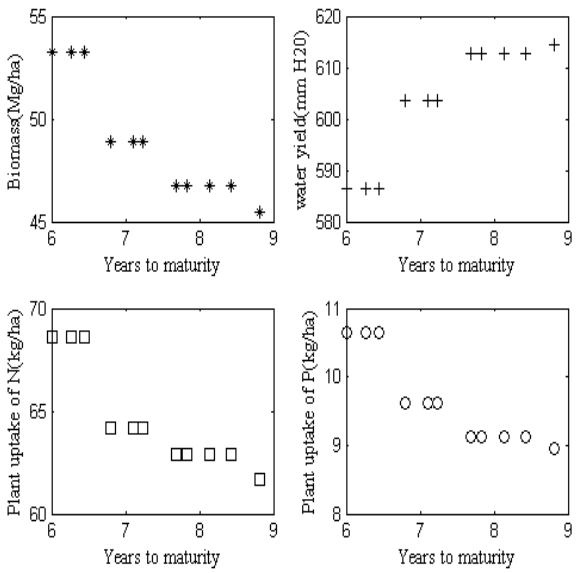

(b) Years to reach maturity

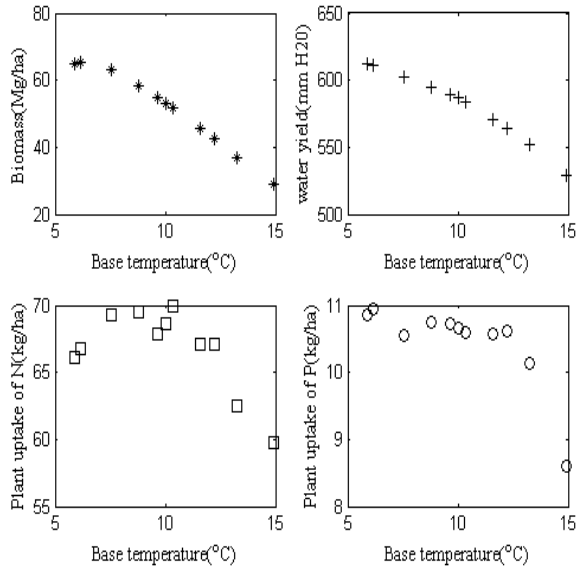

(c) Base temperature

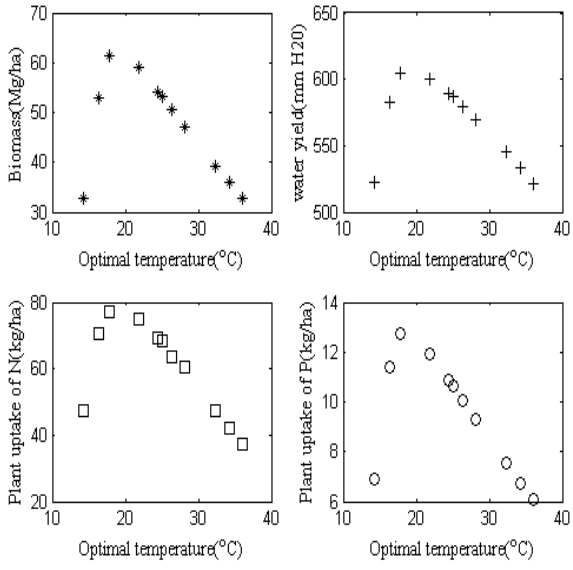

(d) Optimal temperature

Figure B 1 Sensitivity analysis plots of sensitive *Populus* growth parameters

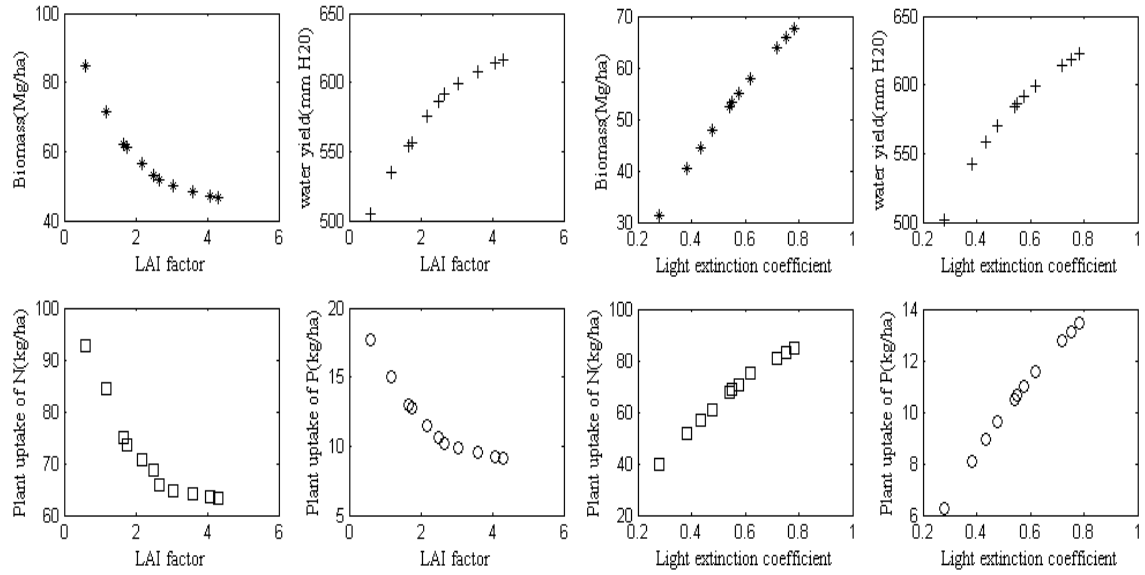

(e) LAI factor (f) Light extinction coefficient

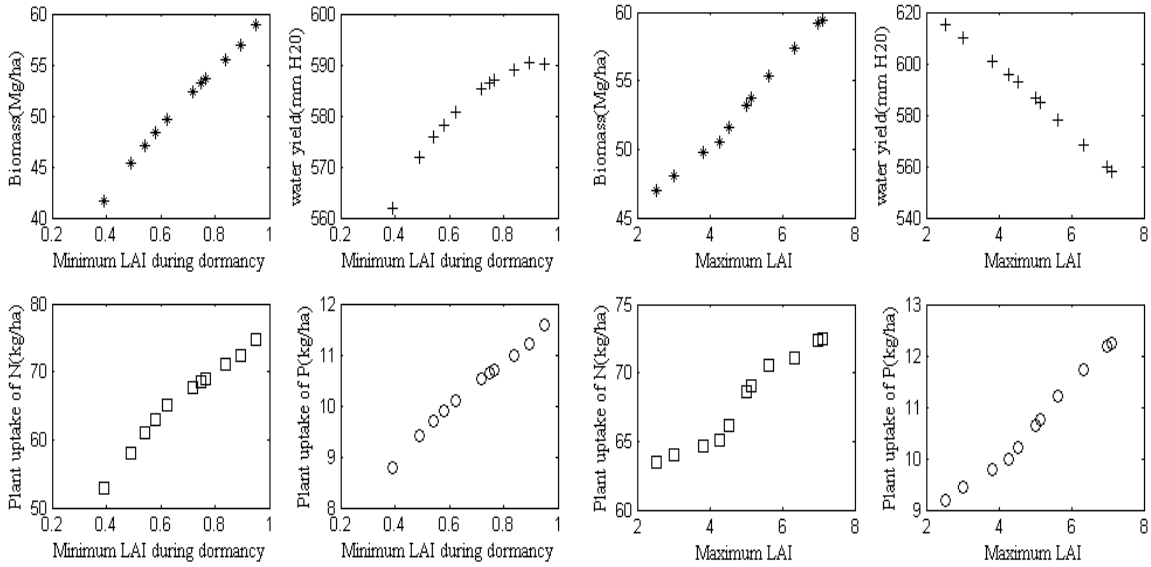

(g) Minimum LAI during dormancy (h) Maximum LAI

Figure B.1 continued

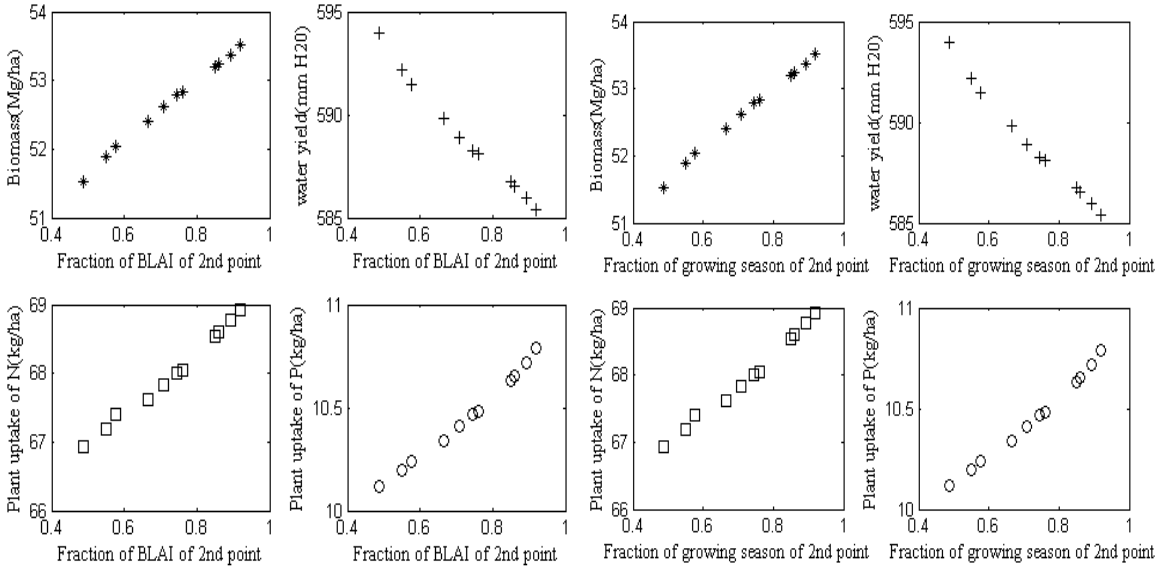

(i) Fraction of BLAI of 2nd point (j) Fraction of growing season of 2nd point

Figure B.1 continued

Table B 4 Relative sensitivity analysis of model outputs to tree growth parameters, ranked by greatest sensitivity of biomass yield for the modified SWAT in Wisconsin

Parameter	Parameter definition	Biomass (t ha^{-1})	Water yield (mm H_2O)	Plant uptake of Nitrogen (kg ha^{-1})	Plant uptake of Phosphorus(kg ha^{-1})
BIO_E	Radiation Use Efficiency in ambient CO_2 (kg ha^{-1})/(MJ/m^{-2})	0.987	0.252	0.982	0.977
MAT_YRS	Number of years required for tree species to reach full development (years)	-0.972	0.541	-0.670	-1.26
T_BASE	Base Temperature (°C)	-0.964	-0.154	-0.188	-0.285
T_OPT	Optimal Temperature (°C)	-0.873	-0.189	-0.521	-0.944
EXT_COEF	Light Extinction Coefficient	0.713	0.199	0.678	0.706
TREED	LAI Decline Factor	-0.413	0.173	-0.393	-0.568
ALAI_MIN	Minimum LAI for plant during dormancy	0.395	0.039	0.236	0.306
BLAI	Maximum leaf area index (LAI)	0.325	-0.112	0.175	0.413
LAIMX2	Fraction of BLAI corresponding to 2nd point on optimal leaf development curve	0.097	-0.038	0.051	0.197
FRGRW2	Fraction of growing season coinciding with LAIMX2	-0.047	0.019	-0.013	-0.100
BMX_TREES	Maximum biomass for a forest (metric t ha^{-1})	0.027	0.011	-0.015	-0.018
FRGRW1	Fraction of growing season coinciding with LAIMX1	-0.021	0.007	-0.019	-0.052
LAIMX1	Fraction of BLAI corresponding to 1st point on optimal leaf development curve	0.016	-0.005	0.015	0.039
WAVP	Rate of decline in radiation use efficiency per unit increase in vapor pressure deficit	-0.012	-0.004	-0.009	-0.012
PLTNFR3	Plant N fraction at maturity (whole plant)	-0.009	-0.002	-0.362	-0.023
GSI	Maximum stomatal conductance	0.008	-0.260	-0.271	0.000
PLTNFR1	Plant N fraction at emergence (whole plant)	-0.005	-0.001	0.597	-0.005
PLTNFR2	Plant N fraction at 50% maturity (whole plant)	-0.004	-0.001	1.308	-0.001
CHTMX	Maximum canopy height (m)	-0.000	0.021	-0.000	0
FRGMAX	Fraction of GSI corresponding to the 2nd point the stomatal conductance curve	0	-0.005	0	0

Table B.4 Continued.

VPDFR	Vapor pressure deficit (kPa) corresponding to 2nd point on the stomatal conductance curve	0	-0.003	0	0
RSDCO_PL	Plant residue decomposition coefficient	0	-0.000	0	0
PLTPFR1	Plant P fraction at emergence (whole plant)	0	0	0	0.283
DLAI	Point in growing season when LAI declines	0	0	0	0
RDMX	Maximum rooting depth (m)	0	0	0	0
CNYLD	Plant N fraction in harvested biomass	0	0	0	0
CPYLD	Plant P fraction in harvested biomass	0	0	0	0
PLTPFR2	Plant P fraction at 50% maturity (whole plant)	0	0	0	0
PLTPFR3	Plant P fraction at maturity (whole plant)	0	0	0	0
USLE_C	Minimum crop factor for water erosion	0	0	0	0
CO2HI	Elevated CO_2 atmospheric concentration ($\mu L\ CO_2\ L^{-1}$ air) corresponding the 2nd point in the radiation use efficiency curve	0	0	0	0
BIOHI	Biomass-energy ratio corresponding to 2nd point on the radiation use efficiency curve	0	0	0	0
WSYF	Lower limit of harvest index ((kg ha^{-1})/(kg ha^{-1}))	0	0	0	0
BM_DIEOFF	Biomass dieoff fraction	0	0	0	0
HVSTI	Harvest index for optimal growing conditions	0	0	0	0

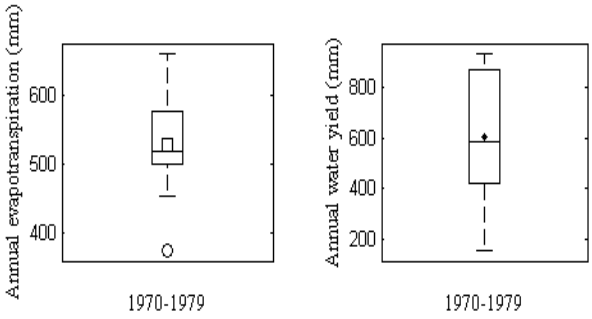

Figure B 2 Boxplots of annual evapotranspiration and water yield (1970-1979) of hybrid poplar site in Wisconsin

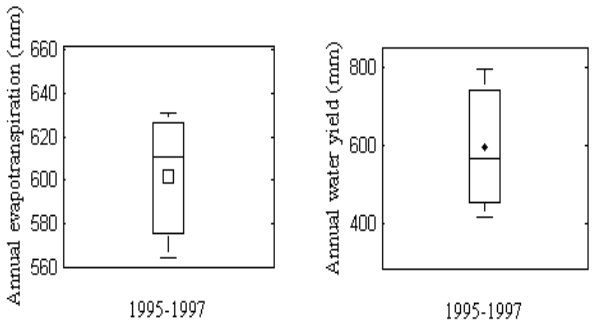

Figure B 3 Boxplots of annual evapotranspiration and water yield (1995-1997) of cottonwood site in Mississippi

References

Arnold, J., Kiniry, J., Srinivasan, R., Williams, J., Haney, E., & Neitsch, S. (2011). Soil and water assessment tool input/output file documentation version 2009. Texas Water Resources Institute Technical Report. (365).

Black, B. L., Fuchigami, L. H., & Coleman, G. D. (2002). Partitioning of nitrate assimilation among leaves, stems and roots of poplar. *Tree Physiology, 22*(10), 717-724.

Ek, A. R., & Dawson, D. H. (1976). Actual and projected growth and yields of *Populus*' Tristis# 1'under intensive culture. *Canadian Journal of Forest Research, 6*(2), 132-144.

Guo, T., Engel, B. A., Shao, G., Arnold, J. G., Srinivasan, R., & Kiniry, J. R. (2015). Functional approach to simulating short-rotation woody crops in process-based models. *BioEnergy Research*, *8*(4), 1598-1613.

Hansen, E. A. (1983). Intensive plantation culture: 12 years research. General Technical Report, North Central Forest Experiment Station, USDA Forest Service (NC-91).

Joslin, J., & Schoenholtz, S. (1997). Measuring the environmental effects of converting cropland to short-rotation woody crops: A research approach. *Biomass and Bioenergy, 13*(4), 301-311.

Kiniry, J. R., Williams, J. R., Gassman, P. W., & Debaeke, P. (1992). A general, process-oriented model for two competing plant species. *Trans. ASAE*, *35*(3), 801-810.

Landsberg, J., & Wright, L. (1989). Comparisons among *Populus* clones and intensive culture conditions, using an energy-conservation model. *Forest Ecology and Management, 27*(2), 129-147.

McLaughlin, R. A., Hansen, E. A., & Pope, P. E. (1987). Biomass and nitrogen dynamics in an irrigated hybrid poplar plantation. *Forest Ecology and Management, 18*(3), 169-188.

Michael, D., Dickmann, D., Isebrands, J., & Nelson, N. (1990). Photosynthesis patterns during the establishment year within two *Populus* clones with contrasting morphology and phenology. *Tree Physiology, 6*(1), 11-27.

Monsi, M., & Saeki, T. (1953). The light factor in plant communities and its significance for dry matter production. *Japanese Journal of Botany, 14*, 22-52.

Neitsch, S., Arnold, J., Kiniry, J., & Williams, J. (2011). Soil and water assessment tool theoretical documentation version 2009. Texas Water Resources Institute Technical Report.

Pettry, D., Schoenholtz, S., Dewey, J., Switzer, R., & Mitchell, B. (1997). *Environmental impacts of conversion of cropland to short rotation woody biomass plantations*. Annual Progress Report, Mississippi State University, submitted to Tennessee Valley Authority, Muscle Shoals, AL and Oak Ridge National Laboratory, Oak Ridge, TN.

Strong, T., & Hansen, E. (1993). Hybrid poplar spacing/productivity relations in short rotation intensive culture plantations. Biomass and Bioenergy, 4(4), 255-261.

Strong, T. F., & Zavitkovskj, J. (1983). Effect of harvesting season on hybrid poplar coppicing.

Thornton, F. C., Dev Joslin, J., Bock, B. R., Houston, A., Green, T., Schoenholtz, S., Pettry, D., & Tyler, D. D. (1998). Environmental effects of growing woody crops on agricultural land: first year effects on erosion, and water quality. *Biomass and Bioenergy, 15*(1), 57-69.

Zavitkovski, J. (1981). Characterization of light climate under canopies of intensively-cultured hybrid poplar plantations. *Agricultural Meteorology, 25*, 245-255.

VITA

VITA

Tian Guo was born and raised in a city near the Yangtze River in China. In June 2009 she graduated from Wuhan Polytechnic University in China with a degree in Biological Engineering. In September 2009 she began graduate studies at Southwest University in China in the Department of Resources and Environment. Her master's work focused on soil and water conservation study. She completed her Master's of Science in Agriculture in June 2012 and joined Agricultural and Biological Engineering Department's Ph.D. program at Purdue University in August 2012. Her dissertation research has primarily focused on the development and modification of Soil and Water Assessment Tool (SWAT) to model biomass production of bioenergy crops and hydrologic and water quality responses to their growth. She will complete her Doctor of Philosophy in May 2016, and soon after begin postdoctoral research at Purdue University.

PUBLICATION

PUBLICATION

Guo, T., Engel, B. A., Shao, G., Arnold, J. G., Srinivasan, R., & Kiniry, J. R. (2015). Functional approach to simulating short-rotation woody crops in process-based models. *BioEnergy Research*, *8*(4), 1598-1613.